Proceedings of a Workshop on the Physical Properties of Volcanic Seafloor

Woods Hole Oceanographic Institution
Woods Hole, Massachusetts 02543 USA

N00014-90-J-1319

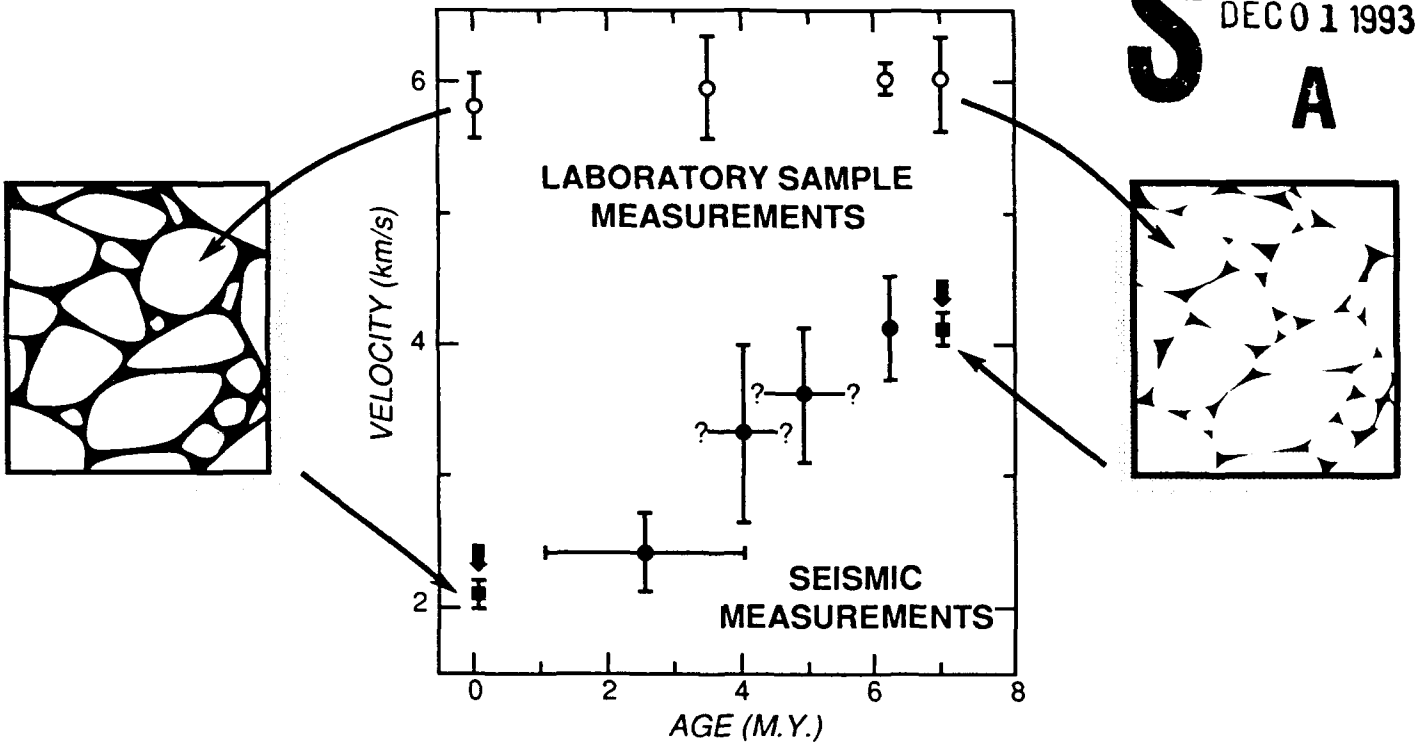

April 24-26, 1990

Convenors: G.M. Purdy and G.J. Fryer

Sponsored by the U.S. Office of Naval Research
and the Joint Oceanographic Institutions, Inc./U.S. Science Support Program

Acknowledgements

This workshop and the preparation and reproduction of this report was supported by the U.S. Office of Naval Research and by the Joint Oceanographic Institutions, Inc. as part of the U.S. Science Support Program for the Ocean Drilling Program. We appreciate the encouragement and guidance of Dr. R.S. Jacobson of ONR and Dr. Ellen Kappel of JOI in the planning and execution of this workshop. The organization of the meeting and the preparation of this report benefitted greatly from the competence and hard work of Faith Hampshire.

The success of the workshop was due to the diligence and leadership of the Discussion Group chairmen whose names are listed in Appendix 1.

CONTENTS

SUMMARY

The volcanic ocean floor, defined by the uppermost basaltic lavas of oceanic Layer 2, is the single largest and most consistent contrast in physical properties on the earth's surface. More than 60% of our planet is coated by this boundary that constitutes a contrast in both compressional and shear wave velocity of several km/s. Propagation through the ocean floor, and reflection and scattering from it, cannot be understood quantitatively without a knowledge of the properties of this boundary.

The compressional wave velocity of the volcanic seafloor on the scale of tens to hundreds of meters is almost one third (i.e., ~2.1 km/s) the velocity when measured in the laboratory at the scale of centimeters (~6 km/s); and evidence exists to suggest that at the large scale of 10-100 meters this velocity doubles during the first 7-10 my after the formation of the crust (or within a few hundred kilometers of the ridge axis). Both these phenomena are illustrated in the figure on the cover of this report.

A knowledge and understanding of the spatial variability in structure of the uppermost oceanic crust is a key to the understanding of both the temporal and along-axis variability in accretion processes. This is currently one of the most important unknowns that blocks progress in the quantitative modeling of mid-ocean ridge systems.

The significance of these issues and the substantial progress in recent years towards their understanding prompted the organization of a workshop in April 1990 held at Woods Hole Oceanographic Institution and sponsored by the Office of Naval Research and the U.S. Science Advisory Committee/Joint Oceanographic Institutions, Inc. The objectives of the workshop, which was attended by approximately 80 earth scientists and acousticians, were to review our state of knowledge concerning the processes that control the physical properties of the uppermost several hundred meters of the igneous ocean crust and to describe the measurements and experiments that, during a 5-10 year long program would solve the key problems. The workshop was extremely successful, inviting lively and constructive discussion, and many contributed manuscripts that are included in this report providing a first class overview of this field of research.

Several common themes emerged from the workshop and high priority objectives were defined that must be achieved before a thorough understanding is possible of how the upper oceanic crust evolves. It is clear that the processes we are studying are controlled by a multiplicity of variables. It is clear that the temporal and spatial scales upon which changes occur in the upper crust vary from thousands to tens of millions of years, and from millimeters to hundreds of kilometers. Our research plan must be exceptionally systematic in its approach and we propose to focus all data collection within a small number of evolutionary flow-line corridors. A minimum of two corridors should be identified, one on the East Pacific Rise, the other on the Mid-Atlantic Ridge. Their along-axis extent should be 50-100 km and they should extend onto at least 20 my crust.

Wide ranging programs to collect the background regional data within these corridors should be initiated as soon as possible. Within these evolutionary corridors approximately five ~10 kilometer square detailed survey areas should be identified and *pairs* of drill holes should be located within them. In addition, in both the Atlantic and Pacific oceans, scarps that constitute 'windows' into the crust and provide unparalleled views of the lateral continuity of basic structures, should be identified and subjected to comparable detailed studies; a drilling program should be designed to provide a truly three dimensional view of the structures observable in two dimensions on the scarp.

The large and diverse data sets generated by this ambitious program should be used to:

- determine and contrast the architectures of Atlantic and Pacific crust and define the processes that control the differences and influence the variability.

- identify the nature and timescales of the alteration processes and understand the linkages between these processes and the evolving physical properties of the crust.

- quantify the controls that determine the nature and timing of the key alteration phenomena.

- establish robust correlations between the geological architecture and the compressional and shear wave velocity structure and the magnitude and nature of the porosity.

- fully define the systematic evolutionary changes in the physical properties of the upper crust and identify correlations with key parameters (topography, sediment cover, spreading rate, etc.).

These objectives can only be accomplished if substantial advances in modeling capabilities are made, thus allowing the researcher to integrate these diverse observations into a coherent picture of how the various processes interact to produce such apparently systematic changes in physical properties.

The magnitude of the effort embodied in the above recommendations is sufficiently large that some priorities must be set. Three primary areas of research are identified below.

- Determination of the fundamental architecture of the upper oceanic crust: this most fundamental of objectives must take precedence over other efforts. The highest priority must be given to the determination of the nature of the surficial low velocity layer, and of its lowermost boundary. Two programs can be described that would most effectively provide substantial progress towards this goal. Firstly a combined detailed survey/seismics/drilling program on young (0-1 my) Pacific crust, that would for the first time combine a pair of drill holes through the uppermost crust (and associated downhole experiments) with a three dimensional seismic image of the crust from a careful on-bottom source and receiver tomography experiment, and a comprehensive suite of near-bottom geophysical and sampling data. And secondly, a coordinated geophysical and drilling program focussed (again on Pacific crust) on a scarp exposure of a substantial section of the upper crust: from this an unparalleled view of structural heterogeneity in three dimensions can be obtained.

- Alteration and Variability: this program also has two components: a detailed survey area (~10 km square) on 20 my old Pacific crust must be chosen within which a *pair* of drill holes through the upper crust (with as close to total recovery as possible) will provide the baseline data (when compared with the results from the younger drill hole results described above) in studies of alteration, cementation and secondary mineral deposition. Again, an on-bottom seismic tomography experiment should fully characterize the three dimensional structure around the holes. And secondly, spot seismic velocity measurements should be made along the flow line between the young and this 20 my site to unequivocally establish one example of how the velocity of the uppermost 100m evolves with age.

- Modeling: complex interactions between widely varying processes (e.g., alteration to fluid flow to permeability to faulting) must be understood and quantified if our objectives are to be achieved. This is only feasible if substantially more effort is directed towards the development and construction of careful models that adequately describe the primary evolutionary processes. There are many steps between the cementation of grains within a basaltic breccia and seismic velocity: these can only be understood quantitatively via the insights yielded by good physical models.

Substantially more than half the area of the seafloor in the Central and North Pacific ocean is covered by less than 100 meters of sediment. This means that the nature of the interaction of low frequency sound with the seafloor is dominantly controlled by the physical properties of the underlying igneous crust, rather than by the sediments. Because of our knowledge of the substantial age related changes in the compressional wave velocity structure of the uppermost crust, we predict major spatial changes in nature of bottom interaction.

Specifically because we suspect the shear velocity of the upper crust when it is formed is below the compressional wave velocity in the water column, but that this reverses itself as an ocean basin is traversed (due to the aging process), then profound changes in bottom interaction are predicted. The research program described in this report will provide the understanding of the controlling processes on crustal evolution that are key to the prediction of this spatial change in physical properties. This will provide a quantum leap in the quality of predictions of bottom loss in long range low frequency propagation problems.

INTRODUCTION

The workshop was held at Woods Hole Oceanographic Institution, Massachusetts on April 24-26, 1990. The convenors were G.M. Purdy of Woods Hole Oceanographic Institution and G.J. Fryer of the University of Hawaii. Guidance in the planning and execution of the workshop was provided by a steering committee consisting of N.I. Christensen of Purdue University, K. Becker of Rosenstiel School of Marine and Atmospheric Science and O. Diachok of the Naval Research Laboratory.

The objectives of the workshop were to define what we know, and what we do not know of the processes that control the physical properties of the uppermost several hundred meters of the igneous ocean crust. And then given this framework, outline a science plan that includes the measurements and experiments that, during a 5-10 year long program, would furnish solutions to these previously established problems. The scientific rationale for the focus on the physical properties of just this uppermost section of the oceanic crust lies in two substantially different areas: within this section of the volcanic sequence lies a complete fossil record of the temporal and spatial (particularly along-axis) changes in the crustal emplacement process. If key relationships between structure and physical properties can be established then remote mapping methods (e.g., seismic, electrical) can be used to exploit these relationships to investigate the episodicity of the accretion process and its variability with distance from axial discontinuities and transform faults.

The second rationale follows from the well-known property of the uppermost crust, first recognized by Bob Houtz and John Ewing in the mid 1970's: at the seismic scale of several hundred meters the compressional wave velocity of the upper crust almost doubles during a period of several million years following its formation (see cover figure). Especially in thinly sedimented oceans like the North Pacific this evolutionary process is the dominant factor controlling systematic changes in seafloor reflectivity. If these processes can be understood sufficiently well that quantitative predictions can be made of changes in physical properties, then useful maps of spatial variations in acoustic bottom losses for long range low frequency propagation in the water column can be computed that are of substantial interest to the Navy acoustics community.

Workshop participants, whose names and affiliations are included in *Appendix 2*, totalled approximately 60 individuals representing diverse disciplines ranging from geochemistry to acoustics and including a large group of seismologists. Attendees at the three day meeting (see Agenda in *Appendix 1*) were organized into three primary 'process' oriented groups focussed on the three key phenomena that control the physical properties of the uppermost crust - volcanic emplacement, tectonics (faulting, cracking, fissuring) and alteration (both of the individual basaltic units and of the medium as a whole through the precipitation of secondary minerals in inter-pillow cavities and in micro cracks and fissures). A fourth group focussed on the overall impact and relative importance of these phenomena on the acoustic properties of the seafloor.

Having used these groups, stimulated and well-directed by a set of keynote speakers, to define the Scientific Objectives, the workshop then split by technique to discuss various measurement and experimental approaches. Three 'Technique' groups were formed to deliberate upon how seismic and acoustic experiments, downhole and other geophysical measurements and sampling and laboratory measurements could be used to tackle the previously established scientific objectives. The 'wish lists' that these groups produced were, not surprisingly, extensive and ambitious. We used the 'Process' oriented groups (Volcanics, Tectonics and Alteration) to review these recommendations and reorganize them into coherent plans to tackle the high priority issues.

This workshop report is presented in three sections. The first provides an account of the Workshop Proceedings, describing the primary conclusions of the discussion groups and presenting a summary of the primary recommendations. The second section consists of eight keynote papers that are summaries of the keynote presentations that at the start of the workshop, served to summarize the primary issues and objectives. The final section is a compilation of contributed papers all of which pertain to issues relevant to the understanding of the physical properties of the uppermost sections of the igneous ocean crust.

We do not intend this report to serve as a blueprint for all research in the structure of the upper crust. More refinement, detailed discussion and prioritization is needed than is possible within the context of a single three day workshop. We do hope however, that this report will provide a framework within which more specific planning can take place and that it will serve as a useful reference work to provide the interested researcher with a rapid overview of the key issues surrounding this important and exciting topic of research.

If the reader of this report wishes a brief but scholarly overview of the important components of the problem of understanding the volcanic seafloor, then the Keynote Papers (Section B) will be of primary interest. If detailed and diverse views of processes, techniques and physical properties are wanted then the Papers Contributed to the Workshop (Section C) are the best source. If an account of wide-ranging discussion about processes and program plans is of interest, then the reader is referred to the Workshop Proceedings in Section A. It is in this section that attempts are made to outline key elements of the research and data collection that are needed to achieve progress in the understanding of the volcanic seafloor.

Section A: Workshop Proceedings

1: Introduction

2: Processes

3: Measurements

4: Strategies

5: Modeling

6: Issues

7: Towards an integrated plan.

A1: Introduction

Understanding of the physical properties of volcanic seafloor requires a knowledge of the processes that create and alter the igneous oceanic crust. For this reason the nuclei of the workshop around which the primary deliberations were organized were three groups that considered Volcanic processes (led by Bob Detrick of the University of Rhode Island), Tectonic processes (led by Brian Lewis of the University of Washington) and Alteration processes (led by Joe Cann of the University of Leeds and Woods Hole Oceanographic Institution). To maintain linkage to practical issues related to Acoustics, a fourth group was formed led by Orest Diachok of the Naval Research Laboratory.

Because planning research programs necessarily involves the application of data collection techniques then three parallel groups deliberated on experimental approaches: Seismo-Acoustics (co-chaired by Ralph Stephen, LeRoy Dorman and Orest Diachok), Downhole and other Geophysical Measurements (co-chaired by Dave Goldberg, Dan Moos and Paul Johnson) and Laboratory Measurements and Bottom Sampling (co-chaired by Jeff Karson, Rick Carlson and Roy Wilkens).

The following three sections of text ('Processes', 'Measurements' and 'Strategies') represent summaries of the conclusions of these groups arrived at by consensus and presented to the plenary sessions of the workshop. Some editing by the convenors has been necessary to produce a consistent and readable document. Because of the fundamental importance of modeling to gaining understanding of all key processes, a special section has been added (contributed by Jian Lin of Woods Hole Oceanographic Institution) in order to provide emphasis to this often neglected field.

The Keynote speakers contributed lists of questions and issues that they considered of particular importance to their subject of interest. Although some overlap exists between these 'questions' and the subjects covered in Sections A and B, they were considered such a useful and rich source of insight into the most important unknowns, that they have been edited and collated into a separate section entitled 'Issues'.

Finally an attempt has been made by the convenors to identify the common threads among the wildly diverse recommendations generated at the workshop discussions and begin the definition of a long range research plan. Without such a program directed at the shallow igneous crust it is clear we can understand neither bottom interaction of low frequency sound nor the temporal and spatial variability of the crustal accretion process.

A2: Processes

The physical properties of volcanic seafloor are controlled in large part by the mineralogy of the rocks from which it is constructed and the shape, size and distribution of the cracks, voids and fissures that we know pervade its structure. The mineralogy of the basalts and the magnitude and nature of the porosity of the shallowmost crust is determined by the volcanic processes that intrude and extrude the magma into the shallow crust and onto the seafloor. Tectonic processes of extension, uplift, fissuring and faulting modify the porosity and in some cases lift deeper crustal materials close to the seafloor. Immediately following emplacement, alteration processes begin to modify the mineralogy of the crustal matrix and substantially change the porosity and mean crack shape by precipitation of secondary minerals.

Thus if we are to understand the physical properties of the shallow igneous crust well enough so that on the one hand we can predict their values given basic regional data (crustal

age, spreading rate, sediment cover, etc.) and on the other hand use measurements of these properties to infer some characteristics of the environment in which the crust was created (e.g., proximity to distal end of segment, during a period of high or low magma budget, etc.), then it is essential we understand the linkages between the volcanic, tectonic and alteration formative and evolutionary processes and those physical and chemical characteristics that determine the physical properties.

There follows summaries of the key process oriented objectives that workshop attendees considered essential components of research programs design to address:

Volcanic Processes: The overall goal here is to understand the volcanic processes involved in the construction of oceanic crust and to understand how they contribute to and control the physical properties of the uppermost crust.

To achieve this goal we must determine the factors that control the eruptive style, composition, volume and episodicity of volcanic activity. For example, we need to know the relative proportion of different eruptive types in layer 2. We need to understand the controls on the eruptive style (pillows, flows) and how this changes during a volcanic emplacement event. And most fundamentally we need to know the temporal variability of magmatism.

A prominent barrier to our understanding is a lack of knowledge of the basic architecture of the uppermost crust. Are there systematic structures (e.g., layering) within the uppermost crust and if so what are their modes of formation? If fundamental structural units can be defined then a knowledge of their lateral and vertical extent is vital. We must determine both the width of the zone over which the crust is formed by volcanic processes and the length of time over which a single structural unit is emplaced.

Of specific interest to this research program is the direct understanding of the role that primary volcanic construction plays in determining the upper crustal physical properties. What volcanic processes give rise to acoustically identifiable boundaries? What creates anisotropy in the crust? How do volcanic structures control the primary porosity and permeability of the crust? Most generally, how do volcanic processes control compressional and shear velocity and attenuation, density and roughness?

Although the shallow crust is known to be substantially heterogeneous, little is known concerning either the scales or the origins of this heterogeneity. What is the nature of the structural heterogeneity of the upper crust on the scales of tens of meters to kilometers and is it deterministic or stochastic? What is the size spacing and orientation of cracks and what is their aspect ratio distribution? How does the structure of the upper crust vary regionally with tectonic setting? The interrelationships of volcanism with hydrothermal and tectonic processes during crustal emplacement are important unknowns. What is the relationship between stress regime, eruptive style and architecture of the upper crust? How does volcanic structure control subsegment-scale processes?

Key issues within this plethora of questions were identified to be the determination of the fundamental architecture of the uppermost crust: do systematic structures exist, what are the primary structural units and how are they related to eruptive style, composition and volume? Also important is the determination of the scales of heterogeneities (from local to regional).

Tectonic Processes: Like no other process, it is clear that first order differences which determine the role that tectonics plays in the formation of the crust exist between the major ocean basins. It appears that lithosphere accretion can be divided into roughly two

classes, one having very low levels of seismic energy release and a thin axial lithosphere (e.g., East Pacific Rise), the other having high levels of seismic energy release and a thick axial lithosphere (e.g., Mid-Atlantic Ridge). Hypotheses to explain these differences include consideration of mantle temperature and composition, and magma budgets.

Tectonic extension on parts of the Mid-Atlantic Ridge may reach 100%, but on the East Pacific Rise it is probably only a few percent. What controls this fundamental difference in the amount and style of extension? It is certainly more complex than simply spreading rate dependency.

To what extent is the tectonic emplacement of crustal material important? How extensive are gabbros and serpentinites at the seafloor and how do they influence seismic velocity? To what extent does tectonics control porosity of the upper crust (compared, for example, with porosity due to volcanic structures)? Are faults and fissures important contributors to the large scale porosity? To what extent does tectonics control permeability? Are faults primary conduits for fluid flow deep into the crust? What is the relative importance of volcanic cycles and tectonics in controlling seafloor morphology? Mass wasting must be a primary contributor to small scale seafloor heterogeneity in topographically rough environments but how is this controlled by tectonic activity? Cracks and faults form because of the presence of stresses in the crust: what is the stress field and how does it vary in space and time? And of course a most fundamental issue is: how do cracks form and evolve?

Alteration Processes: *The seismic properties of shallow oceanic crust are* profoundly influenced by the metamorphic history of the plate as it moves off-axis and ages. Three major types of processes modify the volcanic and tectonic structure inherited from crustal accretion at the ridge axis: 1) mechanical processes, such as sedimentation, mass wasting, brecciation, collapse and compaction; 2) low temperature (<70°C) seawater interaction, which can be active for several millions of years off-axis; and 3) high temperature (>70°C) seawater interaction, which is believed to occur primarily near-axis. Ophiolite and drilling studies reveal major provinces of alteration within oceanic crust, with an upper layer of cold, oxidative seawater alteration, overlying a layer of low temperature hydrothermal alteration (e.g., zeolite facies), overlying a zone of higher temperature hydrothermal interaction (e.g., greenschist facies), although the thickness of these layers varies substantially. It is clear that extreme variability exists in the nature, scale and geometry of alteration in oceanic crust This heterogeneity reflects the complicated physico-chemical processes and feedback loops associated with seawater-rock interactions, which are influenced by parameters that include: permeability structure, thermal regime, fluid composition and water-rock ratio. The evolution of these parameters with time and depth, and the controls exerted on them by tectonic setting, all need to be identified in order to understand fully the alteration of oceanic crust and its effect on physical properties. The objectives of a program to understand the influences of alteration on the physical properties of the volcanic seafloor should be as follows:

— The evolution of alteration in the upper oceanic crust with increasing crustal age, and the influence on this of other crustal variables must be understood.

  - What is the spatial scale of alteration type, geometry, and intensity, vertically and laterally?

  - On regional spatial scales, what is the influence of: crustal age, spreading rate, and degree of crustal rifting?

- On local spatial scales, what is the influence of topography, rock type, sediment type, fissuring, sediment cover and fracturing?
- What are the chemical fluxes into and out of the crust?
- Is the lower boundary of the axial low velocity cap alteration-controlled?
- What is the mechanical evolution of the upper crust?

— The links between alteration and physical properties on hand specimen and logging scale must be determined.

- How is alteration mineralogy and chemistry related to physical properties?
- How does rock volume, pore space geometry and fracture filling vary with alteration? How does this relate to physical properties?

— The links between alteration and physical properties at seismic scales must be determined.

- What is the seismic structure of the upper crust as a function of age? Does the velocity of the upper layers indeed double? Why? How does the shear velocity evolve?
- What are the relations between seismic/acoustic observables and scale and degree of alteration?
- What are the relations between different alteration scales in ophiolites? Do these extend to the ocean basins?
- What is the geometry of off-axis active hydrothermal systems?
- What are the links between seismics, alteration and other physical observables?

A3: Measurements

Discussion of the physical and chemical processes that control shallow crustal properties is a fine academic exercise that is not useful unless observational strategies can be devised that will provide ways to test and validate models and ideas. With this practical thought in mind, three discussion groups were formed to define the measurements and experiments needed to achieve the objectives summarized in the previous section. The division of responsibilities between the groups was somewhat arbitrary and inevitably resulted in some overlap and is most simply described by the group titles.

Downhole and Other Geophysical Measurements: It is necessary first to define a framework within which this broad range of measurements can be made. The primary recommendation in this respect is the establishment of two crustal evolutionary corridors, that have a width comparable to that of a distinct recognizable spreading segment, and that extend from the rise crest onto approximately 20 m.y. old crust. The two corridors should be located over contrasting spreading regimes (e.g., Atlantic and Pacific) and the following fundamental properties should be mapped within them (not arranged in order of priority).

Required Properties:

- Seismic velocity, both compressional and shear, and attenuation.
- The structure of the crust in three-dimensions.
- Topography of the seafloor and the igneous basement.
- Alteration of the crust in three dimensions and with time.
- Thermal structure.
- Seismicity: distribution in depth, spatial distribution relative to surface morphologies and source mechanisms.
- Electrical properties (and especially their relationships with porosity).
- Fine-scale magnetics (possible linkages to alteration and faulting?).
- Sampling, both surface and subsurface.
- In situ stress measurements.
- Sediment type, distribution and physical properties.
- Seafloor reflectivity.
- Porosity and permeability (both small and large scale).
- Seismic anisotropy (both azimuthal and horizontal).

Criteria for Selection of Crustal Evolution Corridors:

- The corridors should be located over 'normal' oceanic crust away from anomalous disturbances like hot spot traces, ridge jumps, propagators, etc. The two spreading systems should be chosen for their contrasting character. One should be characterized by large amplitude topography and be dominated by tectonic processes; the other should have low amplitude topography and be dominated by volcanic processes.

- Both corridors should have similar and consistent sedimentation histories.

- The upper crustal structure within the corridors must be mappable using presently available seismic methods.

- Because of the importance of carrying out subseafloor observation and sampling on a broad spectrum of scales, then the corridor on the tectonically dominated system should include a good scarp that provides adequate opportunity to perform such experiments.

- On the volcanically dominated system, the corridor should not be positioned to include a 'window into the crust' because this would necessarily require the location to be an unusual area. Instead, a separate and additional survey should be carried out over an appropriate feature perhaps located nearby (for logistical ease) but certainly that provides observational opportunities into similarly formed crust.

- The corridors should be centered upon flow lines from the center of discrete spreading segments of modest length, so that it is practical that the total width of the corridors encompasses all the crust generated at that spreading segment.

- Logistical considerations should play some role in choice of location of the corridors (weather, proximity to ports from which research vessels can operate, magnitude and quality of existing data coverage, etc.).

Key Emphases:

- Because so few observations exist pertaining to the scales of variability in structure in the shallow crust then special emphasis should be given to drilling *pairs* of holes so that direct observations of geological stratigraphies can be compared. Such 'twin holes' would also allow innovative cross-hole geophysical experiments that would provide further insights into the lateral continuity and heterogeneity of observed structures.

- Progress in learning about evolutionary processes in the shallow crust is not limited by lack of ideas or insufficient understanding of the fundamental physics and chemistry that controls the processes, but by an extreme lack of appropriate data that can be used to test, validate and enhance models of the changes that occur in the crust. Thus substantial emphasis should be placed on the systematic collection of consistent datasets using the best of the available new technologies.

Measurement Strategies:

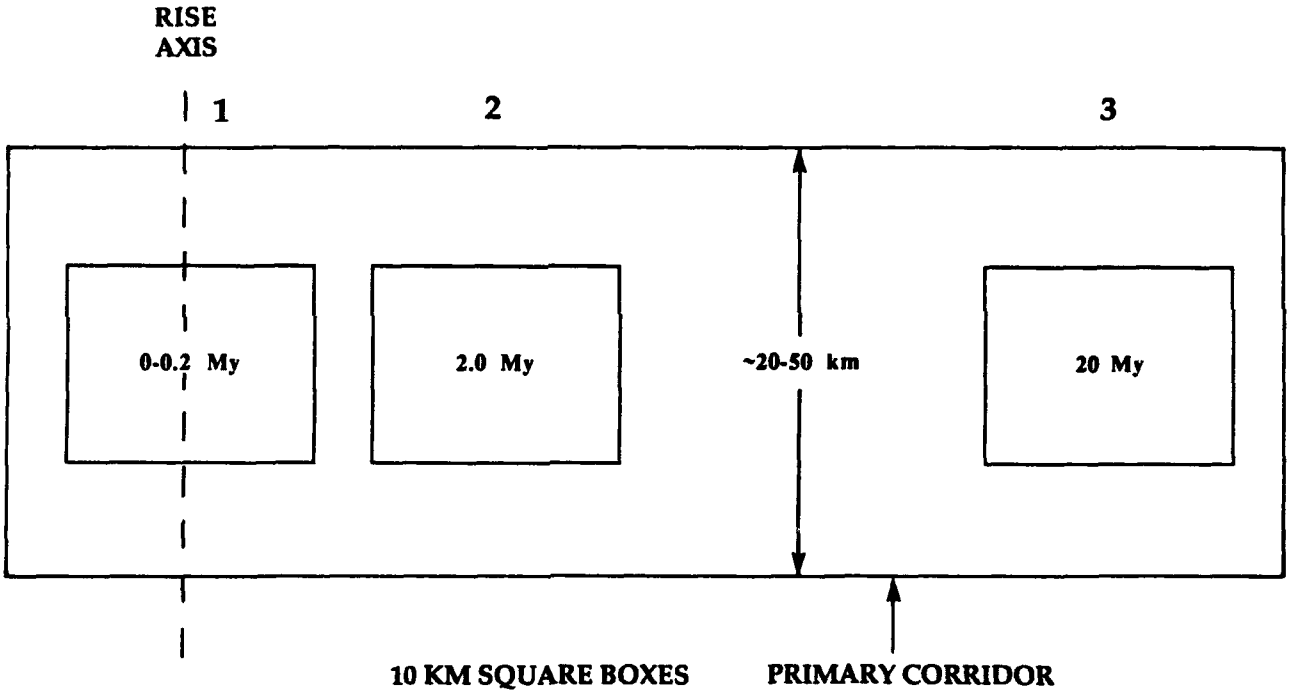

Within the primary corridor basic regional mapping should be carried out including:

- Multibeam bathymetry and side scan sonar.
- Single channel and multichannel seismic mapping reflection profiling (including 3.5 kHz).
- OBS and seismic refraction experiments.
- Magnetics and gravity.
- Heat flow and sediment cording where appropriate.
- Dredging (where possible).
- Rock drilling (using seafloor drill to recovery small oriented cores).

However, the focus of the work should be in ~three small detailed survey areas each about 10 km square, distributed over 0, 2 and 20 my crust. These

measurements in these areas should be organized around pairs of drill holes that penetrate several hundred meters into the volcanic basement.

Area 1: 0-0.2 my, one pair of drill holes and a complete set of near bottom deep tow surveys. Extensive logging, downhole and cross-hole experiments in the drill holes (see Table).

Area 2: centered on 2 my, one pair of drill holes, near bottom surveys, heat flow (where feasible in sediment pockets) and additional detailed surface surveys as appropriate. Extensive logging, downhole and cross-hole experiments in the drill holes (see Table).

Area 3: centered on 20 my, two pairs of drill holes, modest near bottom survey effort as appropriate, additional surface surveys and a comprehensive heat flow measurement program. Extensive logging, downhole and cross-hole experiments in the drill holes (see Table).

In the above, 'near bottom surveys' include video and high resolution side-scan imaging, deep tow magnetics, seafloor gravity, active electromagnetic methods, on-bottom refraction experiments, deep tow seismic reflection profiling.

In addition to the three 'primary' detailed survey boxes here, consideration should be given to the siting of one survey of a substantial scarp that provides a 'window' into the crust. And to the possibility of siting a survey over very old crust (~100 my) to provide end-member observations to the evolutionary process.

Seismic and Acoustic Methods: Process objectives addressed by seismo-acoustic methods are as follows:

- Determine the fundamental architecture of the uppermost crust.
- What scales of heterogeneity are present in the upper crust?
  - What is the nature of the structural heterogeneity?
  - What are the size, capacity, orientation and aspect ratio distribution of cracks in the crust?
  - How does the structure of the upper crust vary regionally with tectonic setting?
- What are the physical properties of the upper crust (compressional and shear velocities, compressional and shear attenuation, density, roughness).
- What is the width of the zone over which the crust forms by volcanic processes?
- How extensive are gabbros and serpentinites at the seafloor?
- To what extent does tectonics control porosity of the upper crust?
- How do cracks form and where?
- What is the stress field in the upper crust?
- What are the links between alteration and physical properties at seismic scales?
- What is the seismic structure of the upper crust as a function of age? Does the velocity of the upper layers double? How does the shear velocity vary?

Table

BOREHOLE MEASUREMENTS

PROPERTY	VERTICAL RESOLUTION					NEW
	≤CM	CM-M	M	10-100M	≥100M	
POROSITY		(neutron)				
DENSITY		density				gravity
P-WAVE VEL.		sonic	mcs	vsp	ose	x-hole seismic
S-WAVE VEL.			mcs			vsp(s);ose(s); x-hole
ANISOTROPY					ose	sonic(s)+above
ATTENUATION		sonic	mcs	vsp	ose	above
CHEMISTRY		nuclear				
FLUID CHEM.						wire-line packer
PERMEABILITY				packer		flowmeter+w-1 packer
TEMPERATURE		temp				
RESISTIVITY	FMS	SFL,DIL	DLL	LSR		IP;oblique EM
MAG.FIELD		3-axis Mag				
SUSCEPTIBILITY		susc.				
STRUCTURE	BHTV;FMS		DLL			
STRESS		BHTV;FMS				Hydr. Fract.
FRACTURING	BHTV;FMS					

Seismo-acoustic tools to address the objectives:

Survey Tools:

- Seabeam (multi-beam bathymetry) to determine seafloor morphology.
- Multi-channel seismic methods to determine V_p, in the upper crust (and possibly V_s?). Track the shallow layer off axis. Would roughness effects make the resolution too poor to be meaningful? Resolution is about 50m vertically and 500m horizontally. V_p and V_s studies will require either a longer streamer (~6 km) or two ships.
- DTAGS is a deep tow, high frequency (200-600 Hz) multi-channel system which would be used to map basement topography below sediments. With modifications to lower frequency it could be used to map heterogeneity within the crust. In sediments the resolution is 50m vertically and 200m horizontally.
- Horizontal arrays can be used with broad side sources to measure the time spread and angle spread of basement reflections and to study anisotropy in the reflections.
- There is a critical need for a rapid, inexpensive survey tool to measure V_s in the upper crust.

Small Scale Experiments

- A vertical array of hydrophones in the water column can be used to determine the phase velocities of VLF sound in the ocean and to separate the sound field into modes, which are sensitive to upper crustal shear speed.
- Bottom refraction experiments using OBS's, OBH's, or borehole sensors and bottom sources are the most promising technique for determining V_p, V_s, Q_p and Q_s in small (~2 km) blocks of upper crust. With enough source-receiver combinations, tomographic inversions of the data can be carried out. Resolution would be 30m vertically and 50m horizontally. Also useful for heterogeneity and anisotropy.
- Bottom interface wave experiments are particularly promising for mapping shear velocity and anisotropy in the upper crust. Resolution is about 10m vertically and 100m horizontally.
- Borehole seismometers are well coupled to the earth and provide high quality polarization measurements necessary to anisotropy studies. (Shear wave splitting is the most diagnostic feature of anisotropy.) Oblique seismic experiments measure the lateral variability in the upper crust at scales of 100m to 2 km. Borehole seismics also link the borehole scale measurements (cm-m) to regional geophysical scales (100m - 1 km).
- Microearthquake activity can be monitored with long term OBS deployments and will constrain the tectonic behaviors of the crust. Structural resolution is poor and needs improvement.
- Shear modulus experiments based on seafloor response to surface gravity waves are potentially very useful but resolution is currently limited to about 200m in the upper crust.
- Borehole shear sources and deep seafloor shear sources should be developed and deployed to give improved shear velocity measurements in the upper crust.
- Conventional tomography using ocean bottom seismometers and near surface shots can be quite useful in mapping shallow upper crustal structure.

Modeling/Analysis Techniques

- Finite difference and finite element forward modeling techniques give us insight into propagation and scattering in random and strongly heterogeneous media.

- Reflectivity forward modeling techniques for anisotropic media are essential to elucidate the physics of this complicated phenomena.
- WKBJ, reflectivity and SAFARI methods are used to study propagation in one-dimensional structures. They would be more useful if they were faster.
- Elastic coupled normal mode codes and elastic PE codes should be developed and applied to long range bottom interaction problems.
- Waveform and travel-time inversion techniques should be applied to the acquired data to quantitatively constrain the structural models.
- We urge the development of electrical methods for upper crustal investigations and the correlation of electrical and seismic observatories.

Laboratory Measurements and Bottom Sampling: Samples should be recovered from a minimum of two evolutionary corridors, each of which should be a minimum of 10 km in width and each extending out to 40 my old crust with some sampling beyond 100 my. The two corridors should be located on contrasting spreading systems (slow vs. fast spreading, and rough vs. smooth topography). Drilling must be a primary sample recovery tool with penetrations of several hundred meters into the volcanic basement being necessary.

Surveys and Sample Recovery

Four classes of primary data collection are proposed:

- Regional: It is essential that the setting and evolutionary history of all recovered samples be well known. Therefore regional scale measurements of the following parameters is essential: morphology (multibeam and side scan), sediment distribution (both thickness and type), magnetic field, heat flow, gravity field, multichannel seismic reflection profiling.

- Geological Mapping: At a reconnaissance scale using conventional dredging and coring, and in selected small area, in detail using submersibles and ROV's.

- Seismic Structure: It is impossible to relate the results of laboratory measurements to the evolutionary problem unless accurate determinations of velocity structure are made at the sites from which samples are recovered.

- Drilling: This is the primary tool for sample recovery. 2-3 deep (~1000m) holes and 8-10 shallow holes are needed along each corridor. Spatial distribution of holes should not be uniform but directed towards tackling specific problems. New drilling techniques must be developed to substantially improve recovery so a complete picture of crack distribution and alteration style can be obtained. Comprehensive programs of downhole logging and other downhole experiments should be carried out.

- Other Opportunities: In parallel with the above described primary studies, advantage should be taken of the special opportunities for observation and sample recovery provided by ophiolite formations, subareal volcanic systems (e.g., Hawaii, Iceland) and major seafloor scarps ('windows' into the crust).

Measurements:

There are eight factors that determine the seismic properties of samples in the laboratory:

Primary mineralogy
Glass content
Alteration products
Porosity
Pore fluid
Confining pressure
Temperature
Pore pressure

And there are seven general classes of physical properties that are measurable in the laboratory:

Seismic velocities
Seismic attenuations
Density
Electrical properties
Thermal properties
Magnetic properties
Permeability

In addition, dating of the samples is important (though not yet routinely feasible with precision in any direct manner), and most critically the study of the fabric of the samples, quantifying deformation and crack geometries. Important problems are the quantification of the effects of alteration on the magnitude and nature of the porosity, specifically the way in which cracks are progressively healed with time; the effects of temperature on seismic velocity are exceptionally poorly known; very few good measurements of attenuation exist and the effects of pore pressure require further investigation; and the results of expensive downhole logs would be substantially more useful if reliable calibrations (especially for porosity) were available.

Theory and Modeling

The result of laboratory studies of recovered samples could be better applied to the study of ocean floor processes if improved models and a better quantitative understanding of the following phenomena were available:

- Hydrothermal circulation: obviously a huge topic but it is probably the key process that controls alteration (and consequently perhaps porosity and crack geometry). Improved models are needed to provide insight into the spatial scales of the processes, the effects of topography and sediment cover, the nature of the primary conduits.

- Cracks: an understanding of the formation and evolution of cracks (on all scales) is essential.

- Anisotropy: single velocity measurements alone are uninterpretable without a knowledge of the nature of the anisotropy and how it effects the seismic measurements.

- Frequency dependency: The relationship between measurements made in the laboratory at very high frequencies and those on the seafloor at a few tens of herz is unknown. Improved insight into how to scale these measurements would be extremely helpful.

Required New Technologies

Many of the required measurements cannot be made in any practical manner given current technology. The following is a list of areas in which the development of improved measurement and sampling techniques is particularly important.

- Deep drilling: capability for recovery of oriented samples is critical along with the development of ways to substantially improve percentage recovery.

- Dating young volcanics: construction of the shallow crustal section and its very early evolution cannot be understood until methods are developed to date young basalts.

- Rock drill for operation by a submersible or ROV: this is the only way to reliably recover fresh oriented samples from the seafloor or from an outcrop and be able to place that sample in its proper geological context on the spatial scale that we know the stratigraphy of the crust to vary.

- Wireline rock drill: even a few meters of sediment blocks conventional dredging. Sampling is thus very heavily biassed to very young crust because of the expense of using a drilling vessel to recovery volcanic material from older crust. A wireline rock drill, though limited in penetration, would vastly improve the distribution in age and variety of the samples available for study.

- Improved seismic methods: continued development of higher resolution techniques capable of mapping three dimensional structures is crucial

- High Temperature Laboratory Data: new approaches and instrumentation are needed to permit laboratory measurements of physical properties to be carried out in a meaningful way at very high temperatures (including the case where some melt is present).

A4: Strategy

The greatest challenge faced at the workshop was the task of merging the diverse array of measurements and experiments described in the previous section with the process oriented problems, with which we began, to generate a reasonable overall research strategy. We achieved mixed success: some components were well treated but inevitably omissions occurred and some ideas received inappropriate emphasis.

Volcanic Processes: the first order priority here is to determine the fundamental architecture of the uppermost crust. We must learn whether systematic structures exist and how they are related to eruptive style, composition and volume and how this structure varies, and over what lateral scales. This understanding cannot be gained unless we learn to link geophysical observations to the outcrop scale geology of the upper crust.

- Strategy: an evolutionary corridor concept is favored within which to carry out regional reconnaissance and detailed observations within about five small areas. The distribution of the detailed survey areas is shown in the cartoon below: the numbers alongside each box represent the priority.

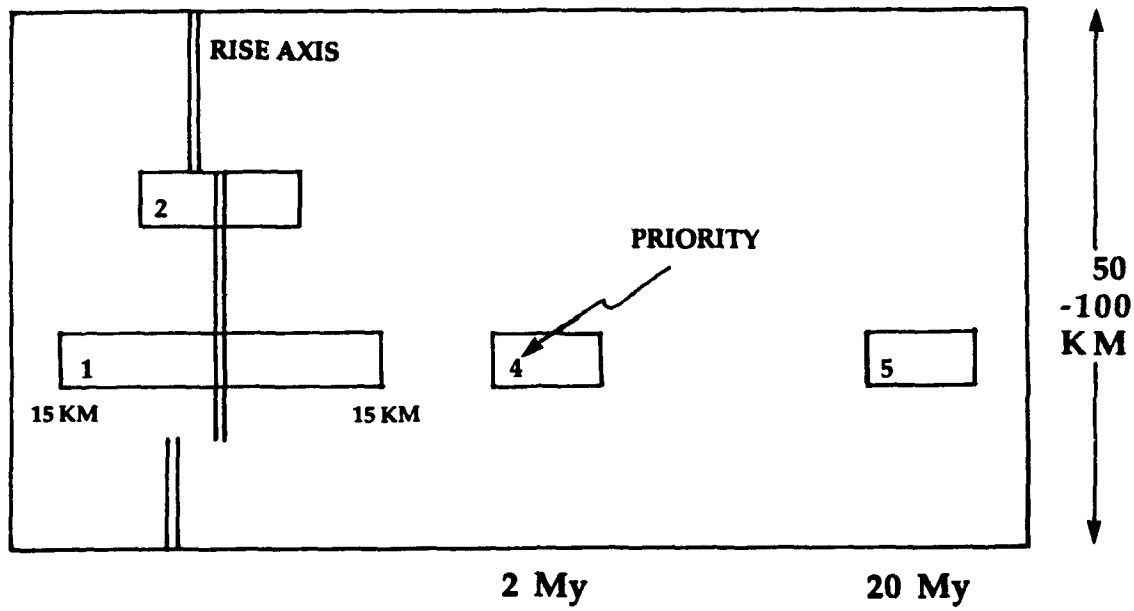

Priority 1: On-axis and near-axis (out to .2-.3 Ma).
Priority 2: Along-axis near the end of an accretionary segment.
Priority 3: Near-axis scarp (fresh exposure, youngest possible crust, long, single geological setting) to provide a 'window' into the internal structure.
Priority 4: ~2 my old crust.
Priority 5: ~20 my old crust.

The highest priority is to study a magma dominated system (e.g., EPR) rather than a tectonics dominated ridge (e.g., MAR) for both the evolutionary corridor and for the scarp surveys. Strictly from the point of view of studying volcanic processes the highest priority is to obtain zero age coverage at both fast and slow spreading ridges, as opposed to more extensive off-axis coverage.

- Techniques and Experiments

1. On the corridor scale two groups of observations are necessary:

   - Regional scale geological/geophysical coverage i.e., multibeam bathymetry, side-scan sonar, magnetics gravity, single channel seismics.

   - Multi-channel seismic reflection profiling (as well as perhaps underway active electromagnetic experiments) to provide some means of extrapolating structure between the detailed survey areas within the corridor.

2. On the scale of the detailed survey areas within the corridors six primary sets of measurements can be identified as follows

- Morphology: high resolution bathymetry and deep tow sidescan and video imaging to fully define the surficial features.

- Systematic seismic structure: high resolution three dimensional tomography experiments using on-bottom sources and receivers.

- Shallow porosity structure: near bottom active electromagnetic measurements and seafloor gravity determinations.

- Shallow structure and local heterogeneity: paired drill holes penetrating several hundred meters into volcanic basement.

- Shallow structure and state of stress: downhole physical property measurements, permeability, porosity formation microscanner, televiewer.

- Composition: submersible and ROV bottom sampling, wireline drilling, deep drilling from drill ship.

3. Full advantage must be taken of the 'window' into the shallow crust provided by some fault scarps. A unique opportunity is presented of placing the results of a drill hole in an appropriate regional context by drilling a site sufficiently close to a scarp that the drill hole stratigraphy can be correlated with that mappable in two dimensions on the scarp (see cartoon).

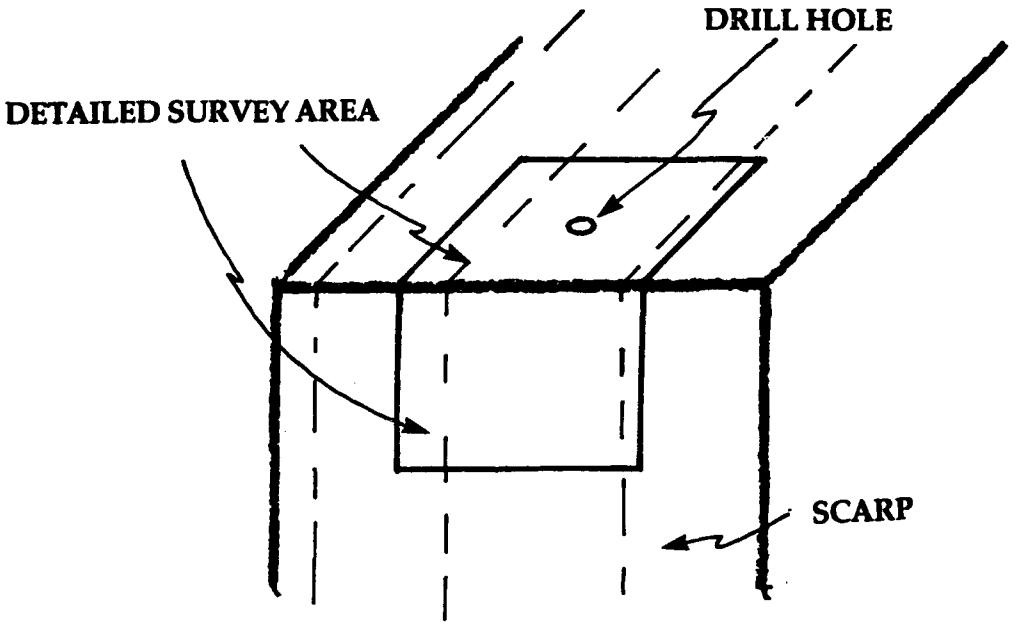

- High resolution deep tow acoustic imaging and bathymetry of all the seafloor and especially of the scarp face (and deep tow magnetics).

- On-bottom seismic experiments must be carried out that take advantage of the unique geometries provided by the scarp. Bottom shots to downhole sensors could provide completely new observations pertaining to scales of lateral variability.

- A complete geological map of the scarp face must be produced, and of the seafloor between the scarp and the drill hole. Extensive sampling must be carried out in the context of these maps.

- The drill hole must extend into and beyond the deepest unit observed on the scarp. An extensive suite of logging and downhole experiments must be carried out.

- Modeling: There are four high priority areas in which modeling studies could improve our understanding of how volcanic processes control the physical properties of the volcanic seafloor:

  - Physics of crustal magma chambers: insights are needed into the parameters that control the three dimensional geometry and longevity of a magma chamber.

  - To understand temporal variations in the accretion process time dependent thermal models must be constructed that describe the behavior of an episodic magma chamber and its response to time varying mantle flow, melt migration and dike injection.

  - Understanding of dike injection processes would be improved by three dimensional models of dike injection (both lateral and vertical) from a magma reservoir.

  - Controls on eruptive style are little known (and their relationship to *porosity structure*): again *even* simple models could greatly enhance our comprehension.

Tectonic Processes: As previously stated, the variation in tectonic processes between ocean basins is profound. It is reasonable to hypothesize that:

- the structure of the Mid-Atlantic Ridge is dominated by tectonism; detachment faults extend into the mantle to depths of up to 10 km; and these faults are primary pathways along which water reaches the upper mantle and altered rocks reach the seafloor;

- the East Pacific Rise is dominated by volcanic cycles and tectonism is limited to the upper 2 km; and tectonism does not substantially alter the crust beyond about 1 km from the axis;

- these processes result in substantially different upper crustal properties; velocity structure, porosity structure and especially the nature of spatial variability will be profoundly different.

It follows from this that a program directed towards elucidating how tectonic processes control upper crustal structure be focussed directly on the ridge axis; and that because the effects of tectonism in every respect are greater on the Mid-Atlantic Ridge that the highest priority effort be directed to a typical segment of that ridge encompassing the segment ends and their interaction with transform or non-transform offsets. Existing models suggest that major changes in tectonic style occur along axis within a particular segment: thus it is essential that these studies extend over a complete segment length. Evidence exists that deep crustal rocks are exposed on the seafloor in the Atlantic due to

tectonic phenomena: this process would dominate the spatial variability in physical properties if, for example, strips of serpentinized ultrabasics are exposed alongside basaltic pillow lavas. This characteristic could so dominate the spatial variability of physical properties in the Atlantic Ocean that it should constitute the highest priority objective with regards to program planning and data collection.

Proposed Program

The highest priority data collection should be located over a well defined segment of the Mid-Atlantic Ridge: four types of data collection should be undertaken in varying degrees of detail over seafloor that extends out to 1-2 my old crust.

- Seafloor mapping and sampling: the goal here is to produce a geological map of the seafloor that unequivocally identifies the primary outcrops, scarps, faults, talus piles, recent volcanic extrusions, etc. The intensity of this survey effort must be varied intelligently over the area so that it is a practical task because the total coverage required may exceed 1000 sq. km. The primary tools will be deep tow side-scan and video imaging, ROV and submersible sampling all integrated into a first class base of high resolution topographic data.

- Near-bottom geophysics: a comprehensive deep-tow magnetics program will fully characterize the spatial variability in magnetization from which inferences about faulting may be gained. On bottom seismic experiments using seafloor sources and receivers will be used to map the sub-bottom shape and extent of outcrops observed by submersible and ROV imaging.

- Long term earthquake monitoring: unequivocal identification of the depth extent and nature of faulting is only possible by the thorough characterization of the local earthquake activity. Ocean bottom seismometer deployments should be long term (>1 year) so that temporal patterns in activity can be recognized, and should extend over a complete ridge segment so changes in the patterns of faulting towards the distal ends can be characterized.

- Drilling: only drilling can provide the ground truth for models (based on the previous datasets) of how extension is taking place. In addition, comprehensive programs of logging and downhole experiments can further constrain estimates of the stress regime and permeability, etc.

Modeling

Two areas of effort deserve special emphasis and are rich in possibilities for substantial progress in understanding basic processes:

- Mechanisms of shallow crust cracking and fissuring:

  - Three-dimensional models of thermal stress-induced cracks should be constructed specifically to investigate the dependence of crack geometry and spatial distribution on the stresses and material properties.
  - Models that relate large-scale faulting and local cracking and especially topography-induced cracks are needed.
  - Models that relate crack geometry and effective porosity and permeability of the crust would permit linkages to be made to hydrothermal models.

- Mechanisms of large-scale brittle and ductile deformation of the lithosphere:

  - Two- and three-dimensional mechanical models of asymmetric rifts and large-scale discrete faults (including high angle and detachment faults).
  - Models of ductile/non-linear deformation of the lithosphere at high temperature and high strain conditions (lower crust/upper mantle conditions).
  - Models of interactive processes between large-scale lithospheric deformation and upper mantle convective flow; between crustal faulting and dike injection/propagation, and between faulting and magma chamber inflation/deflation.

Alteration Processes:

- Baseline surveys

  - Select corridor in thinly-sedimented, smooth crust, on basis of prior aeromagnetic survey work.

    Conduct large aperture multichannel seismic reflection survey both along and across corridor (to provide first cut at compressional wave velocity structure and determine if internal reflectors can be identified).

    Conduct multibeam and side-scan survey and single channel seismics and magnetics and gravity to provide basic background data.

    Conduct reconnaissance dredging and sediment coring and heat flow survey ($\rightarrow$ regional variation at seafloor) (suggest corridor north of Clipperton to - far enough to miss equatorial high sediment rates but missing complications due to Mathematicians seamounts).

- Select scarp (newly exposed crust)
  (10-15 km length of scarp).
  Detailed surveys of potential field
  Side-looking side-scan.
  Dredging
  Submersible
  Devise small-scale seismic experiment to look at structure and variability.
  Sea-floor resistivity.

- Choose/survey detailed survey areas in corridor (tentatively three areas at ages of 0.2, 2, 20 my).

  - Detailed survey for drill site.

all sites	Near bottom underway geophysics side-scan, microbathymetry, magnetics, deep-towed seismic reflection.
2 my, 20 my	Detailed heat flow.
all sites	Photography and sampling (including wireline rock drill) of outcrops.
all sites	Array of seismic experiments.
all sites	Electrical experiments.
0.2 my, 2 my	Plume sniffing.

- Drilling
  1 pair of holes in 0.2 my, 2; 2 pairs of holes in 20 my. Depth to be defined by seismics (?3-400m deep). In each pair of holes (with re-entry cones) continuous coring for laboratory work; full standard set of logs; offset VSP; cross-hole seismic tomography; long-spacing resistivity; hydrogeological tests (much of this may be carried out by wireline re-entry from conventional ship.)

  *Top priority overall is one leg of drilling on 20 my crust with a full suite of associated experiments.

- Laboratory investigations:

  - Full characterization of alteration mineralogy, petrology, geochemistry.
  - Full characterization of laboratory physical properties (acoustic, electrical, magnetic).
  - Microstructural study of pores, fractures, shears.
  - Pore fluid chemistry in sediments.

- Modeling

  - Modeling of hydrothermal flow based on geophysical, geochemical measurements.
  - Modeling of relationships between seismic observables, electric observables, magnetic observables, fractures, pores, etc.
  - Modeling of progressive reactions during fluid flow.

- Ophiolites

  - Mapping and comparative petrography of alteration to link hand specimen and seismic scales.

- Select a corridor in rifted (rough) topography (suggest west from MARK area, to include axial surveys and DSDP Sites 395A, 417 and 418). Repeat same surveys as defined above for corridor and associated scarp. (Diversity of rock types may require more detailed sampling.)

- Select detailed survey areas (one at axis, one around 395A, one at 20 my, one around 417, 418 to take advantage of previous work). Conduct full suite of experiments as in (B) above.

- Drilling

  a) Drill a paired hole to Site 395A, located on the flanks of the MAR near 23°N. The new hole should be 1-200m away and be fully cored.

  b) Two pairs of holes on 20 my old crust. Conduct full suite of experiments/ observations as above, and laboratory measurements and modeling as above.

A5: Modeling

The following is a menu of ideas for areas in which quantitative models of processes would substantially improve understanding of mechanisms that control shallow crustal properties:

Mechanisms of large-scale brittle and ductile deformation of the lithosphere:

- Two- and three-dimensional mechanical models of asymmetric rifts and large-scale discrete faults (including high angle and detachment faults).
- Models of ductile/non-linear deformation of the lithosphere at high temperature and high strain conditions (lower crust/upper mantle conditions).
- Models of interactive processes between large-scale lithospheric deformation and upper mantle convective flow; between crustal faulting and dike injection/propagation, and between faulting and magma chamber inflation/deflation.

The physics of crustal magma chamber, dike intrusion, and extrusive volcanic flows:

- Physical models of magma chamber - investigate the parameters that control the three-dimensional geometry and longevity of a magma chamber.
- Time-dependent thermal models that describe the behavior of an episodically existing magma chamber and the associated episodic mantle flow, melt migration, and dike injection.
- Three-dimensional models of dike injection vertically and laterally from a magma reservoir.
- Models that examine the relative importance of magma transport by flow in existing crustal channels and by dike propagation in unfractured crust.

Mechanisms of shallow crust cracking and fissuring:

- Three-dimensional models of thermal stress-induced cracks (dependence of crack geometry and spatial distribution on the stresses and material properties).
- Models that relate large-scale faulting and local cracking; topography-induced cracks.
- Models that relate crack geometry and effective porosity and permeability of the crust.

Mechanisms of mass wasting and sedimentation:

- Application of on-land land-slide theories to underwater mass wasting (stability analysis of fault scarps; shape and geometry of rockfalls; and the effects of mass wasting on modifying basement morphology).
- Dynamics of sedimentation (dependence on ocean currents; sediment supply; and sediment compaction).

The physics of crustal hydrothermal circulation and alternation:

- Three-dimensional porous flow models of hydrothermal circulation.
- Interaction of faulting and hydrothermal system (permeability due to faulting is highly anisotropic).
- Mechanisms of two-phase flow (in the high temperature boundary layer of a magma body).

- Models of hydrothermal circulation that output testable predictions of chemical and isotope alteration.

A6: Issues

From the keynote speakers and during the workshop, lists of questions emerged that well represent the myriad off problems we face in trying to understand the volcanic seafloor. This section will inevitably repeat some of the material contained elsewhere in this report but not to include its content would have the more serious consequence of omitting some succinct statements of the key issues.

- Key issues pertaining to the evolution with age of the seismic velocity of the uppermost sections of oceanic crust:
  - We cannot hope to understand the evolution of uppermost crust until we learn its basic architecture.
  - What are the relationships between upper crustal compressional and shear velocities and age?
  - How consistent are these relationships? Are there systematic differences between crust generated at different spreading centers?
  - What is the nature of the 2A/2B boundary and how does this evolve with age?
  - What processes are the primary controls on the evolution of seismic velocities?
  - If the key process is indeed a modification in crack and void geometry (rather than a change in total porosity), then how is this achieved? Is it tectonics, magmatics or geochemistry that is the primary control?
  - If it is indeed the cementation of loosely packed extrusives that is the first-order process, then which geochemical reactions control this and what environmental parameters determine the rate at which these alteration processes occur?
  - Does a correlation exist between seismic velocities and cracks and fissures observed on the seafloor?
  - What controls velocity anisotropy in the uppermost crust?
  - Does the degree of velocity anisotropy change with age? If so, what controls this?
  - Does a correlation exist between sediment cover and the velocity of the upper crust?
- Porosity
  - Basic Questions:

    What is the porosity structure of young crust and how does it affect seismic structure?
    How can we estimate the porosity structure from seismic measurements?
    How can we expect seismic structure to change with age or alteration history?
    How should we perform an actual seismic measurement?

- Needs:

  "Adequate" models relating seismic velocities to porosity.
  Direct observations of void density, shape, orientation (televiewer and FMS images; measurements from outcrops; laterolog).
  Geochemical models for how sealing proceeds.
  Geochemical ground truth: observations of crack sealing, hydrothermal deposition, vein formation (ophiolites, dredged and drilled rock, geochemical logs).

  Seismic measurements.

- Considerations for Seismic Experiments:

  To avoid confusion from lateral variability, use small experiments to 'see' below the scale of the variation.
  Anisotropy means the direction of energy propagation must be considered.
  Modeling already shows that complete identification of the porosity structure is impossible from compressional waves alone. Shear wave observations are essential.

- Downhole Measurements: Important problems and issues:

  - Scientific Issues

    How representative are single vertical sections?
    True measure of porosity and nature of porosity.
    Fracture assessment: orientation and extent.
    Alteration history from geochemical logs.
    Continuous vs. bulk measurements of permeability.
    Accurate shear wave logging.

  - Technical Problems

    Calibration of log responses in igneous crust.
    Technology for hole-to-hole experiments.
    Technology for long-term experiments.
    High-temperature instrumentation.

- Physical Properties

  - Key Questions:

    How does temperature affect shear velocities and V_P/V_S ratios in volcanics?
    How does pore pressure affect velocities at high temperature?
    Is the influence of pore pressure on velocities dependent upon crack aspect ratios as well as crack porosity?
    How does crack geometry relate to compressional wave anisotropy and shear wave splitting in cracked volcanic rocks?
    How can we separate the effects of porosity on physical properties from that of alteration products?
    Is Q characterized by mineralogy at high pressures rather than cracks and their saturation condition?
    Is there a Q-density relation similar to velocity-density relationships?

Is attenuation anisotropic in cracked volcanics?
Is an effective pressure law applicable for Q?
Are Q_p/Q_s ratios diagnostic of porosity?

- Significant observations needed:

  What is the spatial distribution of crustal cracks?
  How deep do these cracks penetrate into the crust?
  How does this large-scale cracking vary as a function of time?
  Are there observable correlations between cracking, heat flux, and crustal physical properties?

- Geological questions:

  How does crustal cracking control the thermal environment?
  Is fluid flux controlled by large- or small-scale permeability?
  What types of crustal alteration are occurring off-axis? Where?
  Is the crustal fluid circulation system open or closed? What horizontal scale?
  Is crustal cracking coherent on a local scale, or on a segment/ridge-wide scale?
  What are the relevant fluid/rock reactions, and the associated thermal environment during alteration?

- Towards relationships between chemical and physical properties

  - A key first step is to define chemical and mineralogical changes in the volcanic crust as a function of:

    Rock type - pillow, sheet flow, dike, glass, holocrystalline.
    Original composition - primitive tholeiite, differentiated, alkali.
    Topography - basement high, low.
    Sediment cover - type (calcareous ooze, pelagic clay, hydrothermal), thickness (0 to 400m).
    Time - progression, sequence and rate in zonations in rock.
    - distance from ridge axis.
    Temperature - mineral facies, assemblages, 0°-400°C.
    Water - rock ratio - high, low.
    Eh - oxidative, reductive.
    Depth in crust - 0 to 500m, and how composition, temperature, water-rock ratio etc. change with depth.

  - Then correlate these chemical and mineralogical changes with changes in physical properties of hand specimens.

    Density
    Porosity
    Magnetics
    Resistivity
    Conductivity

  - And finally, correlate changes in hand specimens with integrated field geophysical observations:

    Acoustic properties
    Magnetics
    Heat flow
    Downhole logging

- Acoustics of the upper crust (top 300m):
  - Geoacoustic Parameters

    Objectives: measure and learn how to predict:

    1st order

    Changes in compressional (V_p) and shear (V_s) velocity versus age and sediment thickness.

    2nd order

    V_p (θ, Z); V_s (θ) anisotropy versus age and sediment thickness.

    ΔV_p; ΔV_s variability versus age and sediment thickness.

    L (V_p); L (V_s) correlation length versus age and sediment thickness.

    α_p; α_s attention coefficients versus age and sediment thickness.

    RMS (θ) boundary RMS roughness versus age and spreading rate.

    L (θ) boundary correlation length versus age and spreading rate.

    ϕ RMS boundary RMS slope versus age and spreading rate.

  - Geoacoustic provinces:

    1st order

    Normal crust, sediment thickness <100m (majority of Pacific).

    2nd order

    Normal crust, 100m < sediment thickness <200m
    Seamounts
    Mid-Ocean Ridges
    Fracture Zones
    Subduction Zones

    3rd order

    Normal crust sediment thickness >200m.

A7: Towards an Integrated Plan

The scope of the problems described in the previous sections is extremely broad: it is unrealistic to attempt to compress the wide-ranging recommendations into a succinct summary statement. However, common themes have emerged and high priority objectives

have been recognized that must be achieved before a thorough understanding is possible of how the upper oceanic crust evolves. It is clear that the processes we are studying are controlled by a multiplicity of variables. It is clear that the temporal and spatial scales upon which changes occur in the upper crust vary from thousands to tens of millions of years, and from millimeters to hundreds of kilometers.

Thus the research plan must be exceptionally systematic in its approach to these problems in order to prevent the waste of resources on fruitless research directions. It is for this reason that the conventional 'flow-line corridor' approach, that is espoused throughout this document, is valid; and it is for this reason that the large volumes of background data, that define the controls on the evolutionary processes that determine the velocities and physical properties, are essential.

The first order recommendation is to identify two corridors, one on the East Pacific Rise the other on the Mid-Atlantic Ridge, within which data collection efforts will be focussed. The along-axis extent of these corridors should be 50-100 km and they should extend onto ~20 my crust. Wide ranging programs to collect the background regional data within these corridors should be encouraged and initiated as soon as possible. Within these evolutionary corridors approximately five intelligently distributed ~10 kilometer square detailed survey areas should be identified and high resolution seismic and other geophysical data should be collected, along with seafloor video and acoustic imaging. On the basis of these detailed surveys, *pairs* of drill holes should be located within each of the areas: the hole separations should be determined by our evolving understanding of the important scales of lateral variability. In addition, in both the Atlantic and Pacific oceans, scarps that constitute 'windows' into the crust and provide unparalleled views of the lateral continuity of basic structures, should be identified and subjected to comparable detailed studies; a drilling program should be designed to provide a truly three dimensional view of the structures observable in two dimensions on the scarp and to provide key samples for laboratory investigations of possible heterogeneity in physical properties.

The large and diverse data sets generated by this ambitious program should be used to:

- determine and contrast the architectures of Atlantic and Pacific crust and define the processes that control the differences and influence the variability.

- establish robust correlations between the geological architecture and the compressional and shear wave velocity structure and the magnitude and nature of the porosity.

- fully define the systematic evolutionary changes in the physical properties of the upper crust and identify correlations with key parameters (topography, sediment cover, etc.).

- identify the nature and timescales of the alteration processes and understand the linkages between these processes and the evolving physical properties of the crust.

- quantify the controls that determine the nature and timing of the key alteration phenomena.

These objectives can only be accomplished if substantial advances in modeling capabilities are made, thus allowing the researcher to integrate these diverse observations into a coherent picture of how the various processes interact to produce such apparently systematic changes in physical properties.

The magnitude of the effort embodied in the above recommendations is sufficiently large that some priorities must be set. Below we identify three primary areas, and two secondary areas upon which we believe effort should be focussed at the earliest opportunity.

- Determination of the fundamental architecture of the upper oceanic crust: this most fundamental of objectives must take precedence over other efforts. The key unknowns have been detailed elsewhere in this report, but the highest priority must be given to the determination of the nature of the surficial low velocity layer, and of its lowermost boundary. Two programs can be described that would most effectively provide substantial progress towards this goal. Firstly a combined detailed survey/seismics/drilling program on young (0-1 my) Pacific crust, that would for the first time combine a pair of drill holes through the uppermost crust (and associated downhole experiments) with a three dimensional seismic image of the crust from a careful on-bottom source and receiver tomography experiment, and a comprehensive suite of near bottom geophysical and sampling data. And secondly, a coordinated geophysical and drilling program focussed (again on Pacific crust) on a scarp exposure of a substantial section of the upper crust: from this an unparalleled view of structural heterogeneity in three dimensions can be obtained and unique opportunities are presented for innovative on-bottom to downhole experiment geometries that could provide unequivocal ground truth measurements of geophysical properties.

- Alteration and Variability: this program also has two components: a detailed survey area (~10 km square) on 20 my old Pacific crust must be chosen within which a *pair* of drill holes through the upper crust (with as close to total recovery as possible) will provide the baseline data (when compared with the results from the younger drill hole results described above) in studies of alteration, cementation and secondary mineral deposition. Again, an on-bottom seismic tomography experiment should fully characterize the three dimensional structure around the holes. And secondly, spot seismic velocity measurements should be made along the flow line between the young and this 20 my site to unequivocally establish one example of how the velocity of the uppermost 100m evolves with age.

- Modeling: complex interactions between widely varying processes (e.g., alteration to fluid flow to permeability to faulting) must be understood and quantified if our objectives are to be achieved. This is only feasible if substantially more effort is directed towards the development and construction of careful models that adequately describe the primary evolutionary processes. There are many steps between the cementation of grains within a basaltic breccia and seismic velocity: these can only be understood quantitatively via the insights yielded by good physical models.

Two secondary areas worthy of special attention are as follows:

- Electromagnetic methods (and their integration with seismic results): improved ways of making remote estimates of upper crustal porosity are desperately needed. Recent developments in deep tow active electromagnetic sounding show great promise by providing a completely independent (though admittedly still ambiguous) estimate of porosity. However when combined with seismic results perhaps meaningful constraints can be produced.

- Structural variability of the Atlantic seafloor: the profound heterogeneity that would ensue from the widespread presence of tectonically emplaced lower crustal rocks on the seafloor in the Atlantic would dominate the variability in physical properties to such a degree, and in such a complex manner, that the existence/non-existence of this phenomena must be established at the earliest opportunity. A comprehensive geological map of one segment of the Mid-Atlantic ridge must be produced and a supporting program of earthquake monitoring to map and characterize all the active faulting must be carried out.

Section B: Keynote Papers

1: Processes

2: Geophysical Measurements

3: Physical Properties

Section B1: Processes

1: Seawater-Rock Interaction: G. Thompson

2: Volcanic Processes: R. Batiza

3: Tectonic Regulation of the Physical Properties of the Sea Floor: The View from the Juan de Fuca Ridge: P. Johnson

SEAWATER-ROCK INTERACTION

Geoffrey Thompson
Woods Hole Oceanographic Institution

The volcanic seafloor, once formed, undergoes progressive changes in physical, chemical and mineralogical properties due to interaction with seawater. This ageing process, or crustal evolution, is the key to interpreting the geophysical surveys we routinely make over the ocean floor.

1. Effects

Seawater-rock interactions influence:

(a) *Acoustic Properties*

Compressional wave velocities are directly influenced by the density of the substrate. Seawater-rock interactions reduce the density of the rocks.

(b) *Magnetic Properties*

The Ti-Fe rich minerals that control magnetism undergo oxidation and break-down during seawater-rock interactions; the initial high remanent magnetization and susceptibility gradually decrease, and the Curie temperature changes.

(c) *Porosity*

Cracks, pores and voids in the rock are progressively infilled by precipitation of new minerals produced as a result of seawater-rock interaction.

(d) *Heat Flow*

Observations and measurements of heat flow are directly affected by seawater circulation in the volcanic crust which efficiently extracts heat from the basaltic lavas. Downflow and upflow zones of circulating hydrothermal cells can be pinpointed from heat flow distributions.

(e) *Chemical Composition*

Exchange of ions between seawater and the volcanic rocks takes place resulting in chemical fluxes that may influence controls on seawater composition, and produce an oceanic crust compositionally different from the original precursor.

(f) *Mineralogy*

Seawater-rock interactions produce a variety of new minerals, often hydrated, generally less dense than the originals, and with different mechanical and physical properties.

Fig. 1. Summary of observed chemical gains and losses from basaltic rock during seawater reactions at different temperatures. Species in perentheses do not always show the loss or gain as indicated and are probably dependent on other parameters such as oxidation, rock-water ratio, presence of sulphides or other phases.

CHEMICAL EXCHANGE

Low Temperature
(< 100°C)

Rock Gains		Rock Losses	
H_2O		Si	
K		Ca	
P		Mg	
Mn		(Na)	
(Fe)			
B	U	(Sr)	
Li	Cu		
Rb	Zn		
Cs	LREE		
	(Ba)		

High Temperature
(> 150°C)

H_2O		Si	
Mg		Ca	
(S)		K	
		Mn	
		(Fe)	
		B	Sr
		Li	(Cu)
		Rb	(Ni)
		Cs	(Zn)
		Ba	(U)

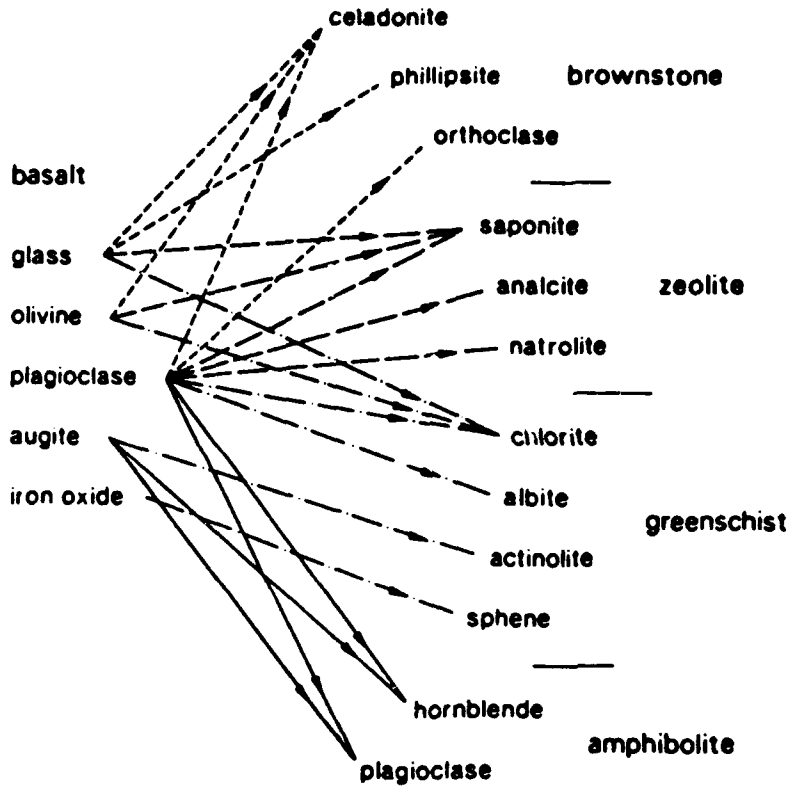

Fig. 2. Metamorphic facies and congruent mineral reactions for basalt-seawater reactions over a range of temperatures (from Cann, 1979).

2. Controls

The extent and rate of seawater-rock interactions are controlled by:

(a) *Solution Circulation*

The amount of seawater seen by the rock, the water-rock ratio, is primarily a function of the permeability. This latter property is controlled by the morphology of the individual rock and the type of geological formation.

(b) *Temperature of Reaction*

In general the higher the temperature, the faster and greater the extent of reaction. However, as the temperature increases so does the direction of the reaction for some elements, i.e., some elements are added to the rock from seawater at low temperature but may be leached from the rock at higher temperature. The minerals formed and precipitated from seawater-rock interactions change as the temperature increases and thus the physical properties of the resulting rock.

3. Observations

We have some observations and measurements with regard to the alteration of the oceanic crust but we lack good quantification of the effects and direct correlations between extent of alteration and physical properties. One of the aims of this workshop is to define how we might systematically define and measure such a relationship. Some of the effects of seawater rock interactions that we do know include:

(a) *Effects on Composition*

In general, seawater-rock interaction (seawater-basalt in this particular case) result in a net exchange of ions dependent on temperature. Figure 1 summarizes our knowledge. Low temperatures are generally at bottom water temperatures but include reactions up to about 70°C. High temperature reactions include those from 100° to 400°C.

(b) *Effects on Mineralogy*

Variable new mineral assemblages are produced as the temperature of interaction increases Figure 2 shows typical facies and assemblages that may define the degree of metamorphism. Present observations indicate that brownstone and greenstone assemblages dominate in the upper oceanic crust. Low temperature assemblages are ubiquitous and probably play a dominant role in defining the physical properties. High temperature reactions take place deep in the crust, 1-2 kms generally. They are only found in the upper levels in the upflow zones of high temperature hydrothermal cells, or when tectonics may expose deeper levels through faulting.

Some of the complexities and variables that control the effects of seawater-rock interaction have been summarized by such workers as Honnorez (1981), Thompson (1983, 1984), Honnorez *et al.* (1985), Alt *et al.* (1986), Gillis and Robinson (1990), and references therein. Major differences appear to be observed as a function of depth in the seafloor:

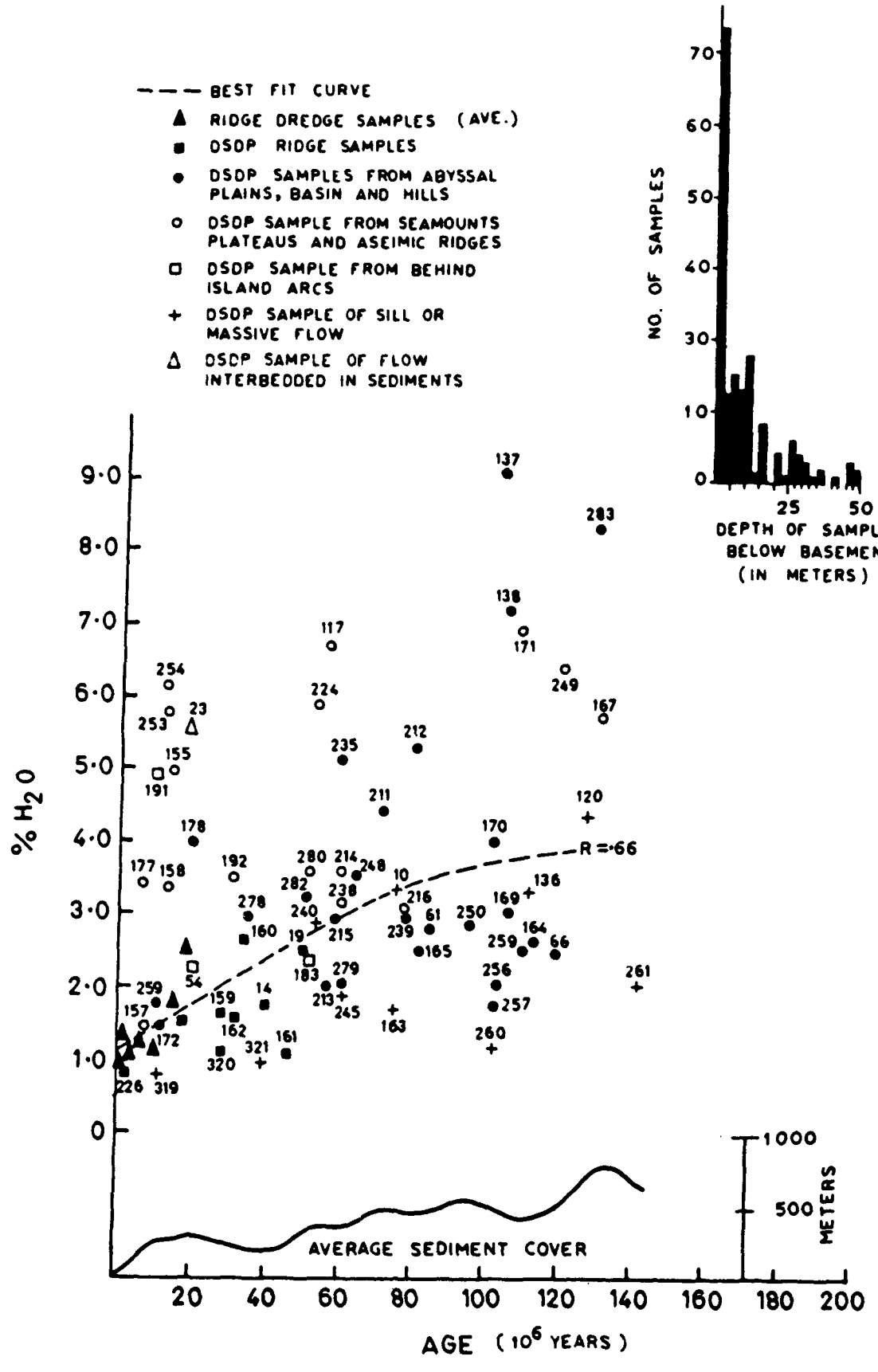

Fig. 3. Average H_2O contents of basalts from DSDP basement sites as a function of age (from Hart, 1976). Most of these sites are shallow (less than 10m penetration) and continue to show water for over 100 million years.

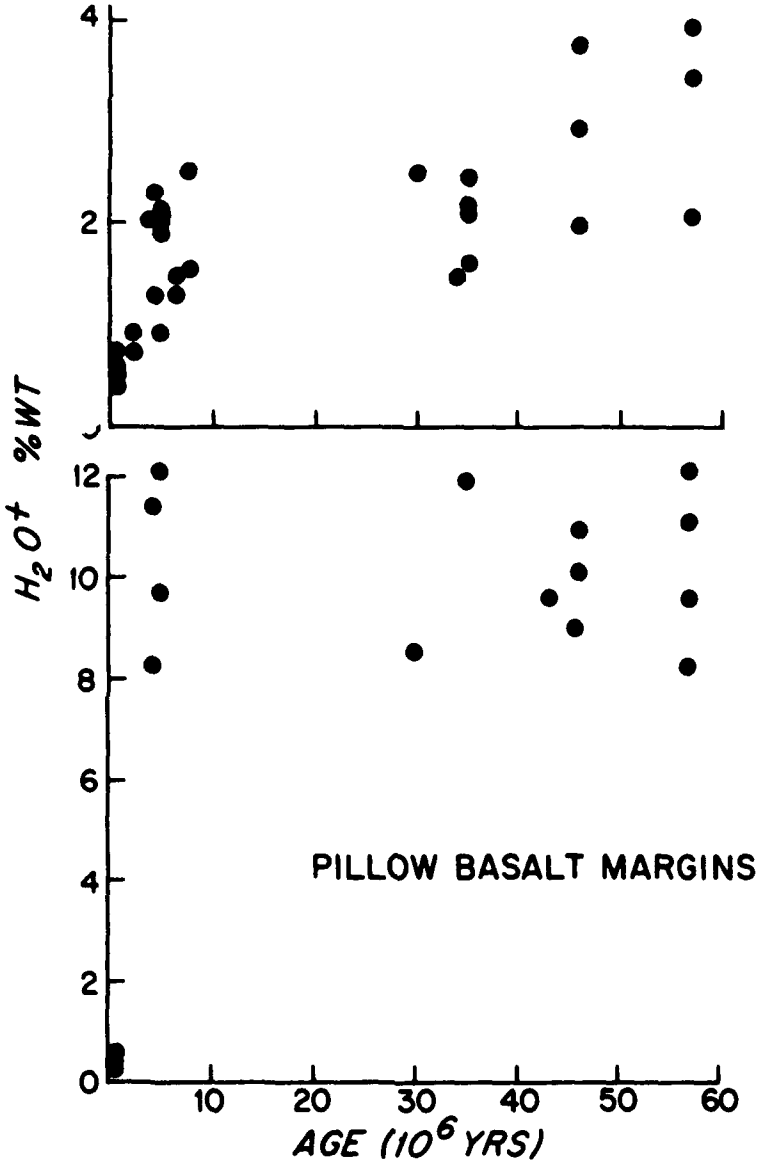

Fig. 4. Variation in composition of pillow interiors and margins as a function of age (from Thompson et al., in preparation). (A) H_2O vs. age for interiors and margins.

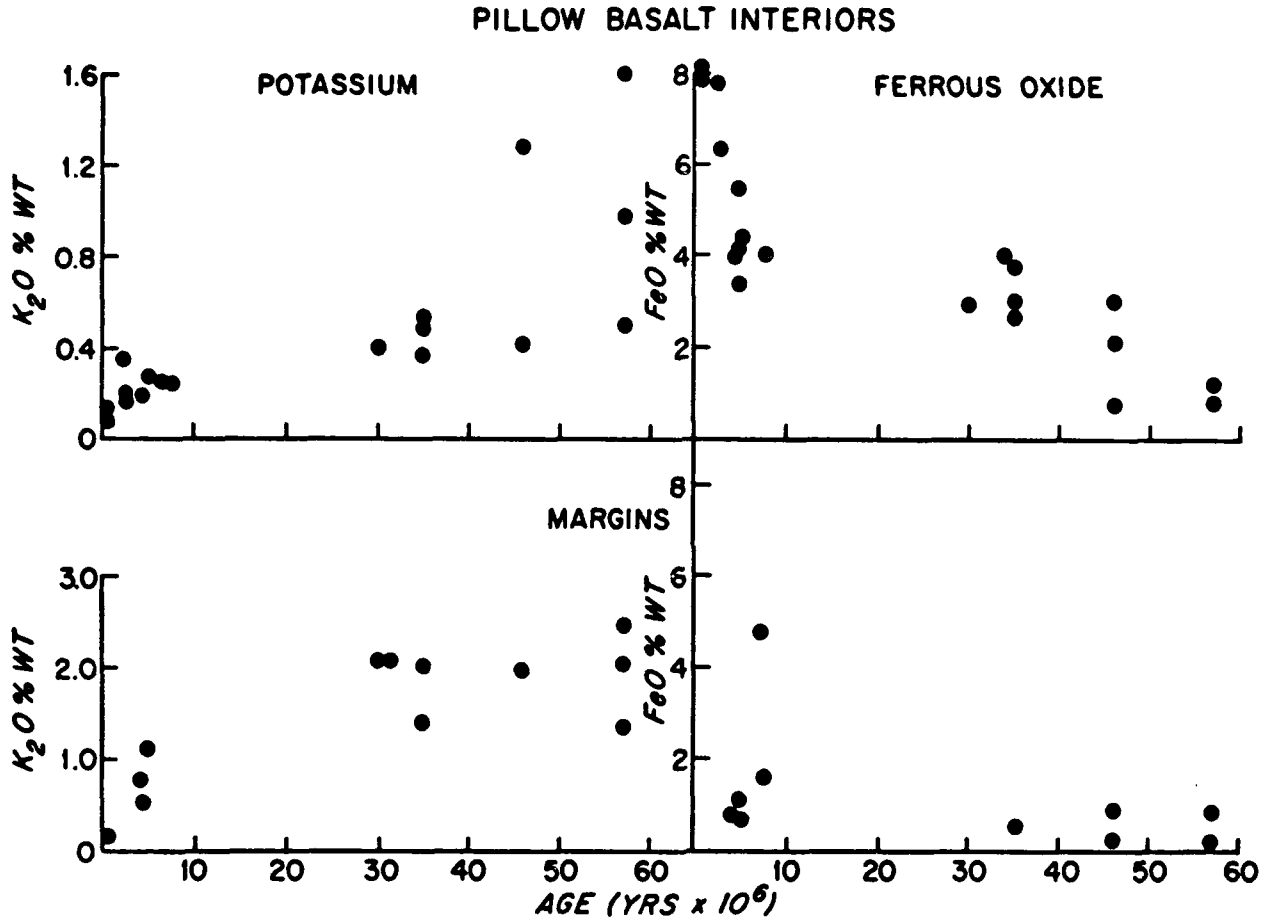

Fig. 5. . Variation in composition of pillow interiors and margins as a function of age (from Thompson et al., in preparation). (B) K_2O and FeO vs. age for interiors and margins. Note that the pillow interiors continue to show increases in H_2O and K_2O, and oxidation of ferrous iron for over 60×10^6 years; the pillow margins rapidly oxidize and hydrate in less than 10×10^6 years, and potassium uptake is very rapid also.

(i) *Upper Oceanic Crust*

Generally the alteration of the upper few tens of meters of the volcanic layer is controlled by low temperature and high water to rock ratios. The depth and extent of weathering is a function of permeability in the geologic formation and the individual rock morphology, and the duration of the reaction. Observations are based primarily on dredged rock specimens and from the upper sections of drill cores from the Ocean Drilling Program. The reaction appears to be progressive with time, possibly up to 80-100 x 10^6 years. Figure 3 shows data for H_2O contents of upper level rocks from Hart (1976). In the early 1970's we did an experiment to evaluate some of these time-related effects by doing a series of dredge hauls from the axis to the flanks of the ridge at 23°N in the Atlantic that covered about 1000 km or nearly 60 x 10^6 years. Based principally on pillow basalt observations, the most common form of volcanic morphology in the shallow upper levels of the crust, the results indicated that the extent of alteration increased with time and as a function of the original mineralogy. Figures 4 and 5 show differences in the contents of a number of components — H_2O, K, and Fe oxidation — for both the glassy margins and the crystalline interiors of pillows. These diagrams summarize the bulk effects — the glass is quickly altered and then remains relatively constant, the interiors progressively alter through 60 x 10^6 years. Typically in any given specimen the extent of alteration is variable and concentric zones of discoloration are observed parallel to exposed surfaces, joints, or cracks, with each zone varying in composition and mineralogy. The sequence of chemical changes and mineralogical effects for palagonitization are well documented (e.g., Honnorez, 1981) but the sequences, rates or degrees of alteration in the interiors is less well documented or quantified. The degree of oxidation, or Eh, of the local environment is clearly a variable that can result in differing chemistries and mineralogy. Non-oxidative alteration can produce Fe-sulfides such as pyrite or marcasite as well as clay minerals with differing Fe/Mg contents compared to oxidative conditions. Criteria for documenting the extent of alteration, e.g., K, H_2O gains, Fe oxidation, Si and Ca losses, change in Sr and O_2 isotopes, change in magnetic properties, are variable in rate and extent for any single component and have not been closely correlated with each other, zonation or other bulk physical properties.

ii) *Lower Oceanic Crust*

Deeper portions of the volcanic crust, up to a few hundred meters, as observed in drill cores also show variable alteration, although generally to a lesser extent and different to that of the upper portion. They are probably more typical of low temperature, low water-rock ratios. There is much more unaltered material, although extensive alteration around fissures or joints attest to water-rock interactions continuing to great depths. Non-oxidative alteration is more common than in the upper levels. The extent of chemical exchange is generally much less (in terms of mass fluxes). Mineralogically blue-gray Fe-rich smectites, sulfides, phyllosilicates such as celadonite and saponite are more common than in the upper portions. Also in both oxidative and non-oxidative zones carbonates (calcite and aragonite) are much more common. In the upper levels such minerals are rare. Progression of alteration with time is much less definitive. Studies of vein mineralogies (Hart and Staudigel, 1978) and geochronology suggest that much of the alteration takes place within 3 x 10^6 years after formation, carbonate deposition may continue and minor alteration to 10 x 10^6 years then very little changes are observed after that period as the lower portions of the volcanic pile are effectively

sealed from further seawater penetration due to sediment cover and infilling of local porosity by secondary minerals.

iii) *Other Effects*

There is some evidence, not well quantified, that the depth and extent of alteration may be a function of local topography — basement highs are generally more altered than basement lows. This has been confirmed by extensive studies of the low temperature alteration of the Troodos ophiolite by Gillis (1990). The extent and type of basement cover inhibits water penetration and further alteration, although again this is not well quantified. Locally, volcanics exposed at the sea surface typically become covered with ferromanganese precipitates which increase in thickness with time. Only in long exposed regions, such as seamounts, does this cover become sufficiently thick, tens of cm, to inhibit circulation or change the bulk physical properties. In some regions, particularly where local upwelling of hydrothermal solutions may occur, manganese oxides and clay minerals such as montmorillonite and nontronite may occur in sufficient thicknesses and extent to also inhibit water penetration and to locally absorb sound of certain wavelengths.

Temperature of interaction strongly affects the degree and extent of alteration. Figure 6 from DSDP holes 417A and B shows a marked change in alteration (exemplified by K content, but true for many other components, and the mineralogy and physical properties) for two sites within a few hundred meters. In one case we believe warm waters of 30°C (part of a circulation cell funnelled to a topographic high), reacted with that particular region some 2 to 3 million years after crustal formation. How typical such regions are of the oceanic crust is not clear.

DSDP hole 5048 on the Costa Rica Rift is the deepest and one of the better studied drill holes in the crust. Here the evidence demonstrates that the crustal section has seen a variety of solutions and temperatures of reaction as it moved away from the ridge axis. These varying stages of alteration and temperature produced a sequence of mineral assemblages that can be related to temperature, and subsequent changes in chemical composition. This study is well documented by Alt *et al.* (1986) and points to the complexity and painstaking detailed work required to interpret the subsequent effects of alteration.

Very high temperature alteration, 200°-400°C produces metamorphic mineral assemblages. Chemically the basalts lose alkali metals, Si and Ca, but gain Mg and other metals. Although these reactions typically take place 1-2 km depth in the volcanic pile, they may locally be exposed in the upper zone where upflow zones of high temperature fluids penetrate. Tectonic displacements may also result in local outcropping of greenstones on the ridge flanks or median valley walls. How extensive such exposures may be is unknown. Their mineralogy (Fig. 7) and composition (Fig. 1) produce very different physical properties for the crust.

4. Objectives

Our principal objective is to systematically evaluate and quantify the effects of alteration on the physical properties of the oceanic crust. Because of the many variables that control alteration, this requires an integrated approach that combines a study of morphology, mineralogy, and chemistry of an extensive section of seafloor combined with geophysical measurements.

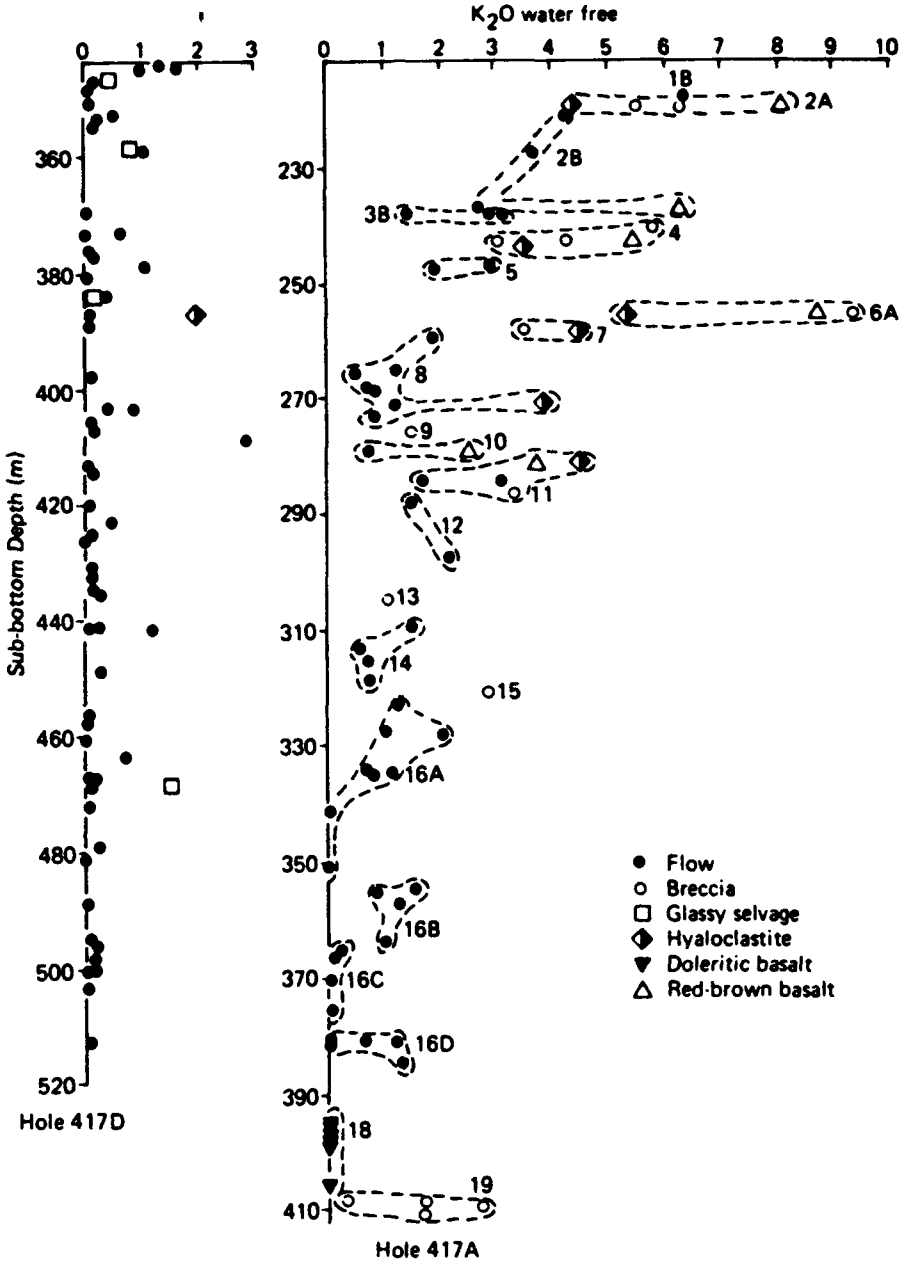

Figure 6. *Weight per cent K_2O, calculated on a water-free basis, versus depth in Holes 417A and 417D. The tops of the basalt have been matched in position. Lithologic units, as defined in the Site 417 Report (this volume), are circles where more than one sample is given, and identified by italicized number. "Doleritic basalt" refers to massive basalt of Unit 18.*

Fig 7. Metamorphic facies and reported minerals observed in each facies

Facies	Mineralogy
Halmyrolysis	Celadonite, phillipsite, palagonite, saponite, montmorillonite, nontronite, Fe-Mn hydroxide orthoclase
Zeolite	Analcite, stilbite, heulandite, natrolite-mesolite-scolectite, chlorite-smectite, saponite
Prehnite-pumpellyite	Prehnite, chlorite, calcite, laumontite, epidote
Greenschist	Albite, actinolite, chlorite, epidote, quartz, sphene, hornblende, tremolite, talc, magnetite, nontronite
Amphibolite	Hornblende, plagioclase, actinolite, leucoxene, quartz, chlorite, apatite, biotite, epidote, magnetite, sphene

(a) Define Chemical and Mineralogical changes in the volcanic crust as a function of:

a.	*Rock type*	— pillow, sheet flow, dike, glass, olocrystalline.
b.	*Original composition*	— primitive tholeiite, differentiated, alkali.
c.	*Topography*	— basement high, low.
d.	*Sediment cover*	— type (calcareous ooze, pelagic clay, hydrothermal).
		— thickness (0 to 400m).
e.	*Time*	— progression, sequence and rate in zonations in rock.
		— distance from ridge axis.
f.	*Temperature*	— mineral facies assemblages, 0°-400°C.
g.	*Water-rock ratio*	— high, low.
h.	*Eh*	— oxidative, reductive.
i.	*Depth in crust*	— 0 to 500m, how variables a-h change with depth.

(b) Correlate chemical and mineralogical changes with changes in Physical Properties of hand specimen:

a. Density
b. Porosity
c. Magnetics
d. Resistivity
e. Conductivity

(c) Correlate changes in hand specimens with Integrated field Geophysical Observations:

a. Acoustics
b. Magnetics
c. Heat flow
d. Down hole logging

5. Achievement of Objectives

(a) *Field Experiment*

i. Select a transect from ridge axis to flank, 2-5 km wide, 100-200 km long.
ii. Survey with seabeam and sidescan sonar (for topography and morphology).
iii. Measure acoustic properties (various wavelengths, to define sediment thickness, density, local reflections, etc.).
iv. Measure magnetic properties (preferably near seabottom so local effects are well measured and observed).
v. Measure heat flow (to define circulation cells, upflow and downflow zones).
vi. Photograph (to define nature and extent of volcanic outcrops, local hydrothermal precipitation, type of sediment cover).
vii. Recover rock samples at intervals along segment based on results of i-vi surveys. Exposed, *in situ*, samples can be recovered by ROV or submersible. Closely spaced shallow drill samples (10-20m), using new

technology, sited as a function of changes in physical properties, observations, and variable morphology and topography. Finally, deep drill samples (100-200m) at selected intervals based on all previous measurements and recoveries.

viii. Down hole logging of drill sites to measure bulk physical properties — density, porosity, etc.

(b) *Laboratory Measurements*

i. Recovered rocks systematically studied and measurements made, in detail, on same selected subsamples.
ii. Mineralogy — petrography, diffraction, microprobe analyses.
iii. Chemical composition — bulk samples, alteration zones, vein mineralogies. Include H_2O, Fe oxidation, alkalis (K, Na, Li, Rb, Cs) alkaline earths (Ca, Ma, Sr, Ba), metals (Fe, Mn, Ti, Ni, Co, Cr, V), other elements (e.g., B, Y, Zr, REE), transuranics (U, Th, Pb), isotopes (O_2, S, B, Pb).
iv. Geochronology — U/Th, Rb/Sr, ^{14}C, etc.
v. Temperature — C, O_2 isotopes.
vi. All measurements to be correlated with each other and with the various physical properties from integrated field surveys and down hole measurements. Where feasible and meaningful, the physical properties of individual samples should also be measured.

References

Alt, J.C., J. Honnorez, C. Laverne and R. Emmerman, 1986. Hydrothermal alteration of a 1 km section through the upper oceanic crust, DSDP Hole 504B: mineralogy, chemistry and evolution of seawater-basalt interactions. *J. Geophys. Res., 91*: 10309-10335.

Gillis, K.M. and P.T. Robinson, 1990. Patterns and processes of alteration in the lavas and dykes of the Troodos Ophiolite, Cyprus. *J. Geophys. Res.*, in press.

Hart, R.A., 1976. Progressive alteration of the oceanic crust. In: *Initial Repts. D.S.D.P. Leg 34, vol. 34, pp. 433-437.*

Hart, S.R. and H. Staudigel, 1978. Oceanic crust age of hydrothermal alteration. *Geophys. Res. Letters, 5*: 1009-1012.

Honnorez, J., 1981. The aging of the oceanic crust at low temperature. In: *The Oceanic Lithosphere*, (E. Emilioni, ed.), vol. 7, pp. 525-587.

Honnorez, J., C. Laverne, H.W. Hubberten, R. Emmerman and K.Muehlenbacks, 1985. Alteration processes in layer 2 basalts from DSDP Hole 504B, Costa Rica Rift. In: *Initial Reports of DSD, vol. LXIX*, pp.509-546.

Thompson, G., 1983. Hydrothermal fluxes in the ocean. In: *Chemical Oceanography* (J. Riley, ed.), vol. 8, pp. 271-337.

Thompson, G., 1984. Basalt-seawater interaction. In: *Hydrothermal Processes at Sea-floor Spreading Centers* (P.A. Rona et al.), pp. 225-278.

VOLCANIC PROCESSES

Rodey Batiza
Hawaii Institute of Geophysics, University of Hawaii,
2525 Correa Road, Honolulu, HI 96822

Construction of the upper oceanic crust is largely due to primary volcanic processes. Thus understanding the causes of its characteristic internal structure, physical properties and heterogeneity requires insight into the fundamental factors that control melt supply, melt migration, the formation and behavior of magma chambers, dike intrusion and volcanic eruptions. Variations in the nature and rates of these processes exert a strong control on the thickness of the oceanic crust and such variations may occur on a variety of geographic length scales (e.g., intra segment, regional) and time scales. Volcanic processes result in earthquakes and inflation/deflation of active mid-ocean ridges and probably are causally related to faulting, fissuring and hydrothermal processes, which also profoundly influence the architecture and physical properties of the volcanic ocean crust. In this brief paper, I first quickly review what is known about the factors that control each volcanic process. Then I discuss possible approaches to obtaining further knowledge about each process and the key experiments, observations, measurements or modeling studies that are needed to do so.

Melt Supply: The process of melting upper mantle periodotites to form MORB magma may be very complex in detail, however many of the fundamental controls on melting are reasonably well understood. The initial temperature of the mantle material that upwells beneath active mid-ocean ridges controls the depth of initial melting (e.g., Verhoogen, 1973; Yoder, 1976; McKenzie, 1984). At mid-ocean ridges, melting probably begins at depths of 60-80 km (Figs. 1 and 2), though this is controversial. The depth of initial melting may vary, leading eventually to differences in crustal thickness (McKenzie, 1984; Dick and Fisher, 1984; Michael and Bonatti, 1985; Klein and Langmuir, 1987). The thermal structure of the upper mantle and the mantle upwelling rate control the amount of heat loss from the upwelling and thus also affect the total amount of melt that can be produced (crustal thickness).

The along-axis shape and cross-axis width of the upwelling control the initial amount and distribution of melt. The along-axis shape can be partly constrained by petrologic and geophysical studies (e.g., Macdonald, 1989; Langmuir et al., 1986; Lin et al., 1990; Batiza et al., 1988) and studies of ophiolites (e.g., Rabinowicz et al., 1987). Theoretical and modeling studies also provide additional constraints (e.g., Schouten et al., 1985). The cross-axis width of the upwelling has been considered in numerous theoretical studies (e.g., Scott and Stevenson, 1989; Sleep, 1988; Phipps-Morgan, 1987) and can be constrained partly by the chemistry of zero-age near-axis seamount lavas (Fig. 3; Batiza et al., 1990a) and U-Th disequilibrium studies (McKenzie, 1985a).

Melt Migration: In order to erupt, melt produced in the mantle must obviously migrate upward. At the same time, melt may also migrate laterally, which could produce crustal thickness variations that might not be readily inferred from the initial mantle melt distribution alone. The mode and rate of melt migration relative to the solid residue of melting and its eventual segregation from this residue depend upon a large number of factors, many of which are only poorly known. These include: melt buoyancy, the rheological properties of partly molten mantle, the viscosities of melt and partly molten mantle, the stress state and other factors. At depth, melt migration is probably by porous flow (e.g., McKenzie, 1984, 1985b; Phipps-Morgan, 1987; Speigelman and McKenzie, 1987; Ahearn and Turcotte, 1979) however at appropriate condition, formation of melt veins and dikes leads to rapid

segregation and melt transport upward and perhaps laterally (e.g., Sleep, 1988; Nicolas, 1986). The efficiency of melt migration and extraction is an important issue, as it affects the magma budget for on and off-axis eruptions.

Melt Storage: Since upward melt transport is thought to be driven primarily by the buoyancy of the melt, when the melt reaches a level of neutral buoyancy in the crust, it may pool in magma chambers (Ryan, 1987). Since the density of MORB melt is a strong function of composition (e.g., Sparks and Huppert, 1984), the depth of ponding is partly a function of melt composition. In addition, of course, the density structure of the crust also controls the depth of magma chambers and may influence their shape. The rates of resupply and emptying of the chamber, its size and shape, and internal dynamic processes are all important because they affect the thermo-mechanical properties of the material surrounding the chamber. In turn, these characteristics, through feedback mechanisms, may affect not only volcanic processes, but also tectonic activity and hydrothermal processes. Whether chambers are sill-like, dike-like or equant in shape, they may migrate laterally, leading eventually to variations in crustal thickness. Such migration could result from swelling during resupply, or interactive dynamic changes in mass and density distribution in the lid of the chamber.

Dike Intrusion: Dike intrusion in rift zones is a relatively well-studied and understood process (Figs. 4-6; e.g., Walker, 1987; Knight and Walker, 1988; Rubin and Pollard, 1987; Rubin, 1990). Where studied in detail, flow of magma in dikes is seldom exactly vertical or horizontal, providing additional support for the concept of blade-like dikes emanating outward and upward along the axis of rifting. The main controls on the propagation of such dikes are the vertical and lateral magma pressure gradients (partly determined by the density distribution of the shallow crust) and the ambient state of stress in the crust. Laminar flow velocity of magma in dike is controlled by the magma pressure gradient, the viscosity of the magma and the thickness of the dike. If magma pressure is sufficiently high, magma moving in dikes will erupt at the surface. Otherwise, the dike will simply be emplaced at depth.

Volcanic Eruptions: Deep-sea photography, submersible observations and other techniques have provided a wealth of observational data on the variety and types of submarine eruptive products (e.g., Ballard et al., 1979; Ballard and Moore, 1977; Francheteau et al., 1979; Lonsdale and Spiess, 1980). However very few studies have been systematic and as a result, the physical volcanology of deep-sea eruptions (vs. subaerial ones, Fig. 7) is very poorly understood. Bonatti and Harrison (1988) discuss the role of thermo-elastic stresses in submarine lava flows and the effect of magma temperature, viscosity and discharge rate. Additional important controls on the style (and thus primary porosity) of submarine MORB eruptions are conduit geometry, eruption velocity (Fig. 8), topography, rate of shear during flow and others (e.g., Smith and Batiza, 1989; Batiza et al., 1990b; Wohletz, 1986; Moore, 1975; Peterson and Tilling, 1980). The discharge rate, duration of eruptions, style of eruption and topography will determine the size and shape of basaltic lava flows, neither of which are presently known. It is to be expected, however, that these characteristics would exert a control of the extent and scales of lateral heterogeneity of the volcanic portion of the ocean crust. Of additional interest are the questions of eruption frequency and the nature of eruption trigger mechanisms at ridge crests.

Scientific Objectives: From the foregoing very brief review, it is clear that many fundamental controls on the volcanic processes that build the ocean crust remain poorly understood. The great progress that has been made in understanding the behavior of Hawaiian and Icelandic rifts, indicates that understanding how mid-ocean ridge volcanoes work is a realistic scientific objective. In fact, studies of subaerial rifts can provide valuable guidelines and hypotheses that can be tested at mid-ocean ridge axes. Of fundamental importance is determining the interplay of magmatic, tectonic and hydrothermal processes and how these vary spatially and temporally. Establishing the actual patterns of crustal

thickness variations in the vicinity of active mid-ocean ridges would provide very important clues. However this information alone does not necessarily constrain deeper volcanic processes because magma is capable of moving laterally as well as vertically. In order to make progress, it is possible to identify several scientific objectives which, if met, would provide valuable constraints on the processes discussed previously. Some of these are (not in priority order):

1.) Define the geometry of mantle upflow in three dimensions.

2.) Determine the three-dimensional patterns of crustal thickness variations on zero age and older crust.

3.) Determine the density structure of volcanic sea-floor.

4.) Map the distribution, size and shape of sub-axial magma chambers.

5.) Determine the state of stress of young volcanic crust.

6.) Determine, if possible, the average dike width in ocean crust.

7) Determine the shape and volume of individual submarine lava flows.

8.) Determine the fundamental controls on eruptive style and flow morphology of submarine eruption products.

9.) Determine the scales of heterogeneity in volcanic ocean crust.

Key Measurements, Observations and Modeling Studies: Successfully completing work on this ambitious list of scientific goals clearly will require much effort, time and resources. However because actual measurements may address more than one goal, a great deal of progress may be possible with a few key programs. Below is a partial, unprioritized list of measurements, experiments, etc. and the processes which they will shed light on, directly and indirectly.

Volcanic Processes

Observations/Measurements:

1.) density structure of volcanic crust - zero age and off-axis

   a.) within a spreading segment
   b.) at several spreading rates
   (direct bearing on magma migration and eruption dynamics)

2.) geodetic (x,y,z) measurements at active ridge crests
   (to determine inflation, deflation and correlation with eruptive/intrusive activity - direct bearing on magma migration, supply and emptying of chambers and stress state)

3.) seismologic monitoring of active ridge crests
(same as 2, plus important information on tectonic processes)

4.) measure in-situ stresses at active ridge axes and off-axis
(bears directly on the nature of magmatic-tectonic interactions and dynamics of dike intrusion)

5.) systematic measurements of flow morphology and volumes
(bears directly on magma pressure, eruption dynamics and magma budgets)

6.) systematic studies of zero-age seamounts lavas
(constrains deep thermal regime and width of mantle upflow zone)

7.) systematic dating--petrologic studies along flow lines
(constrains internal dynamic processes, resupply and emptying frequency of magma chambers)

8.) systematic and detailed studies of petrology-age of "zero age" along-axis flows
(constrains the three-dimension upwelling geometry and indirectly constrains other processes).

Modeling and Laboratory Studies:

1.) theoretical modeling studies of thermal structure, stress distribution and melting beneath active mid-ocean ridges - especially dynamic, three-dimensional studies incorporating temporal variation

2.) measurements of viscosity and rheological properties of melt-solid mushes

3.) measurements of melt geometry (at micro scale) in partly melted peridotite under conditions of non-hydrostatic stress

4.) measurements of melt permeability in partly melted peridotite under a variety of conditions.

References

Ahearn, J.L. and Turcotte, D.L., 1979, Magma migration beneath an ocean ridge, *Earth Planet. Sci. Lett., 45*, 115-122.

Ballard, R.D. and Moore, J.G., 1977, Photographic Atlas of the Mid-Atlantic Rift Valley, Springer Verlag, New York.

Ballard, R.D., Holcomb, R.T. and van Andel, T.H., 1979, The Galapagos rift at 86°W, 3. Sheet flows, collapse pits and lava lakes on the rift valley, *J. Geophys. Res., 84*, 5407-5422.

Batiza, R., Melson, W.G. and O'Hearn, 1988, Simple magma supply geometry inferred beneath a segment of the Mid-Atlantic Ridge, *Nature, 335*, 428-431.

Batiza, R., Niu, Y. and Zayac, W.C., 1990a, Chemistry of seamounts near the East-Pacific Rise: Implications for the geometry of sub-axial mantle flow, *Geology* (submitted).

Batiza, R., Smith, T.L. and Niu, Y., 1990b, Geological and petrologic evolution of seamounts near the EPR based on submersible and camera study, *Mar. Geophys. Res., 11*, 169-236.

Bonatti, E. and Harrison, C.G.A., 1988, Eruption styles of basalt in oceanic spreading ridges and seamounts: effect of magma temperature and viscosity, *J. Geophys. Res., 93*, 2967-2980.

Dick, H.J.B. and Fisher, R.L., 1984, Mineralogic studies of the residues of partial melting: abyssal and alpine-type perioditites, in Kimberlites II: The mantle and crust relationships, ed. J. Komprohst, 295-308.

Francheteau, J., Juteau, T. and Rangin, C., 1979, Basaltic pillars in collapsed lava pools on deep ocean floor, *Nature, 281*, 109-211.

Klein, E.M. and Langmuir, C.H., 1987, Global correlations of ocean ridge basalt chemistry with axial depth and crustal thickness, *J. Geophys. Res., 92*, 8089-8115.

Knight, M.D. and Walker, G.P.L., 1988, Magma flow directions in dikes of the Koolau Complex, Oahu, determined from magnetic fabric studies, *J. Geophys. Res., 93*, 4301-4320.

Langmuir, C.H., Bender, J.F. and Batiza, R., 1986, Petrologic and tectonic segmentation of the East Pacific Rise, 5°30'N-14°30'N, *Nature, 322*, 422-429.

Lin, J., Purdy, G.M., Schouten, H., Sempere, J.-C. and Zervas, C., 1990, Evidence for focused magmatic accretion along the Mid-Atlantic Ridge, *Nature* (submitted).

Lonsdale, P. and Spiess, F.N., 1980, Deep tow observations at the crest of the East Pacific Rise, 8°45'N, *DSDP v. 54*, 43-62.

Macdonald, K.C., 1989, Tectonic and magmatic processes on the East Pacific Rise, in The Geology of North America, v. N, The Eastern Pacific Ocean and Hawaii, 93-110.

McKenzie, D., 1984, The generation and compaction of partially molten rock, *J. Petrol., 25*, 713-765.

McKenzie, D., 1985a, 230Th-238U disequilibrium and the melting processes beneath ridge axes, Earth Planet. *Sci. Lett., 72*, 149-157.

McKenzie, D., 1985b, The extraction of magma from crust and mantle, *Earth Planet. Sci. Lett., 74*, 81-91.

Michael, P.J. and Bonatti, E., 1985, Peridotite compositions from the North Atlantic: regional and tectonic variations and implications for partial melting, *Earth Planet. Sci. Lett., 73*, 91-104.

Moore, J.G., 1975, Mechanism of formation of pillow lava, *Am. Sci., 63*, 269-278.

Nicolas, A., 1986, A melt-extraction model based on structural studies in mantle peridotites, J. Petrol., 27, 999-1022.

Peterson, D.W. and Tilling, R.I., 1980, Transition of basaltic lava from pahoehoe to aa, Kilauea Volcano, Hawaii: Field observations and key factors, *J. Volc. and Geotherm. Res., 7*, 271-293.

Phipps-Morgan, J. 1987, Melt migration beneath mid-ocean ridge spreading centers, *Geophys. Res., Lett., 14*, 1238-1241.

Rabinowicz, M., Ceuleneer, G. and Nicolas, A., 1987, Melt segregation and flow in mantle diapirs below spreading centers: Evidence from the Oman ophiolite, *J. Geophys. Res., 92*, 3475-3486.

Rubin, A.M., 1990, A comparison of rift-zone tectonics in Iceland and Hawaii, *Bull. Volc., 52*, 302-319.

Rubin, A.M. and Pollard, D.P., 1987, Origin of blade-like dikes in volcanic rift zones, *USGS Prof. Paper 1350*, 1449-1470.

Ryan, M.P., 1987, Neutral buoyancy and the mechanical evolution of magmatic systems, in: Magmatic Processes: Physicochemical Principles, ed. B.O. Mysen, 259-287.

Schouten, H., Klitgord, K.D. and Whitehead, J.A., 1985, Segmentation of mid-ocean ridges, *Nature, 317*, 225-229.

Scott, D.R. and Stevenson, D.J., 1989, A self-consistent model of melting, magma migration and buoyancy-drive circulation beneath mid-ocean ridges, *J. Geophys. Res., 94*, 2973-2988.

Sleep, N.H., 1988, Tapping of melt by veins and dikes, *J. Geophys. Res., 93*, 10,255-10,272.

Smith, T.L. and Batiza, R., 1989, New field and laboratory evidence for the origin of hyaloclastite flows on seamount summits, *Bull. Volc., 51*, 96-114.

Sparks, R.S.J. and Huppert, H.E., 1984, Density changes during fractional crystallization of basaltic magma: Fluid dynamic implications, *Contrib. Mineral. Petrol., 85*, 300-309.

Spiegelman, M. and McKenzie, D., 1987, Simple 2-D models of melt extraction at mid-ocean ridges and island arcs, *Earth Planet. Sci. Lett., 83*, 137-152.

Verhoogen, J., 1973, Possible temperatures in the oceanic upper mantle and the formation of magma, *Geol. Soc. Amer. Bull., 84*, 515-522.

Walker, G.P.L., 1987, The dike complex of Koolau Volcano, Oahu: Internal structure of a Hawaiian rift zone, *USGS Prof. Paper 1350*, 961-993.

Wohletz, K.H., 1986, Explosive magma-water interactions: thermo dynamics, explosion mechanics and field studies, *Bull. Volc., 48*, 245-264.

Yoder, H.S., 1976, Generation of basaltic magma, National Academy of Science Press, 265 pp.

Figure Captions

Figure 1. P-T melting relations of peridotite showing adiabatic ascent paths for mantle of different temperature. The fine lines (e.g., phi = 0.3) are percent partial melt (porosity) produced as a function of initial temperature during adiabatic upwelling. From McKenzie (1984).

Figure 2. From McKenzie (1984), showing how crustal thickness varies as a function of initial mantle temperature (and depth of initial melting) for a simple melting model.

Figure 3. From Batiza et al. (1990a), showing that zone of mantle upwelling at the East Pacific Rise is probably wide (~100 km) vs. narrow (10-20 km). This conclusion comes from a petrologic comparison of zero-age seamount and EPR axial lavas.

Figure 4. Blade-like dikes intruded along the axes of rift zones (from Rubin and Pollard, 1987). Pm is magma pressure and S is remote crustal stress perpendicular to the dike plane.

Figure 5. Various factors that affect magma pressure and remote stress distribution. Density structure of the upper crust is the most likely and significant factor leading to dike propagation in this model. (From Rubin and Pollard, 1987.)

Figure 6. From Rubin (1990), this figure provides an explanation for the fact that Icelandic dikes do not result in surface eruptions as commonly as those of Hawaiian rift zones. In Iceland, because of large horizontal remote stresses, dikes propagate under the influence of large driving forces (Pm-Sh) but small head.

Figure 7. From Williams and McBirney, "Volcanology," 1979, Freeman, Cooper and Co.--this figure is adapted from Peterson and Tilling (1980) and shows the inferred controls one aa vs. pahoehoe eruption style.

Figure 8. From Smith and Batiza (1989), this schematic diagram shows the inferred eruption style leading to submarine hyaloclastite deposits. Submarine lava fountaining must involve high eruption velocity, however no systematic studies of submarine lava flows have been conducted. Such studies are needed to test hypotheses regarding the controls on submarine eruption styles.

Figure 1

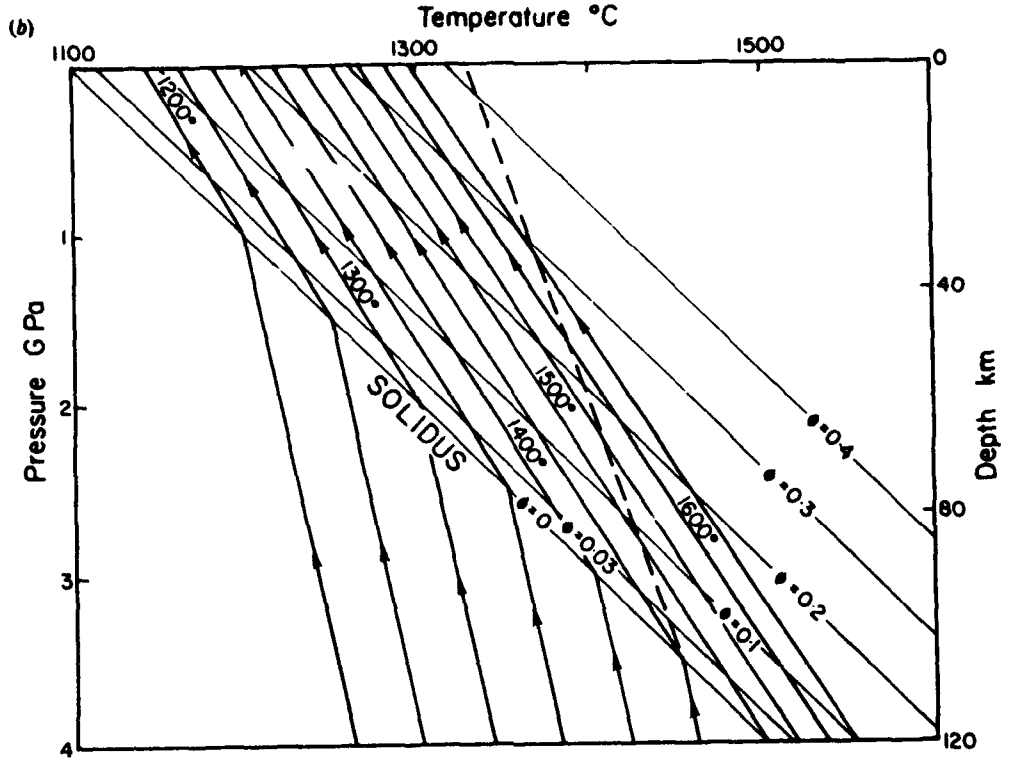

Figure 2

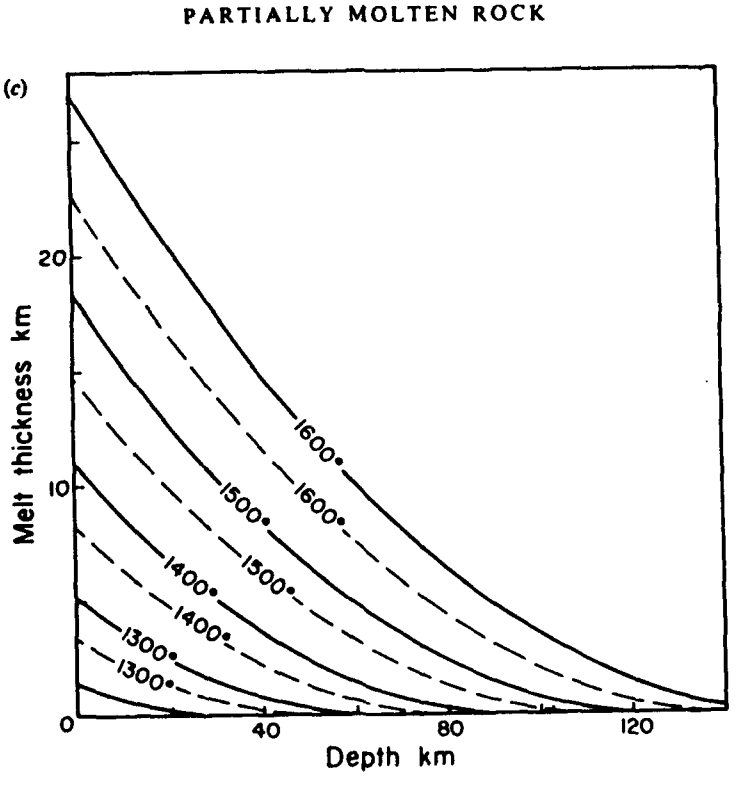

Figure 3

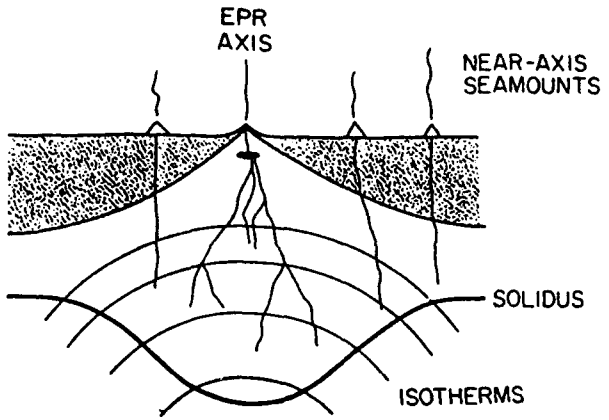

Figure 4

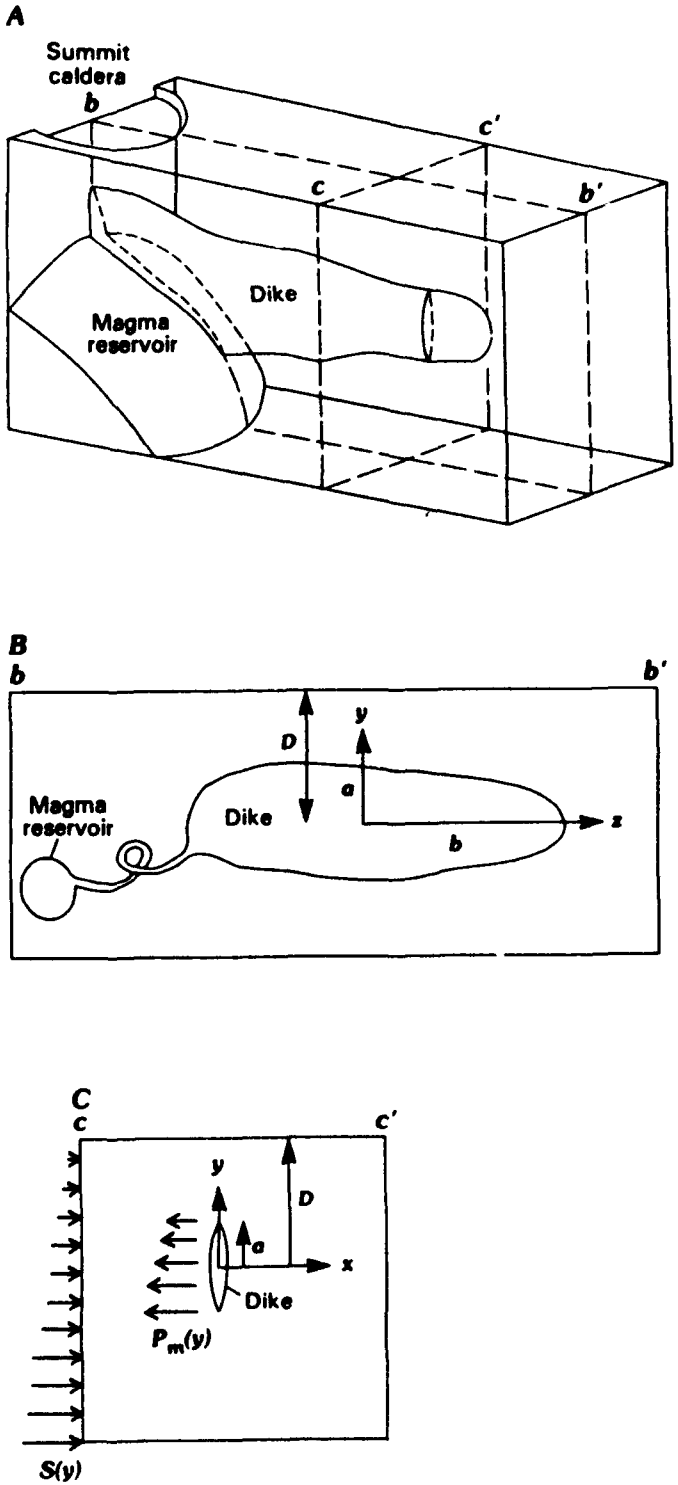

Figure 5

53. ORIGINS OF BLADE-LIKE DIKES IN VOLCANIC RIFT ZONES

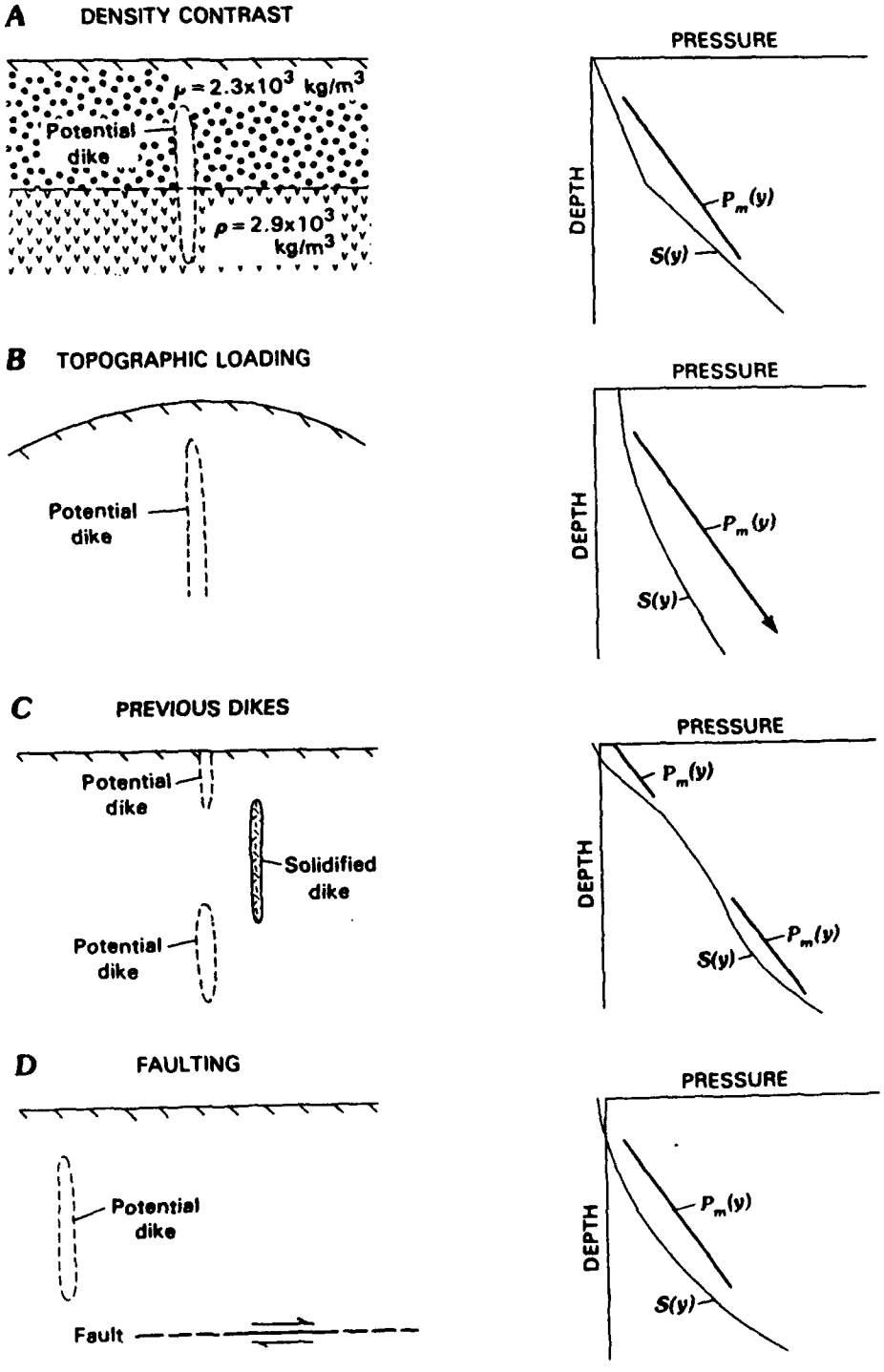

Figure 6

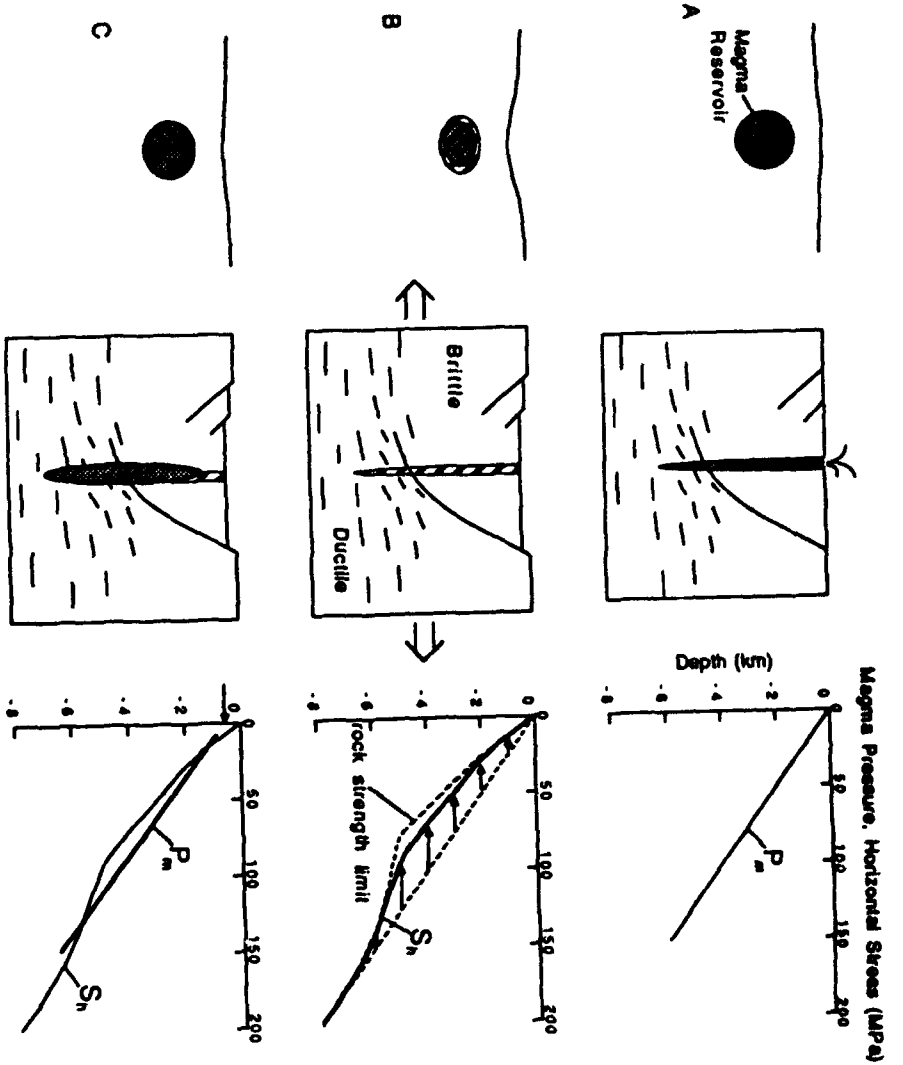

Figure 7

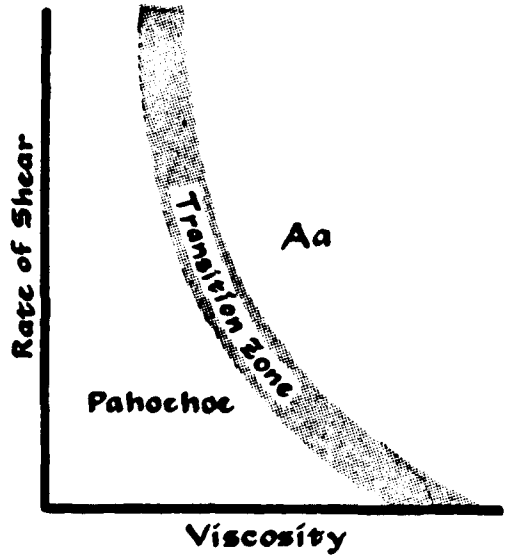

Figure 8

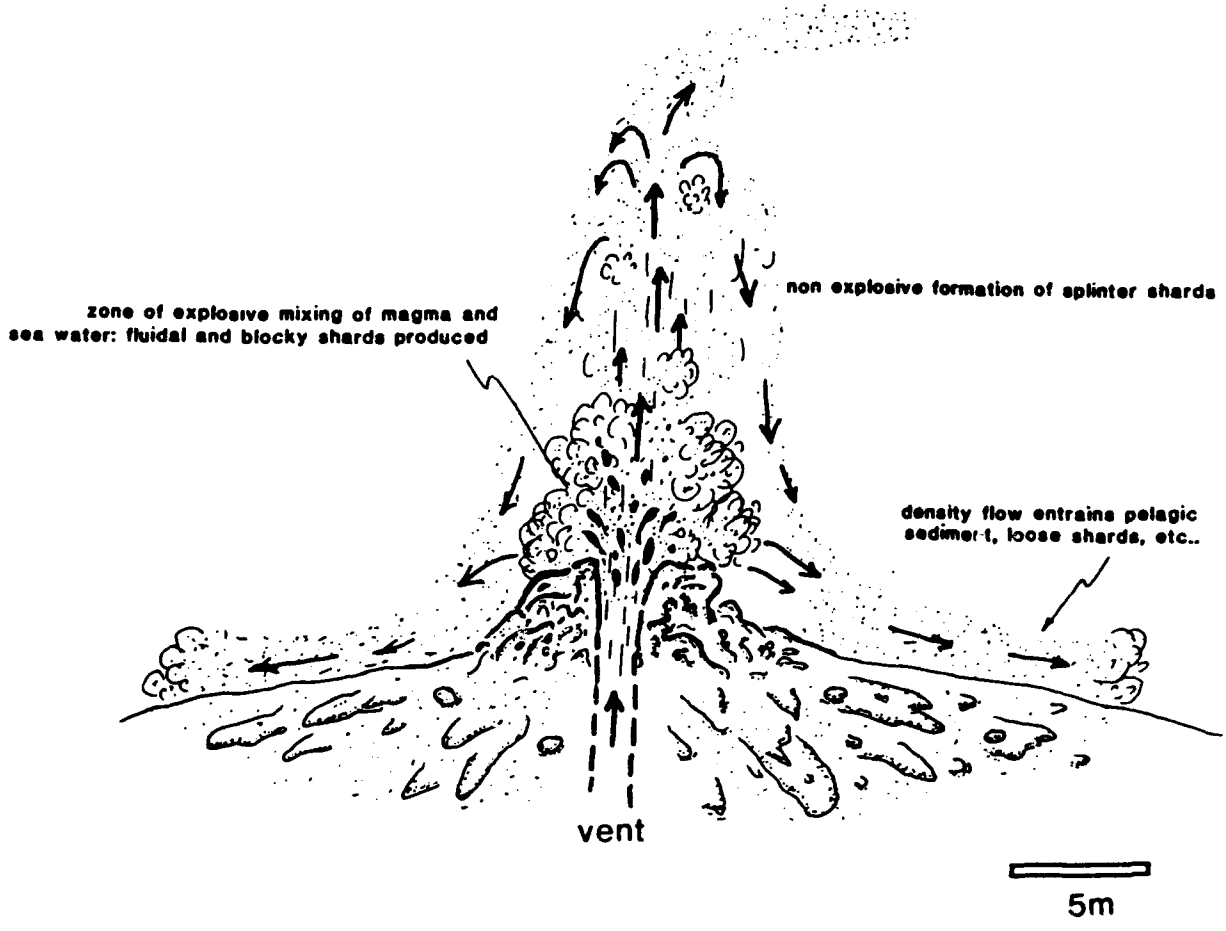

TECTONIC REGULATION OF THE PHYSICAL PROPERTIES OF THE SEA FLOOR: THE VIEW FROM THE JUAN DE FUCA RIDGE

H. Paul Johnson
University of Washington

Introduction

Tectonic processes are extremely active on the floor of the ocean. In many cases, the entire 'character' of the igneous basement is determined by these processes, including the depth of the sea floor, the height and roughness of the abyssal hills, the heat flux out of the crust, and the fluid flux circulating within the crust. Tectonic stress controls the basic geological processes of crustal evolution, including (a) those operating in the near-axis region, where crust is formed; (b) in mid-basin, where crustal re-heating occurs; and (c) approaching a subduction zone, where old faults are re-activated and trapped fluids can be remobilized.

Marine tectonic activity is defined as the irreversible stress usually associated with sea floor spreading process - and many times expressed in igneous crustal rocks as vertical faults and fissures (cracks). These faults and fissures form large scale cracks, which, in our hypothesis at least control the gross permeability of the crust. Our scale length for this discussion is on the order of 10's to 100's of meters in length. By controlling the large-scale permeability, these crustal cracks may control the fluid flux paths, which in turn control the alteration of the associated igneous rock. This alteration, in all probability, ultimately controls the physical properties of ocean basement rocks.

In any discussion of crustal evolution, it seems important to address several fundamental geological questions related to the tectonic control of the physical properties of ocean crust. First, and perhaps foremost, how does crustal cracking control the thermal environment of the crust? During crustal formation, the upper extrusive rocks are quenched by exposure to sea water, are later re-heated by heat transfer from the lower crustal layers, cooled and then re-heated again during the process of subduction. In our hypothesis, these thermal cycles are controlled, both spatially and temporally, by the cracks which are induced within the crustal plate. Whether or not this deep crustal cracking actually occurs in the real ocean is an important question to resolve; the remaining questions are sub-sets to this primary question.

We can organize the next set of questions into several groups:

a. Where does the crustal cracking that controls permeability occur - near the ridge axis, or at some characteristic distance from the axis?

b. Does the associated alteration of the crustal rocks occur immediately after cracking, or at some later time?

c. Is the fluid circulation within the crust open or closed [i.e., does fluid from either the upwelling or downwelling limbs 'leak' through the sediments]?

d. Is the cracking/alteration uniform along a ridge segment, or is it local in distribution and non-uniform?

GEOLOGICAL QUESTIONS

- How does crustal cracking control the thermal environment?
- Is fluid flux controlled by large- or small-scale permeability?
- What types of crustal alteration are occurring off-axis? Where?
- Is the crustal fluid circulation system open or closed? What horizontal scale?
- Is crustal cracking coherent on a local scale, or on a segment/ridge-wide scale?
- What are the relevant fluid/rock reactions, and the associated thermal environment during alteration?

TECTONIC STRESS
↓
CRUSTAL CRACKING
↓
PERMEABILITY
↓
FLUID FLUX
↓
ALTERATION
↓
PHYSICAL PROPERTIES

e. Finally, what are the relevant fluid/temperature/rock reactions in the environment that are causing these changes? How can we define them, how can we get a sample of the components of the reactions, and how can we model them on a global scale?

Life History of a Crack

It has been generally accepted that crustal cracking, fissuring and faulting is a monotonic process, one that occurs at or near the axis of spreading, and further, that this initial cracking does not continue during the life history of the plate. Second-generation tectonic models, on the other hand, argue that there are periods when cracks possess varying degrees of control over crustal permeability. In these models, it is possible to construct a hypothetical sequence of events where these crustal crack open, seal closed and then re-open.

In the beginning of the proposed tectonic cycle, existing lower crustal cracks are covered by the 'last lava flow' associated with crustal formation. Thermal contraction produces surficial cracks, which, since they are cooling the underlying lava flow, can produce shallow-source hydrothermal phenomena. Many small-scale hydrothermal deposits can have this type of superficial cracking as their source. Subsequent tectonic extension can deepen these cracks (in either the on- and off-axis environment). The spatially fixed, deep-source rock of these types of crack can produce large-scale, hydrothermal deposits such as those present on the Endeavour and Explorer ridges, in the NE Pacific.

Percolation of mineral-laden fluid through these cracks can seal the crustal section through the process of internal deposition, causing the fracture-induced permeability to become unconnected rock porosity, and trapping the circulating fluid within the crust. Finally, as the plate approaches the subduction zone, tectonic stress associated with plate flexure prior to subduction can re-activate old, previously sealed crustal cracks, and convert the porosity back into connected permeability again. This is a very hypothetical model of crustal cracking, but there is some data behind it, and it is a place from which to start discussions.

Crack Parameters

If we are to consider the effects that cracking has on the properties of a igneous crustal plate, then we need to define what are the relevant crack parameters. Since the material science people have studied cracks for decades, this preliminary work has already been done for us, it is only necessary to redefine those parameters that are geologically relevant. The basic parameters are, of course:

a. fracture length,

b. surface width,

c. depth of closure,

d. depth of fracture,

e. crack spacing, and

f. the variation of crack with depth.

LIFE HISTORY OF A CRACK

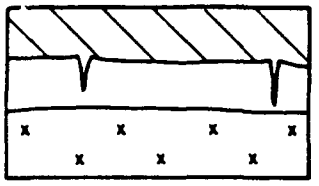

CRUSTAL FORMATION

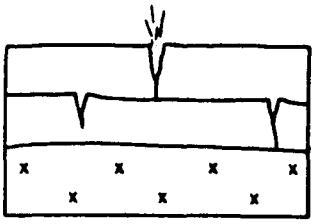

SURFICIAL CRACKING

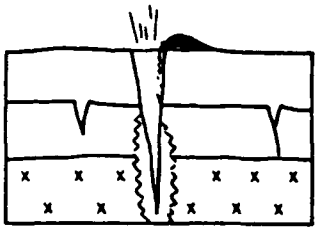

TECTONIC DEEPENING

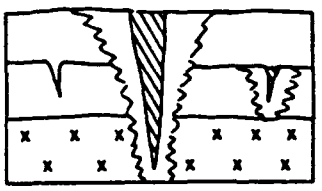

CRACK SEALING

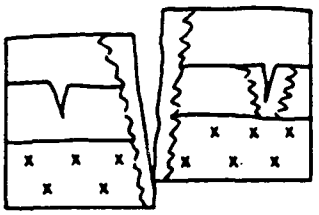

CRACK RE-ACTIVATION

CRACK PARAMETERS

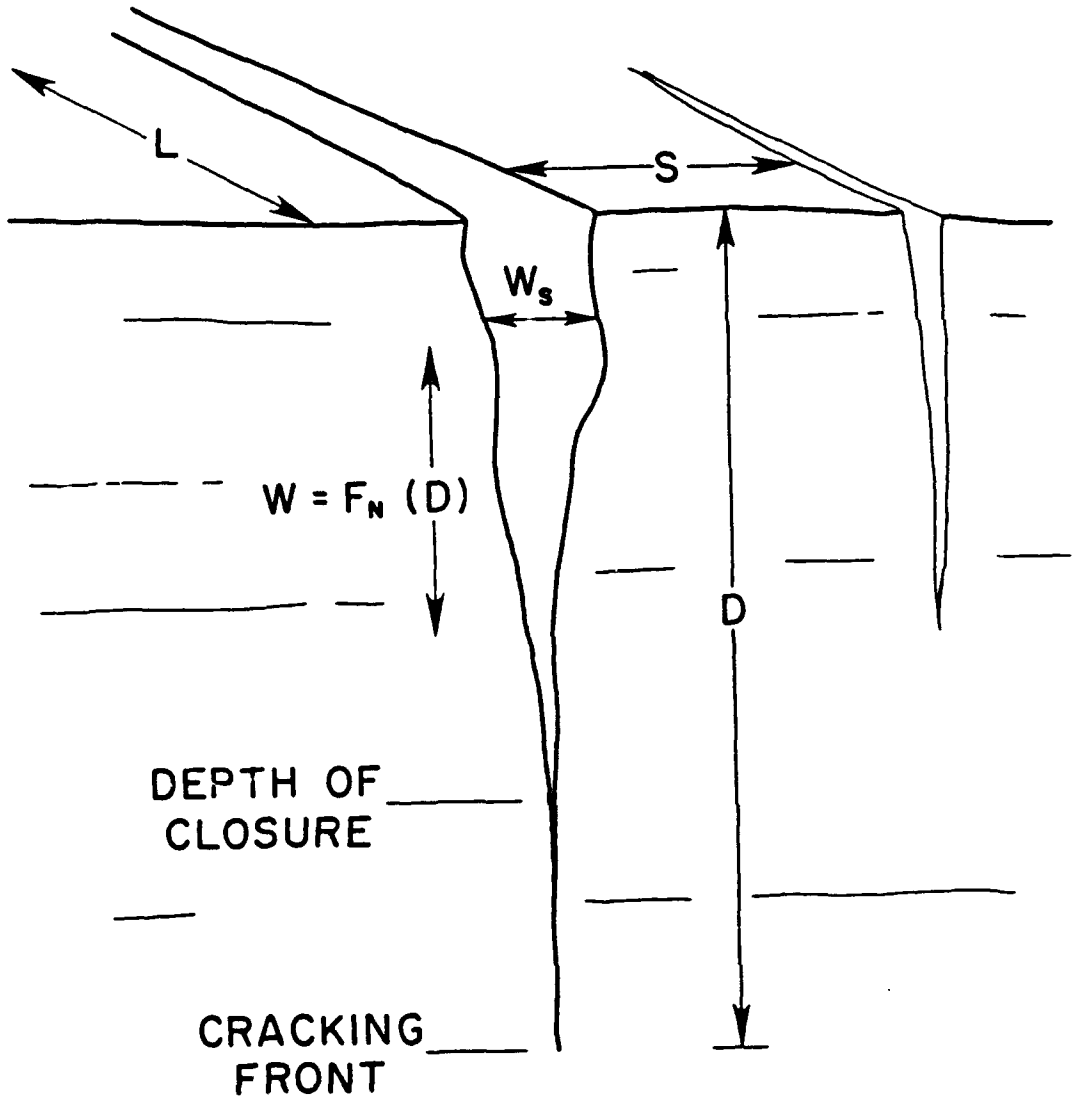

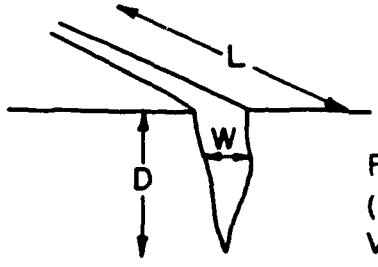

From: Geertsma and Haackens;
(1979) Journal of Energy Resources
Volumn 101, pp. 8-19.

$$W(x=0) = C\left[\frac{(1-\nu)\,D^2}{GL}\right]^{1/4}$$

$W(x=0)$ = FRACTURE WIDTH

C = CONSTANT

ν = POISSON'S RATIO

G = SHEAR MODULUS

L = FRACTURE WIDTH

D = FRACTURE DEPTH

$$[\text{DEPTH}] \propto [\text{WIDTH}]^2\,[\text{LENGTH}]^{1/2}$$

For the marine geologist, crack length and spacing can be fairly easily determined from side-scan sonar surveys; surface width can, in principal at least, be determined fairly readily from near-bottom observations - but hardly ever is. The last three critically important parameters - fracture depth, depth to closure, and the related 'width as a function of depth' have never been determined anywhere; and have only recently been perceived as important in marine geology. The determination of these parameters must be a high priority for any study that hopes to understand the physical properties of ocean crust.

With existing laboratory data (generally obtained from non-geological samples), we can begin to look at what sort of relationships might be possible between these parameters; although any study that models ocean crust as a uniform, isotropic elastic medium is definitely 'grasping at straws'. If oceanic basement were this ideal material, however, we could propose a relationship between depth, length and width of a crack; with depth of cracking being a strong function of crack width, and a very weak function of length. For example, if we had 2 cracks in the same isotropic elastic medium, and one crack was 4 times as long as the other, we would expect the longer one to only be twice as deep. On the other hand, if we have the same two cracks, now the same length but one twice as wide, the wider one would be 4 times as deep. An obvious application of this principal in marine geology is that if we are looking for deep cracks, we should (as our intuition tells us) go with the wide cracks, not the long ones.

Crustal Evolution Model

As an example of our current understanding of crustal evolution, it seems useful to consider the well-studied Juan de Fuca Ridge, a spreading center that is characterized by a topographic high, with an axial notch at the precise axis of spreading. We approached the problem of crustal evolution by looking at the source of the central (within Brunhes) magnetic anomaly high; a well-define magnetic anomaly directly over the axis and one that is associated with all medium to fast spreading ridges. Historically, our first observation, made from the SeaMARC II data in the region, is that crustal cracking on the Juan de Fuca is non-uniformly distributed; with regions that are extensively cracked, and other (surprisingly) regions which are uncracked and unfaulted. Our second observation was that the Juan de Fuca has a very continuous Central Anomaly Magnetic High (CAMH) over the axis. A recent aeromagnetic survey by the Canadian government over the Endeavour segment of the Juan de Fuca shows that the CAMH is continuous along ridge strike, and remains well-defined even when the axial morphology goes from an axial ridge to a topographic low. Our deep-tow magnetics survey over the same region showed that the zones of magnetization contrast that produce the CAMH are strongly correlated with the zones of observed surface cracking in the side-scan. We assume from this observed correlation that the cracked zones are associated with low crustal magnetization and the uncracked zones with high magnetization.

These observations led us to the preliminary model that the Central Magnetic Anomaly High is produced by cracking and alteration - low temperature alteration which lowers the magnetization of the crust immediately off-axis. On the Juan de Fuca Ridge, the "split bow-form ridges" that were formerly axial highs form abyssal hills with inward-facing scarps that move progressive away from the axis. In order to test the crustal evolution hypothesis that cracking controls the rate of alteration, we extended the initial deep tow magnetometer lines to include the flanking ridges that are both on the east and west of the axial ridge. These flanking abyssal hills are regions of uncracked crust (topographic highs) bounded by fissured topographic lows. What we found was that in areas both near and far from the ridge axis, those regions of fissured and cracked crust (in the side-scan images) are zones of low magnetization, while areas of unfissured (at the surface) crust are regions of high magnetization.

PREDICTIONS OF CRUSTAL EVOLUTION MODEL

TYPE I - uncracked

TYPE II - cracked

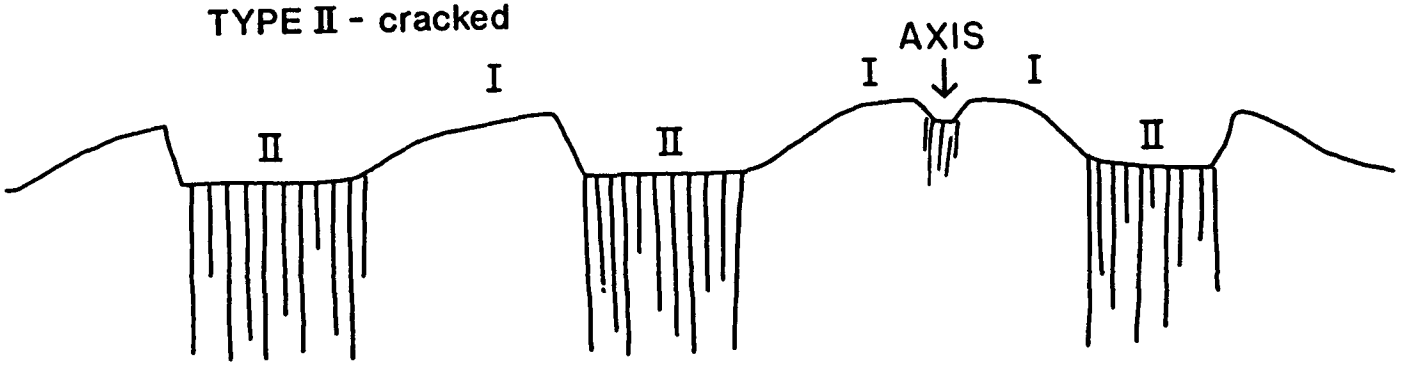

I. LOW PERMEABILITY AND HEAT FLOW: HIGH MAGNETIZATION
(no alteration)

II. HIGH PERMEABILITY AND HEAT FLOW: LOW MAGNETIZATION
(alteration initiated)

VERTICAL CRUSTAL FRACTURING

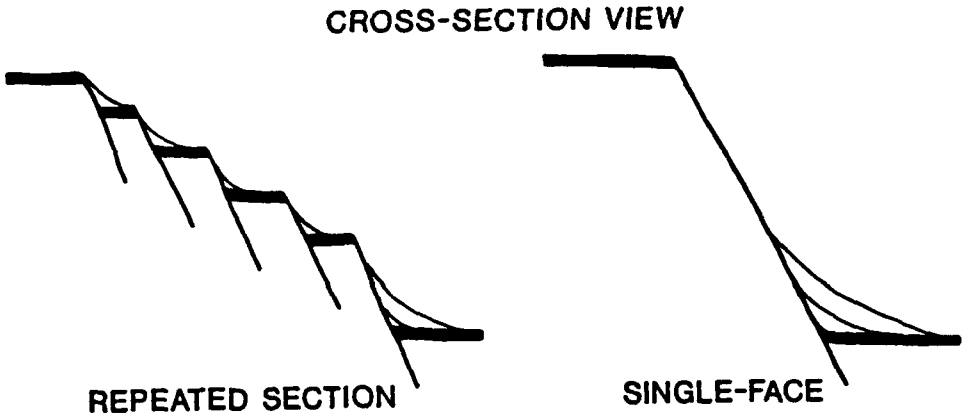

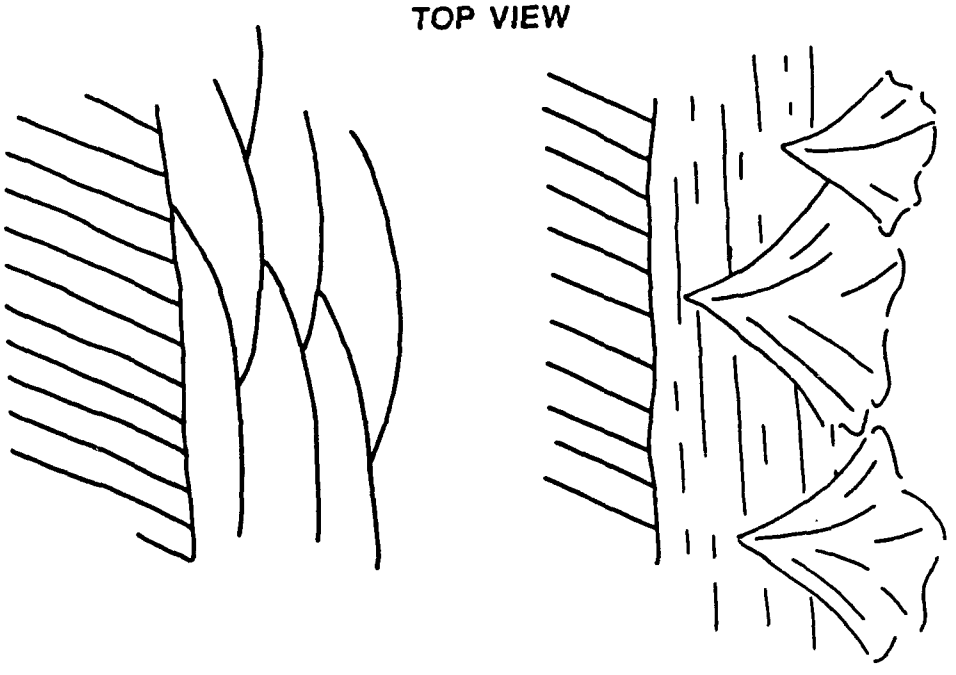

Analysis of the full set of deep-tow magnetics, side-scan and bathymetry data then led us to the model of crustal evolution:

* Cracking of the crust allows water to penetrate deep within the upper extrusives - rocks that are the primary source of the magnetic anomalies.

* This water circulation, within the warm rock, causes the magnetic minerals to alter, and the magnetization of the crustal rock to be substantially decreased.

* On the Juan de Fuca at least, these cracked high permeable zones are the topographic lows, and the unfissured ridges are uncracked and unaltered.

This simple model of crustal evolution allows us to make some predictions about the changes of the physical properties of the igneous rocks. The crustal evolution model that we are proposing is a simple one; crustal cracking controls the fluid flux, which - in turn - alters the basement rock and changes the physical properties of the crust, including a reduction in the magnetization. The actual reality associated with ocean crustal evolution is certainly more complex than this proposed model, but for the first-order tests we have been able to apply, our model seems to work.

Blanco Fracture Data - depth of cracks

Now we can pursue some of the ramifications of tectonic control of crustal physical properties. In order to do that, we need to look in some detail at perhaps the most dramatic expression of tectonic activity in the ocean, geological features called fracture zones; we will concentrate on the Blanco Fracture Zone in particular. The Blanco Fracture Zone is located at the southernmost end of the Juan de Fuca ridge, and, in addition to having about 6 cm/yr of transverse motion across it, has a substantial cross-trend extensional component. This dilational component expresses itself on the Blanco as a series of pull-apart basins, which are regions of crustal extension. These deep elongate basins, the Blanco Trough being the relevant example, are extremely steep-sided, tectonically defined topographic lows. The steep boundary walls (which are actually closer in slope to 45 degrees than 90 degrees), provide us with some clear examples of deep crustal sections exposed by vertical tectonic movement.

Oceanic igneous crust breaks in many different ways, but the two end members of this continuous suite can be described as 'single-face' and 'repeated section'. The former is the simplest to interpret, and consists of a single vertical exposure of the full crustal section. The latter is perhaps the more common style of crustal breaking, with the same vertical section near the top being exposed repeatedly, like a deformed deck of playing cards. The single-face exposures can tell us a lot about the vertical structure of ocean crust - without the need for drilling; while the 'repeated section' style of breakage cannot. Many fracture zones have both styles of breakage; one style on one side of the Fracture Zone, and the other style on the other side. The single-face breakages seem to be more coherent along the fracture strike, and present a distinctive uniform pattern when observed with side-scan, while the repeated sections are less coherent along-strike - and show a 'braided' backscatter pattern.

The single-face crustal breakages, which present the entire crustal section in vertical exposure, represent an tremendous opportunity for those who want to see below the surface of ocean crust. As an example, the north wall of the Blanco, which is a single-face break, can give us some insight into the fundamental question of the depth of surface crack penetration. Our SeaMARC II coverage of the Blanco allows us to look at the edge of the wall of the Trough, and to see surface fissuring that is continuous - down the entire face of

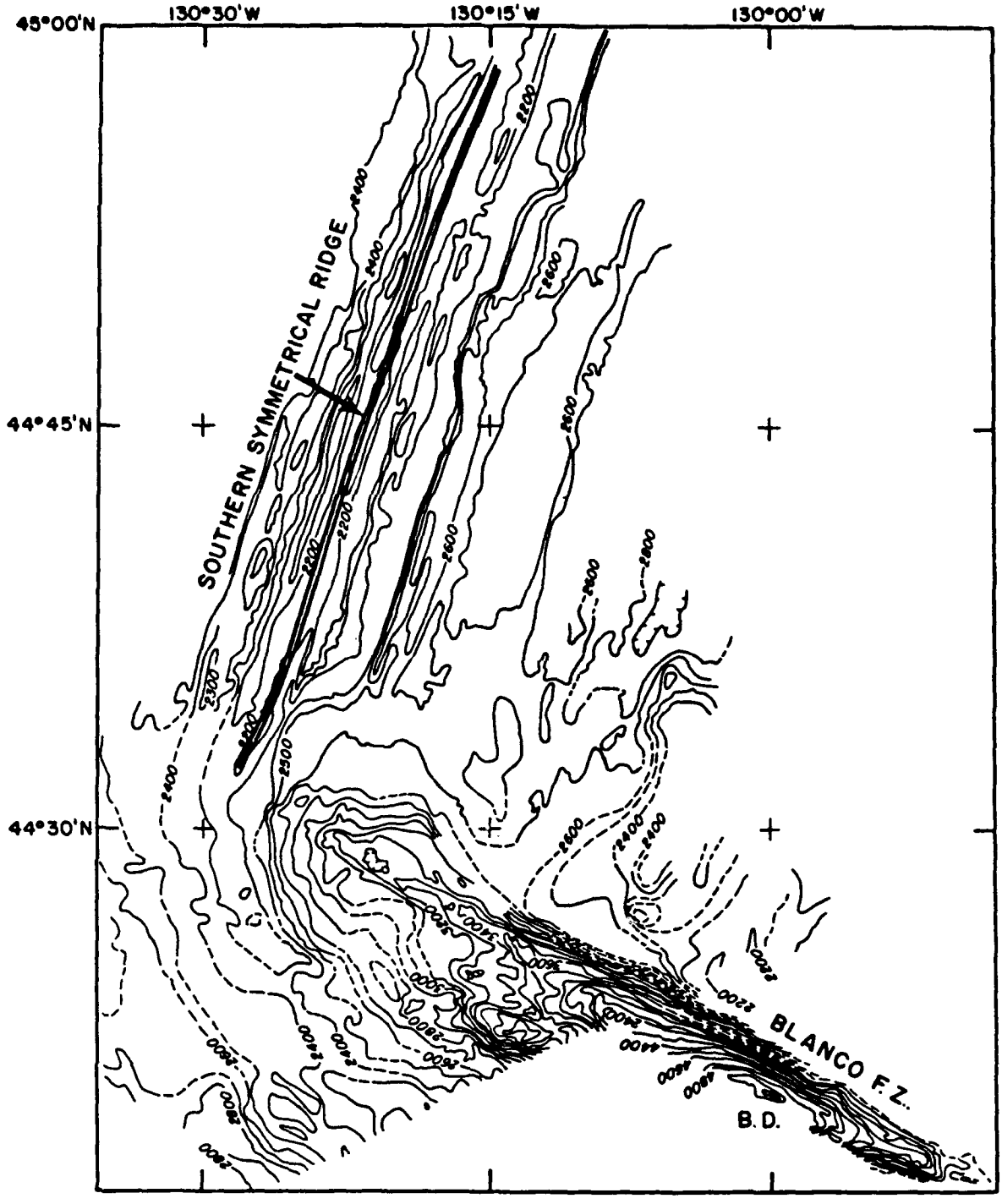
45°00'N
130°30'W
130°15'W
130°00'W
44°45'N
44°30'N
SOUTHERN SYMMETRICAL RIDGE
BLANCO F.Z.
B.D.

2400
3000
3500
4000
3500
4000

the cliff. We can actually follow individual side-scan reflectors that are visible as crustal fissures at the surface, down the face of the wall, to a depth of over 1.2 km within the crust.

While not completely satisfying (crust adjacent to a fracture zone may not be a normal basement section) this data provides us with a strong indication that the fissuring visible at the surface CAN penetrate deeply into the crustal section. This example of the deep penetration of cracks is an important component to our model of crustal evolution.

Crustal Re-heating

As a last topic, I am going to try to demonstrate that tectonic activity, at least in the form of abyssal hill formation, can play a major role in the post-formation evolution of oceanic basement. I will describe a heat flow survey of the Juan de Fuca plate - originally done by Jean Moran and Clive Lister - across Cascadia Basin, which I will re-interpret in terms of crustal reheating and remagnetization.

Moran and Lister measured the heat flow as a function of age in Cascadia Basin, showing values that rise up to join the 'conduction only' curve at about 170 km from the axis. Given their measured heat flow values away from the axis of spreading, and the appropriate sediment thermal conductivity, it is possible to calculate the temperature at the sediment/basalt interface as a function of distance from the spreading center. If this crustal temperature as a function of age is then plotted, it is obvious that the Juan de Fuca Plate, at least, is undergoing serious crustal re-heating to temperatures of close to 200 degrees C. Data compiled from DSDP cores and logging, particularly Sites 504B and 395A, argues that this phenomena has more general applicability to ocean crust than just the Juan de Fuca plate.

The maximum temperature that a given section of crust will reach during post-formation reheating depends, for the most part, on the crustal age where the insulating sediment blanket becomes complete and the heat flow values intersect the conduction curve. If this intersection is close to the axis, crustal re-heating of the extrusive rocks will be substantial (i.e., 100-200 deg C); if the intersection of the two curves is distant from the axis, the general crustal re-heating will not be significant in terms of alteration (i.e., less than 100 deg C). As two extreme examples, the Juan de Fuca Ridge, because of the high sedimentation rate and low topographic relief, has a complete insulating sediment blanket formed very near (<20 km) the axis. The Mid-Atlantic Ridge, however, has more extreme topographic relief, and is not 'insulated' until after the lithosphere has cooled substantially.

Conclusions

It would be easy to over-generalize from these preliminary observations, but a conservative interpretation of the data above would be that there are many sites within the Pacific basin which have experienced substantial basement re-heating, while most of the younger Atlantic crust has not been substantially re-heated. If the crustal rocks have been reheated, then the physical properties of these rocks, and the material in the void spaces between them, are also likely to have been effected.

It is easy to see why there should be a fundamental difference in thermal and alteration history between the two oceans. The Atlantic, for example, is topographically rough with large relief on the abyssal hills, and is not completely insulated with a sediment blanket until it has cooled substantially. Under these circumstances, the sea floor will not undergo substantial reheating. On the other hand, the Pacific crustal abyssal hills are much smaller, and the sedimentation entirely covers the warm crust before the lithosphere cools substantially.

BASEMENT TEMPERATURES vs AGE

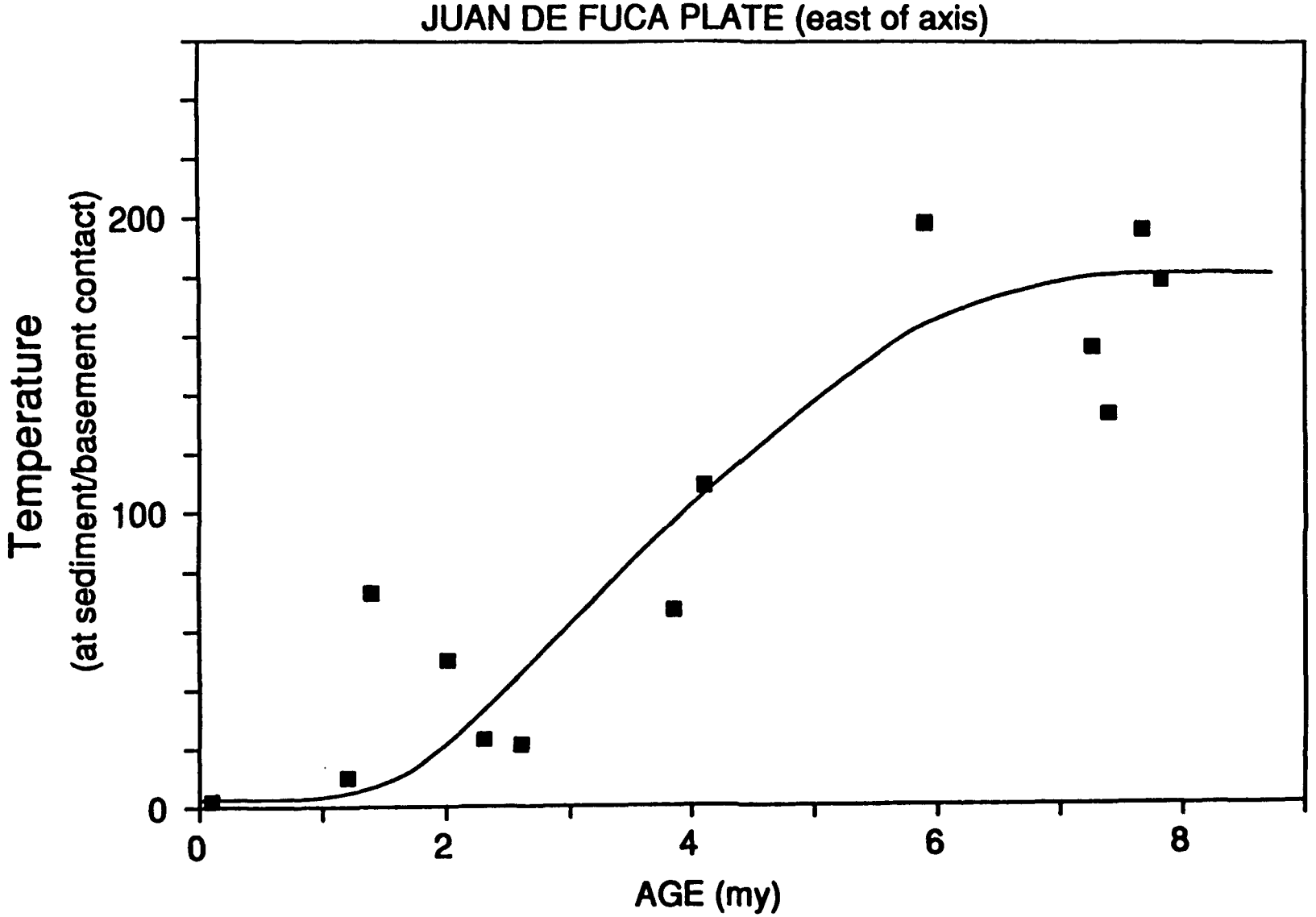

A plot of crustal temperature versus age, near the Juan de Fuca Ridge (in Cascadia Basin). Temperatures are those extrapolated for the sediment-basement interface, from heat flow and sediment thermal conductivity. In this area, sediment cover becomes significant at about 1 million years (30 km from the axis). Data from Moran, 1985; and Moran and Lister, 1986.

CRUSTAL REHEATING

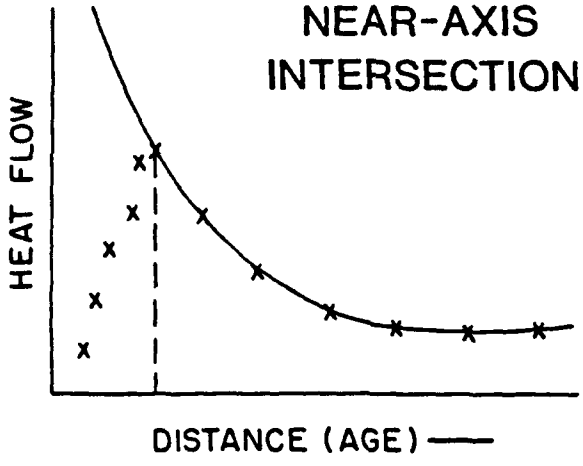

HIGH SEDIMENTATION; LOW RELIEF
HIGH CRUSTAL REHEATING

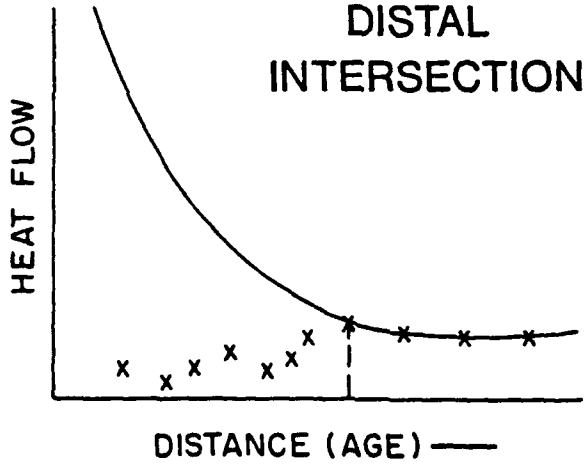

LOW SEDIMENTATION; HIGH RELIEF
LOW CRUSTAL REHEATING

DEPTH TO BASEMENT FOR TWO SPREADING CENTERS

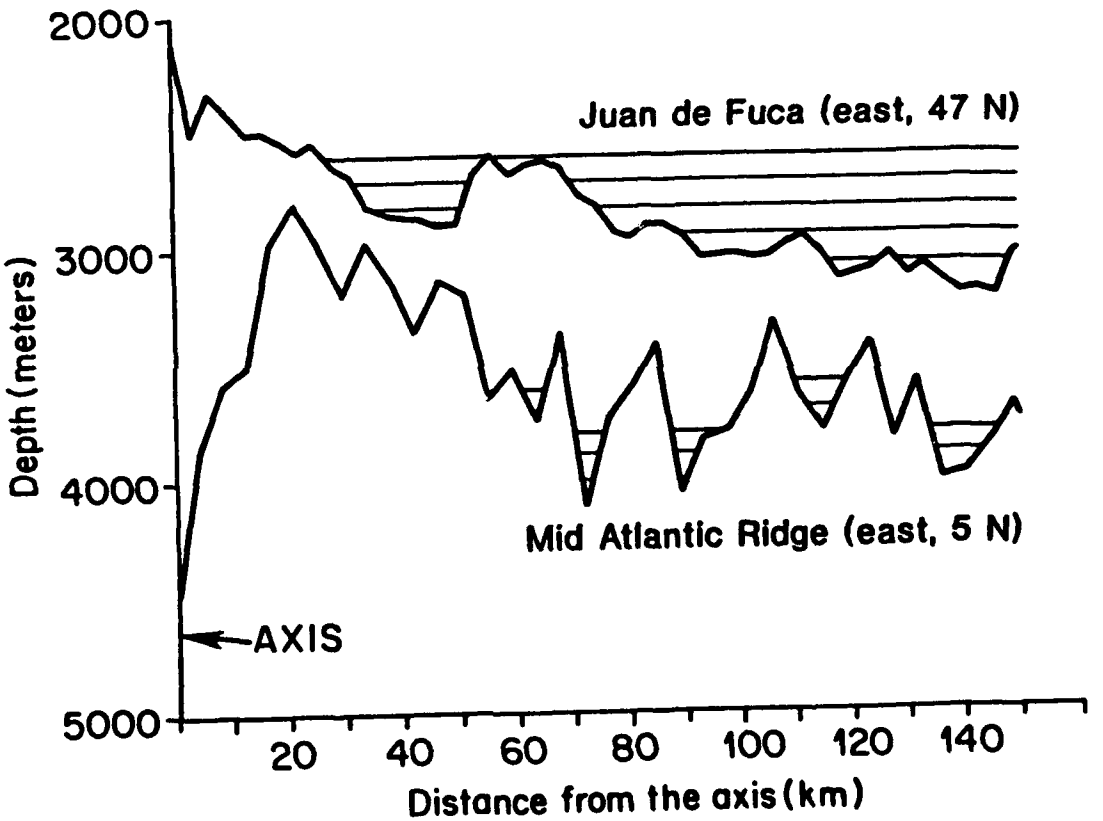

In this environment, the basement rocks will warm up off-axis, to temperatures high enough to undergo substantial intermediate temperature alteration.

Abandoning the conservative interpretation, it is possible to speculate that there are at least two fundamentally different types of crustal evolution processes that are tectonically controlled; one results in substantial crustal reheating off-axis (in the Pacific) and the other does not (in the Atlantic). The details may not yet be fully resolved, but it is clear that tectonic processes are a major controlling factor associated with crustal evolution. The alteration associated with this re-heating process is a primary independent variable in determining the physical properties of the ocean crust.

SIGNIFICANT OBSERVATIONS NEEDED

- What is the spatial distribution of crustal cracks?
- How deep do these cracks penetrate into the crust?
- How does this large-scale cracking vary as a function of time?
- Are there observable correlations between cracking, heat flux, and crustal physical properties?

Section B2: Geophysical Measurements

1: Seismic Structure of the Uppermost 0.5-1 km of Zero Age Oceanic Crust: E.E. Vera and J.B. Diebold

2: The Evolution in Seismic Structure of the Uppermost 0.5-1 km of Oceanic Crust: G.M. Purdy

3: Resolution of the Structure and Physical Properties of the Upper Oceanic Crust using Downhole Measurements: K. Becker

SEISMIC STRUCTURE OF THE UPPERMOST 0.5-1 KM OF ZERO AGE OCEANIC CRUST

Emilio E. Vera and John B. Diebold
Lamont-Doherty Geological Observatory
Palisades, NY 10964

Abstract

We discuss the upper seismic structure of zero age oceanic crust at 9°N on the East Pacific Rise as derived from the analysis of Expanding Spread Profiles (ESP). Observed refracted arrivals allow us to determine directly the uppermost crustal velocity structure (layer 2A). At the seafloor we find very low V_p and V_S/V_p values around 2.2 km/s and ≤ 0.43. In the topmost 100 to 200m of the crust V_P remains low (≤ 2.5 km/s), then rapidly increases to 5 km/s at ~500m below the seafloor. High attenuation values ($Q_P < 100$) are suggested in the topmost ~500m of the crust. The intermediate crust from about 0.4 to 1.6 km below the seafloor can be characterized by an approximately 400m thick layer with a nearly constant velocity around 5.3 km/s, overlying a relatively steep velocity gradient zone where velocities around 6.7 km/s are reached within the following 800m. These two layers may be broadly equated with layers 2B and 2C. At the rise crest and within approximately 2 km of the rise crest, the lower part of the gradient is missing, and in its place, there is a sharp decrease in velocity as the top of the AMC is approached.

Introduction

In May and June, 1985, a suite of two-ship multichannel seismic experiments was carried out between 8°50' N and 13°30' N on the East Pacific Rise (EPR) [Detrick et al., 1987]. The seismic experiments were centered in two areas of the axial region, approximately at 9°30' N and 13°N, each of them covering about 100 km along strike and about 10 km (~0.2 m.y.) on either side of the rise crest. In each area several common-depth-point (CDP) reflection lines were shot along and across the rise axis and were complemented by a set of Expanding Spread Profiles (ESP) [Stoffa and Buhl, 1979] shot parallel to the rise axis. Several aspects of the reflection lines have been discussed by Detrick et al. [1987], Mutter et al. [1988] and Fox et al. [1988]. The 13°N ESPs have been analyzed by Harding et al. [1989], and the 9°N ESPs by Vera [1989] and Vera et al. [in press]. In this paper we present a detailed discussion of the upper crustal seismic structure derived from the 9°N ESPs (Figure 1), in particular that from ESP 5AG (airgun part of ESP 5) acquired along the rise crest over zero age crust.

A important result to emerge from the 9°N ESPs as well as from the 13°N ESPs [Harding et al., 1989] is the observation of refracted arrivals from the uppermost crust that allow us to determine the velocity structure of approximately the topmost 500m of the crust. Direct observation of such arrivals in young oceanic crust has only rarely been reported. An exception to this is an experiment on the Mid-Atlantic Ridge at 23°N (Purdy, 1987) where the seismic source and the receiver were located on the seafloor. Previous refraction experiments with the source at the sea surface and the receiver at either the sea surface or the seafloor, however, have been unable to detect this type of arrivals. This is the case, for example, for several seismic experiments in the ROSE area of the EPR at 12°N [Ewing and Purdy, 1982; Bratt and Purdy, 1984; Vera and Mutter, 1988] where the uppermost crustal velocity structure could not be obtained directly, and was instead estimated by a single velocity gradient layer using a method described by Ewing and Purdy [1982]; velocities as low as 2.5 km/s and gradients as high as 4 s^{-1} were inferred for the uppermost several hundred meters of the crust. Purdy [1987] found similar values in the Mid-Atlantic Ridge. Our ESPs confirm these results.

We directly measure very low seafloor velocities around 2.2 km/s and steep velocity gradients with an average of about 5 s^{-1} in the uppermost 500m of the crust. We find, however, that the assumption of a single velocity gradient is too simplistic and does not fit the data. Instead the ESPs support models with a 100 to 200m thick layer with velocities no greater than 2.5 km/s, overlying a very steep velocity gradient zone where velocities above 5 km/s are reached within a few hundred meters.

In what follows, we make use of the terminology for the oceanic crust derived from seismic refraction experiments, where subdivision in layers is based on P-wave velocities. From the top to the bottom of the crust, layers 2A, 2B, 2C and 3 then correspond to average velocities between 3 and 4 km/s, 5.2 ± 0.4 km/s, 6.1 ± 0.2 km/s and 6.9 ± 0.2 km/s respectively [Houtz and Ewing, 1976].

The Uppermost Crust (2A)

P-wave (V_p) Velocity Structure

Figure 2a shows ESP 5AG shot along the rise crest (Figure 1), and Figure 3 its tau-p transform; main arrivals that are used to obtain V_p are labeled in both Figures. The key to the uppermost crustal velocity structure is the retrograde branch T1. The point where T1 and the seafloor reflection, R1, meet gives the velocity at the seafloor. This is particularly clear in the tau-p domain where this happens at a p value of around 0.45 s/km (Figure 3). The reciprocal of this value, 2.2 km/s, is the velocity at the seafloor. The remainder of the T1 branch yields velocities slowly increasing in the uppermost 100m of the crust, and a very rapid increase from 2.4 to 5 km/s in the next 150m.

Figures 2 and 4 compare ESP 5AG with reflectivity and WKBJ synthetic seismograms for our final velocity model (Figure 5). Figure 4 concentrates on the arrivals related to the uppermost crust and shows the excellent agreement between the WKBJ and reflectivity synthetics as well as between the data and the synthetics. One difference between the synthetics is the branch RA, which is produced by reflectivity modeling but not by WKBJ. This arrival comes from the large velocity gradient (noted above) which appears as sharp discontinuity to low frequencies. WKBJ cannot model this effect because it employs a high frequency approximation in which waves experience no interaction with velocity gradients other than geometrical spreading. Thus at offsets less than about 1.5 km, the WKBJ seismograms show only the source wavelet that comprises the first pulse and two bubble pulse reverberations. The branch RA is seen in the data about 80 ms after the seafloor reflection R1. At first inspection RA appears to be simply part of the airgun signature and should therefore be included as part of the source wavelet. On closer inspection, however, we noted that its character changes from trace to trace in a manner that is difficult to attribute to the airgun signature.

We tested several models for the uppermost crust and recognized that a slow uppermost layer overlying a large velocity gradient was needed to match the data. Figure 4d, for example, presents a case where the uppermost crust velocity structure is approximated by a single gradient layer (Figure 5) calculated using the location where T2 meets R1, and the slope of T2 at this point as described by Ewing and Purdy [1982]. As expected, this model predicts the correct traveltimes for branch T2, but completely misses T1. We found that only a very small range of models were allowed if a seafloor velocity of 2.2 km/s and compatibility with branch T2 were imposed as constraints. Even minor changes always resulted in noticeably poorer matches of the data. The thickness of the uppermost layer was thus constrained to ±25m in our final model

S- wave (V_S) Velocities

The 9°N East Pacific Rise ESPs show virtually no shear arrivals from which direct measurements of V_S can be made. A simple estimation of V_S can be obtained from V_P using a constant ratio $V_S/V_P = 0.54$ which is an appropriate value for oceanic basalts samples at approximately 0.5 kbar [Christensen, 1972]. Some indirect determination of V_S, however, can be achieved by analyzing the P-wave arrival amplitudes. This is the case of the seafloor reflection, R1, whose amplitude versus offset pattern is very sensitive to the seafloor V_S. The synthetics in Figure 4 were computed using a seafloor $V_S = 0.95$ km/s ($V_S/V_P = 0.43$). The "normal" case, $V_S/V_P = 0.54$ ($V_S = 1.19$ km/s) produced a decay of the seafloor reflection amplitudes with distance that was faster than that seen in the data (Figure 6). Thus ESP 5AG indicates an uppermost crust where both, V_P at 2.2 km/s and V_S/V_P at 0.43 are anomalously low.

Attenuation

Branch T2 (Figure 2) corresponds to rays turning at depths from about 0.3 to 1.3 km below the seafloor, while R2 is the reflection from the top of the axial magma chamber (AMC) 1.6 km below the seafloor. The overall amplitudes of these arrivals depend strongly on the attenuation in the uppermost crust. The synthetics in Figure 2b, computed using a P-wave quality factor Q_P=80 in the uppermost 600m of the crust, correctly reproduce most of the features of arrivals T2 and R2. It must be noticed, however, that in Figure 2 the data have been amplified more than the synthetics, while in figure 4 the gains are equal. Therefore in Figure 2, the near vertical seafloor reflection amplitudes are not matched because those in the data are 1.67 times larger than those in the synthetics. We estimate that an even larger attenuation ($Q_P \approx 50$) would be needed to match the absolute amplitudes of arrivals T2 and R2. We, however, did not carry out computations with new attenuation values because attenuation is only one of several factors that control amplitudes, including seafloor roughness and overall reflectivity of the uppermost crust which are difficult to evaluate in detail. The use of values of $Q_P<100$ in the uppermost crust is nevertheless required by the data. If no attenuation is used in the synthetics, the T2 and R2 amplitudes are more than three times larger than in the data and many multiple and converted shear arrivals appear in the synthetics, but are not seen in the data.

The Intermediate Crust (2B-2C)

Branches T2 and T3 (Figures 2 and 7) provide the P-wave velocity structure below layer 2A, from about 0.4 to 1.6 km below the seafloor. These branches are present in all of the 9° N ESPs except in the on-axis ESP 5 which does not display a branch T3.

Below layer 2A, our velocity models, except at the rise crest, are characterized by an approximately 400m thick layer with a nearly constant velocity around 5.3 km/s, overlying a relatively steep velocity gradient zone where velocities around 6.7 km/s are reached within the following 800m (Figure 8). These two layers may be broadly equated with layers 2B and 2C. At the rise crest (ESP 5) the lower part of the gradient is missing, and in its place, there is a sharp decrease in velocity as the top of the AMC is approached; this is in direct correspondence with the fact that T3 is also missing in ESP 5.

The intermediate crustal velocity structure is constrained by the amplitudes of arrivals T2 and T3, particularly by an amplitude maximum seen between 7 and 8 km where the two branches meet (see Figure 7). This amplitude pattern requires a crustal velocity structure consisting of a nearly constant velocity layer overlying a steep velocity gradient zone. Together these two layers produce a traveltime triplication with the corresponding concentration of energy at offsets between 7 and 8 km. In ocean bottom hydrophone data acquired between

11°N and 13°N on the EPR, Bratt and Purdy [1984] found a similar amplitude pattern, that they also used to constrain their models. Their velocity structure for 0.5 m.y.-old crust is analogous to our solutions. It is remarkable that despite the differences in location, crustal age and spreading rate, a similar velocity structure is also found at DSDP hole 504B (Figure 8).

Discussion and Conclusions

Uppermost crust

Velocities no greater than 2.5 km/s within the uppermost 100 to 200m of the crust represent a significant discrepancy from values of between 5 and 6 km/s measured on basalt samples from mid-oceanic ridges [Christensen and Shaw, 1970; Christensen, 1972; Hyndman and Drury, 1976]. This discrepancy has been a subject of considerable debate, and several authors [Hyndman and Drury, 1976; Spudich and Orcutt, 1980a,b; Bratt and Purdy, 1984; Purdy, 1987; Vera and Mutter, 1988; among others] have recognized that it may be satisfactorily explained by the presence of large-scale fracturing and voids in the crust that are not present in laboratory samples. Spudich and Orcutt [1980a,b] show how, starting with a basalt having a few percent small-scale porosity and a velocity of 6 km/s, the addition of an extra 10% porosity in the form of large-scale cracks can lower the velocity to values as small as 2.5 km/s. To achieve the same result with spherical pores however, physically unreasonable values of as much as 50% large-scale porosity are required. Purdy [1987] argues against total porosities in excess of 30% at zero age crust because of the lack of plausible mechanisms able to decrease these values with age at a rate fast enough to be compatible with observations made on older crust. Thus, although a mixture of large-scale cracks and pores is expected within the top part of the oceanic crust, cracks probably dominate over spherical pores. Our observation of a relatively low V_S/V_P at the seafloor (≤ 0.43) supports this suggestion. Based on sonic down-hole logging measurements in the upper 150m of oceanic crust at Deep Sea Drilling Project (DSDP) hole 504B, Moos et al. [1986] conclude that low aspect ratio fractures decrease V_S and increase V_P/V_S, whereas equidimensional voids reduce both V_P and V_S without changing their ratio. The presence of large-scale fractures in the uppermost crust is also consistent with, and can be part of the reason for, the high attenuation values ($Q_P<100$) suggested for that zone by our amplitude modeling. At the EPR we then envisage a topmost 100 to 200m thick layer with a large-scale porosity no higher than 20%, predominantly in the form of low aspect ratio fractures.

A clue to the nature of the uppermost crust is suggested by the results obtained at DSDP hole 504B. At this site, the upper 100m of the basement consists of a relatively permeable aquifer made up of pillow lavas, breccias, and a few massive flows. Within this zone the fractures appear to be open and filled with seawater (Anderson et al., 1982). At the base of the aquifer the porosity rapidly decreases and the velocity increases (Becker et al., 1982; Newmark et al., 1985). The slow topmost 100 to 200m is then likely to correspond to an aquifer which is underlain by a zone having a significantly lower porosity and permeability, resulting in a marked seismic transition at the bottom of the aquifer. The changes in porosity and permeability probably occur in response to the closure of large-scale fractures, due mainly to the combined effect of the increasing confining pressure with depth and infilling of voids by hydrothermal alteration products.

Our solutions seem to indicate that the shallow crust evolves with lower velocities occurring with increased age (see Figures 8). It should be pointed out, however, that the variability in structure between crust of approximately the same age (ESP 7 and 8) is about the same as the variability between the youngest and the oldest crust in our experiment (ESP 5 and 1). Thus the crustal evolution suggested by our solutions may not be genuine, but simply an artifact of the structural variability of the uppermost crust. It is worth noticing, however, that a similar trend at 12°50' N on the EPR has been pointed out by McClain et al. [1985], and more

recently by Burnett et al. [1989] and Caress et al. [to be submitted to Journal of Geophysical Research].

Common midpoint ray tracing through a crustal structure defined by our velocity models demonstrates that rays which turn within the upper 300m or so of the crust have sampled crust at distances no greater than 1 km from the midpoint. Thus the uppermost crustal velocity structure derived from our ESPs corresponds only to a small portion of crust around the ESPs' midpoints, and is not necessarily a regional feature. Arrival T1 defining the uppermost crust, however, also appears in other data from the EPR experiment. It can be recognized in a significant number of wide aperture CDPs of along axis lines, and it is extremely clear in ESP 9 shot along the rise crest in the 13°N study area [Harding et al., 1989]. It is, therefore, suggested that the type of uppermost crustal velocity structure inferred from ESP 5AG is a general feature of the EPR from 9° to 13°N, having a lateral extent of at least 10 km away from the ridge axis. Studies in the ROSE area of the EPR at 12°N [Ewing and Purdy, 1982; Bratt and Purdy, 1984; Vera and Mutter, 1988] would indicate that a similar structure might be extended as far as 200 km (4-m.y.) from the axis.

Intermediate Crust

This part of the crust can be characterized by a nearly constant velocity layer overlying a relatively steep velocity gradient zone.

The nearly constant velocity layer with velocity values around 5.3 km/s can be identified as oceanic layer 2B. The velocities in this region compare well with laboratory measurements on basalt samples from mid-oceanic ridges [Christensen and Shaw, 1970; Christensen, 1972; Hyndman and Drury, 1976], which are free of large-scale crustal fracturing and voids. At DSDP hole 504B, layer 2B is a zone composed of pillow basalts, flows, and breccias, characterized by moderate velocity gradient in both P and S-wave velocities, and with an average P-wave velocity around 5.3 km/s [Newmark et al., 1985]. Our nearly constant velocity zone would then consist of extrusives where confining pressure and hydrothermal mineralization, among other factors, have closed a large fraction of the large-scale porosity.

The relatively large velocity gradient zone below the nearly constant velocity zone, would mark the transition from extrusives on top to dikes below. This interpretation is again supported by downhole measurements at DSDP hole 504B, where at the extrusive-dike transition, an increase of the velocity gradient is detected. Within the 700m of transition zone and dikes penetrated at hole 504B, V_p increases from approximately 5.3 km/s at the bottom of the extrusives, to 6.4 km/s at the bottom of the hole (see Figure 8). This trend agrees well with the gradient zone present in all our ESPs. The average velocity in our gradient zone is around 6.1 km/s. In velocity models consisting of constant velocity layers, this velocity would be assigned to this zone which would then be identified as layer 2C. Since our models do not contain sharp discontinuities, the top and bottom of layer 2C is not well defined and this designation should be used with care.

References

Anderson, R.N., J. Honnorez, K. Becker, A.C. Adamson, J.C. Alt, R. Emmermann, P.D. Kempton, H. Kinoshita, C. Laverne, M.J. Mottl, and R.L. Newmark, DSDP Hole 504B, the first reference section over 1 km through layer 2 of oceanic crust, *Nature, 300*, 589-594, 1982.

Becker, K., R.P. Von Herzen, T.J.G. Francis, R.N. Anderson, J. Honnorez, A.C. Adamson, J.C. Alt, R. Emmermann, P.D. Kempton, H. Kinoshita, C. Laverne, M.J.

Mottl, and R.L. Newmark, In situ electrical resistivity and bulk porosity of the oceanic crust Costa Rica Rift, *Nature, 300*, 594-598, 1982.

Becker, K., H. Sakai, et al., *Proc. ODP, Init. Repts. (Pt. A), 111*: College Station, TX (Ocean Drilling Program), 1988.

Bratt, S.R., and G.M. Purdy, Structure and variability of oceanic crust on the flanks of the East Pacific Rise between 11°N and 13°N, *J. Geophys. Res., 89*, 6111-6125,1984.

Burnett, M.S., D.W. Caress, and J.A. Orcutt, Tomographic image of the magma chamber at 12° 50' N on the East Pacific Rise, *Nature, 339*, 206-208, 1989.

Caress, D.W., M.S. Burnett, and J.A. Orcutt, Tomographic image of the axial low velocity zone at 12°50' N on the East Pacific Rise, to be submitted to *J. Geophys. Res.*

Christensen, N.I., Compressional and shear wave velocities at pressures to 10 kilobars for basalts from the East Pacific Rise, *Geophys. J.R. Astron. Soc., 28*, 425-429, 1972.

Christensen, N.I., and G.H. Shaw, Elasticity of mafic rocks from the Mid-Atlantic Ridge, *Geophys. J.R. Astron. Soc., 20*, 271-284, 1970

Detrick, R.S., P. Buhl, E. Vera, J. Mutter, J. Orcutt, J. Madsen, and T. Brocher, Multi-channel seismic imaging of a crustal magma chamber along the East Pacific Rise, *Nature, 326*, 35-41, 1987.

Diebold, J.B., and P.L. Stoffa, The traveltime equation, tau-p mapping and inversion of common midpoint data, *Geophysics, 46*, 238-254, 1981.

Ewing, J.I., and G.M. Purdy, Upper crustal velocity structure in the Rose area of the East Pacific Rise, *J. Geophys. Res., 87*, 8397-8402, 1982.

Fox, P.J., R.S. Detrick, R. Tyce, J. C. Mutter, W.R.J. Ryan, C.H. Langmuir, *ODP East Pacific Rise data synthesis*, 1988.

Harding, A.J., J.A. Orcutt, M.E. Kappus, E.E. Vera, J.C. Mutter, P. Buhl, R.S. Detrick, and T.M. Brocher. The structure of young oceanic crust at 13°N on the East Pacific Rise from expanding spread profiles, *J. Geophys. Res., 94*, 12,163-12196, 1989.

Houtz, R., and J. Ewing, Upper crustal structure as a function of plate age, *J. Geophys. Res., 81*, 2490-2498, 1976.

Hyndman, R.D., and M.J. Drury, The physical properties of oceanic basement rocks from deep drilling on the Mid-Atlantic Ridge, *J. Geophys. Res., 81*, 4042-4060, 1976.

McClain, J.S., J.A. Orcutt, and M. Burnett, The East Pacific Rise in cross section: A seismic model, *J. Geophys. Res., 90*, 8627-8639, 1985.

Mithal, R., and E.E. Vera, Comparison of plane-wave decomposition and slant stacking of point-source seismic data, *Geophysics, 52*, 1631-1638, 1987.

Moos, D., D. Goldberg, M.A. Hobart, and R.N. Anderson, Elastic wave velocities in layer 2A from full waveform sonic logs at hole 504B, *Initial Rep. Deep Sea Drill. Proj., 92*, 563-570, 1986.

Mutter, J.C., G.A. Barth, P. Buhl, R. Detrick, J. A. Orcutt, and A.J. Harding, Magma distribution across ridge-axis discontinuities on the East Pacific Rise from multichannel seismic images, *Nature, 336*, 156-158, 1988.

Newmark, R.L., R.N. Anderson, D. Moos, and M.D. Zoback, Sonic and ultrasonic logging of hole 504B and its implications for the structure, porosity, and stress regime of the upper 1 km of the oceanic crust, *Initial Rep. Deep Sea Drill. Proj., 83*, 479-510, 1985.

Purdy, G.M., New observations of the shallow seismic structure of young oceanic crust, *J. Geophys. Res., 92*, 9351-9362, 1987.

Spudich, P., and J. Orcutt, A new look at the seismic velocity structure of the oceanic crust, *Rev. Geophys., 18*, 627-645,1980a.

Spudich, P., and J. Orcutt, Petrology and porosity of an oceanic crustal site: Results from waveform modeling of seismic refraction data, *J. Geophys. Res., 85*, 1409-1433, 1980b.

Stoffa, P.L., and P. Buhl, Two-ship multichannel seismic experiment for deep crustal studies: Expanded spread and constant offset profiles, *J. Geophys. Res., 84*, 7645-7660, 1979.

Vera, E.E., J.C. Mutter, Crustal structure in the Rose area of the East pacific Rise: One-dimensional travel time inversion of sonobuoys and expanded spread profiles, *J. Geophys. Res., 93*, 6635-6648,1988.

Vera, E.E., *Seismic structure of 0- to 4.5-m.y.-old oceanic crust between 9°N and 13°N on the East Pacific Rise*, Ph.D. Thesis Columbia University, 1989.

Vera, E.E., J.C. Mutter, P. Buhl, J.A. Orcutt, A.J. Harding, M.E. Kappus, R.S. Detrick, and T.M. Brocher, The structure of 0-to 0.2-m.y.-old oceanic crust at 9°N on the East Pacific Rise from Expanded Spread Profiles, *J. Geophys. Res.* (in press).

Figure Captions

Figure 1. R/V R.D Conrad's track in the 9°N survey area. The ESP's midpoints are marked by a dot. The heavy segments on the cross-axis CDP lines represent the axial magma chamber (AMC) event as seen in these lines. The bathymetry is based on a 20-m contour interval chart from a compilation of Sea Beam studies in the area. The dashed contours are extrapolated from measured bathymetry (continuous line contour). Contours are in meters. Areas shallower than 2600m are stippled.

Figure 2. (a) ESP 5AG (Air gun) shot at the rise crest. The main arrivals are labeled: R1, the seafloor reflection; RA, a shallow reflection; T1, rays turned below RA that contain information about the uppermost crustal seismic structure; T2, rays turned below T1; R2 the reflection from the top of the axial magma chamber (AMC); B1 and B2, seafloor reflections for the first and second source bubble pulse reverberation. The AMC event (R2) and its first source bubble pulse reverberation are also indicated by arrows and double arrows respectively. (b) Reflectivity synthetics for the final model (Figure 5). The labels are as in Figure 2a. Note that the gains for the data and the synthetics are not equal, indicating that the T2 and R2 amplitudes are not matched in absolute terms.

Figure 3 tau-p transform of ESP 5AG (Figure 2a) generated by slant stacking including corrections to produce the plane wave decomposition of the x-t point source data [Mithal and Vera, 1987]. The input data were 50 m-equispaced seismograms from

0 to 25 km. The stacking was performed for ray parameters from 0.02 to 0.62 s/km at a 0.002 s/km increment. The labels correspond to those of Figure 2. To clearly map the weak T2 arrivals, the traces up to 2.5 km had to be excluded from the stacking (inset). Note a ray parameter around 0.45 s/km at the point where T1 meets R1 indicating a V_p=2.2 km/s at the seafloor.

Figure 4. Comparison between ESP 5AG and synthetic seismograms for arrivals defining the uppermost crustal velocity structure. A seafloor hyperbolic shift has been applied and the seafloor reflection time, defined as zero. The labels correspond to those of Figure 2. The synthetics include the receiver response and convolution with a source, and the gain has been adjusted to match the amplitude of the data for the near vertical incidence seafloor reflection. (a) Reflectivity calculations of final model (Figure 5). (b) ESP 5AG. The source wavelet was taken from the trace at x=1.2 km retaining the first pulse and the first and second bubble pulse reverberations. (c) WKBJ calculation of final model. (d) WKBJ model where the uppermost crust is approximated by a single velocity gradient (dotted line Figure 5). This model does not produce arrival T1.

Figure 5. Final velocity model and velocity model constructed using the tau-sum recursion [Diebold and Stoffa, 1981] on the postcritical arrivals T1 and T2 (Figure 3). The velocity discontinuity 1.6 km below the seafloor is the axial magma chamber (AMC) interface, and the dotted line corresponds to a model where the uppermost crust is approximated by a single velocity gradient layer [Ewing and Purdy, 1982].

Figure 6. Comparison between WKBJ synthetics for ESP 5AG. The plotting and labels are as in Figure 4. The same P-wave velocity structure (Figure 5) was used in the two cases shown. (a) Seafloor V_S/V_p = 0.43. This case corresponds to the one in Figure 4c and matches the data seafloor reflection amplitudes (R1). (b) Seafloor V_S/V_p = 0.54. The decay of the seafloor reflection amplitudes with distance is faster than in case a and hence faster than in the data.

Figure 7. Comparison between ESP 7AGP (airgun positive) shot 3.1 km west of the rise crest (Figure 1) and reflectivity synthetics for the final model (Figure 8) with emphasis on arrivals T2 and T3. The amplitude maximum around 7.5 km greatly constrains the intermediate crustal velocity structure. Events parallel to and 0.15 s later than the main arrivals correspond to the first bubble pulse reverberation of the source.

Figure 8. ESPs' final velocity models for the upper crust and comparison with hole 504B basement P-wave velocities from *in situ* multichannel sonic logging during Ocean Drilling Program leg 111 [Becker et al.,1988]. Before plotting, the velocity log was smoothed with a 60m running average window. The hole lithology and seismic layers are also shown. There is a remarkable similarity between our solutions and the hole 504B velocities. In both cases the intermediate crustal velocity structure consists of a nearly constant velocity layer overlying a relatively steep velocity gradient zone.

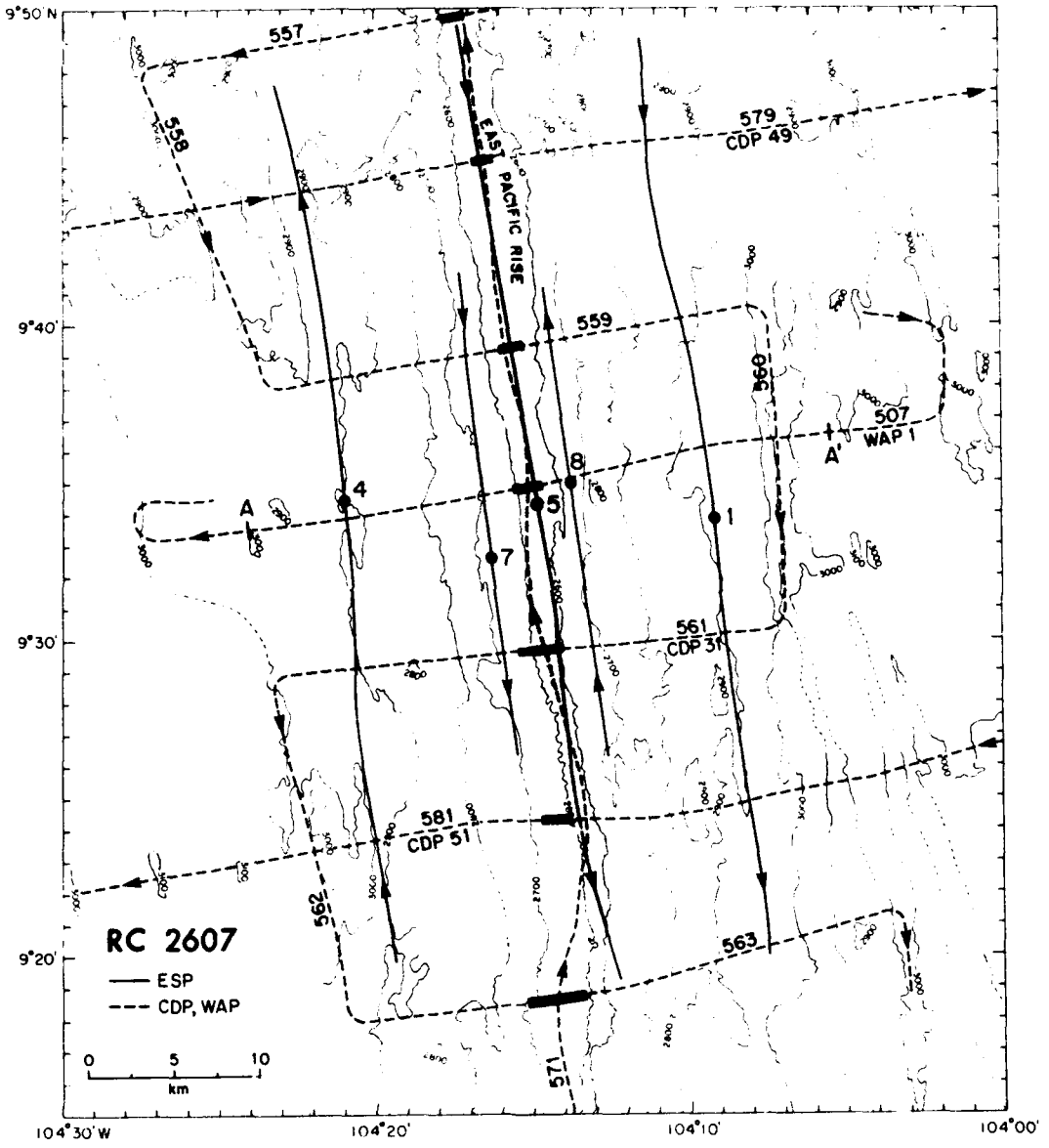
9°50'N
9°40'
9°30'
9°20'
104°30'W
104°20'
104°10'
104°00'
557
558
579
CDP 49
EAST PACIFIC RISE
559
560
507
WAP 1
A
A'
4
5
8
7
1
561
CDP 31
581
CDP 51
562
563
571
RC 2607
ESP
CDP, WAP
0
5
10
km

Fig.1

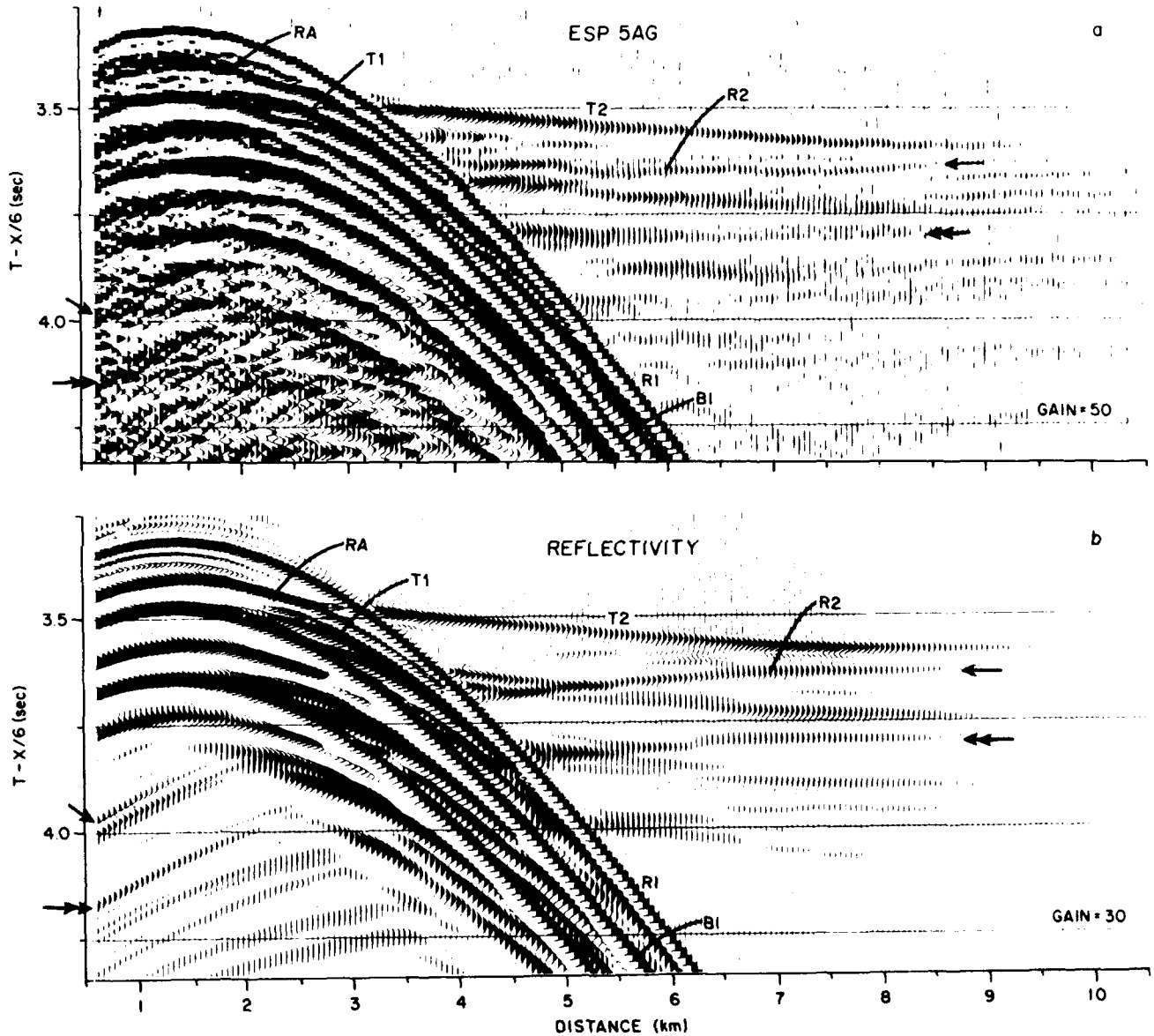
ESP 5AG
a
RA
T1
T2
R2
RI
BI
GAIN=50
T-X/6 (sec)
3.5
4.0
REFLECTIVITY
b
GAIN=30
1
2
3
4
5
6
7
8
9
10
DISTANCE (km)

Fig. 2

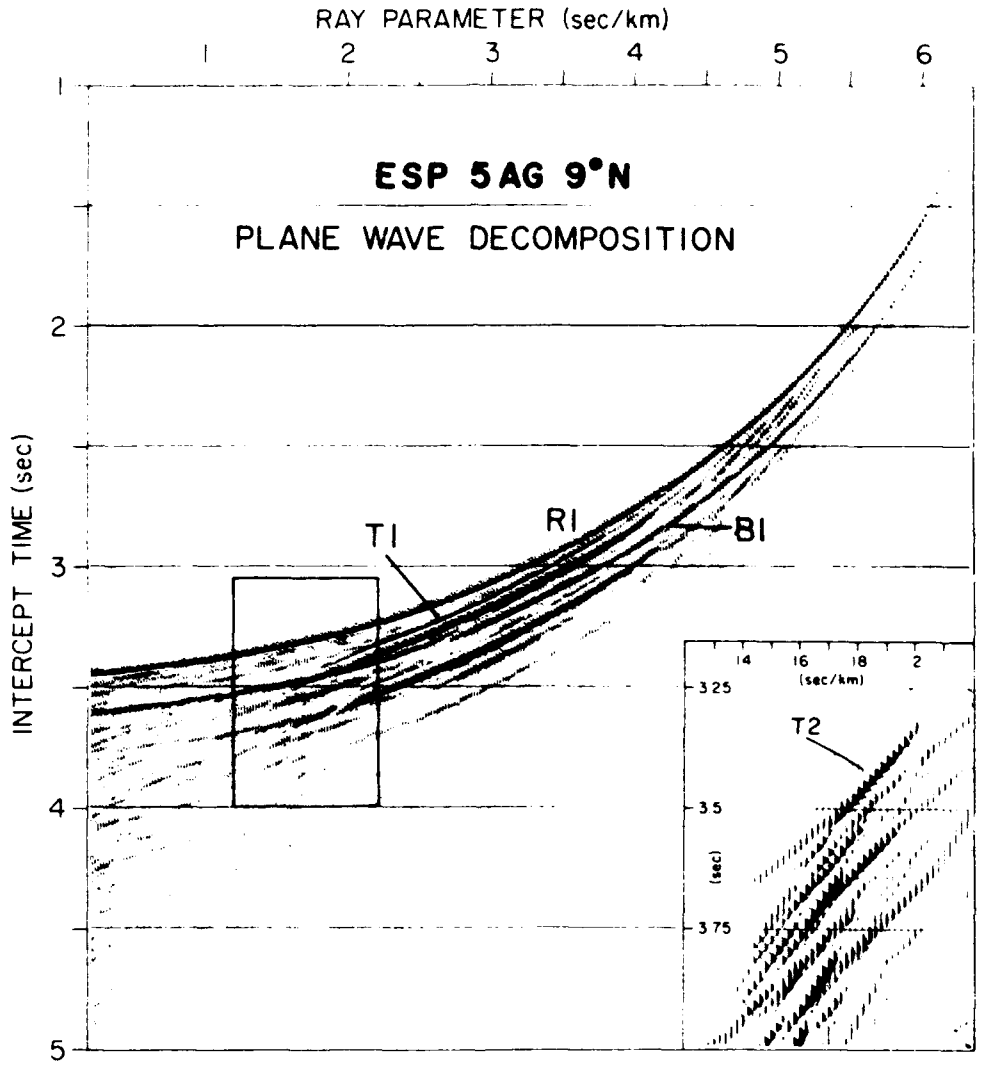
RAY PARAMETER (sec/km)
1
2
3
4
5
6
ESP 5AG 9°N
PLANE WAVE DECOMPOSITION
INTERCEPT TIME (sec)
2
3
4
5
T1
R1
B1
14
16
18
2
(sec/km)
3.25
T2
3.5
(sec)
3.75

Fig. 3

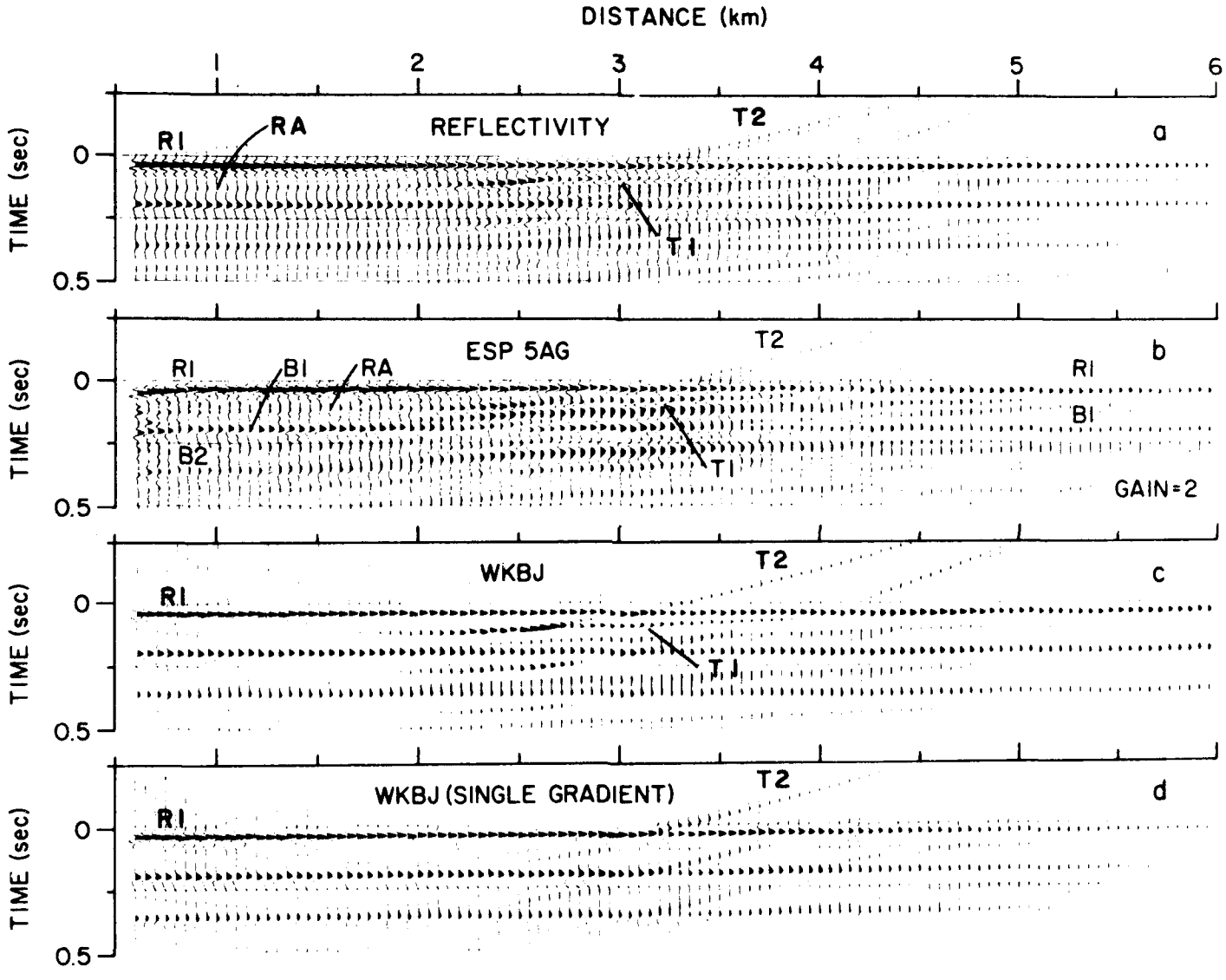
DISTANCE (km)
1
2
3
4
5
6
TIME (sec)
0
0.5
R1
RA
REFLECTIVITY
T2
T1
a
ESP 5AG
B1
B2
GAIN=2
b
WKBJ
c
WKBJ (SINGLE GRADIENT)
d

Fig. 4

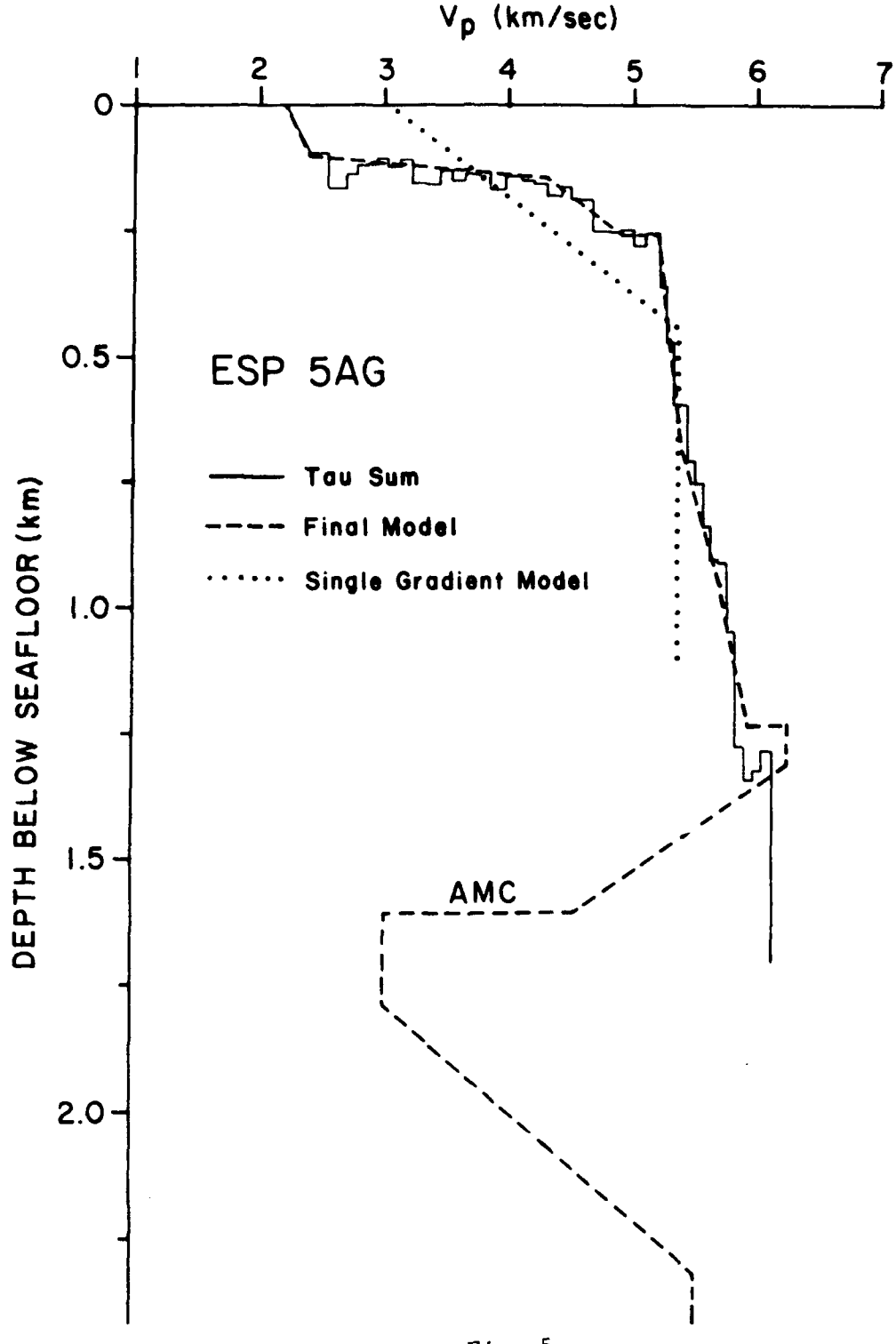
V_p (km/sec)
2
3
4
5
6
7
0
0.5
1.0
1.5
2.0
DEPTH BELOW SEAFLOOR (km)
ESP 5AG
Tau Sum
Final Model
Single Gradient Model
AMC

Fig. 5

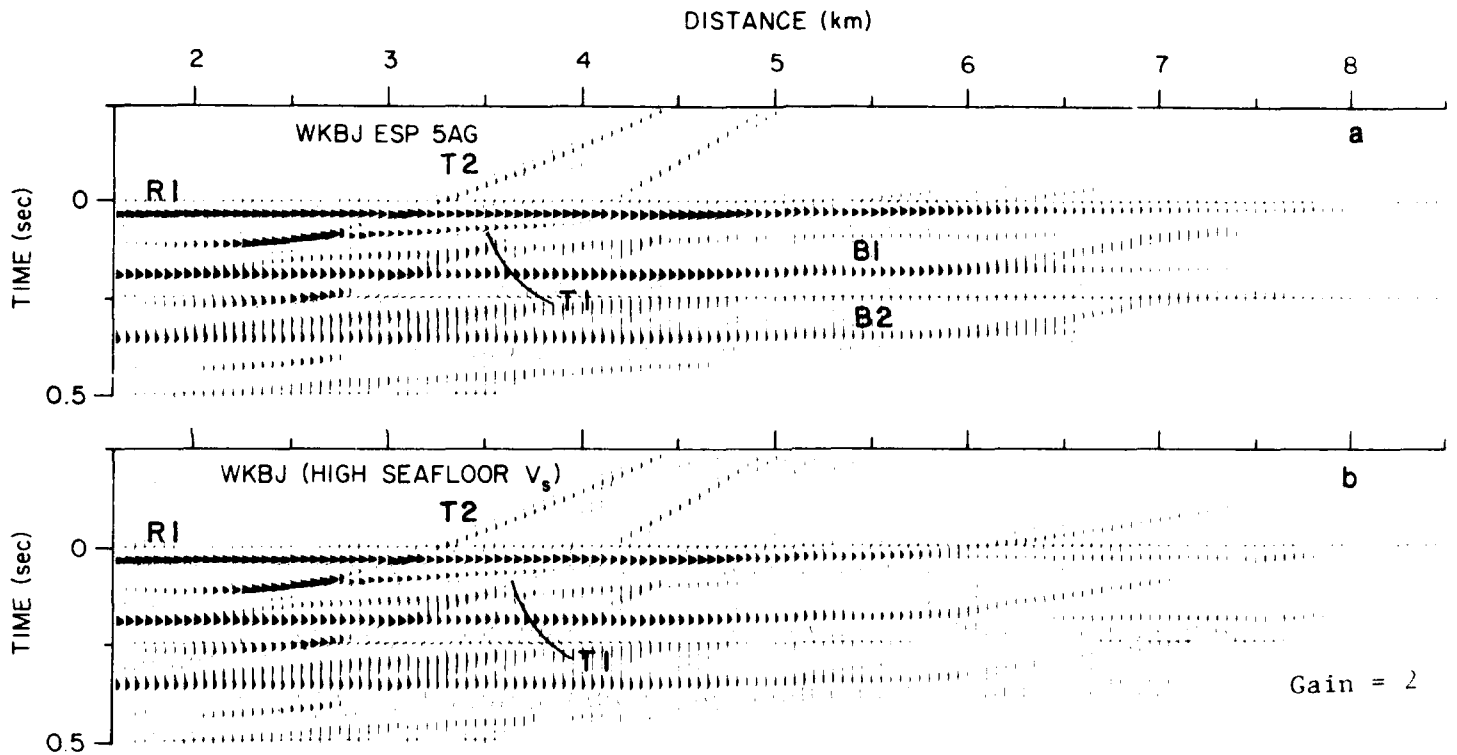
DISTANCE (km)
2
3
4
5
6
7
8
WKBJ ESP 5AG
a
T2
R1
B1
T1
B2
TIME (sec)
0
0.5
WKBJ (HIGH SEAFLOOR V_s)
b
T2
R1
T1
TIME (sec)
0
0.5
Gain = 2

Fig. 6

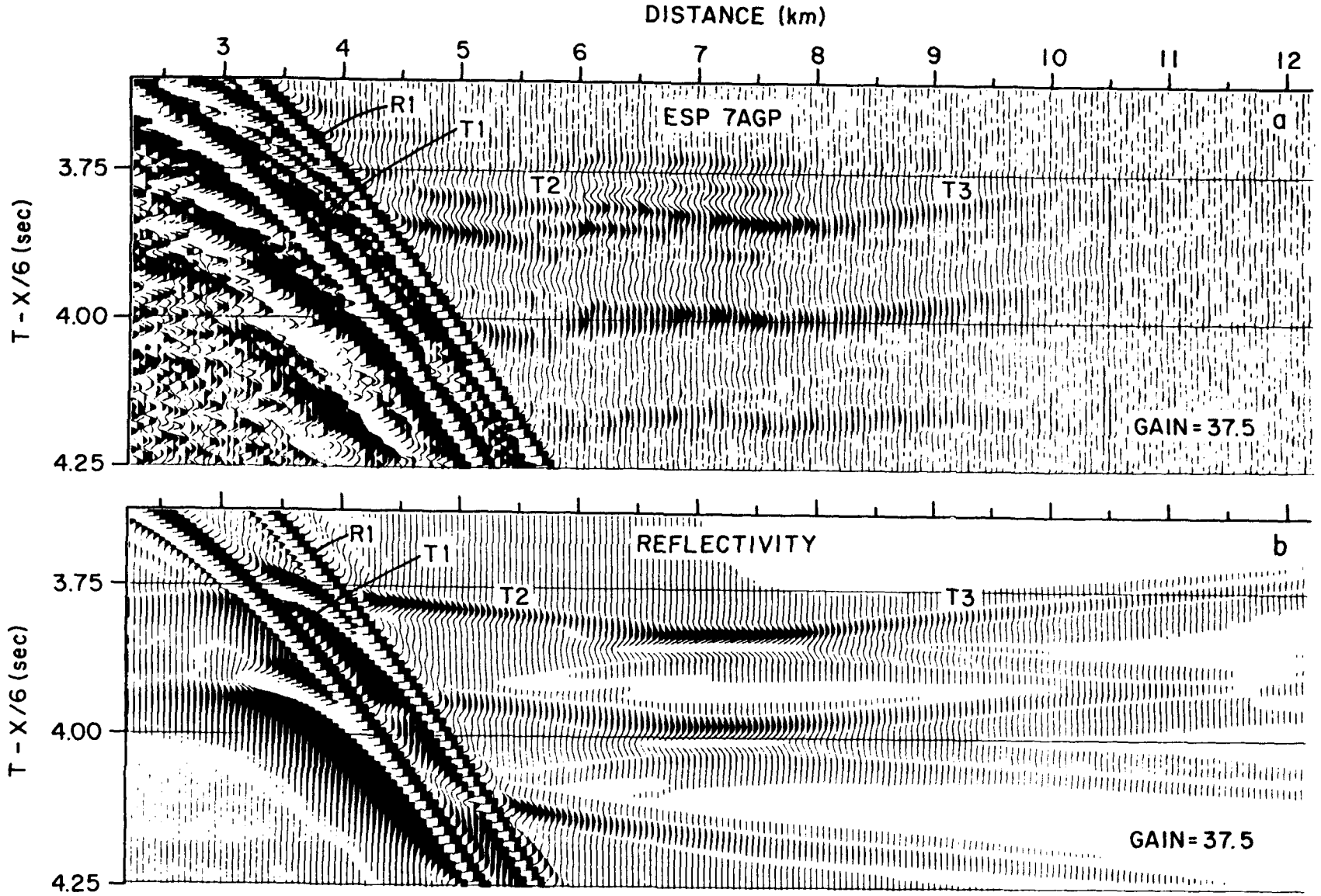
DISTANCE (km)
3
4
5
6
7
8
9
10
11
12
R1
T1
ESP 7AGP
a
T2
T3
3.75
4.00
4.25
T - X/6 (sec)
GAIN = 37.5
R1
T1
REFLECTIVITY
b
T2
T3
3.75
4.00
4.25
T - X/6 (sec)
GAIN = 37.5

Fig. 7

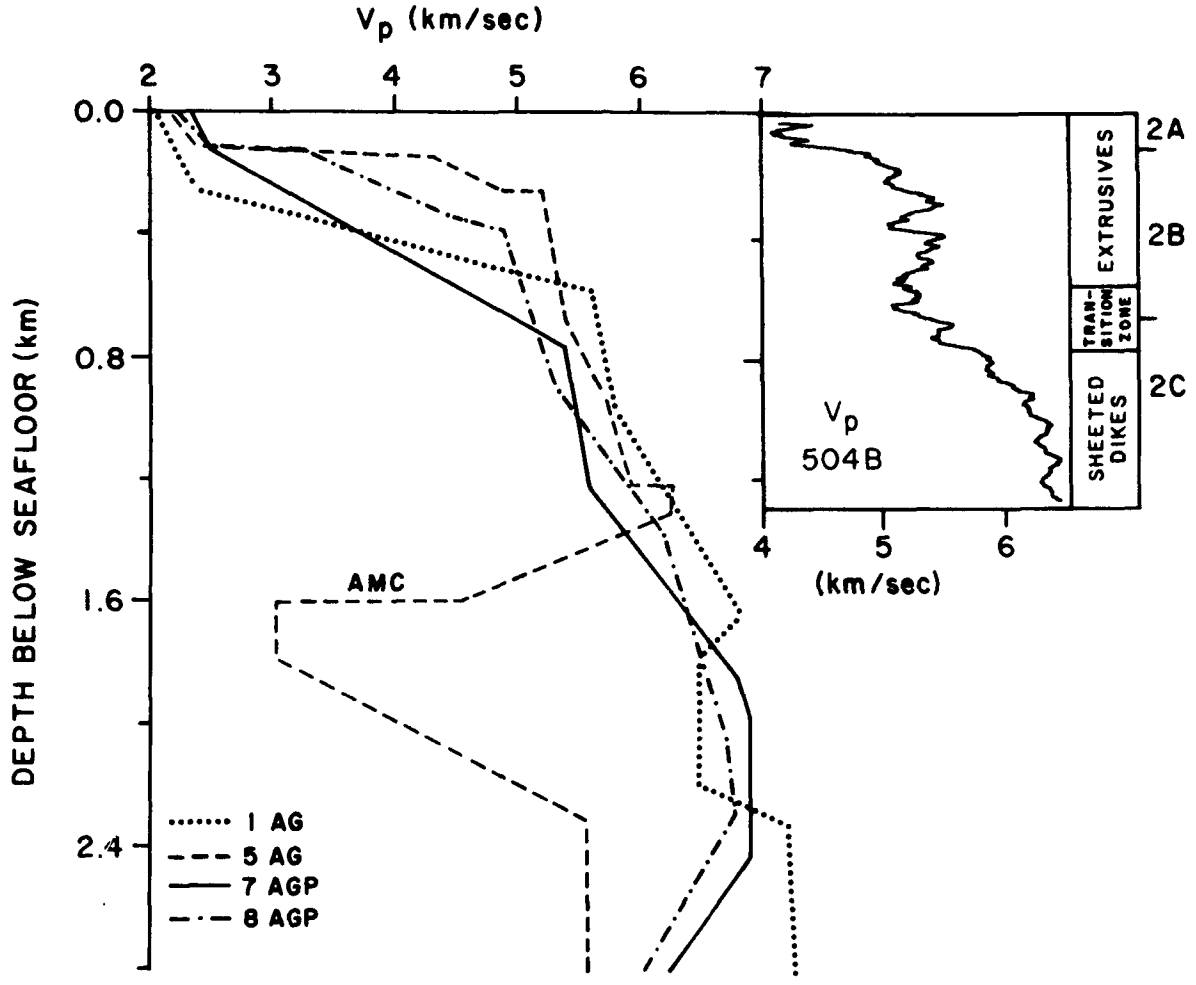
V_p (km/sec)
2
3
4
5
6
7
0.0
0.8
1.6
2.4
DEPTH BELOW SEAFLOOR (km)
AMC
1 AG
5 AG
7 AGP
8 AGP
V_p
504B
4
5
6
(km/sec)
EXTRUSIVES
TRANSITION ZONE
SHEETED DIKES
2A
2B
2C

Fig. 8

THE EVOLUTION IN SEISMIC STRUCTURE OF THE UPPERMOST 0.5 - 1.0 KM OF OCEANIC CRUST

G.M. Purdy
Woods Hole Oceanographic Institution
Woods Hole, MA 02543

Introduction

The single largest and most consistent physical property contrast on the earth's surface is that between the basalts of oceanic layer 2 and the overlying water or sediments. This boundary constitutes the outermost hard rock shell over more than half of the surface area of the globe. Compared with the heterogeneities of the surface of the continents and the structural complexities of the continental margins, the homogeneity on a large scale of this boundary tempts the researcher into the belief that is could contain important and resolvable signals pertaining to the formation and evolution of the oceanic lithosphere. The magnitude of the physical properties change across this boundary also means that it dominates the characteristics of transmitted or reflected seismic energy, and thus is key to the understanding and prediction of long range propagation of low frequency sound in the water column.

The precise architecture of the uppermost 1 km of oceanic crust remains poorly understood. We do not know whether systematic changes in the structure of this uppermost section are caused by differences in accretion rates or by along axis changes in modes of crustal emplacement or simply by temporal changes in the magma supply. Adequate data does not exist to test any of these models. Estimates of the nature of the uppermost crust depend almost exclusively upon careful but ill-constrained analogies with ophiolites (e.g., Spudich and Orcutt, 1980) and to an amazing degree upon the findings at one deep ocean drill hole: 504B (e.g., Becker et al., 1989). One of the few well known characteristics of the top of layer 2 is that its velocity increases with age: we do not know well the rate at which this occurs or indeed whether it occurs uniformly in all oceans. Nor do we understand the physical and chemical processes that control it. But ever since the classic work of Houtz and Ewing (1976), the existence of some kind of substantial systematic age related change in the structure of layer 2 has been well known.

The Results of Houtz and Ewing

This classic paper published in 1976 documented for the first time two important characteristics of oceanic crustal structure. The term 'layer 2A' was introduced to describe a surficial layer of mean velocity 3.64 km/s that was observed widely over young crust in both the Pacific and Atlantic oceans. And they found that over a few tens of millions of years the velocity of this layer increased by more than 1 km/s (Figure 1). Because these results were based on such a large number of consistently interpreted sonobuoy data sets (with nearly identical characteristics) these results were considered robust and credible. Houtz and Ewing concluded that:

> "...layer 2A has either changed diagenetically with the passage of time or that it has been repeatedly intruded by basalts. Any diagenetic change must have taken place under so little overburden pressure that it is difficult to imagine the appropriate process unless it is the filling of voids and cracks by hydrothermal mineralization."

Two primary reasons can be identified to explain why, in the last fifteen years, so little progress has been made in refining and understanding the important relationship illustrated in Figure 1. Knowledge of the architecture of oceanic crust and particularly the upper oceanic crust remains poor. It seems clear that the crust is made up of a set of layers with demonstrably different velocity gradients (e.g., Spudich and Orcutt, 1980; Purdy and Ewing, 1986) but the correlation of the seismic characteristics of these layers with their geological structure remains extremely ambiguous. Within the uppermost crust a number of seismic signatures are tantalizing in their consistency but they cannot be unequivocally linked to their structural cause. With the application of modern multichannel seismic reflection techniques to structure problems in the deep ocean, many identifications have been made of consistent reflectors in the shallow crust (Herron, 1982; Musgrove and Austin, 1983; Detrick et al., 1987; Rohr et al., 1988). Careful analyses of the amplitude relations of short-range (5-10 km) refracted phases (e.g., Bratt and Purdy, 1984; Fischer and Purdy, 1986) has also revealed that major boundaries, across which there are substantial changes in physical properties (i.e., >20%), must occur in the uppermost 1-2 km. However, compiling these scattered observations into a coherent picture of the shallow structure is not simple, as is illustrated in Figure 2 (from Purdy, 1986).

New Measurements

The second primary reason for slow progress is the well known problem that seismic energy turning in the uppermost crust is never observed as a first arrival in a conventional deep ocean seismic refraction experiment. The desire to carry out precise measurements of shallow crustal structure prompted the development of a new deep-towed seismic source (Koelsch et al., 1986) that, along with conventional ocean bottom hydrophones or seismometers, would allow complete small-scale experiments to be carried out actually on the deep ocean floor. The use of this prototype source on the Mid-Atlantic Ridge in 1985 produced the first unequivocal evidence for the presence of extremely low velocities (~2.1 km/s) within the basalts near the seafloor on crust less than a few hundred thousand years old (Purdy, 1987). Although several previous conventional experiments (e.g., Keen and Tramontini, 1970; Talwani et al., 1971; Houtz and Ewing, 1976; Whitmarsh, 1978; Ewing and Purdy, 1982) inferred shallow velocities in the range 2.2-4.0 kms^{-1}, the observations from the MAR using the deep towed explosive source constituted the first unambiguous direct observations. Primary refracted diving waves that had turned within a few tens of meters of the seafloor were observed as first arrivals with phase velocities less than 2.5 km/s. These new observations when combined with other selected shallow crustal measurements suggested an even more dramatic evolutionary story than that proposed by Houtz and Ewing, 1976. The data compilation shown in Figure 3 (from Purdy, 1986) shows that, on the seismic scale of >100m, at zero age the volcanic crust at the seafloor has a velocity that is one third that of the basalts that we know constitute this layer, and secondly that, again at the seismic scale, the velocity at the seafloor doubles during the first few millions of years after its formation.

Confirmation that the very low seafloor velocities (<2.5 km/s) observed by Purdy (1987) in the Atlantic also exist on young Pacific crust is provided by the careful interpretation of expanding spread profile (ESP) results from the East Pacific Rise near 13°N (Harding et al., 1989) and 9°30'N (Vera et al., 1990; Vera and Mutter, this report). An important new observation revealed by these experiments was the presence of a major boundary that marked the base of this surficial low velocity (SLV) layer. The most reasonable explanation why this boundary was not detected by the on-bottom refraction experiments in the Atlantic is that the SLV layer was substantially thicker. Velocity-depth functions determined from airgun refraction data on the MAR (Purdy and Detrick, 1986) and on the Endeavor segment of the Juan de Fuca ridge (Cudrak, 1988), when compared with the EPR structure determined by the ESP's (Figure 4) is suggestive that slower

spreading ridges (like the MAR and Juan de Fuca) generate a substantially thicker SLV layer than the EPR. Insufficient data exists to confirm this, but Figure 4 presents an intriguing observation. The nature of this SLV layer and of the prominent boundary that marks its base are important unknowns.

Evolution on a Different Time Scale?

Although the rates of change of velocity depicted in Figures 1 and 3 are substantially different, both results refer to processes that are occurring over temporal scales of millions of years and spatial scales of hundreds of kilometers. A new set of observations now suggests however that a very different evolutionary process may be occurring in the uppermost crust that influences the structure dramatically during the first 20000 years of its life. In 1985 McClain et al. published a model of the East Pacific Rise that included a narrow zone over the rise crest itself of higher velocity shallow crustal material. Their model suggested that decrease in velocity with age occurred, not an increase. When McClain's dataset was reinterpreted several years later by Burnett et al., 1989 using formal inverse methods, this same high velocity anomaly remained a prominent characteristic of the shallow crust over the rise crest. An independent three-dimensional seismic tomography experiment (Toomey et al., 1990) also carried out on the EPR but at a location 200 nm south of McClain's site, produced an extremely similar result (Figure 5). Most important of all, this experiment established the along-axis continuity of this high velocity anomaly. The limited depth resolution of these tomographic solutions however does not constrain whether or not this anomaly in fact resides within the SLV layer.

Tomographic results from the MAR at 26°N (Kong, 1990) reveal features that have some similarity. Comparable changes in velocity are observed in the uppermost 1 km but the changes occur along axis over distances of 10-15 km, not across axis. On the MAR the shallow high velocity anomaly seems to be located over the along-axis topographic high.

Processes

The goal of this paper is to present a summary of the seismic observations that support the existence of systematic evolutionary processes in the shallow crust. However, it cannot be completed without brief comments about the mechanisms that could be responsible for the profound observed changes in physical properties.

As explained in Purdy, 1987, if the 2 km/s change in velocity seen in Figure 3 is indeed a consequence of age-related modifications to the physical properties of the crust, and if the primary change is in only the total porosity, then a 15-20% reduction in porosity over ~7 my is required to explain these observations. This is extremely unlikely because any such pervasive process capable of causing such a huge porosity change (e.g., off-axis volcanism, secondary mineral deposition, tectonic compression) would have been previously observed in geophysical and sampling data. As explained elsewhere in this report, a far more probable scenario is that the primary change is due not to an alteration in the magnitude of the porosity but by a change in the shapes of the voids and cracks that make up the porosity (accompanied by a modest change of a few percent in the total porosity itself). Such a process is simple to imagine (see Figure 1 of Fryer and Wilkens, this report): when the surfaces of the breccia that make up the SLV layer are coated by a thin hydrothermal deposit, although the porosity is only slightly reduced, the mean aspect ratio of the void spaces changes dramatically.

A robust explanation for the narrow high velocity anomalies observed along the rise crest is much more problematical (Figure 5). Two classes of explanation exist: *Tectonic*, in which the crestal high velocity region is considered to be young unfractured volcanic flows the velocity of which is dramatically reduced within ~1 km of the emplacement zone by faulting and fissuring and *Volcanic* in which the observation of high crestal velocities is considered to be an artifact of the poor depth resolution of the tomographic techniques and is in fact due to a lateral change in the vertical structure of the crust, perhaps the rapid subsidence of the dikes as the extrusive layer is built up over them (Toomey et al., 1990). The second explanation is favored because of the common observation of pervasive fissuring throughout the axial summit region and secondly because it could also serve to explain the MAR observation of Kong 1990, i.e., the dikes reach closest to the seafloor at an along-axis topographic high.

References

Becker, K., H. Sakai, A.C. Adamson, J. Alexandrovich, J.C. Alt, R.N. Anderson, D. Bideau, R. Gable, P.M. Herzig, S. Houghton, H. Ishizuka, H. Kawahata, H. Kinoshita, M.G. Langseth, M.A. Lovell, J. Malpas, H. Masuda, R.B. Merrill, R.H. Morin, M.J. Mottl, J.E. Pariso, P. Pezard, J. Phillips, J. Sparks, S. Uhlig, 1989. Drilling deep into young oceanic crust, Hole 504B, Costa Rica Rift, *Rev. Geophysics, 27*, 79-102.

Bratt, S.R. and G.M. Purdy, 1984. Structure and Variability of Oceanic Lithosphere on the Flanks of the East Pacific Rise between 11° and 13°N, *Jour. Geophys. Res., 89*, 6111-6125.

Cudrak, C.F., 1988. *Shallow Crustal Structure of the Endeavor Ridge Segment, Juan de Fuca Ridge, from a Detailed Seismic Refraction Survey*, Unpubl. Ph.D. Thesis, Univ. of British Columbia, Vancouver, BC.

Detrick, R.S., P. Buhl, E. Vera, J. Mutter, J. Orcutt, J. Madsen, T. Brocher, 1987. Multichannel Seismic Imaging of the axial magma chamber along the East Pacific Rise between 9°N and 13°N, *Nature, 326*, 35-41.

Ewing, J.I. and G.M. Purdy, 1982. The Upper Crustal Velocity Structure in the ROSE Area of the East Pacific Rise, *Jour. Geophys. Res., 87*, 8397-8402.

Fischer, K.M. and G.M. Purdy, 1986. Seismic Amplitude Modeling and the Shallow Crustal Structure of the East Pacific Rise at 12°N, *Jour. Geophys. Res., 91*, 14006-14014.

Harding, A.J., J.A. Orcutt, M.E. Kappus, E.E. Vera, J.C. Mutter, P. Buhl, R.S. Detrick and T.M. Brocher, 1989. Structure of young oceanic crust at 13° N on the East Pacific Rise from expanding spread profiles, *J. Geophys. Res., 94*, 12163-12196.

Herron, T.J., 1982. Lava Flow Layer - East Pacific Rise, *Geophys. Res. Lett., 9*, 17-20.

Houtz, R. and Ewing, J.I., 1976. Upper crustal structure as a function of plate age, *J. Geophys. Res., 81*, 2490-2498.

Keen, C. and C. Tramontini, 1970. A seismic refraction survey on the Mid-Atlantic Ridge, *Geophys. J.R. astr. Soc., 20*, 473-491.

Koelsch, D.E., W.E. Witzell, J.E. Broda, F.B. Wooding and G.M. Purdy, 1986. A Deep-Towed Explosive Source for Seismic Experiments on the Ocean Floor, *Mar. Geophys. Res., 8*, 345-361.

Kong, L.S.L., 1990. *Variations in Structure and Tectonics along the Mid-Atlantic Ridge: 23 N and 26 N*, Ph.D. Thesis, WHOI/MIT Joint Program in Oceanography, Woods Hole Oceanographic Institution.

Musgrove, L.A. and J.A. Austin Jr., 1983. Intrabasement structure in the southern Angola Basin, *Geology, 11*, 169.173.

Purdy, G.M., 1987. New Observations of the Shallow Seismic Structure of Young Oceanic Crust, *Jour. Geophys. Res., 92*, 9351-9362.

Purdy, G.M., 1986. Processes of Evolution of the Uppermost Crust in the MARK Area, *EOS, 67*, p. 1213.

Purdy, G.M. and R.S. Detrick, 1986. The Crustal Structure of the Mid-Atlantic Ridge at 23°N from Seismic Refraction Studies, *Jour. Geophys. Res., 91*, 3739-3762.

Rohr, K.M.M., B. Milkereit and C.J. Yorath, 1988. Asymmetric Structure across the Juan de Fuca Ridge, *Geology, 16*, 533-537.

Spudich, P. and J. Orcutt, 1980. A new look at the seismic velocity structure of the oceanic crust, *Rev. Geophys. Space Phys., 18*, 627-645.

Talwani, N., C.C. Windisch and M.G. Langseth, Reykjanes Ridge Crest, 1971. A detailed geophysical study, *J. Geophys. Res., 76*, 473-517.

Toomey, D.R., G.M. Purdy, S.C. Solomon and W.S.D. Wilcock, 1990. The Three-dimensional Seismic Velocity Structure of the East Pacific Rise near latitude 9°30'N, *Nature, 347*, 639-645.

Vera, E.E., J.C. Mutter, P. Buhl, J.A. Orcutt, A.J. Harding, M.E. Kappus, R.S. Detrick and T. Brocher, 1990. The structure of 0- to 0.2 m.y. old oceanic crust at 9° N on the East Pacific Rise from expanded spread profiles, *J. Geophys. Res., 95*, 15529-15556.

Whitmarsh, R.B., 1978. Seismic refraction studies of the upper igneous crust in the North Atlantic and porosity estimates for Layer 2, *Earth Planet. Sci. Lett., 37*, 451-464.

Figure Captions

Fig. 1 The classic relationship of Houtz and Ewing (1976) shows the velocity of Layer 2A plotted against crustal age in millions of years. Open circles are data points from the Atlantic Ocean, solid dots are from the Pacific. The number of sonobuoy determinations used to compute each mean value is shown by the data point.

Fig. 2 Overview of the key pieces of evidence concerning layer boundaries in the oceanic crust compiled against two-way reflection time in seconds. Selected data is included from drilling (395A and 504B), refraction experiments (B+P = Bratt and Purdy, 1984; F+P = Fischer and Purdy, 1986; NAT = North Atlantic Transect) and reflection profiles (J de F = Juan de Fuca, Rohr et al., 1988; EPR = Detrick et al., 1987).

Fig. 3 Compilation of young shallow igneous crust velocities from laboratory sample measurements (open circles) at the 'classic' drill sites on the Mid-Atlantic Ridge (648B, 332 and 395A) and flanks of the Galapagos spreading center (504B). Solid dots are refraction velocity measurements: the bold arrows indicate the two on-bottom refraction measurements from Purdy (1987). The refraction velocities double over the first few million years and are one third the lab sample values at zero age. From Purdy (1986).

Fig. 4 A comparison of three velocity-depth functions for the uppermost crust: EPR from the East Pacific Rise at 13°N (Harding et al., 1989); J de F from the Endeavor Segment of the Juan de Fuca Ridge (from Cudrak, 1988); MAR from the median valley of the Mid-Atlantic Ridge near 23°N (from Purdy and Detrick, 1986). *Note the dramatic difference in the thickness of the surficial low velocity layer between the fast spreading EPR, and the slow and intermediate spreading rate MAR and Juan de Fuca.*

Fig. 5 A horizontal cross section through a three dimensional P wave velocity structure resulting from tomographic inversion of a seismic refraction data set collected over the crest of the EPR near 9°30'N (from Toomey et al., 1990). The velocity model is represented by perturbations from an average one dimensional model over the area. The y axis is aligned with the regional trend of the EPR (N8°W), and the 0,0 coordinate coincides with the rise axis at latitude 9°30.72'N. The contour interval is 0-2 km/s. The stippling highlights the 1-2 km wide high velocity anomaly that follows the rise crest.

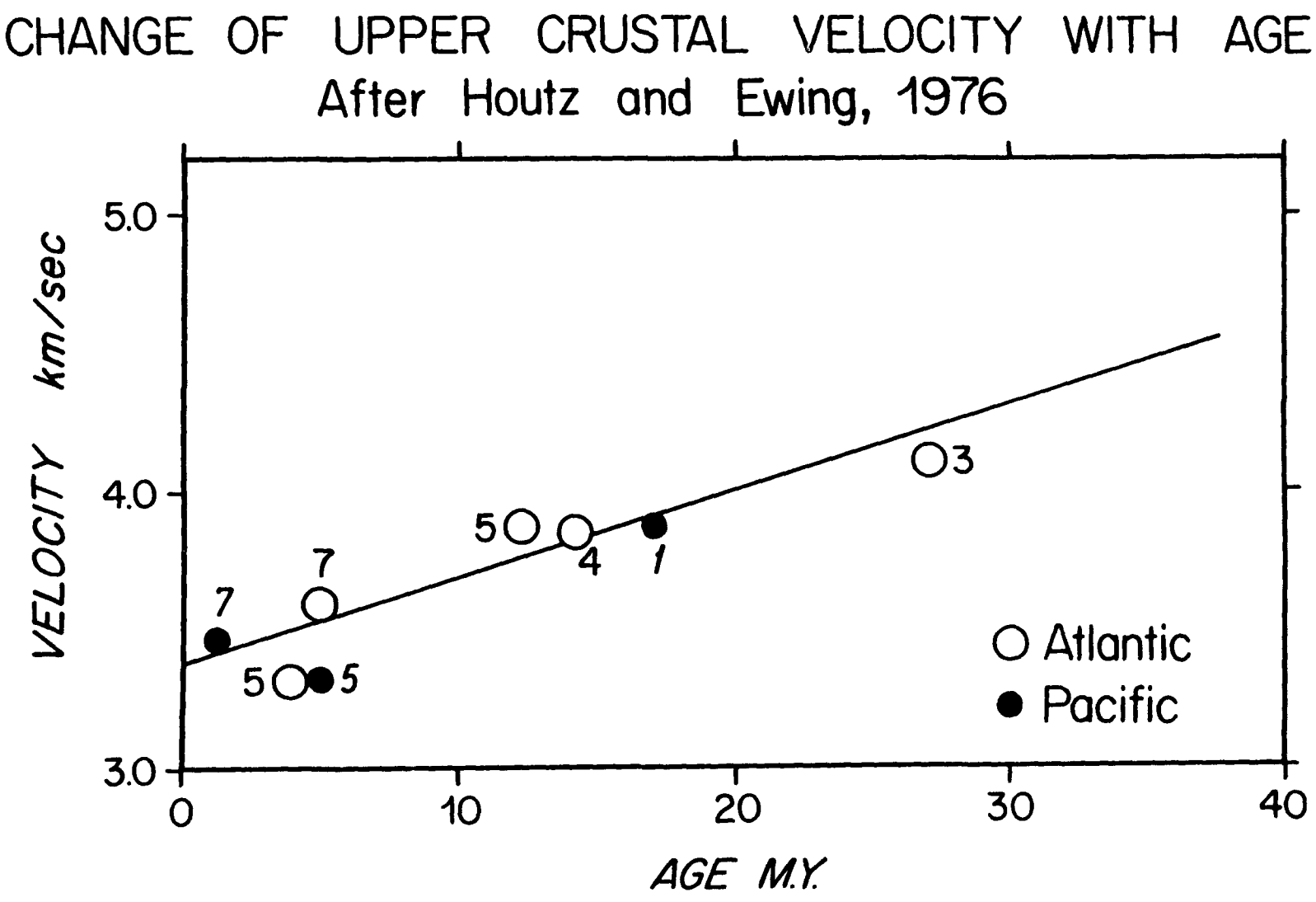
CHANGE OF UPPER CRUSTAL VELOCITY WITH AGE
After Houtz and Ewing, 1976
VELOCITY km/sec
5.0
4.0
3.0
0
10
20
30
40
AGE M.Y.
7
7
5
5
5
4
1
3
Atlantic
Pacific

Figure 1

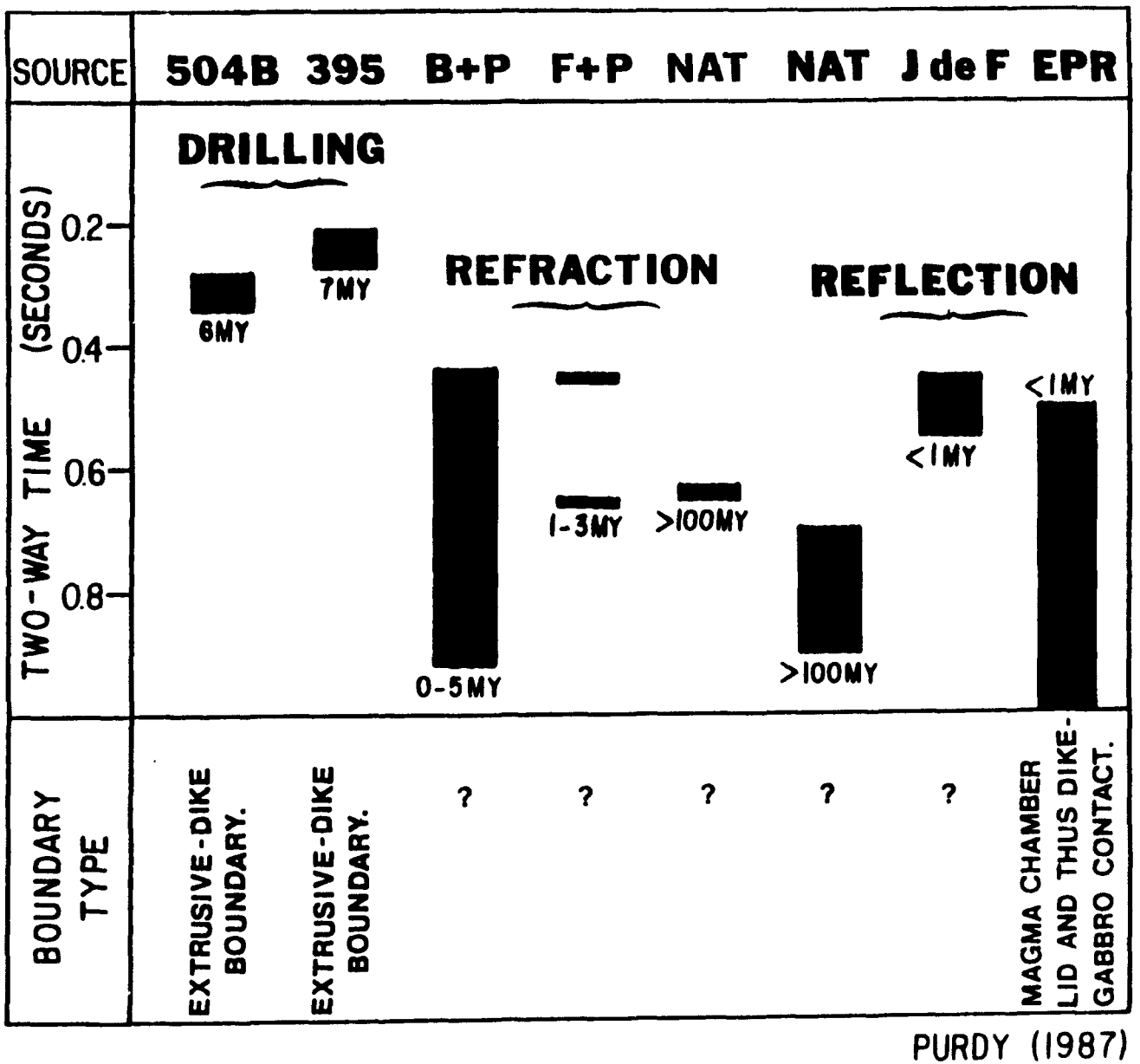
LAYERING OF THE UPPER OCEANIC CRUST
SOURCE
504B
395
B+P
F+P
NAT
NAT
J de F
EPR
DRILLING
REFRACTION
REFLECTION
TWO-WAY TIME (SECONDS)
0.2
0.4
0.6
0.8
6MY
7MY
0-5MY
1-3MY
>100MY
>100MY
<1MY
<1MY
BOUNDARY TYPE
EXTRUSIVE-DIKE BOUNDARY.
EXTRUSIVE-DIKE BOUNDARY.
?
?
?
?
?
MAGMA CHAMBER LID AND THUS DIKE-GABBRO CONTACT.
PURDY (1987)

Figure 2

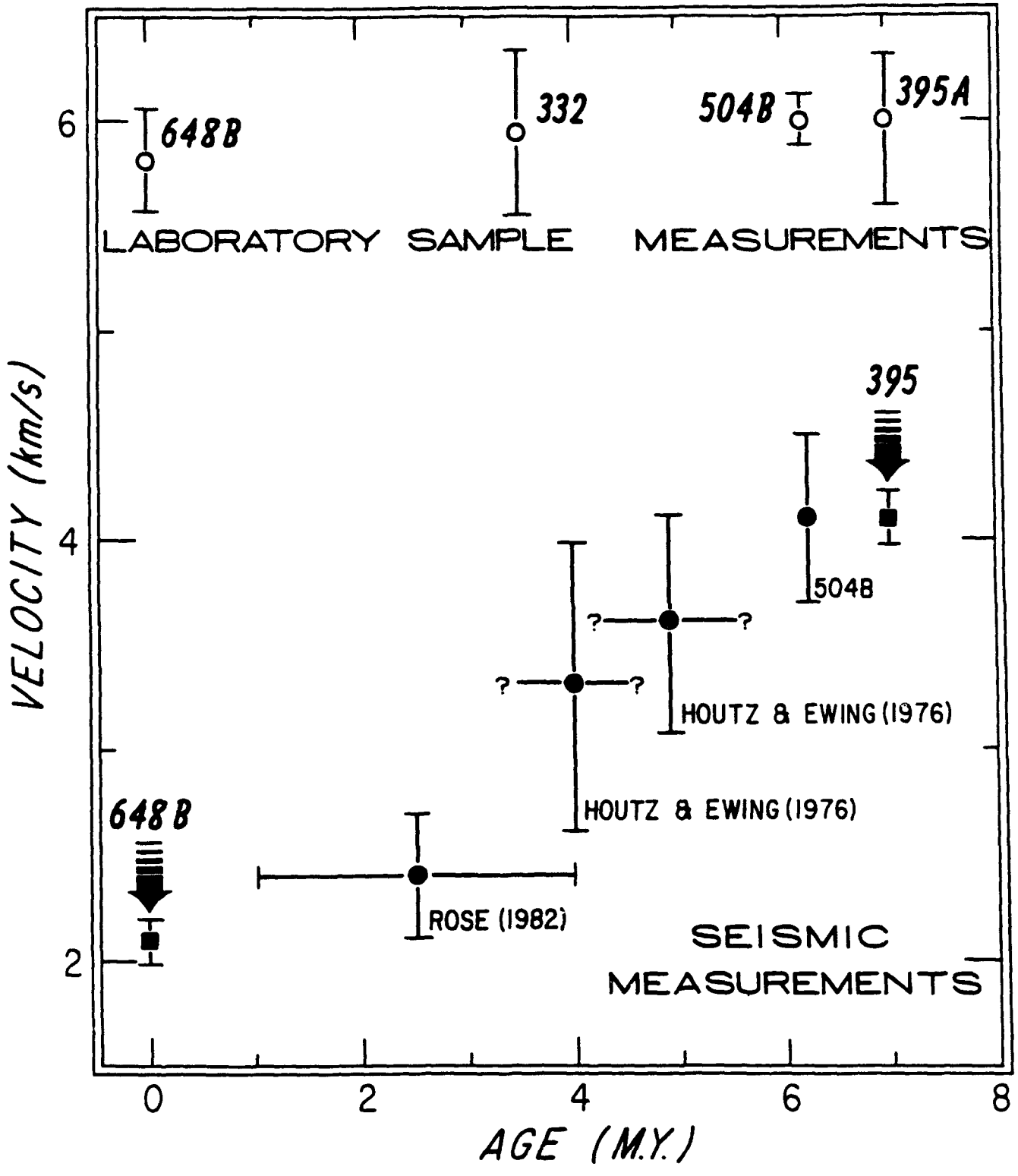
6
4
2
VELOCITY (km/s)
0
2
4
6
8
AGE (M.Y.)
648B
332
504B
395A
LABORATORY SAMPLE MEASUREMENTS
395
504B
?
?
?
?
HOUTZ & EWING (1976)
HOUTZ & EWING (1976)
648B
ROSE (1982)
SEISMIC
MEASUREMENTS

Figure 3

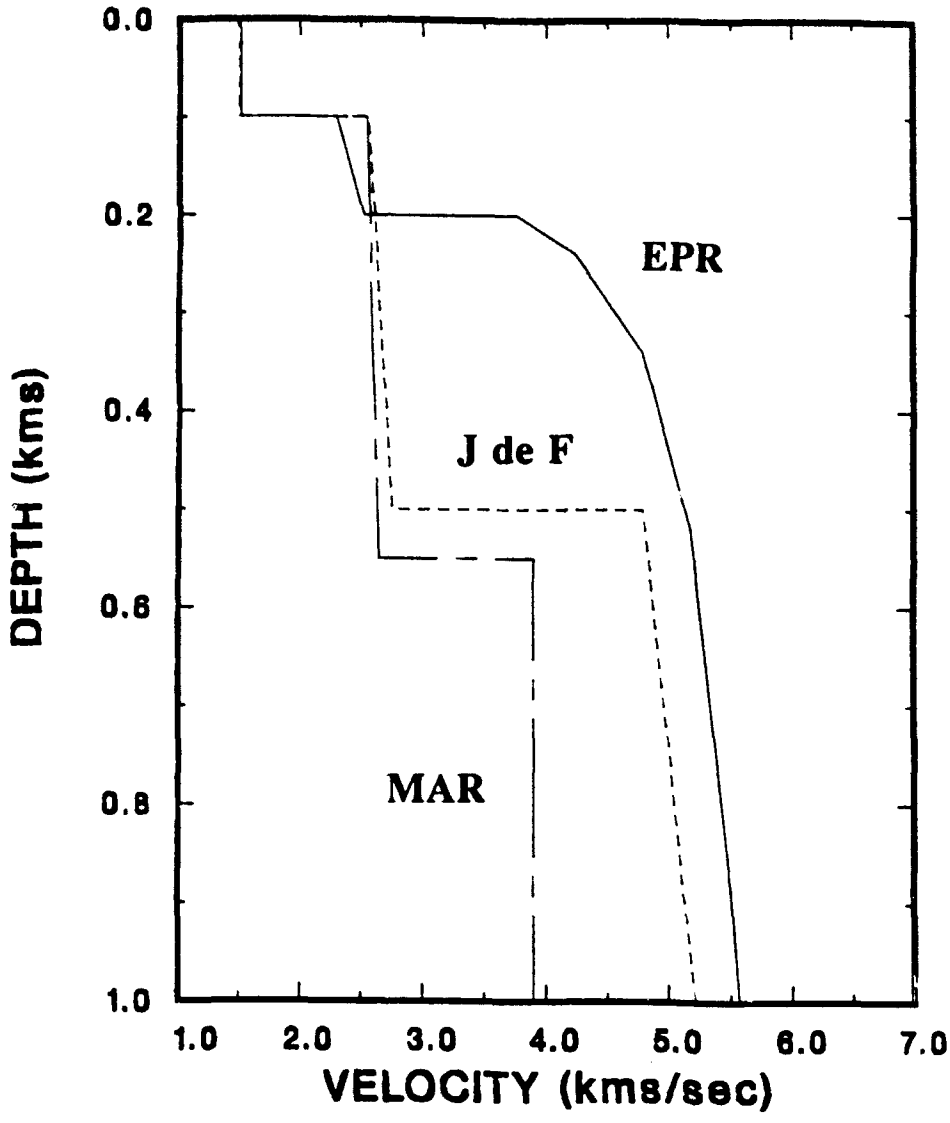
0.0
0.2
0.4
0.6
0.8
1.0
DEPTH (kms)
EPR
J de F
MAR
1.0
2.0
3.0
4.0
5.0
6.0
7.0
VELOCITY (kms/sec)

Figure 4

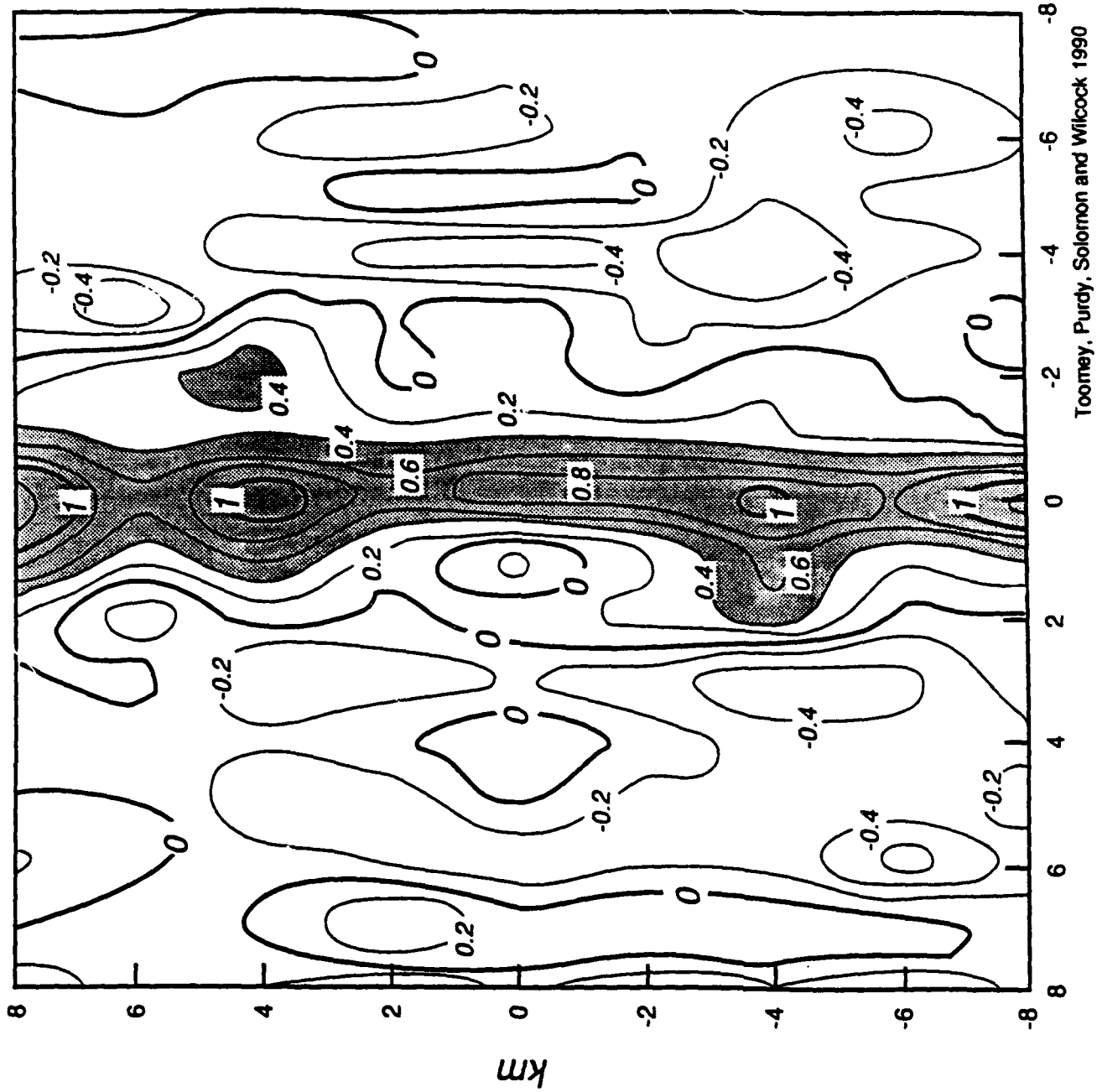

Figure 5

RESOLUTION OF THE STRUCTURE AND PHYSICAL PROPERTIES OF THE UPPER OCEANIC CRUST USING DOWNHOLE MEASUREMENTS

Keir Becker
Division of Marine Geology & Geophysics, University of Miami
Miami, FL 33149

Introduction: Unique Contributions and Limitations of Downhole Measurements

Downhole measurements offer many unique contributions towards the detailed resolution of the structure and physical properties of the upper oceanic crust. Perhaps the most important is the ground truth that downhole measurements provide -- the continuous record of the vertical variation of properties in situ, at averaging scales ranging from cm's up to the hundreds of m's that are typical of remote seismic sensing of the upper crust (Table 1). Without this kind of ground truth, we cannot expect to develop the ability to predict the effect of young volcanic seafloor on acoustic propagation, much less to invert remotely observed signals to assess the structure and evolution of the upper oceanic crust. The recovered cores are of course also important in this regard; however, given the typically poor core recovery in holes that penetrate young volcanic seafloor as well as the possible effects of large-scale porosity that cannot be preserved in the recovered core, downhole measurements provide our best direct resolution of the physical properties of the upper oceanic crust.

Unfortunately, there are practical and technological limitations to the benefits derived from coring and downhole measurements, primarily because young volcanic seafloor is often difficult to drill. As a result, there are relatively few upper crustal reference holes more than a few hundred m deep, and many of these have both poor core recovery and poor hole conditions. These provide difficult conditions for calibration of the responses of downhole tools, but even then the logs provide our best record of the structure and lithology of the crust.

An important implication is that we must reserve our major downhole measurements efforts for detailed studies at a few sites, and that these sites must be well characterized before drilling. A few good examples of deep crustal reference holes have already been drilled and extensively logged (Figure 1), but this group particularly lacks sites in 'normal' crust formed at fast spreading rates like much of the Pacific. The few deep crustal holes tend to dominate our thinking as reference sites, whether or not they are somehow 'characteristic' sites. An important task of this workshop is to specify both what defines a characteristic site and where such characteristic sites are most needed given the great effort that is required to survey and drill them.

Important Issues and Future Developments in Downhole Measurements

The suite of downhole measurements and logs mobilized for ODP is among the most advanced sets of tools used in any drilling program in the world (e.g., Worthington et al., 1989). As is summarized in Table 1, these tools allow the resolution of a number of important properties at a range of vertical and horizontal averaging scales. For example, the properties that are measured best over the widest range in scales are compressional velocity and electrical resistivity. Four crustal reference holes (418A, 395A, 504B, and 735B) were logged with this suite of tools during the first three years of ODP, and good

discussions of these results can be found in the relevant ODP volumes and a JGR special section published in June 1990 (see bibliography).

However, the focus of this brief report is not to summarize these exciting results, but instead to concentrate on those issues which promise even greater returns given further development. Our experience in applying such a powerful set of tools in heterogeneous formations like the upper oceanic crust has shed much light, but also raised a number of important scientific issues and technical problems. Some of these issues are related to specific measurements that have not yet been properly made, and others concern more general scientific matters. In the remainder of this report, some of the more important of these issues are summarized.

How representative are single vertical sections?

This question must always be considered in assessing core and logs from any single vertical hole, and particularly applies to holes that penetrate young volcanic seafloor, which we must expect to be laterally and vertically heterogeneous. For example, the classic reference Hole 504B was originally located in supposedly sealed, 5.9-m.y.-old crust with relatively smooth basement relief, a thick, relatively uniform sediment cover, and conductive heat flow closely matching that predicted by plate theory (Langseth et al., 1983). These are all conditions under which a single hole might be expected to be somewhat representative on a regional scale, yet subsequent geophysical surveys and downhole measurements have revealed considerable lateral variability in geothermal processes (e.g., Mottl et al., 1983; Langseth et al., 1988; Fisher et al., 1990), and in seismic properties (e.g., Stephen, 1985, 1988; Collins et al., 1989).

Such heterogeneity is probably even more pronounced in younger and less-sealed crust, and may also be the case in old crust, so the few reference holes must be carefully sited with respect to geophysical surveys that fully characterize the upper oceanic crust and its lateral variability. In many cases, single holes will be inadequate to determine the in situ properties that account for this variability; instead, carefully selected multi-hole sites will be required to assess the causes for lateral heterogeneity and their effects on remote geophysical observations. Given the great effort required to establish an ODP hole in young oceanic crust, consideration should be given to placing additional holes near existing successful holes, whether or not these sites are ideally 'characteristic' sites. Indeed, there is an initiative now developing within ODP to identify a few such multi-hole, 'crustal characterization' sites, for which likely candidates might be second holes near 395A or 504B.

Developing a True Measure of Porosity

Nearly all of the measurements listed in Table 1 are affected by porosity, and many could in some sense be inverted to estimate porosity. However, none of these inversions can be shown to yield accurate determinations of the in situ porosity and its nature in young oceanic crust. This is partly because of the variable nature and great range of scales of the porosity in young oceanic crust, but is also because no tool truly measures porosity. Even the so-called neutron 'porosity' log does not measure actual porosity, but instead responds to the presence of hydrogen -- which can occur in the upper oceanic crust in other forms (e.g., alteration products) than the seawater that occupies pore space. The best that can be done with any of the logs and present processing techniques is profiles of the relative variations of some apparent porosity derived from the measurement of another parameter. Such profiles may be fairly accurate in a relative sense, and are probably much better than determinations of porosity by remote geophysical methods, but may be in absolute error by as much as 10-20 porosity % units. Improving this absolute accuracy will require a better

understanding of tool responses in irregular, seawater-filled holes that penetrate the heterogeneous and variably-altered upper oceanic crust (e.g., Broglia and Ellis, 1990).

Improving our resolution of porosity and its nature will also depend on finding some solution to the following calibration dilemma: In the upper oceanic crust, porosity is known to take many forms and scales, from the intergranular pores that can be preserved in recovered core to the large-scale fractures and voids that could not be properly assessed even with perfect recovery of the solid portion of the cored section. As core recovery in the upper oceanic crust is typically much less than perfect, we may never be able to resolve what proportions of the unrecovered core represent unrecovered rock versus voids and fractures. Since we cannot adequately sample large scale porosity, we generally cannot calibrate the log-derived porosities against the core. An important exception is in massive units where porosity is low and mostly intergranular and where core recovery is often quite good (e.g., Broglia and Ellis, 1990). Such massive units provide important calibrations of many of the logs for low-porosity formations, and with careful corrections we can obtain fairly accurate values of porosity in relatively unporous formations. However, we still lack calibration for high-porosity formations typical of young volcanic seafloor, where we cannot sample in situ porosity, and as a result we cannot properly scale the log-derived porosities against true porosities for the full range of porosities encountered in the upper oceanic crust.

Accurate Shear Wave Logging

While compressional wave velocities can be logged at a variety of scales and frequencies (Table 1), it has proven very difficult to accurately log upper crustal shear wave velocities. As explained elsewhere in this volume, determining the shear velocity structure is critical in assessing the effects of young volcanic seafloor on submarine acoustic propagation. In addition, accurate shear wave logging would complement compressional wave data to allow good resolution of the nature of the porosity and the in situ seismic structure of the upper oceanic crust. However, standard logging tools with compressional sources excite converted shear energy only below certain cutoff frequencies; in the heterogeneous and porous upper oceanic crust much of this energy is lost by scattering (Moos et al., 1990), and weak shear wave arrivals are difficult to distinguish from other 'normal' or 'pseudo-Rayleigh' borehole modes (e.g., Cheng and Toksöz, 1981; Paillet and White, 1982).

Some shear wave information can be extracted from sonic logs in the upper oceanic crust, but only with very careful processing and only for a small proportion of the logged section (Moos et al.,1990). Thus, the solution to obtaining more accurate and complete shear wave logs does not appear to lie in more sophisticated processing of data collected with existing sonic logs. Instead, a more promising approach will be to develop acoustic sources that will actually produce shear or torsional energy at the appropriate frequencies, rather than rely on the frequency-limited conversion of compressional energy to shear at the borehole wall. Such sources have been shown to have great promise (e.g., Chen, 1988, 1989), and with further development could be essential in assessing the shear velocity structure of the upper oceanic crust in situ.

Fracture Orientation and Extent

Assessing the orientation and extent of fractures is very closely related to understanding the nature of the porosity and the behavior of acoustic energy in the upper oceanic crust. As described above, fractures form the kind of void space that often cannot be adequately recovered in core. Nevertheless, fractures and other structural elements can be imaged quite well where they intersect the borehole wall, using the ultrasonic borehole televiewer

(BHTV) and the formation microscanner (FMS). Fractures are apparent because of the change in reflectivity imaged by the BHTV, and because of the variation in microresistivity imaged by the FMS. Such variations in reflectivity and/or microresistivity may also occur if a fracture is filled with seawater or plugged with alteration products, so it is difficult to distinguish open fractures from sealed fractures using these tools. Moreover, the BHTV and FMS image only the borehole wall and provide no resolution as to the lateral extent of the open or filled fractures. Determining which imaged fractures are open, and then assessing their contribution to in situ porosity and permeability, will require detailed work spanning a range of averaging scales with many additional measurements, including sonic attenuation, shear wave velocity, resistivity, and geochemical logs and detailed permeability measurements (e.g., Goldberg et al., in press; Moos et al., 1990).

Continuous versus Bulk Measurements of Permeability

Permeability is by definition the single most important parameter in controlling the fluid circulation that results in the alteration of the oceanic crust. In the upper few hundred m of young crust, permeability is thought to be dominated by the interconnected, large-scale porosity and fractures which are so difficult to quantify with logs. Unlike porosity, permeability can be directly measured in situ using packers, devices that hydraulically seal the hole. However, such packers generally yield permeability values averaged over vertical intervals (either between a single packer and the bottom of the hole, or between two separate packers) that may be significantly greater than the scale of inter-connected fractures or porosity that actually controls fluid flow and alteration. Thus, truly understanding the fluid flow and alteration, and its effect on acoustic properties of the upper oceanic crust, requires other methods to assess the detailed variation of permeability with depth and its relation to fractures and large-scale porosity. At least four such methods deserve further consideration and development:

(1) the direct measurement of detailed permeability profiles, using a flowmeter/ pressure log under conditions of constant injection into a larger interval isolated using a packer (e.g., Morin et al., 1988),

(2) using acoustic logs resolve the effects of permeability on the propagation of Stoneley waves (e.g., Cheng et al., 1987),

(3) the integrated analysis of the full suite of logs, particularly those sensitive to fractures, with packer interval permeability measurements (e.g., Goldberg et al., in press), and

(4) once multi-hole sites are drilled, hole-to-hole experiments to assess the lateral variability of permeability, porosity, density, and seismic properties.

Determination of Lithostratigraphy and Alteration History from Logs

The lithostratigraphy and alteration encountered in a borehole are a record of the magmatic, tectonic, and alteration processes which control the properties of the oceanic crust. Given the typically poor core recovery in the upper oceanic crust, logs and downhole measurements become especially important in determining lithostratigraphy and alteration history. With poor core recovery, it is difficult to assign depths and unit boundaries to the recovered rocks, and the continuous records provided by logs are then essential in distinguishing lithostratigraphic units and in fixing their boundaries. Logs that are particularly valuable for determining lithology include those that map structures at the borehole wall, the BHTV and FMS (e.g., Pezard and Lovell, 1990), and the Dual

Laterolog (DLL) resistivity log, which seems to average over the proper scale to image typical structural units in the upper oceanic crust particularly well (e.g., Pezard, 1990).

A further problem with poor core recovery in the upper oceanic crust is the bias in the rocks that are recovered, which in many cases has been towards selective recovery of the more competent units, with less representative recovery of altered zones. As a result, a great deal of effort is now being focused on proper interpretation of the neutron activation 'geochemical logs' in the upper oceanic crust, for both original geochemical compositions and the effects of alteration (e.g., Anderson et al., 1990). Much of this effort must be directed towards a calibration dilemma that is similar to that described above for porosity: if the logs can be calibrated only against core recovery that is biased away from the more altered rock, then it is unclear with what accuracy the calibration can be applied to the logs representing this unrecovered, more altered proportion of the crust.

The careful interpretation of the alteration record from geochemical logs will also be important in assessing the history of alteration, in estimating the 'paleo-permeability' that has been sealed by alteration products, and in correcting other logs for the presence of alteration products. For example, the neutron porosity log requires a correction for the effect of hydrogen atoms bound in alteration products (e.g., Broglia and Ellis, 1990), and a proper inversion of electrical resistivity logs for porosity will require a correction for the enhanced conductivities of certain alteration products (e.g., Pezard, 1990).

More Quality Holes!

In some ways the most important issue in downhole measurements is one that is as political as it is scientific or technical, and that is the need for more quality holes. There are very few upper crustal reference holes (Figure 1), but the cores, logs, and downhole measurements from these holes have produced a wealth of information regarding the structure and evolution of upper oceanic crust. However, we cannot assume that these reference holes fully represent the oceanic crust, and we clearly need comparable surveys, coring and downhole measurements at other 'characteristic' sites. More specifically, we need:

(1) more well-surveyed, 'characteristic' crustal drilling sites,

(2) more multi-hole sites, to assess lateral variability in upper crustal properties, using both downhole and cross-hole experiments,

(3) more re-entry cones set to allow the detailed drilling and downhole measurements required to understand the upper oceanic crust (a surprisingly small percentage of DSDP/ODP holes have been drilled utilizing reentry), and

(4) more time for downhole measurements, either from the drillship or by subsequent wireline reentry of those holes established with proper reentry cones.

Reaching these goals will require the political effort to influence policy and funding decisions. This workshop volume will hopefully provide a good start, by assembling the scientific justification for further study of young volcanic seafloor in detail. However, the workshop report alone will not be sufficient with respect to scheduling drilling, as the ODP is specifically a proposal-driven program. Thus, formal ODP proposals will be required for the sites endorsed by this workshop -- and these proposals will be written only if workshop participants are sufficiently committed to act as the proponents for drilling.

References and Recent Bibliography

References cited

Anderson, R.N., Alt, J.C., Malpas, J., Lovell, M.A., Harvey, P.K., and Pratson, E.L., Geochemical well logging in basalts: the Palisades Sill and the oceanic crust of Hole 504B, *J. Geophys. Res.*, *95*, 9265-9292, 1990.

Broglia, C., and Ellis, D., The effect of alteration, formation absorption, and standoff on the response of the thermal neutron porosity log in basalts: examples from DSDP-ODP sites, *J. Geophys. Res.*, *95*, 9171-9188, 1990.

Chen, S.T., Shear-wave logging with dipole sources, *Geophysics, 53*, 659-667, 1988.

Chen, S.T., Shear-wave logging with quadrupole sources, *Geophysics, 54*, 590-597, 1989.

Cheng, C.H., and Toksöz, M.N., Elastic wave propagation in a fluid-filled borehole and synthetic acoustic logs, *Geophysics, 46*, 1042-1053, 1981.

Cheng, C.H., Jinzhong, Z., and Burns, D.R., Effects of in-situ permeability on the propagation of Stoneley (tube) waves in a borehole, *Geophysics, 52*, 1279-1289, 1987.

Collins, J.A., Purdy, G.M., and Brocher, T.M., Seismic velocity structure at DSDP Site 504B, Panama Basin: evidence for thin oceanic crust, *J. Geophys. Res.*, *94*, 9283-9302, 1989.

Fisher, A.T., Becker, K., Narasimhan, T.N., Langseth, M.G., and Mottl, M.J., Passive hydrothermal circulation on the southern flank of the Costa Rica Rift, *J. Geophys. Res.*, *95*, 9343-9378, 1990.

Goldberg, D., Broglia, C., and Becker, K., Fracturing, alteration, and permeability: in-situ properties in Hole 735B, *Proc. ODP, Sci. Results, 118*, in press.

Langseth, M.G., J.R. Cann, R., J.H. Natland, and M.A. Hobart, Geothermal phenomena at the Costa Rica Rift: background and objectives for drilling at Deep Sea Drilling Project sites 501, 504, and 505, *Init. Rep. Deep Sea Drill. Proj.*, *69*, 5-30, 1983.

Langseth, M.G., M.J. Mottl, M. Hobart, and A. Fisher, The distribution of geothermal and geochemical gradients near site 501/504: implications for hydrothermal circulation in the oceanic crust, *Proc. ODP, Init. Rep. (Pt. A), 111*, 23-32, 1988.

Morin, R.H., Hess, A.E., and Paillet, F.L., Determining the distribution of hydraulic conductivity in a fractured limestone aquifer by simultaneous injection and geophysical logging, *Ground Water, 26*, 587-595, 1988.

Moos, D., Pezard, P., and Lovell, M., Elastic wave velocities with oceanic layer 2 from sonic full waveform logs in DSDP Holes 395A, 418A, and 504B, *J. Geophys. Res.*, *95*, 9189-9208, 1990.

Mottl, M.J., J.R. Lawrence, and L.D. Keigwin, Elemental and stable-isotope composition of pore waters and carbonate sediments from Deep Sea Drilling Project sites 501/504 and 505, *Init. Rep. Deep Sea Drill. Proj.*, *69*, 461-473, 1983a.

Paillet, F.L., and White, J.E., Acoustic modes of propagation in the borehole and their relationship to rock properties, *Geophysics*, *47*, 1215-1228, 1982.

Pezard, P.A., Electrical properties of MORB, and implications for the structure of the oceanic crust at DSDP Site 504, *J. Geophys. Res.*, *95*, 9237-9264, 1990.

Pezard, P., Lovell, M., ODP Leg 126 Shipboard Scientific Party, Downhole images: electrical scanning reveals the nature of subsurface oceanic crust, *EOS, Trans. AGU*, *71*, 709, 1990.

Stephen, R.A., Seismic anisotropy in the upper oceanic crust, *J. Geophys. Res.*, *90*, 11383-11396, 1985.

Stephen, R.A., Lateral heterogeneity in the upper oceanic crust at Deep Sea Drilling Project site 504, *J. Geophys. Res.*, *93*, 6571-6584, 1988.

Worthington, P.F., Anderson, R.N., Jarrard, R.D., Becker, K., Bell, J.S., Salisbury, M.H., and Stephen, R.A., Scientific applications of downhole measurements in the ocean basins, *Basin Research*, *1*, 223-236, 1989.

Other recent bibliography

I. Hole 418A:
Salisbury, Scott, et al., *Proc. ODP, Init. Repts.*, *102*, 1986.
Salisbury, Scott, et al., *Proc. ODP, Sci. Results*, *102*, 1988.

II. Hole 504B:
Becker, Sakai, et al., *Froc. ODP, Init. Repts.*, *111*, 1988.
Becker, Sakai, et al., *Rev. Geophys.*, *27*, 79-102, 1989.
Becker, Sakai, et al., *Proc. ODP, Sci. Results*, *111*, 1989.

III. Hole 395A:
Detrick, Honnorez, et al., *Proc. ODP, Init. Repts.*, *106/109*, 1988.
Detrick, Honnorez, et al., *Proc. ODP, Sci. Results*, *106/109*, 1990.

IV. Hole 735B:
Robinson, Von Herzen, et al., *Proc. ODP, Init. Repts.*, *118*, 1989.
Robinson, Von Herzen, et al., *Proc. ODP, Sci. Results*, *118*, in press.

V. Holes 395A, 418A, 504B, and others:
Papers in a JGR special section on results of logging and downhole measurements in DSDP/ODP deep crustal holes, June, 1990.

Table 1

BOREHOLE MEASUREMENTS

PROPERTY	VERTICAL RESOLUTION					NEW
	≤CM	CM-M	M	10-100M	≥100M	
POROSITY		(neutron)				
DENSITY		density				gravity
P-WAVE VEL.		sonic	mcs	vsp	ose	x-hole seismic
S-WAVE VEL.			mcs			vsp(s);ose(s); x-hole
ANISOTROPY					ose	sonic(s)+above
ATTENUATION		sonic	mcs	vsp	ose	above
CHEMISTRY		nuclear				
FLUID CHEM.						wire-line packer
PERMEABILITY				packer		flowmeter+w-1 packer
TEMPERATURE		temp				
RESISTIVITY	FMS	SFL,DIL	DLL	LSR		IP;oblique EM
MAG.FIELD		3-axis Mag				
SUSCEPTIBILITY		susc.				
STRUCTURE	BHTV;FMS		DLL			
STRESS		BHTV;FMS				Hydr. Fract.
FRACTURING	BHTV;FMS					

Figure Caption

Figure 1. Schematic stratigraphy encountered in eight representative deep DSDP/ODP holes. The five holes on the left are the five deepest penetrations into true oceanic basement, shown left to right in order of decreasing basement penetration. Four of these five holes (395A, 418A, 504B, and 735B) were extensively logged during the first three years of ODP (see bibliography). Hole 332B is located in 3.5-m.y.-old north Atlantic crust, but cannot be revisited for logging because the reentry cone and casing have separated. The three holes shown for comparison on the right include, left to right, two deep penetrations into extrusive flows that overlie true igneous basement and have also been logged extensively, 462A in the western Pacific and 642E on the Voring Plateau as well as the deepest hole drilled to date by DSDP or ODP into any lithology, 398D in sediments near the Galicia Bank.

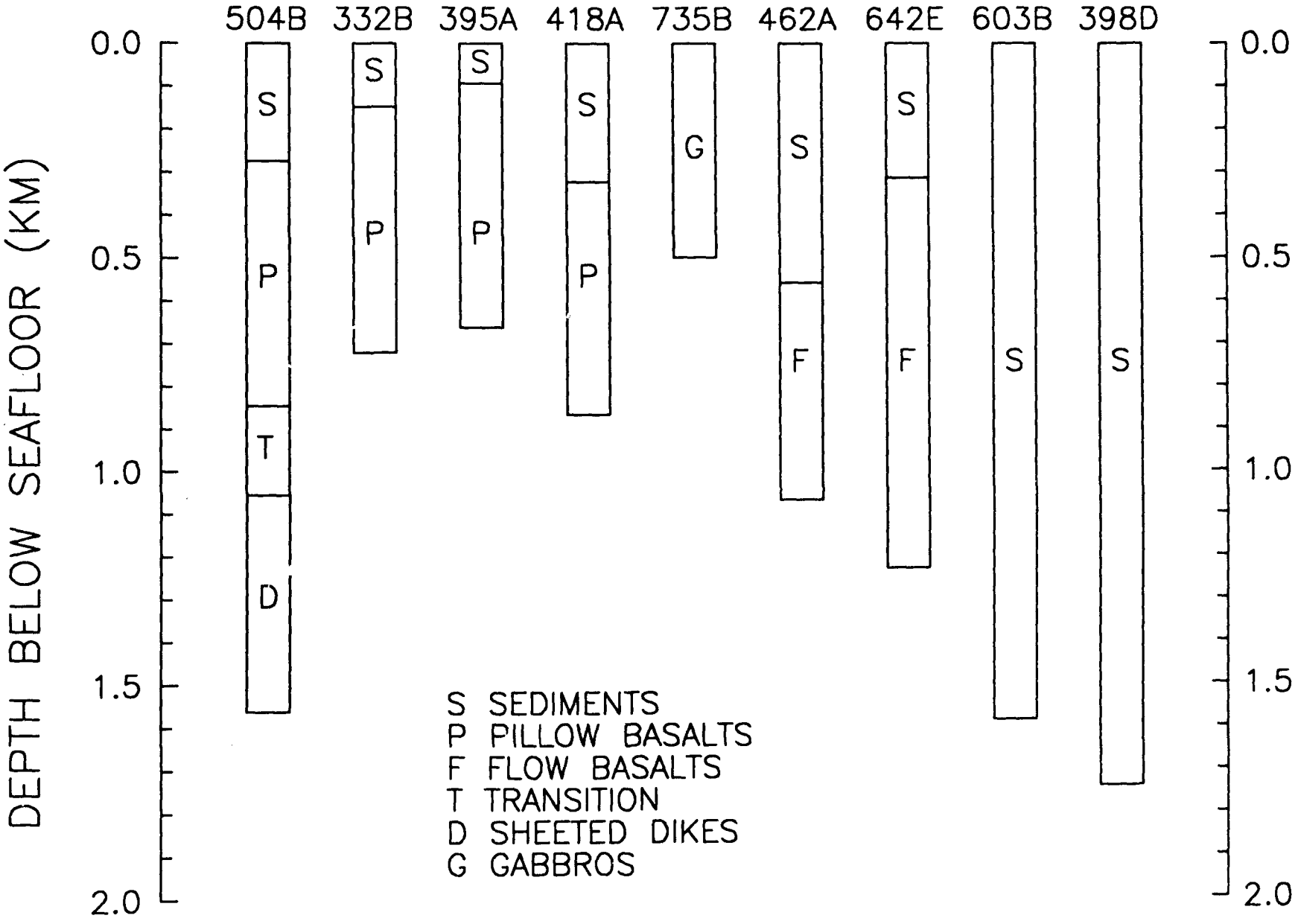
504B
332B
395A
418A
735B
462A
642E
603B
398D
DEPTH BELOW SEAFLOOR (KM)
0.0
0.5
1.0
1.5
2.0
S
P
T
D
G
F
S SEDIMENTS
P PILLOW BASALTS
F FLOW BASALTS
T TRANSITION
D SHEETED DIKES
G GABBROS

Section B3: Physical Properties

1: The Physical Properties of Oceanic Volcanic Rocks: N.I. Christensen

2: Fractures, Cracks and Large Scale Porosity: G.J. Fryer and R.H. Wilkens

THE PHYSICAL PROPERTIES OF OCEANIC VOLCANIC ROCKS

N.J. Christensen
Department of Earth and Atmospheric Sciences
Purdue University
West Lafayette, IN 47907

INTRODUCTION

Beginning in the early 1950s, field and laboratory physical property measurements of the oceanic crust have been the subject of numerous investigations. The results of early refraction studies at sea often showed a simple three-layered crustal model with relatively uniform velocities and thickness of individual layers (Raitt, 1963). Seismic experiments using modern seismic techniques have determined detailed velocity-depth structures through the oceanic crust at several locations. Houtz and Ewing (1976) found that the uppermost basalt of the oceanic crust has relatively low velocities, usually between 3.6 and 4.8 km s^{-1}, which increase rapidly with depth giving rise to compressional wave velocity gradients in the upper 2 km of the crust averaging between 0.5 and 2.0 s^{-1} (Kennett, 1977; Whitmarsh, 1978; Houtz, 1980; Spudich and Orcutt, 1980). More recent experiments (e.g., Vera et al., 1990) report layer 2A velocities as low as 2.2 km/s. In addition, refraction profiles recorded on ocean bottom seismometers by Au and Clowes (1984) confirm similar low shear-wave velocities in the upper basaltic crust followed by a rapid increase in velocity with depth. The low velocities and their variability in the upper oceanic crust immediately underlying deep sea sediments are generally attributed to the presence of high porosity, rubbly pillow basalt and breccia zones at shallow depths (e.g., Hyndman and Drury, 1976) with the rapid increases in velocities with depth originating from decreasing porosity.

Marine heat flow observations, electrical soundings and geophysical logging have established that the pores and cracks are water saturated and often likely to be interconnected (Lister, 1972; Kirkpatrick, 1979; Hermance, Nur and Bjornsson, 1972). This presence of pore water within the upper oceanic crust influences a wide range of properties including fracture strength, electrical conductivity and seismic velocities (Raleigh and Paterson, 1965; Brace and Orange, 1968; Christensen, 1970). These properties are likely to depend not only on the external confining pressure at depth, but also on the fluid pressure within the rock cavities.

Models of upper oceanic crustal structure are based on and expressed largely in terms of seismology, important constraints being provided by dredge and drill sample petrology, gravity, heat flow, electrical and magnetic data. Not surprisingly, interpretations of these data have resulted in several models for the volcanic oceanic crust which differ significantly from one another. Because of the emphasis to date on obtaining geophysical information on the seismic structure of the oceanic crust, the following discussion will center on the interpretation of seismic properties of the volcanic oceanic crust.

Techniques

The technique for velocity measurements commonly employed in laboratories is similar to or slightly modified from the pulse transmission method described by Birch (1960). This consists of determining compressional or shear-wave traveltimes through cylindrical rock specimens. Transducers are placed on the ends of the rock core. The sending transducer converts the input, an electrical pulse of 50 to 500V and 0.1 to 10 μsec width, to

a mechanical signal, which is transmitted through the rock. The receiving transducer changes the wave to an electrical pulse, which is amplified and displayed on an oscilloscope screen (Fig. 1). Once the system is calibrated for time delays, the traveltime through the specimen is determined directly on the oscilloscope or with the use of a mercury delay line (Fig. 2). The major advantage of the delay line is that it increases the precision, especially for signals with slow rise times, because the gradual onset of the first arrival from the sample is approximated by the delay line.

Generally the rock specimens are cores 2.54 cm in diameter and 4 to 6 cm long. Bulk densities are calculated from dimensions and weights. For measurements at elevated pressures, the cores are jacketed with copper foil and rubber tubing to prevent high-pressure oil from entering microcracks and pores (Fig. 1). The core ends are either coated with silver conducting paint, or a strip of brass is spot-soldered to the copper jacket at each end to provide an electrical ground for the transducers. For measurements at high temperatures and pressures where gas is the pressure medium, the samples are usually encased in stainless steel. Velocity measurements as functions of confining and pore pressure require an additional pressure generating system and a more elaborate sample jacketing procedure, since the pore fluid must be isolated from the confining pressure fluid.

Unlike velocity determinations, there is no common method used for measuring seismic attenuation in the laboratory. The three parameters most often reported as the attenuation are the seismic quality factor Q, also referred to as the specific attenuation Q^{-1}, the attenuation coefficient α and the logarithmic decrement δ. These are related for low-loss materials ($Q > 10$) by:

$$\frac{1}{Q} = \frac{\alpha V}{\pi f} = \frac{\delta}{\pi} \qquad (1)$$

where V is the phase velocity and f is the frequency (Johnston and Toksöz, 1981). In both the field and laboratory, difficulties arise in separating the intrinsic dissipation of the rock, i.e., processes by which seismic energy is converted into heat, from geometric spreading, transmission losses, scattering, and other factors. Nevertheless, the utilization of laboratory attenuation measurements to tie seismic data to the anelastic properties of rocks is promising, and the refinement of laboratory techniques and the theory concerning the mechanisms involved has yielded and will continue to supply valuable insights into the structure and composition of the volcanic oceanic crust.

The methods used in determining the attenuation can be separated into three categories: resonance techniques, ultrasonic pulse propagation, and low-frequency methods. Ultrasonic pulse propagation has been used only recently for attenuation measurements in rocks and has provided the only attenuation data presently available for oceanic volcanic rocks (Wepfer and Christensen, 1990). An advantage of wave-propagation methods is the comparative ease with which high pressure measurements, may be performed.

The measurement method is a modified version of the ultrasonic pulse-echo spectral ratio technique described by Winkler and Plona (1982). A diagram of the sample assembly is shown in Figure 3. This method is advantageous in that no separate reference sample need be measured, since one is included in the assembly via the coupling buffer. This means that the technique is source insensitive, i.e., the source need not be repeatable in a separate reference measurement. Because inadequate energy coupling between source and sample can be a problem, a potentially major source of error is eliminated. Another benefit of this approach lies with the sample dimensions, which need to be only 2.5 cm in diameter

and can be as short as 1.5 to 2 cm. Additionally, strain amplitudes are very low and applying in situ conditions, particularly confining pressure, is readily accomplished.

In this technique, a 1 MHz transducer is pulsed by a pulser-receiver and then is used to receive the subsequent reflections. The reflections from the front and back faces of the sample are the arrivals of interest. The first reflection travels only through the brass coupling buffer, which is considered to be non-attenuating (infinite Q) relative to the sample and is therefore the reference waveform (cf. Toksöz et al. (1979) and Sears and Bonner (1981), both studies using aluminum). The second reflection travels through both the buffer and the sample and contains the desired attenuation information. Each reflection is windowed and the Fourier transforms are calculated. The spectra are then corrected for diffraction effects as described by Winkler and Plona (1982). From the amplitude spectra and the appropriate energy considerations, the attenuation of the sample is determined. The equation which gives the attenuation coefficient α in decibels per unit length (dB/length) is:

$$\alpha(\omega) = \frac{8.686}{2L} \ln\left[\frac{|R_{23}|}{|R_{12}|}\frac{|A(\omega)|}{|B(\omega)|}\left(1 - R_{12}^2\right)\right] \tag{2}$$

(Winkler and Plona, 1982) where L is the sample length, $A(\omega)$ and $B(\omega)$ are the amplitude spectra of the first and second reflections, respectively, R_{12} is the reflection coefficient between the coupling buffer and the sample, R_{23} is the reflection coefficient between the sample and the backing buffer, and the constant 8.686 converts to decibels. As with most pulse techniques, α is measured and Q is derived using the equation:

$$\frac{1}{Q} = \frac{\alpha V}{\pi f} \tag{3}$$

(Johnston and Toksöz, 1981), where V is the phase velocity, f is the frequency, and α is in 1/length.

Laboratory Data

Several laboratory studies have reported seismic properties of oceanic volcanic rocks. These have provided a basic understanding of many factors that influence velocity and attenuation of rocks sampled from oceanic layer 2. The effects of some of these parameters are briefly reviewed below.

Pressure and Temperature

The effect of confining pressure on velocities has been reported in a number of investigations. An example of data for a typical crystalline rock is shown in Figure 4. The characteristic shape of the curve of velocity vs pressure is attributed to the closure of microcracks. As can be seen from Figure 4, much of the closure takes place over the first 100 MPa.

Fewer data are available on the influence of temperature on rock velocities. It has been well known since the early work of Ide (1937) that the application of temperature to a rock at atmospheric pressure results in the creation of cracks that often permanently damage the rock. Thus, reliable measurements of the temperature derivatives of velocity must be

obtained at confining pressures high enough to prevent crack formation. In general, pressures of 200 MPa are sufficient for temperature measurements to 300°C.

A wide variety of techniques have been employed to measure the influence of temperature on rock velocities (for example, see Birch, 1943; Kern, 1978; Christensen, 1979). An example of data showing the influence of temperature on velocities is shown in Figure 5. This is the only published temperature data for an oceanic volcanic rock.

Increasing temperature decreases velocities, whereas increasing pressure increases velocities. Thus, in a homogeneous crustal region, velocity gradients depend primarily on the geothermal gradient. The change of velocity with depth is given by:

$$\frac{dV}{dz} = \left(\frac{\partial V}{\partial P}\right)_T \frac{dP}{dz} + \left(\frac{\partial V}{\partial T}\right)_P \frac{dT}{dz} \qquad (4)$$

where z is depth, T is temperature, and P is pressure. For regions with normal geothermal gradients (25° to 40°C/km), the change in compressional velocity with depth dV_P/dz is close to zero (Christensen, 1979). However, in high heat-flow regions, crustal velocity reversals are expected if compositional changes with depth are minimal.

All investigations have found that Q increases with increasing confining pressure. Beginning with Birch and Bancroft (1938), every experimental technique has observed a sharp increase in Q at low pressures, which then levels off at high pressures, a response similar to that observed for velocities. The form of the Q vs P curve is generally attributed, therefore, to the closure of microcracks. As with velocity measurements, few researchers have studied attenuation as a function of temperature. At temperatures below the boiling point of the rock's volatiles, Q appears to be temperature independent, and above this, Q increases, indicating outgassing of pore fluids and/or thermal cracking (Johnston and Toksöz, 1980; Tittmann and others, 1974). At the onset of partial melting, Q decreases (Spetzler and Anderson, 1968).

Pore Pressure

The influence of pore pressure on velocity and attenuation has been widely studied for sedimentary rocks; however, only a limited amount of data are available for crystalline rocks and only a single oceanic basalt has been studied (Christensen, 1984). In Figure 6, velocities are shown as functions of confining pressure at atmospheric pore pressure and constant differential pressure (confining pressure minus pore pressure). The dramatic lowering of velocities with increasing pore pressure appears to be a common feature for crystalline rocks and may be one of many possible explanations for crustal low-velocity zones. Of significance, increases of pore pressure in crustal regions will be accompanied by marked increases in Poisson's ratios (Christensen, 1984). Although pore pressure attenuation data is sparse for crystalline rocks, the investigations on sedimentary rocks have found that fluid flow in microcracks is the mechanism responsible for the observed drop in Q with increasing saturation (Winkler and Nur, 1979; Clark and others, 1980). This effect should be seen in crystalline rocks such as basalts.

Porosity

Oceanic basalts at in situ confining pressures show wide ranges in compressional and shear wave velocities (Fig. 7). The samples with relatively low velocities and densities have relatively high porosities and often contain abundant alteration products. Figure 8

shows the relation between compressional wave velocity and porosity for volcanic rocks from a borehole located in the Azores (Hyndman et al., 1979). A knowledge of the porosity and its form in the upper oceanic crust and in islands is important for an understanding of alteration processes, and for rough estimates of the permeability available for hydrothermal circulation processes (e.g., Francis, 1976; Whitmarsh, 1978). The relation may be useful for the estimation of upper crustal porosities from seismic refraction measurements, although much of the upper crustal pore space probably is in large fractures and voids so is not represented by small samples. Figure 8 also shows the predicted velocity-porosity relations for various pore aspect ratios (or elongations) from the non-interaction theory of Toksöz et al. (1976) as applied to the upper oceanic crust by Whitmarsh (1978). A mean aspect ratio of 1/10 gives the best fit in rough agreement with the large scale upper crustal values suggested by Whitmarsh.

Conclusions

Since the early 1970s, much has been learned about elastic wave propagation in oceanic volcanic rocks. Velocities are available at pressures that exist in the upper oceanic crust for a wide variety of basalts. Additional important contributions include laboratory measurements of shear-wave velocities, Vp/Vs ratios, and the influence of temperature and pore pressure on velocities.

For future studies, it is desirable to obtain additional velocity data at high temperatures. This is especially true for shear-wave measurements. As more detailed crustal velocity data become available, it may become apparent that seismic anisotropy is a common and important upper crustal feature. Thus, systematic laboratory studies of compressional wave anisotropy and shear-wave splitting in cracked volcanic rocks could be critical in understanding crustal composition, just as they have been in investigations of the upper oceanic mantle.

Many researchers have obtained high-quality attenuation data, and a number of loss-mechanism theories have proven quite successful. Although a variety of methods have been employed to measure Q, certain trends are evident. The magnitude may vary from one study to the next, but the relative effects of pressure, temperature, and saturation state are fairly consistent, and efforts to relate these conditions to the micro- and macrostructure of rocks should continue. Also, it would seem that the behavior of Q parallels some already well-established velocity characteristics such as dependence on confining and pore pressure and frequency. This raises some interesting questions: Is Q characterized by mineralogy at high pressures rather than cracks and their saturation condition? Is there a Q-density relation similar to the velocity-density relationship mentioned above? Is attenuation anisotropic in crustal and upper-mantle rocks? Are Qp/Qs ratios diagnostic, as suggested by Winkler and Nur (1979)? Is an effective pressure law applicable for Q? Finally, far too little laboratory attenuation work has been done on crystalline oceanic rocks. This must become a priority if significant use is to be made of seismic attenuation data of the oceanic crust.

References

Birch, F., Elasticity of igneous rocks at high temperatures and pressures, *Bull. Geol. Soc. Am.*, *54*, 263-286, 1943.

Birch, F., The velocity of compressional waves in rocks to 10 kilobars, Part 1, *J. Geophys. Res.*, *65*, 1083-1102, 1960.

Birch, F. and D. Bancroft, Elasticity and internal friction in a long column of granite, *Seis. Soc. Am. Bull., 28*, 243-254, 1938.

Christensen, N.I., Compressional wave velocities in rocks at high temperatures and pressures, critical thermal gradients, and crustal low-velocity zones, *J. Geophys. Res., 84*, 6849-6857, 1979.

Christensen, N.I., Pore pressure and oceanic crustal seismic structure, *Geophys. J.R. astr. Soc., 79*, 411-424, 1984.

Clark, V.A., B.R. Tittmann and T.W. Spencer, Effect of volatiles on attenuation (Q^{-1}) and velocity in sedimentary rocks, *J. Geophys. Res., 85*, 5190-5198, 1980.

Hyndman, R.D., N.I. Christensen and M.J. Drury, Seismic velocities, densities, electrical resistivities, porosities and thermal conductivities of core samples from Bermuda and the Azores, *in* Talwani et al. (eds.), Deep Drilling Results in the Atlantic Ocean: Ocean Crust, Maurice Ewing Series, *Am. Geophys. Un.*, 94-112, 1979.

Ide, J.M., The velocity of sound in rocks and glasses as a function of temperature, *J. Geol., 45*, 689-716, 1937.

Johnston, D.H. and M.N. Toksöz, Thermal cracking and amplitude-dependent attenuation, *J. Geophys. Res., 85*, 937-942, 1980.

Johnston, D.H. and M.N. Toksöz, Definitions and terminology, *in* Johnston, D.H. and M.N. Toksöz (eds), Seismic Wave Attenuation, Tulsa, Oklahoma, *Society of Exploration Geophysicists, Geophysics Reprint Series No. 2*, p. 1-5, 1981.

Kern, H., The effect of high temperature and high confining pressure on compressional wave velocities in quartz-bearing and quartz-free igneous and metamorphic rocks, *Tectonophysics, 44*, 185-203, 1978.

Spetzler, H. and D.L. Anderson, The effect of temperature and partial melting on velocity and attenuation in a simple binary system, *J. Geophys. Res., 73*, 6051-6060, 1968.

Tittmann, B.R., R.M. Housley, G.A. Alers and E.H. Cirlin, Internal friction in rocks and its relationship to volatiles on the moon, *in* Proceedings of the 5th Lunar Science Conference, Geochimica et Cosmochimica Acta, supplement 5, 3, 2913-2918, 1974.

Toksöz, N., C.H. Cheng and A. Timur, Velocities of seismic waves in porous rocks, *Geophysics, 41*, 621-645, 1976.

Vera, E.E., J.C. Mutter, P. Buhl, J.A. Orcutt, A.J. Harding, M.E. Kappus, R.S. Detrick and T.M. Brocher, The structure of 0 to 0.2 M.Y. old oceanic crust at 9°N on the East Pacific Rise from expanded spread profiles, *J. Geophys. Res.* (in press), 1990.

Wepfer, W.W. and N.I. Christensen, Compressional wave attenuation in oceanic basalts, *J. Geophys. Res.* (in press), 1990.

Whitmarsh, R.G., Seismic refraction studies of the upper igneous crust in the North Atlantic and porosity estimates for layer 2, *Earth Planet. Sci. Lett., 37*, 451-464, 1978.

Winkler, K.W. and A. Nur, Pore fluids and seismic attenuation in rocks, *Geophys. Res. Lett.*, *6*, 1-4, 1979.

Winkler, K.W. and T.J. Plona, 1982, Technique for measuring ultrasonic velocity and attenuation spectra in rocks under pressure, *J. Geophys. Res.*, *87*, 10776-10780, 1982.

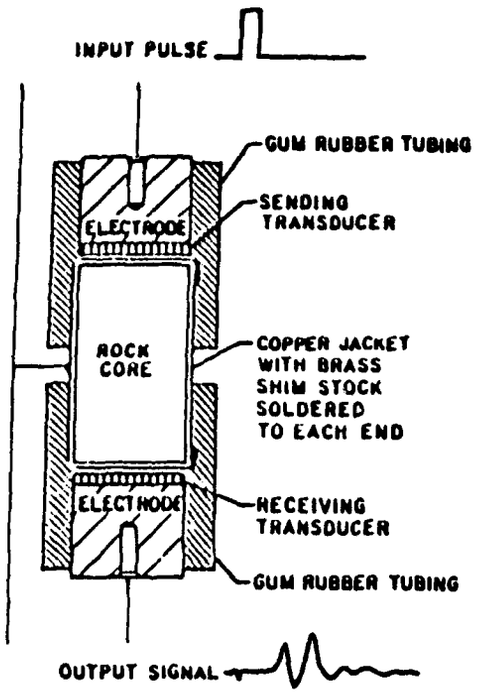

Figure 1

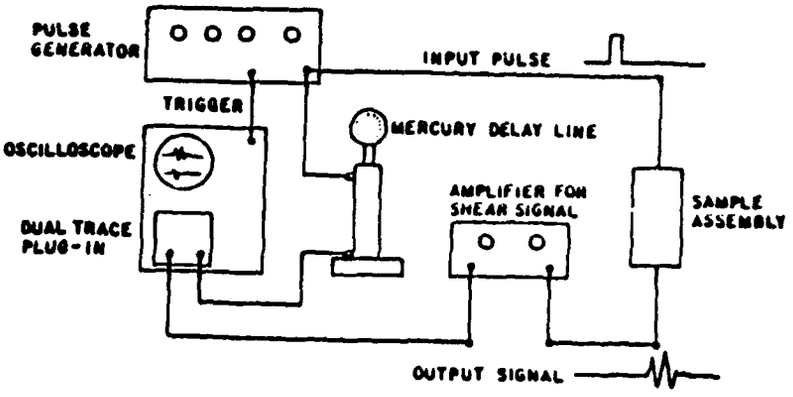

Figure 2

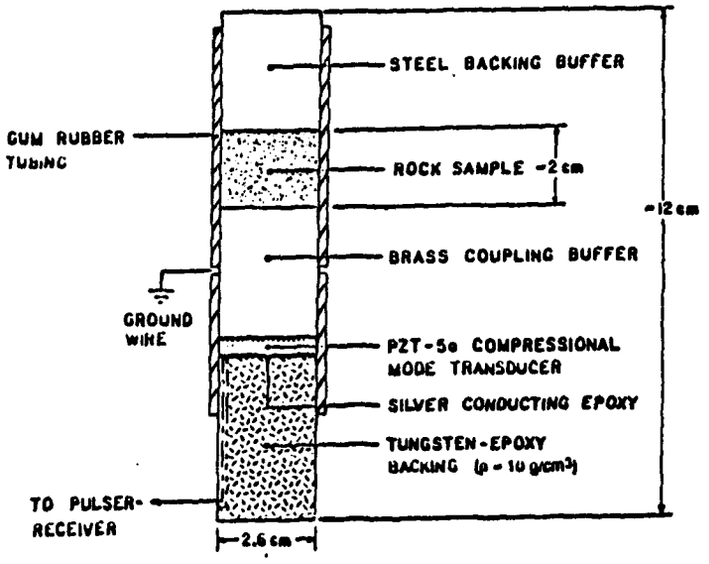

Figure 3

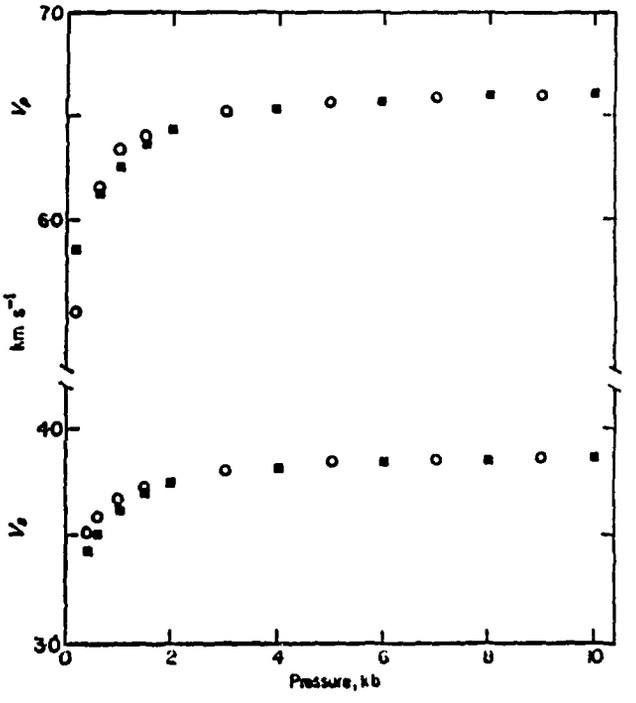

Figure 4

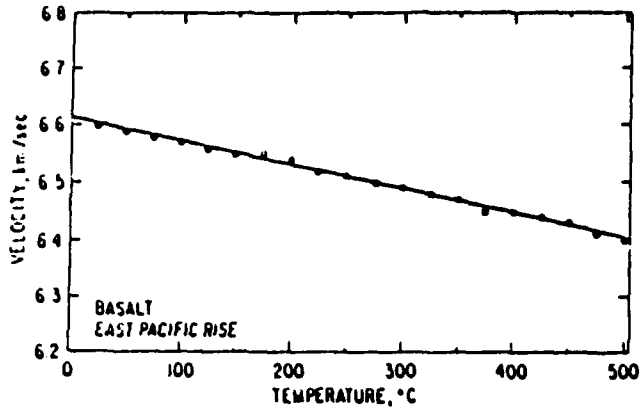

Figure 5

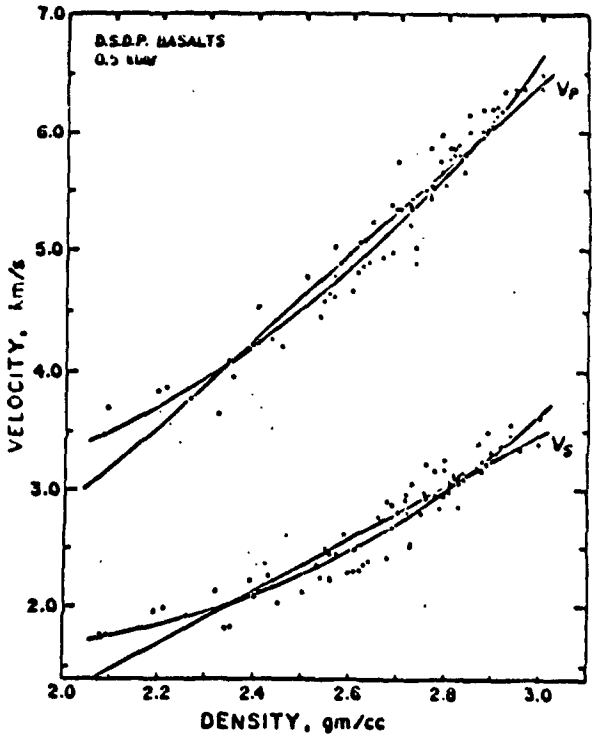

Figure 6

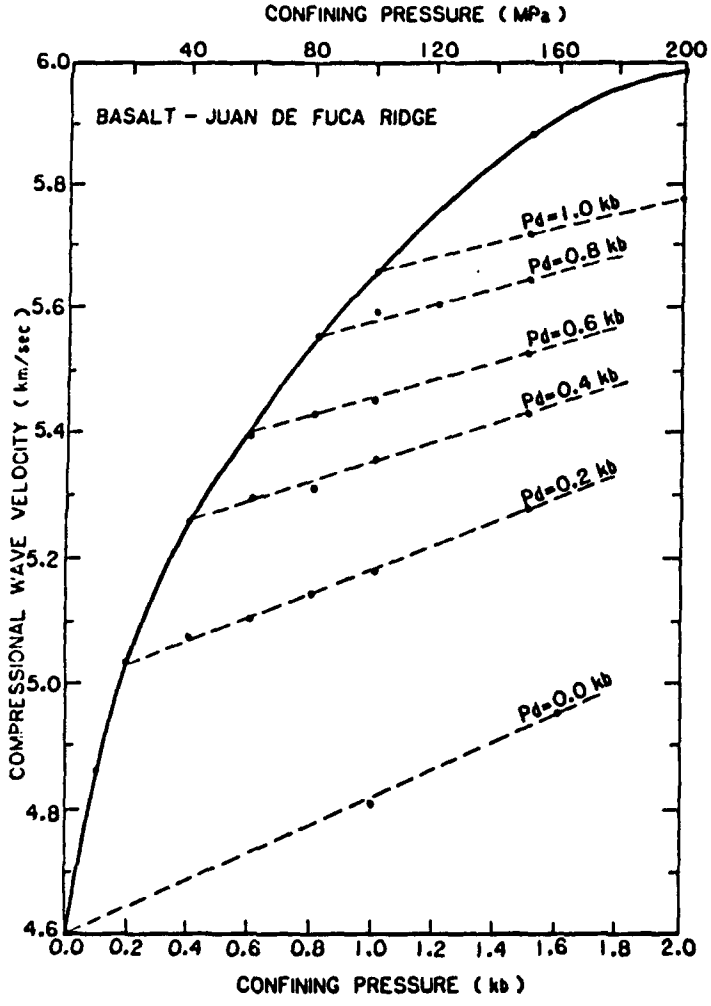

Figure 7

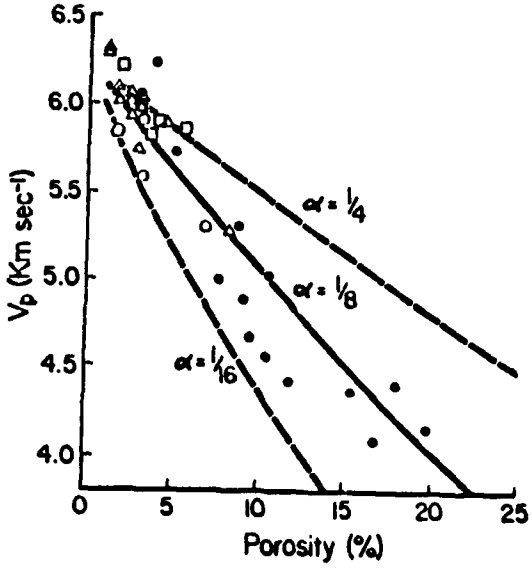

Figure 8

FRACTURES, CRACKS, AND LARGE-SCALE POROSITY

Gerard J. Fryer and Roy H. Wilkens
School of Ocean & Earth Science & Technology
University of Hawaii at Manoa
Honolulu, HI 96822

Fracturing, brecciation, and vesiculation in the uppermost oceanic crust drastically reduce seismic wavespeeds from their laboratory values, and, if this void space is aligned, induce an elastic anisotropy. The void space is slowly filled by alteration products and by direct precipitation from hydrothermal fluids, so the seismic structure varies with depth, with age, and with the local history of hydrothermal activity. The dependence of seismic velocities on porosity and other parameters of the void space (aspect ratio, crack density, crack orientation) suggests that seismic experiments could be used not only to look at the processes of crustal formation and crustal ageing, but also (with suitable small-scale experiments) to explore the geometry of both active and fossil hydrothermal cells. This review briefly summarizes the reasons for this optimistic view, discusses some of the problems to be addressed, and considers both seismic experiments and drilling targets.

Random Porosity

Laboratory measurements of *P*-velocities in oceanic basalts typically fall in the range 6-7 km/s, while seismic measurements of shallow seismic structure are invariably less, as low as 2.1 km/s (Purdy, 1987). As has long been recognised, this discrepancy must be due to porosity at a scale unsampled by dredging or drilling (Hyndman & Drury, 1976; Spudich & Orcutt, 1980). While the seismic structure is dominated by porosity effects, no serious attempts have yet been made to try to estimate the porosity structure from marine seismic data because of major data and theory shortcomings: the required high-resolution seismic measurements of the upper few hundred meters of the crust have, until recently, been nonexistent, and all theories relating seismic properties to porosity that have been proposed so far become invalid at the very high porosities inferred for the shallowest volcanic seafloor.

With sketchy data and inadequate theories, however, it is still possible to explore qualitatively what is going on in the uppermost crust. Purdy (1987) measured an increase of P-wave speed with age from 2.1 km/s at near-zero age crust to 4.1 km/s at 7-m.y.-old crust, a rate of increase which appeared to require staggering porosity reduction. Fryer & Wilkens (1988), however, noted that such large porosity change is only required if void space in the crust is characterized by a single aspect ratio. Since void space varies from thin cracks to more equidimensional spaces between blocks of rubble, the crust must instead have a spectrum of aspect ratios. As such a fractured structure undergoes alteration, the thinnest void space will seal first, changing the aspect ratio spectrum. A cartoon of such change is shown in Fig. 1. Velocities are strongly dependent on both aspect ratio and porosity, as shown in Fig. 2, so the aspect ratio change cannot be ignored if the seismic results are to be explained. Applying the theory of Kuster & Toksöz (1974) (which is strictly valid only for low porosities) to a material with a spectrum of aspect ratios, Fryer & Wilkens (1988) showed that when the thinnest void space is sealed first, the observed velocity increase can be explained by a total porosity reduction of only a few percent (Fig. 3). Marion & Moos (1989), using a very different approach, came to a similar conclusion.

Variation in mean aspect ratio is also consistent with the observed velocity variation with depth. From downhole logs, Fryer & Wilkens (1989) reported systematic variations in velocity-porosity relationships with depth at site 504B (Fig. 4). This variation suggests an increase in mean aspect ratio (i.e., a tendency towards more spherical voids) with depth, exactly what would be expected from the depth-dependent increase in crack sealing from hydrothermal deposition indicated by the geochemical data (Alt, et al., 1986). Downhole logs also support the idea of age-dependent increase in aspect ratio accompanied by a decrease in overall porosity (Fig. 5).

Near-Vertical Fractures and Azimuthal Anisotropy

Any Earth material with a well-developed fabric, be it from parallel fractures, flow layering, or alignment of minerals, will display a variation of seismic velocities with direction. The bathymetric and backscattering fabric of the ocean floor, so apparent in sidescan sonar images, implies a fracture system which should have substantial anisotropic effect. An azimuthal variation in velocity, apparently resulting from parallel, near-vertical fractures and fissures, was first discovered in the upper oceanic crust by Stephen (1981) and has since been identified at many locales in both young and old crust (White & Whitmarsh, 1984; Shearer & Orcutt, 1984, 1986; Stephen, 1985). In young crust, P-velocity variation with azimuth of as much as 20% is not unusual, and the velocity variation is consistent (with the possible exception of the White & Whitmarsh measurement) with ridge-parallel near-vertical fractures. Anisotropy thus almost certainly has the same explanation as the bathymetric fabric: near-axis extension and normal faulting.

With clear azimuthal anisotropy, apparently from near-vertical fractures, the next step would seem to be to back out fracture properties (such as crack density and orientation) from the measured elastic properties. Other than fracture orientation, no one has yet managed to estimate fracture properties, but a necessary intermediate step, determination of elastic parameters describing the behaviour of the fractured crust, has been attempted. These attempts, made by Stephen (1985) and Shearer & Orcutt (1986), have added significantly to our understanding of the crustal structure, and have dramatically demonstrated the importance of recording shear waves in marine seismic experiments. Unfortunately, these attempts were made with inadequate knowledge of the properties of a fractured solid, and as a consequence their results are somewhat misleading.

In a vertically fractured solid, the fastest shear wave is the *SV* wave propagating parallel to the fracture planes (Schoenberg, 1983; Schoenberg & Douma, 1988) and this imposes a severe constraint on any inversion for elastic parameters (in fact it reduces the number of parameters to be fit from five to four). In their work on crustal anisotropy, both Stephen (1985) and Shearer & Orcutt (1986) attempted to extract elastic parameters from their data without imposing the *SV*-speed constraint. In both studies, the final elastic parameters presented are actually incompatible with a fractured solid (Schoenberg, et al., 1987). If we assume that upper crustal anisotropy is indeed the result of fractures, such contrary findings can be explained only by inadequate data or lateral variability. Lateral variability at Stephen's site (DSDP Hole 504B) is extreme, with horizontal velocity change almost as rapid as the vertical change (Stephen, 1988). With such rapid variation, any attempt to quantify upper crustal anisotropy using surface shots and ocean bottom or downhole receivers cannot be successful; the experiment will inevitably integrate over too broad a range of structures. The geometry of seismic experiments to measure anisotropy from near-surface fractures obviously has to be reconsidered.

Flow Layering, Horizontal Fractures, and Transverse Isotropy

In addition to the anisotropy from near-vertical fractures, there must be an additional anisotropy resulting from interleaved flows and breccia zones. Any such anisotropy would be accentuated by horizontal fractures, which have been identified in the upper few hundred meters at hole 504B from acoustic televiewer images (Newmark et al., 1985) and from resistivity measurements using the dual laterolog (Pezard & Anderson, 1989). Vertical fractures induce an azimuthal anisotropy which can be detected from azimuthal variation of velocities or from shear-wave splitting (the occurrence of two shear waves with different polarization and velocity). The anisotropy from flow layering or horizontal fracturing, however, is transversely isotropic: it displays no azimuthal variation. Such anisotropy does not result in split shear waves for compressional sources, so this form of anisotropy is effectively concealed from marine seismology. By ignoring this anisotropy, however, depth errors are introduced into seismic interpretations (Fig. 6), and it is from such errors that the anisotropy can be inferred. Fryer et al (1989) point out that because the anisotropy affects *P* and *S* waves differently, the depth errors from *P*-wave data will be systematically greater than those from *S*-waves, which will result in an anomalously low Poisson's ratio (Poisson's ratio depends on the ratio of *P*-wave speed to *S*-wave speed). Poisson's ratios which are anomalously low in comparison to the values inferred from ophiolites are routinely reported from marine seismic experiments (Spudich & Orcutt, 1980; Au & Clowes, 1984; Shearer & Orcutt, 1986). These anomalies cannot be explained simply from porosity effects (Shearer, 1988), so they are almost certainly the result of depth errors introduced by ignoring anisotropy.

Fundamental Questions

The "porosity structure" (the full suite of parameters that describe the void space: overall porosity, crack density, aspect ratio spectrum, crack orientation, pore connectivity) is clearly of fundamental importance, not only in in determining the physical properties of the bottom, but also in controlling its subsequent alteration. The most obvious questions to be asked are:

1. What is the porosity structure of the crust at the time of formation, how does it vary with geologic setting and spreading rate, and what is the resulting seismic structure?

2. How is the porosity structure modified by off-axis processes, and how does this modification affect seismic structure?

3. How does porosity (and degree of void filling, and aspect ratio) vary within a hydrothermal cell? Are there significant structural differences in downwelling and upwelling zones?

Needs

The delicate sensitivity of seismic structure on porosity, aspect ratio, fracture orientation, etc., would seem to imply that from seismic measurements alone the porosity structure could be determined and the above questions answered. Unfortunately, complete description of the elastic behaviour of fractured and porous ocean floor entails far more parameters than can ever be measured seismically. Seismology can thus contribute to an improved understanding of the structure and evolution of the uppermost crust only if the design of seismic experiments and the interpretation of seismic data are guided by direct measurements of physical properties and by knowledge from other disciplines.

Apart from more and better seismic measurements, a variety of non-seismic and theoretical studies are required to advance towards answers to the fundamental questions raised above. The more obvious studies are:

1. Drilling on very young or zero age crust. Apart from seismic measurements which still are of too low a resolution to define the structure of the uppermost crust with much confidence, our only knowledge of the porosity structure of very young crust is by inference from measurements made on crust of greater age. Because of the rapid changes going on in very young crust we need drill holes in both zero age crust and crust of a few thousand year's age. This would allow both sonic and porosity logging (and, it is hoped, other logging as well) as well as laboratory measurements of velocity and porosity on core samples. We elaborate on drilling objectives below.

2. Porosity modeling. We need to develop "adequate" models relating seismic velocities to the porosity structure. An abundance of theories exist which relate seismic properties to void and crack properties, both for random voids (e.g., O'Connell & Budiansky, 1974; Kuster & Toksöz, 1974) and for aligned voids (e.g., Hudson, 1981). All these theories are correct to first order in the crack density, which effectively means that they work up to porosities of a few percent. But porosities in the shallow ocean crust may be as high as 30%. Higher-order models have been proposed for both random (Cheng, 1978) and aligned (Nishizawa, 1982) voids, but these have yet to be applied to oceanic problems and, in particular, have yet to be tested at very high porosities. Theoretical investigation of the applicability of these and competing models to seafloor conditions is urgently needed; the first-order (low porosity) models currently in use as an aid in interpreting downhole logs and seismic data are at best of only qualitative value.

3. Direct measurement of pore space. At present we have little idea what porosity structure the seafloor has. The aspect ratio spectrum of the void space, in particular, is largely conjecture. What is required is systematic mapping of the large-scale porosity: the number, shape, and orientation of cracks, fractures and inter-rubble voids. At the largest scale this can be done by counting fractures (and measuring their dimensions, spacing, and orientation) on sidescan sonar images of the bottom. At the smallest scale it means measuring cracks in hand specimens and drill cores. Measurements should be made from all possible sources: from televiewer or formation microscanner images of borehole walls, from Deep Tow images of fault scarps, by direct measurement of flow and void dimensions in ophiolites.

4. Geochemical studies. Just as we need to know the geometry of any void space, we also need to know the physical properties the void-filling material, and any change in the properties of the rock matrix. Such properties are most conveniently inferred from the geochemistry. Extensive geochemical studies have been made on ocean drill samples, the most valuable for our purposes being those in which attempts have been made to construct a chronology of alteration (e.g., Alt, et al., 1986). Especially valuable is the radiogenic dating of alteration (Peterson, et al., 1985) as this suggests that it might be possible to construct a predictive model for physical properties using age as an independent variable. But we also need to know about that part of the crust not recovered in a drill core, so the core analyses must be supplemented by investigations of ophiolites (e.g., Staudigel, et al., 1986) and by geochemical logging (Anderson, et al., 1990). Just as in the direct measurement of pore space described above, we would like a geochemical assessment of crack sealing, vein formation, and alteration in general from as wide a range of tectonic settings as possible and using all the available sources of information: ophiolites, dredged and drilled rock, geochemical logs.

Seismic Measurements

From modern expanding-spread profiling (e.g., Vera & Mutter, 1988; Harding, et al., 1989) and on-bottom refraction (Purdy, 1987), it is clear that data with adequate resolution to investigate the structure of the upper few hundred meters will soon be available. From what we know so far of the structure of the uppermost crust we know we must consider the following in planning seismic experiments:

1. Because of the extreme lateral variability of young crust (Stephen, 1988), we must run experiments capable of sampling structure at a scale smaller than the scale of the lateral variation (whatever that is). For MCS work this may mean using deep-towed streamers (e.g., Fagot, 1986), and for refraction experiments it demands ocean-bottom receivers and near- or on-bottom shots (e.g., Purdy, 1987; Hildebrand, et al., 1989).

2. Because of anisotropy we must consider the direction of energy propagation. We must address both the azimuthal anisotropy resulting from vertical fractures, and the transverse isotropy resulting from flow layering and horizontal fractures. To deal with the azimuthal anisotropy we must either align shot lines closely parallel or perpendicular to strike (and interpret the data accordingly), or (better) collect data over a range of azimuths. To deal with the anisotropic effects of layering we must collect data over a range of angles of incidence. This means normal-to-wide-angle reflection (preferably using a deep-towed streamer) or surface MCS and on-bottom refraction.

3. Crude ray tracing and synthetic seismogram modeling of anisotropic ocean floor shows that seismic measurement of the critical parameters of the porosity is difficult to impossible from compressional waves alone. Shear waves are essential and *SH* waves are particularly valuable. *SV* properties should be measurable from on-bottom shots and receivers, but to record *SH* will demand the development of a special source.

Drilling

Until the rock physics theories can be worked out and appropriate seismic experiments designed, the key information for determining the porosity structure and its evolution will come from drilling, and by far the most valuable information from drilling (from the point of view of determining the large-scale porosity structure) will come from downhole measurements. Apart from the routine sonic and neutron porosity logs, the most valuable logs are those which image the borehole walls, such as the televiewer (acoustic imaging) and the formation microscanner (electrical). These are followed closely in importance by geochemical logging, from which the degree of crack infilling and alteration of the host rock can be inferred, and electrical logs (especially the dual laterolog), which provides both an independent measure of the porosity (Pezard, 1990) and an idea about crack orientation (Pezard & Anderson, 1989).

Our understanding of the ocean crust owes a tremendous amount to the phenomenal successes at hole 504B. But extrapolation from that one hole to all oceans is dangerous and must inevitably lead to some bias. Ideally, we would like to complete the matrix of loggable reference holes shown in Table I, bearing in mind that loggable holes may themselves provide a biased view of the ocean floor.

Table I: *Desired matrix of loggable reference holes*

	Fast (Pacific?)	Intermediate (Galapagos?)	Slow (Atlantic?)	Backarc (Marianas?)
Zero Age				
Young-but-not-zero age				
3--7 Ma		504B	395A	
Old	801C		418A	--

Logging zero-age and very young sites will demand the development of slimline tools capable of withstanding high temperatures. Producing such tools will be a formidable undertaking, but the potential rewards are great so the development of the tools should be given every encouragement.

Boreholes in the ocean floor are an unparalleled scientific resource. The experience at hole 504B has been that as technology advances and better logging tools are developed, there is significant science to be gained by relogging (e.g., Becker, et al., 1989). No loggable hole should be abandoned. It is to be hoped that as many of the proposed reference holes in Table I as possible can be logged and relogged, so that the 504B level of understanding can be extended to other locales.

Five Year Targets

We seek to understand the processes by which the uppermost crust is formed and by which it evolves. Data required to gain this understanding are perhaps best obtained by attempting to define the structure of the upper few hundred meters of young crust (over areas at least incorporating an entire hydrothermal cell) in a series of investigations on successively older crust, preferably along a flow line. These investigations would have to be interdisciplinary, and should, if possible, be performed in the vicinity of the geophysical reference holes. The seismic component of such an investigation would have to be a multi-institution effort, using MCS, ocean-bottom or downhole seismometers, and on-bottom sources, with adequate areal coverage to define lateral variability and anisotropy. Before any such large-scale seismic experiment is attempted, however, we should practise and refine our MCS and on-bottom refraction techniques to ensure that desired level of resolution can be achieved.

References

Anderson, R. N., J. C. Alt, J. Malpas, M. A. Lovell, P. K. Harvey, and E. L. Pratson, 1990, Geochemical well logging in basalts: The Palisades Sill and the oceanic crust of Hole 504B, *J. Geophys. Res.*, **95**, 9265-9292.

Au, D., and R. M. Clowes, 1984, Shear-wave velocity structure of the oceanic lithosphere from ocean bottom seismometer studies, *Geophys. J. R. Astron. Soc.*, **77**, 105-123.

Becker, K., H. Sakai, A. C. Adamson, J. Alexandrovich, J. C. Alt, R. N. Anderson, D. Bideau, R. Gable, P. M. Herzig, S. Houghton, H. Ishizuka, H. Kawahata, H. Kinoshita, M. G. Langseth, M. A. Lovell, J. Malpas, H. Masuda, R. B. Merrill, R. H. Morin, M. J. Mottl, J. E. Pariso, P. Pezard, J. Phillips, J. Sparks, S. Uhlig, 1989, Drilling deep into young oceanic crust, Hole 504B, Costa Rica Rift, *Rev. Geophysics*, **27**, 79-102.

Fagot, M. G., 1986, Development of a deep-towed seismic system: A new capability for deep-ocean acoustic measurements, in *Ocean Seismo-Acoustics: Low-Frequency Underwater Acoustics* (T. Akal and J. M. Berkson, eds.), pp. 853-862, Plenum, N.Y.

Fryer, G. J., D. J. Miller, and P. A. Berge, 1989, Seismic anisotropy and age-dependent structure of the upper oceanic crust, in *Evolution of Mid Ocean Ridges* (J. M. Sinton, ed.), pp. 1-8, Am. Geophys. Union, Washington, D.C.

Fryer, G. J., and R. H. Wilkens, 1988, Porosity, aspect ratio distributions, and the increase of seismic velocity with age in young oceanic crust [Abstract], *Eos, Trans. Am. Geophys. Union,* **69,** 1323.

Fryer, G. J., and R. H. Wilkens, 1989, Making sense of seismic velocities in the shallow oceanic crust [Abstract], *Seismological Research Letters,* **60,** 16.

Harding, A. J., J. A. Orcutt, M. E. Kappus, E. E. Vera, J. C. Mutter, P. Buhl, R. S. Detrick, and T. M. Brocher, 1989, Structure of young oceanic crust at 13°N on the East Pacific Rise from expanding spread profiles, *J. Geophys. Res.*, **94,** 12,163-12,196.

Hildebrand, J. A., L. M. Dorman, P. T. C. Hammer, A. E. Schreiner, and B. D. Cornuelle, Seismic tomography of Jasper Seamount, *Geophys. Res. Letters,* **16,** 1355-1358.

Hyndman, R. D., and M. J. Drury, 1976, The physical properties of oceanic basement rocks from deep drilling on the Mid-Atlantic Ridge, *J. Geophys. Res.*, **81,** 4042-4052.

Kuster, G. T., and M. N. Toksöz, 1974, Velocity and attenuation of seismic waves in two-phase media: Part 1. Theoretical formulations, *Geophysics,* **39,** 587-606.

Marion, D., and D. Moos, 1989, Seismic velocities and the morphology of oceanic pillow basalts [Abstract], *Eos, Trans. Am. Geophys. Union,* **70,** 1302.

Newmark, R. L., R. N. Anderson, D. Moos, and M. D. Zoback, Sonic and ultrasonic logging of Hole 504B and its implications for the structure, porosity, and stress regimes of the upper 1 km of the oceanic crust, *Init. Repts. Deep Sea Drill. Project,* **83,** 479-510, 1985.

Peterson, C., R. Duncan, and K. F. Scheidegger, 1985, Sequence and longevity of basalt alteration at Deep Sea Drilling Project Site 597, *Init. Repts. Deep Sea Drill. Project,* **92,** 505-515.

Purdy, G. M., 1987, New observations of the shallow seismic structure of young oceanic crust, *J. Geophys. Res.*, **92,** 9351-9362.

Schoenberg, M., 1983, Reflection of elastic waves from periodically stratified media with interfacial slip, *Geophys. Prospecting,* **31,** 265-292.

Schoenberg, M., and J. Douma, 1988, Elastic wave propagation in media with parallel fractures and aligned cracks, *Geophys. Prospecting,* **36,** 571-590.

Schoenberg, M., D. J. Miller, and G. J. Fryer, 1987, Refraction travel times to an OBS through azimuthally anisotropic oceanic crust [Abstract], *Eos, Trans. Am. Geophys. Union,* **68,** 1372.

Shearer, P. M., 1988, Cracked media, Poisson's ratio and the structure of the upper oceanic crust, *Geophys. J.*, **92,** 357-362.

Shearer, P. M., and J. A. Orcutt, 1985, Anisotropy in the oceanic lithosphere - theory and observations from the Ngendei seismic refraction experiment in the south-west Pacific, *Geophys. J. R. Astron. Soc.,* **80,** 493-526.

Shearer, P. M., and J. A. Orcutt, 1986, Compressional and shear wave anisotropy in the oceanic lithosphere - the Ngendei seismic refraction experiment, *Geophys. J. R. Astron. Soc.,* **87,** 967-1003.

Spudich, P., and J. Orcutt, 1980, Petrology and porosity of an oceanic crustal site: Results from waveform modeling of seismic refraction data, *J. Geophys. Res.*, **85,** 1409-1433.

Staudigel, H., K. Gillis, and R. Duncan, 1986, K/Ar and Rb/Sr ages of celadonites from the Troodos ophiolite, Cyprus, *Geology*, **14**, 72-75.

Stephen, R. A., 1981, Seismic anisotropy observed in upper oceanic crust, *Geophys. Res. Letters*, **8**, 865-868.

Stephen, R. A., 1985, Seismic anisotropy in the upper oceanic crust, *J. Geophys. Res.*, **90**, 11383-11396.

Stephen, R. A., 1988, Lateral heterogeneity in the upper oceanic crust at DSDP Site 504, *J. Geophys. Res.*, **93**, 6571-6584.

Vera, E. E., and J. C. Mutter, 1988, Crustal structure in the ROSE area of the East Pacific Rise: One-dimensional travel time inversion of sonobuoys and expanded spread profiles, *J. Geophys. Res.*, **93**, 6635-6648.

White, R. S., and R. B. Whitmarsh, 1984, An investigation of seismic anisotropy due to cracks in the upper oceanic crust at 45°N, Mid-Atlantic Ridge, *Geophys. J. R. Astron. Soc.*, **79**, 439-467.

Figure Captions

Figure 1. Cartoon of an uncemented breccia (left). The large amount of connected void space makes the material compliant (it deforms easily) so that the velocity of a compressional wave passing through the material is low. If the surfaces of the breccia are covered with a thin hydrothermal deposit (right), the porosity may be only slightly reduced, but the structure, being cemented together, will be much less compliant. A compressional wave will pass through the structure much more rapidly. Note the difference in mean aspect ratio between the two figures: the proportion of long thin void space is reduced on the right.

Figure 2. Aspect ratios shown schematically (above) and the effect of void aspect ratio (alpha) on compressional wave velocity in basalts (below). Lower aspect ratios have a much greater influence on velocities than more spherical pores.

Figure 3. Velocity-porosity trajectories as a rock with a spectrum of void aspect ratios is sealed, computed using Kuster-Toksöz theory. Void sealing has been approximated by removing the thinnest cracks at each step. Reduction in porosity from 26 to 20% more than doubles the compressional wave velocity.

Figure 4. Velocity-porosity distributions at Hole 504B from downhole logs. There is a clear decrease in the slope of the distribution downhole, indicating an increase in the mean aspect ratio (see Fig. 2). Basement begins at 300 meters below seafloor (mbsf).

Figure 5. Velocity-porosity distributions from downhole logs for the 550m of basement penetrated at Hole 418A (110 m.y. old) (top) compared to the uppermost 500m of basement at Hole 504B (6 m.y. old) (bottom). The slope of the distribution for 418A is clearly less than for 504B, suggesting that 418A has the higher mean void aspect ratio expected from the greater degree of sealing.

Figure 6. Depth errors introduced into refraction results by the anisotropy induced by flow layering and horizontal fractures. (a) the *P*-refraction travel time curve for source and receiver on a laminated ocean bottom with a velocity gradient. (b) The true raypath through the anisotropic medium (heavy curve), and the raypath assumed by any isotropic inversion procedure (light curve). (c) True *P*-velocities v_{PH} and v_{PV} for horizontally and vertically propagating *P*-waves, and the velocity returned by the inversion scheme, v_{PI}. It has been assumed here that the anisotropy is zero at the ocean floor, but that is almost certainly wrong. If anisotropy extends to the ocean floor, depth errors will be larger.

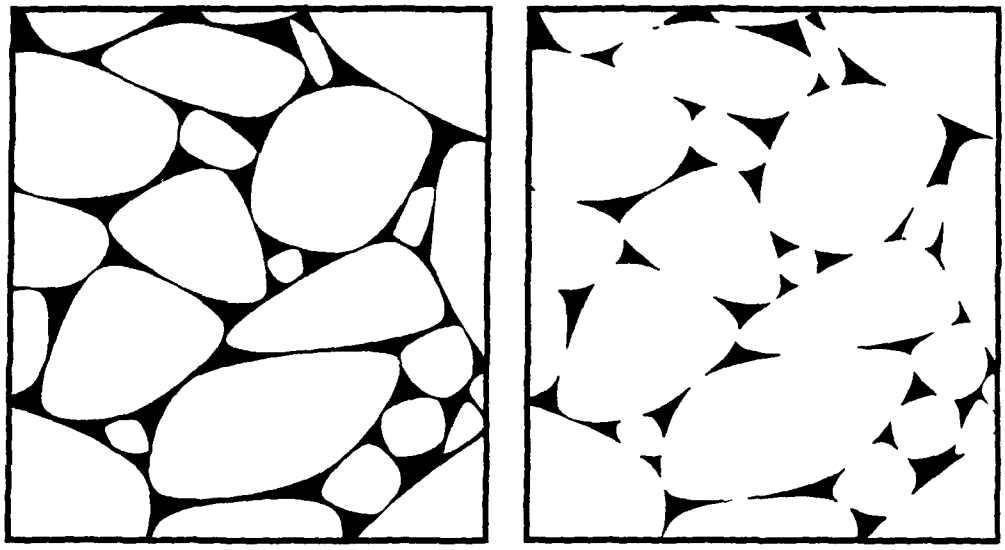

Figure 1

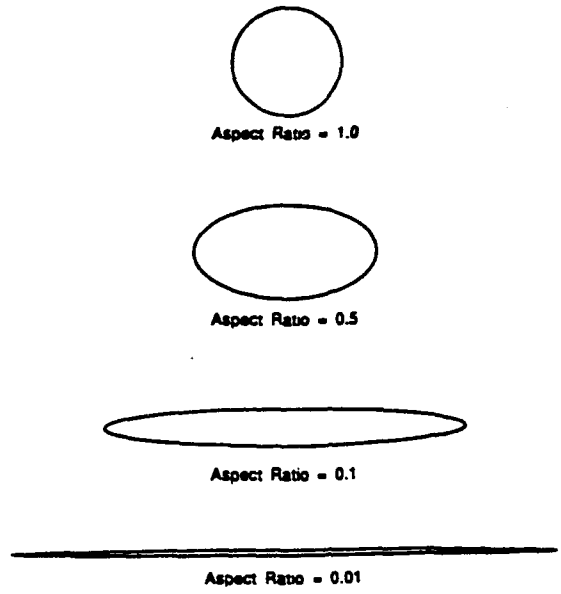
Aspect Ratio = 1.0
Aspect Ratio = 0.5
Aspect Ratio = 0.1
Aspect Ratio = 0.01

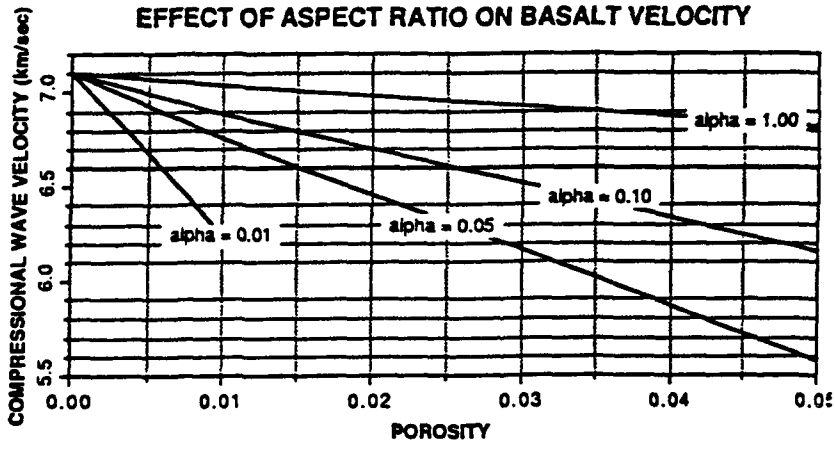
EFFECT OF ASPECT RATIO ON BASALT VELOCITY
COMPRESSIONAL WAVE VELOCITY (km/sec)
7.0
6.5
6.0
5.5
0.00
0.01
0.02
0.03
0.04
0.05
POROSITY
alpha = 1.00
alpha = 0.10
alpha = 0.05
alpha = 0.01

Figure 2

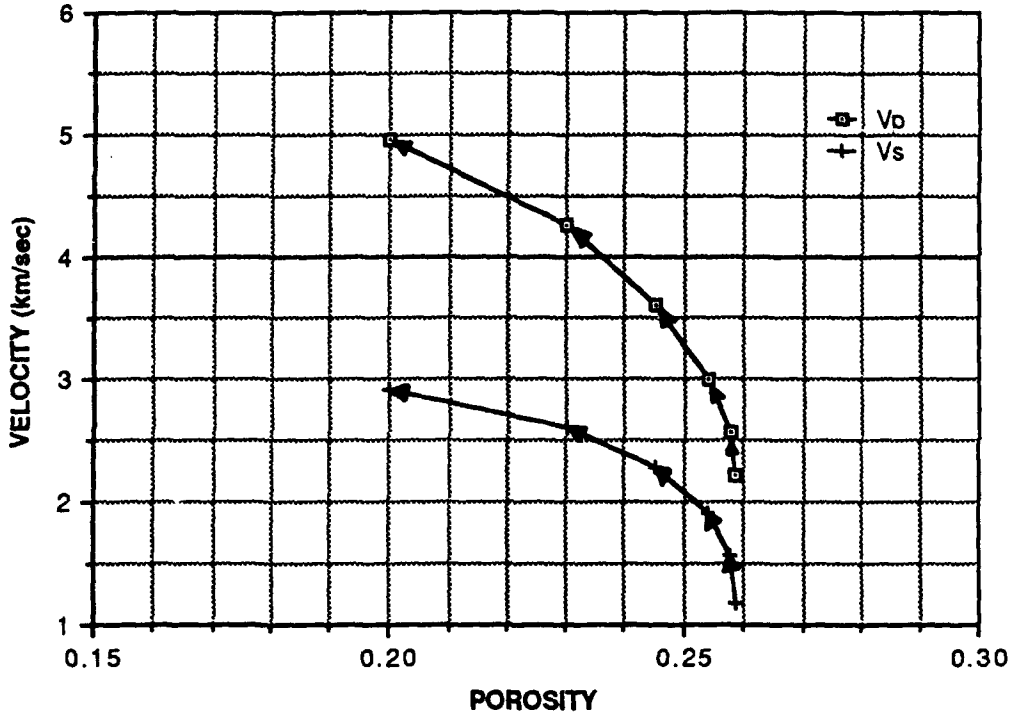

Figure 3

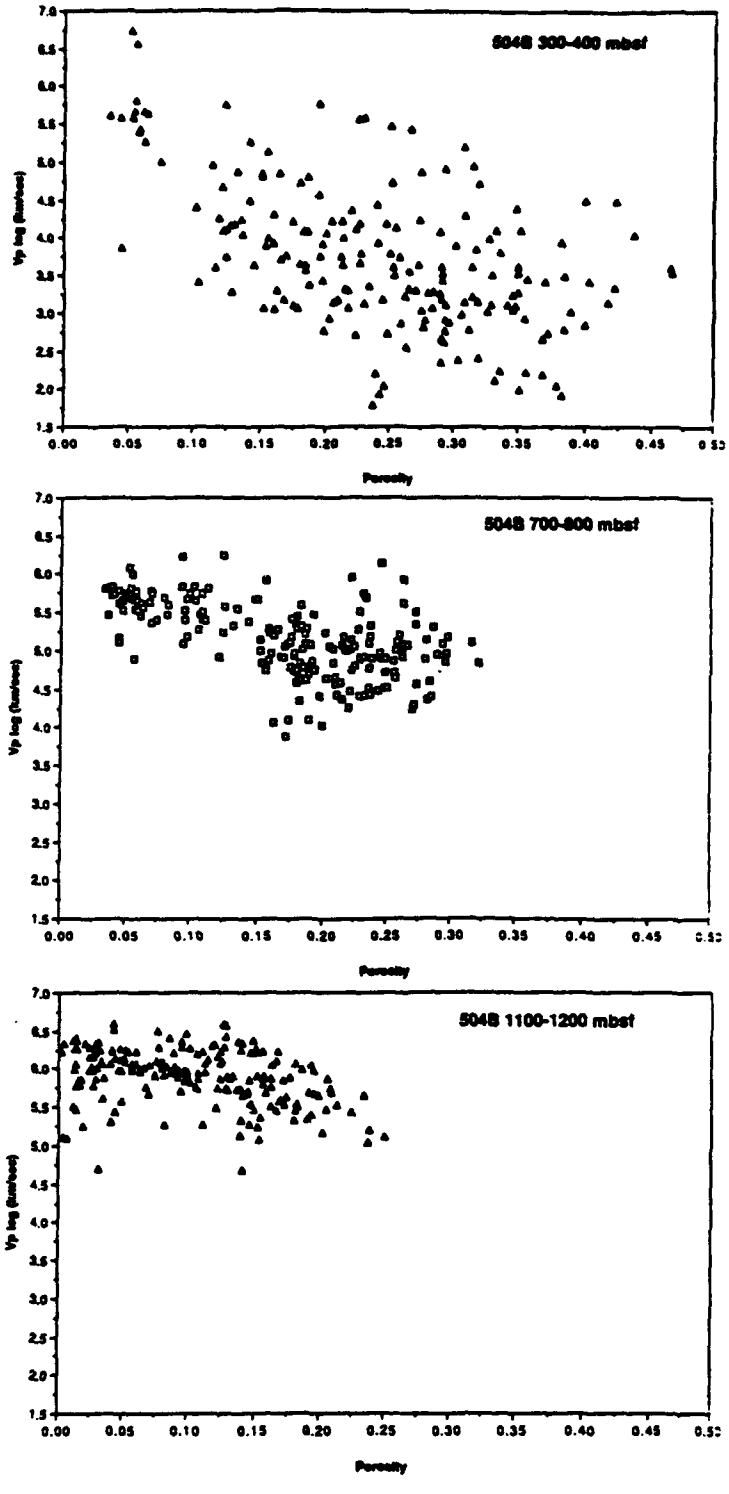
504B 300-400 mbsf
504B 700-800 mbsf
504B 1100-1200 mbsf
Vp log (km/sec)
Porosity
7.0
6.5
6.0
5.5
5.0
4.5
4.0
3.5
3.0
2.5
2.0
1.5
0.00
0.05
0.10
0.15
0.20
0.25
0.30
0.35
0.40
0.45

Figure 4

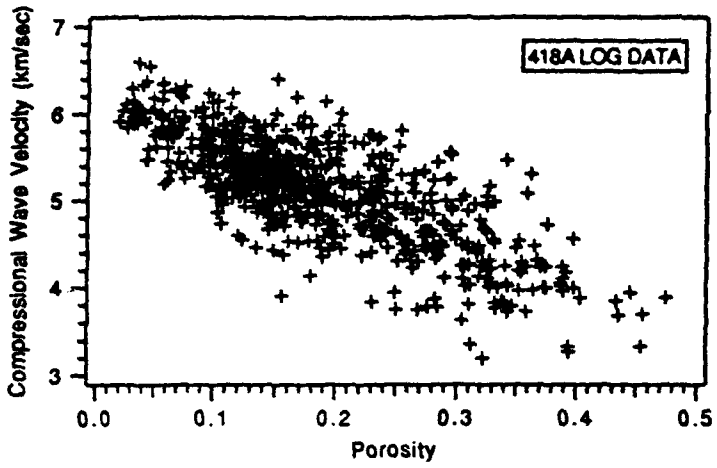
418A LOG DATA
Compressional Wave Velocity (km/sec)
7
6
5
4
3
0.0
0.1
0.2
0.3
0.4
0.5
Porosity

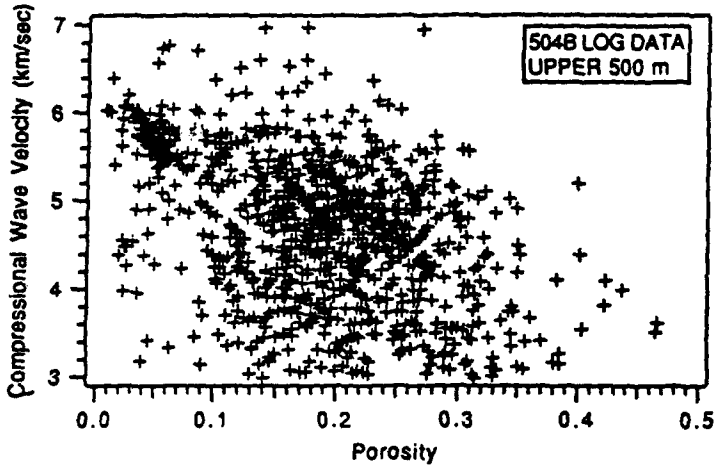
504B LOG DATA
UPPER 500 m
Compressional Wave Velocity (km/sec)
7
6
5
4
3
0.0
0.1
0.2
0.3
0.4
0.5
Porosity

Figure 5

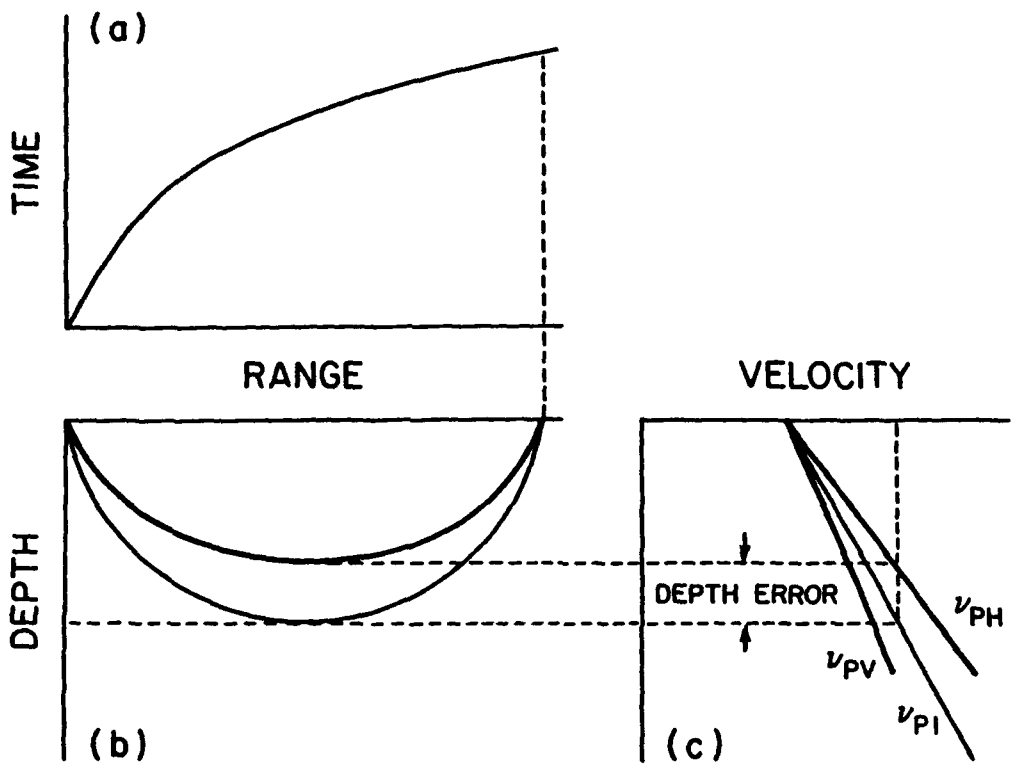

Figure 6

Section C: Papers Contributed to the Workshop

1: **Processes**

2: **Techniques**

3: **Seismics**

4. **Physical Properties**

Section C1: Processes

1: Tectonic Disruption of Volcanic Units of the Oceanic Crust: J.A. Karson

2: The Effect of Alteration on Acoustic Properties in the Ocean Crust: An Example from Ocean Drilling Program Hole 637A: D. Goldberg

3: Implications of In Situ Electrical Resistivity Measurements for the Accretion, Structure, and Hydrology of Medium Spreading-Rate Oceanic Crust: P.A. Pezard

TECTONIC DISRUPTION OF VOLCANIC UNITS OF THE OCEANIC CRUST

Jeffrey A. Karson
Department of Geology, Duke University
Durham, NC 27706

Near-bottom studies of the oceanic crust along spreading centers document the nature of the upper surface of the oceanic basement. These observations help to define the style of faulting of the oceanic crust as well as secondary structures that result from faulting. In addition, tectonic escarpments with significant vertical exposures provide cross sections of the uppermost crust. The following is a very brief summary of these observations to date emphasizing slow-spreading crust where faulting is most pervasive.

Oceanic plate separation with a magma deficit results in tectonic extension of the axial lithosphere along spreading centers. Such lithospheric necking (Tapponier and Francheteau, 1978) may result in relatively minor faulting and fissuring or brittle deformation through the full thickness of the crust (Harper, 1983; Toomey et al., 1985; 1988). In general, the "magma budget" at any point along the spreading axis reflects the time-averaged rate of magmatic construction and thermal structure of the crust. These two parameters control the style of lithospheric extension (Karson et al., 1987; Karson, in press). A low magma budget, characteristic of many slow-spreading ridge segments (Figure 1) results in substantial extensional faulting with significant horizontal (heave) and vertical (throw) fault displacements.

Numerous extensional fault geometries have been documented in continental lithosphere (e.g., Wernicke and Burchfiel, 1982) and many of these have been suggested for oceanic spreading centers on the basis of morphology (e.g., Harrison and Steiltjes, 1977; Macdonald and Luyendyk, 1977). However, only a few of these have been documented to date by near-bottom studies of the oceanic crust.

Observations of sea floor geology from submersibles and camera sleds show that along slow-spreading centers youthful lava flows are quickly reduced to isolated blocks of coherent material surrounded by loose rubble mixed with variable amounts of pelagic ooze. Downslope transport of debris slides often bury blocks of coherent material. Along fast-spreading ridges only local disruption occurs, except at transforms, overlapping spreading centers, propagating rifts, etc.

Although many authors have discussed mid-ocean ridge fault geometries in vertical cross sections, it is important to recognize that extensional strain must be considered in three dimensions. Three dimensional "extensional systems" involve assemblages normal and strike-slip (or oblique-slip) faults (Figures 2-4) that act in concert to accommodate a general strain.

Extensional systems may be considered on a number of scales (Figures 2-4) ranging from ridge segments and transform faults (or overlapping spreading centers) down to normal fault strands of finite length separated by minor transfer or tear faults. Substantial variations in fault geometries exist at all scales.

The widest regions of faulting are associated with normal faults. Hanging wall deformation is primarily a function of the geometry of the underlying master fault (planar, listric, ramp/flat), its dip, and the total amount of displacement. Lower dips result in wider regions of hanging wall deformation which may have a variety of fault styles. Footwall

deformation depends on the same parameters but may show substantial deformation due to isostatic uplift in response to unloading.

The response to brittle extension is in part a function of the mechanical properties of shallow crustal lithologies including dominantly basaltic lavas and diabase dikes. Lithologic contacts and other discontinuities with systematic orientations may help determine fault or slump geometries. Although extreme faulting has exposed plutonic (gabbroic and ultramafic) rocks along spreading centers (e.g., Karson et al., 1987; Karson, in press) placing them in seismic layer 2 (Figure 1), they will not be considered further here. Basaltic pillow lavas and lesser tabular flows constitute the bulk of the upper crust in most places. These units are pervasively fractured and jointed as a result of eruptive and cooling processes. This shattered material is extremely weak and generally cannot support steep fault scarps created by tectonic displacements. Extensive scarp modification occurs by calving of slump masses along headwalls and downslope erosion and deposition by resultant debris slides characterizes all mature fault scarps.

Large-scale inhomogeneities within the volcanic crust may help to localize slip along surfaces bounding slump masses or fault blocks. These could include older fissures, lava flow contacts, pelagic sediment or breccia interbeds, etc. The stratigraphic contacts have orientations related to pre-existing volcanic topography. Different directions of dip would promote different secondary fault geometries.

At deeper levels, originally vertical dikes may foster vertical slip along their margins. However, observations from the sea-floor and ophiolites indicate that faults commonly cut dikes at moderate angles and blocks containing dikes are rotated.

At present detailed fault geometries at spreading centers are not well known. Several areas have been studied in some detail but show substantial differences. The distribution and frequency of the different extensional styles are poorly known especially along fast-spreading ridges. In general, it appears that most areas of slow-spreading crust include a variable thickness of slump and fault breccias overlying a nearly pervasively fractured substrate. Along-strike variations in the breccia thickness and intensity of fracturing is controlled by the geometry of extensional systems. Future studies will help to show how different extensional systems affect crust formed at different spreading rates and in different tectonic settings.

References

Allerton, S. and Vine, F.J., *Geology, 15*, 593-597 (1987).

Gibbs, A., *J. Geol. Soc. Lond., 141*, 609-620 (1984).

Harper, G.D., *Tectonics, 4*, 393-409 (1983).

Harrison, C.J.A. and Stieltjes, L., *Tectonophysics, 38*, 137-144 (1977).

Karson, J.A., Proc. Symp. Ophiolites and Oc. Lithos-TROODOS'87 (in press).

Karson, J.A. and Rona, P.A., *Geol. Soc. Amer. Bull.* (in press).

Karson, J.A., Rona, P.A., and others, *Nature, 328*, 681-685 (1987).

Macdonald, K.C. and Luyendyk, B.P., *Geol. Soc. Amer. Bull., 88*, 621-636 (1977).

Tapponier, P. and Franchetean, J., *J. geophys. Res., 83*, 3955-3970 (1978).

Toomey, D.R., Solomon, S.C., Purdy, G.M. and Murray, M.H., *J. geophys. Res., 90*, 5443-5458 (1985).

Toomey, D.R., Solomon, S.C. and Purdy, G.M., *J. geophys. Res., 93*, 9093-9112 (1988).

Varga, R.J. and Moores, E.M., *Geology, 13*, 846-850 (1985).

Wernicke, B. and Burchfiel, B.C., *J. Struct. Geol., 4*, 105-115 (1982).

SPECTRUM OF EXTENSIONAL STYLES ON THE M.A.R. (c.a. 20mm/yr)

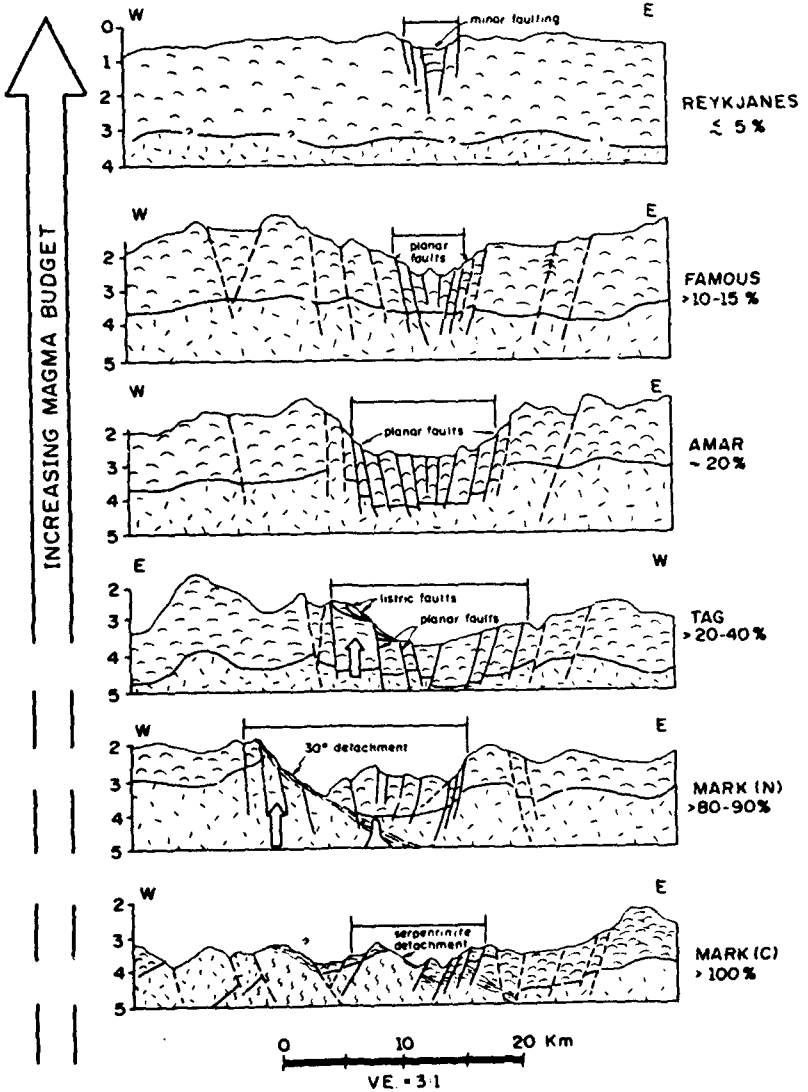

Figure 1

ALONG-AXIS DISCONTINUITIES LINKING DISCRETE SPREADING CELLS

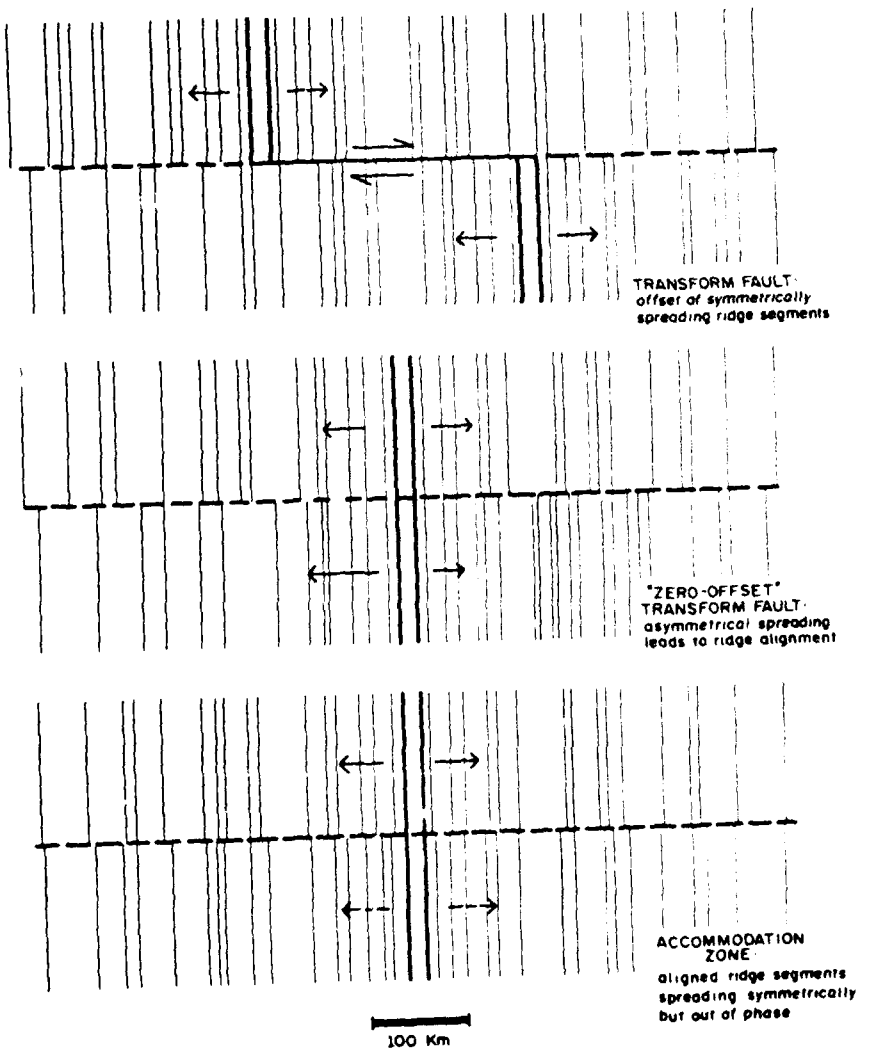

Figure 2

ACCOMMODATION ZONES REQUIRED BY ALONG-AXIS VARIATIONS IN EXTENSIONAL STYLE

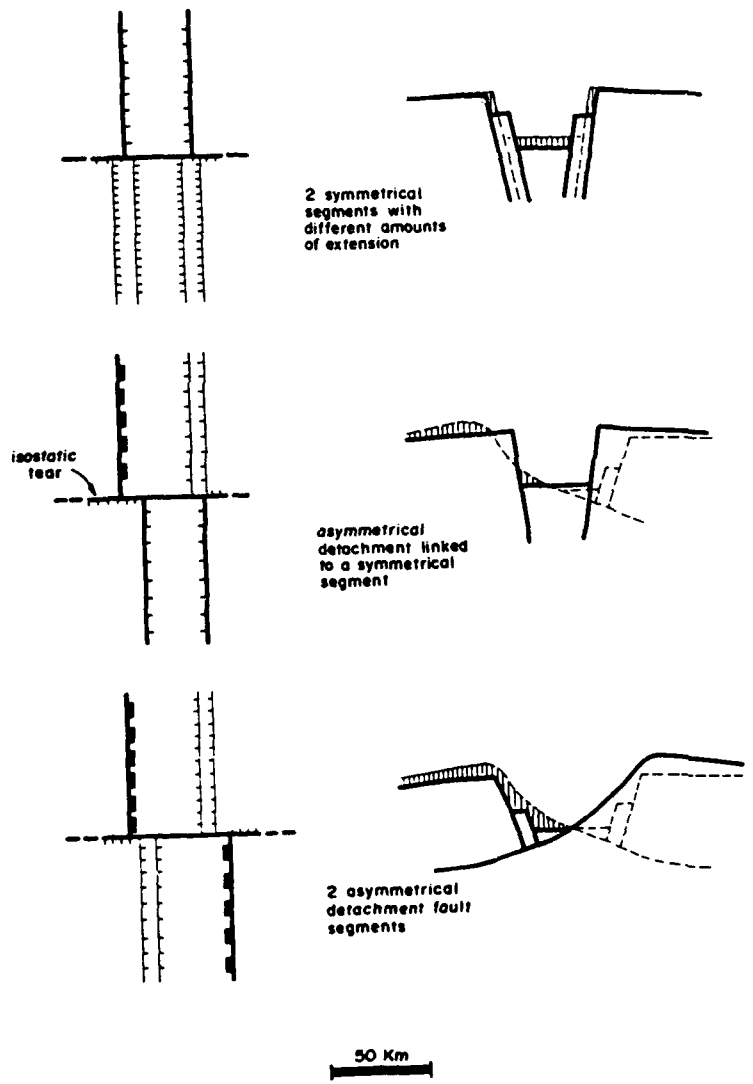

Figure 3

TRANSFER FAULTS BOUNDING TILT DOMAINS

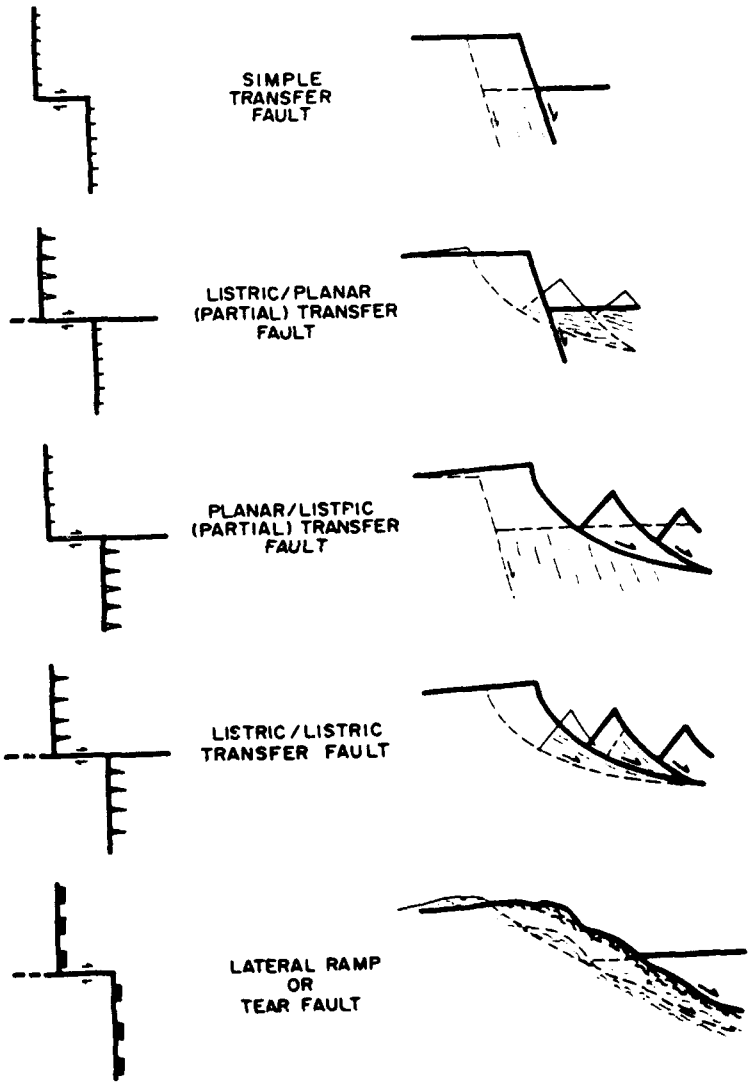

Figure 4

THE EFFECT OF ALTERATION ON ACOUSTIC PROPERTIES IN THE OCEAN CRUST: AN EXAMPLE FROM OCEAN DRILLING PROGRAM HOLE 637A

D. Goldberg
Lamont-Doherty Borehole Research Group, Palisades, NY 10964.

INTRODUCTION

The elastic properties of in-situ materials are routinely determined by industry-standard logging techniques which provide a measure of the compressional velocity in the 10-20 kHz (sonic) frequency band [Pickett, 1963; Arons et al., 1978]. The measurement of attenuation from sonic waveforms, however, poses both theoretical and experimental problems, one of the most difficult being the separation in intrinsic (frictional absorption) and extrinsic (scattering) losses affecting the compressional head wave [Anderson and Castagna, 1984; Goldberg, 1984]. In sonic logs, extrinsic losses and intrinsic attenuation are typically both important, yielding large apparent attenuation of compressional waves, and as as result they have often been used to identify highly attenuating features, such as fractures [e.g., Morris et al., 1964; Paillet, 1980; Seeberger and Zoback 1982; Moos and Zoback, 1983; Haimson and Doe, 1983; Anderson and O'Malley, 1985]. With data from Ocean Drilling Program (ODP) Hole 637A, a similar correlation of in-situ sonic amplitudes with alteration and brecciation in peridotite is presented here.

At Site 637, 74m of folitated peridotite was penetrated from 212 to 285.6m below seafloor (mbsf). The peridotite is clinopyroxene-bearing spinel harzburgite, which is more than 90% serpentized and is pervasively cut by veins of calcite and serpentine [Boillot and Winterer, 1987]. Microscopic inspection shows that the calcite veins cut matrix serpentinite, and interparticular spaces and microfractures are pervasive. The sub-interval that was both logged and cored is only 22m thick (230-252 mbsf), and because of the intense alteration and foliation that varied throughout the core at a scale of 0.1 to 0.5 cm, the physical properties in this interval are both vertically and horizontally anisotropic. The average bulk porosity in this interval, however, varied only slightly between 18 and 19%, perhaps due to bias in sampling the recovered core

DISCUSSION

The compressional velocity, semblance and amplitude logs were calculated from sonic waveforms by signal correlation and are plotted as a function of depth in Figure 1 [Goldberg and Zinszner, 1988]. The borehole diameter, representative core recovery, and comparative alteration of the core are also shown. The alteration log illustrates the relative degree of leaching and, in particular, the major brecciated zones and intervals cut by calcite veins [C.A. Evans, pers. comm., 1987]. The 10-in. borehole diameter varies by only about 1 in. and does not correlate with alteration or poor core recovery. Because acoustic waves are strongly dependent on borehole geometry [Paillet and White, 1982], the poor correlation of borehole diameter with peak amplitude suggests strong amplitude control by other changes in structure. Scattering and poor energy coupling across breccias and veins, which have different elastic moduli than the matrix, will decrease the compressional-wave amplitude. In Figure 1, low compressional amplitudes clearly correlate to brecciated zones and calcite veining; low amplitudes in zones that were not sampled may indicate rocks missed (fractures) or poorly sampled (breccias) during coring. The apparent compressional attenuation may therefore by a useful indicator of such zones, and in general, better depth-to-core correlation can be obtained in the intervals of poor recovery by interpretation of

acoustic logs. In particular, we recommend that compressional amplitudes be exploited for correlations beyond simple fracturing, as their sensitivity to environmental changes reveals important information that is often poorly represented by coring.

Laboratory Vp data are also displayed at effective pressure commensurate with the overburden stress in the well [Goldberg and Zinszner, 1988]. The comparison of laboratory and log-derived Vp data are in good agreement, surmounting the difficulties of laboratory measurements on impermeable and fragile samples, and have estimated experimental errors of about 10%. The differences in laboratory and log-derived velocities may arise, in part, from depth uncertainty in the core samples and from large-scale features, such as fractures, that influence the sonic log, but not the laboratory measurements. The overall agreement of the laboratory velocity with sonic log velocity is not biased by the effects of dispersion, because the measurements were made under pressure by a resonance method in the same 10-20 kHz frequency band [Goldberg and Zinszner, 1988]. Resonance results are generally more reliable, though more time-consuming and limited by sample size and fragility, than ultrasonic experiments. With this in mind, ultrasonic measurements should be interpreted with caution, particularly in conjunction with sonic logging and seismic data, as the difference in frequency and sample size are not simply correlative.

REFERENCES

Anderson, J.A., and Castagna, J.P., 1984. Analysis of sonic log compressional wave amplitudes using borehole compensation techniques. *Trans. Soc. Prof. Well Log Anal. Annu. Symp., 25*: Paper K.

Anderson, R.N., and O'Malley, H., 1985. Frequency response and attenuation changes across highly altered fracture zones crosscutting a fast formation: the oceanic crust of the Mid-Atlantic Ridge. *Trans. Soc. Prof. Well Log Anal. Annu. Symp., 26*: Paper LLL.

Arons, J., Murray, J., and Seeman, B., 1978. Formation compressional and shear interval transit time logging by means of large spacings and digital techniques. *Trans. Soc. Pet. Eng. AIME Annu. Tech. Conf., 53*: Paper 7446.

Boillot, G., Winterer, E.L., 1987. Site 637, In Boillot, G., Winterer, E.L., et al., *Proc. ODP, Init. Repts., 103*: College Station, TX: (Ocean Drilling Program), 123-219.

Goldberg, D.S., Kan, T.K., and Castagna, J.P., 1984. Attenuation measurements from sonic log waveforms. *Trans. Soc. Prof. Well Log Anal. Annu. Symp., 25*: paper NN.

Goldberg, D., and Zinszner, B., 1988. Acoustic properties of altered peridotite at Stie 637 from laboratory and sonic waveform data. In Boillot, G., Winterer, E.L. et al., *Proc. ODP, Sci. Results, 103*: College Station, TX: (Ocean Drilling Program), 269-276.

Haimson, B.C., and Doe, T.W., 1983. State of stress, permeability and fractures in Precambrian granite of northern Illinois. *J. Geophys. Res., 88*: 7355-7371.

Moos, D., and Zoback, M.D., 1983. In-situ studies of velocity in fractured crystalline rocks. *J. Geophys. Res., 88*: 2345-2358.

Morris, R.L., Grine, D.R., and Arkfeld, T.E., 1964. Using compressional and shear acoustic amplitudes for the location of fractures. J. *Pet. Tech., 16*.

Paillet, F.L., 1980. Acoustic propagation in the vicinity of fractures which intersect a fluid-filled borehole. *Trans. Soc. Prof. Well Log Anal. Annu. Symp., 21*: paper D.

Paillet, F.L., and White, J.E., 1982. Acoustic modes of propagation in the borehole and their relationship to rock properties. *Geophys., 47*: 1215-1228.

Pickett, G.R., 1963. Acoustic character logs and their application in formation evaluation. *J. Petr. Tech., 15*: 659-667.

Seeberger, D.A., and Zoback, M.D., 1982. The distribution of natural fractures and joints at depth in crystalline rock. *J. Geophys. Res., 87*: 5517-5534.

FIGURE CAPTION

Figure 1. Geophysical logs of borehole diameter (in.), compressional velocity (km/s), normalized semblance, and amplitude (dB) for altered peridotite drilled at ODP Hole 637A. Laboratory resonance data with 10% error bars are also shown in the compressional velocity column and are in good agreement with the velocity log. Generalized alteration and core recovery logs from shipboard descriptions are shown; low compressional amplitudes correlated well with highly altered and brecciated zones that were poorly sampled during coring of this hole.

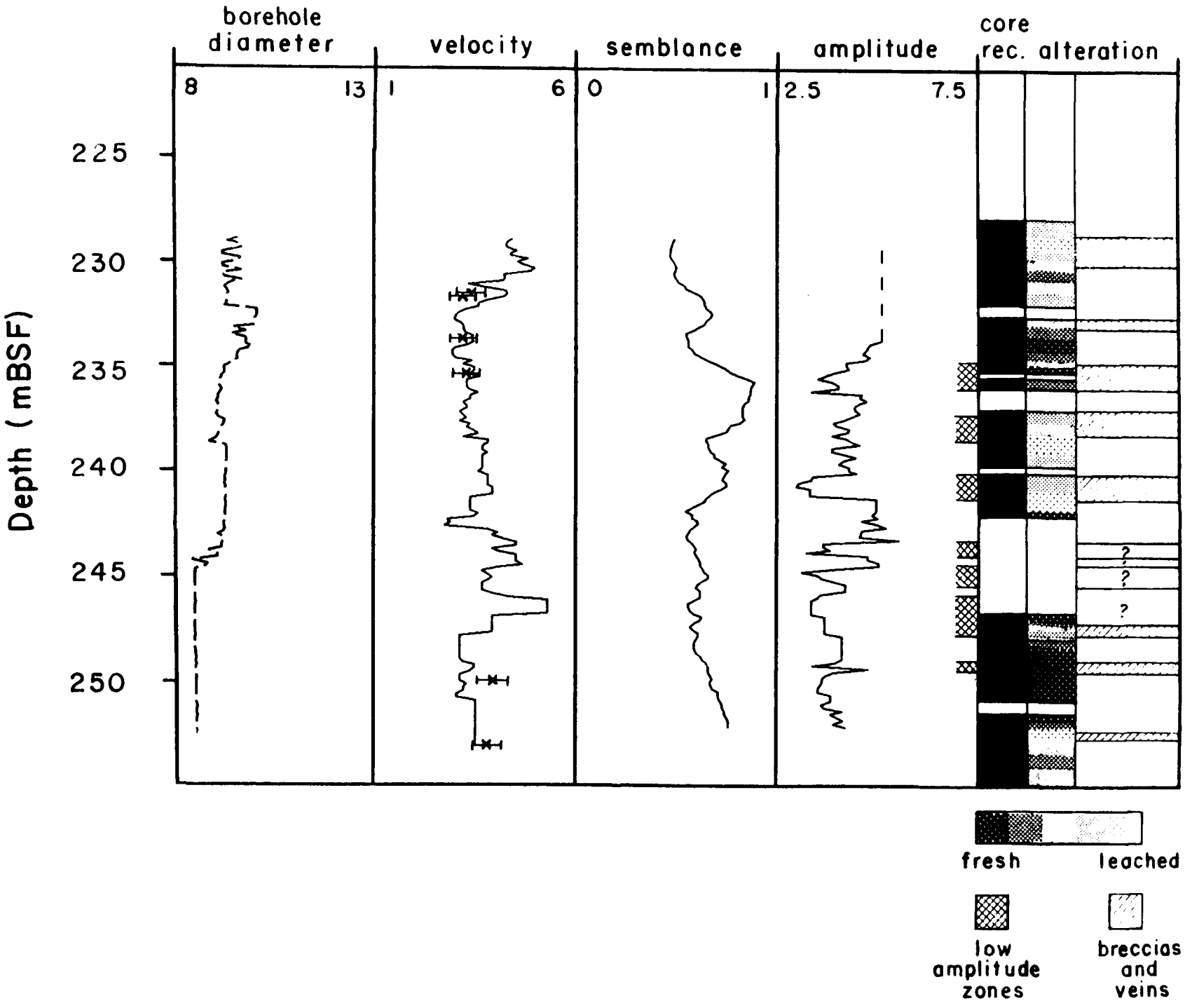
borehole diameter
8
13
velocity
1
6
semblance
0
1
amplitude
2.5
7.5
core rec.
alteration
Depth (mBSF)
225
230
235
240
245
250
?
?
?
fresh
leached
low amplitude zones
breccias and veins

IMPLICATIONS OF IN SITU ELECTRICAL RESISTIVITY MEASUREMENTS FOR THE ACCRETION, STRUCTURE, AND HYDROLOGY OF MEDIUM SPREADING-RATE OCEANIC CRUST

Philippe A. Pezard
Borehole Research Group of the Lamont-Doherty Geological Observatory.

DSDP Hole 504B is located in 5.9 ma oceanic crust, to the south of the Costa Rica Rift (Figure 1), an active ridge now spreading at 7.0 cm/yr (full rate). Hole 504B was re-entered during Leg 111 of the Ocean Drilling Program, and a continuous electrical resistivity profile was recorded [Becker et al., 1989]. This profile permitted to discriminate the large-scale seismic-layers of the upper oceanic crust, to isolate individual lithologic units (such as pillows and massive flows), and to describe the overall morphology of the upper crust in relation with alteration facies observed in thin-sections (Figure 2). In the extrusive part of the crust, the massive flows (10-meters-thick or more) are found to constitute permeability barriers, and subsequently to constrain fluid circulation [Pezard, 1990]. Whereas the flows of Unit 2D (located 50-m into basement) are associated with the under-pressured aquifer located within Layer 2A, Unit 27 is the boundary between low-temperature, oxidative alteration facies of basalt, and higher-temperature alteration phases developed under a reducing environment [Alt et al., 1986]. This relationship between morphology and hydrological regime, and therefore alteration of the basaltic basement might thus be viewed as related to the accretion process of the upper oceanic crust at intermediate spreading-rate.

The volcanic edifice sampled by Hole 504B has been studied with respect to episodic accretion models developed from seafloor observations [Lewis,1979; Kappel and Ryan, 1986; Gente, 1987]. In these morphotectonic models, excessive volcanism periodically builds a crestal ridge along the axis of seafloor-spreading (Figure 3). As the volcanic activity decreases, an elongated summit depression (ESD) develops in the spine of this axial structure due to crustal stretching. In this context, the continuous and vertical nature of borehole measurements provides stratigraphic and structural data that cannot be obtained from seafloor studies.

Due to the zonation of MORB alteration and its relation to lava morphologies [Friedrichsen, 1985; Alt et al., 1986; Pezard, 1990], the 650-m-thick effusive section penetrated in Hole 504B is postulated to be accreted in two main volcanic sequences (VS1 and VS2). The massive lava flows (10-m-thick or more) are interpreted as corresponding to the onset of these volcanic sequences, and consequently as being emplaced onto collapse structures, on the floor of an ESD (Figure 2). The underlying lava, necessarily accreted at the end of the previous volcanic episode, are made of pillows with large porosity values and numerous fractures. On top of such highly heterogeneous intervals, the thick flows constitute crustal permeability barriers, thereby constraining the circulation of hydrothermal fluids. Whereas the interval corresponding to the end of the first volcanic episode is today observed to be sealed by alteration minerals, the second-one is still open to fluid circulation and is now the site of an under-pressured aquifer [Anderson and Zoback, 1982].

Considering that most of the extrusives are emplaced within a narrow neo-volcanic zone, as the crust moves away from the spreading-axis, the lower section of the volcanic pile is that accreted near the ridge-axis, hence exposed to the most intense hydrothermal circulation (such as that associated with black smokers) due to the proximity of the magma chamber (Figure 4). Once capped by a massive flow at the onset of the next volcanic phase (VS2), the lower interval is hydrologically separated from ocean-waters and a reducing

environment develops below it, resulting in the precipitation of sulfides. The upper part of the volcanic edifice is thus ideally never exposed tc fluids reaching deep into the crust, while the lower one is. The fluid circulation in the upper interval is therefore constrained by the amount of heat conducted through the impermeable barrier.

As the first unit extruded for a given vertical cross-section is necessarily emplaced at the ridge-axis, it remains the deepest extrusive rock of the volcanic pile. In Hole 504B where a 250-m-long Transition Zone from dikes to extrusives was discovered, the first extrusive unit is difficult to identify. This Transition Zone is interpreted as the relict of a massive unit flooding the axial ESD at the onset of the first volcanic episode, later ruptured and intruded by numerous dikes necessary to feed the upper part of the volcanic edifice (Figure 5). Further from the axis, the same massive unit constitutes a potential permeability cap for crustal sections accreted earlier. As such, the upper 50 meters of the basement might be considered as the far-end expression of massive outpours extruded near the ridge-axis (Figure 4). The geophysical data recorded in the volcanic section of Hole 504B are thus found to support the non steady-state models of crustal accretion for intermediate spreading-rates of Lewis, [1979], Kappel and Ryan [1986] and Gente [1987] which, in turn, provides a framework to analyze the structural, hydrological (Figure 6), and mineralogical observations made in the hole over the past ten years.

References

Alt, J.C., Honnorez, J., Lavene, C., and Emmermann, R., 1986. Hydrothermal alteration of a 1-km section through the upper oceanic crust, DSDP Hole 504B: the mineralogy, chemistry and evolution of seawater-basalt interactions, *J. Geophys. Res., 91*: 309-335.

Anderson, R.N., and Zoback, M.D., 1982. Permeability, underpressures, and convection in the oceanic crust near the Costa Rica rift, *J. Geophys. Res., 87*: 2860-2868.

Archie, G.E., 1942. The electrical resistivity log as an aid in determining some reservoir characteristics, *Journal of Petroleum Technology, 5*: 1-8.

Becker, K., Sakai, H., et al., 1989. Drilling deep into young oceanic crust, Hole 504B, Costa Rica Rift, *Rev. of Geophysics, 27*, 1, 79-102.

Friedrichsen, H., 1985. Strontium, oxygen and hydrogen isotope studies on primary and secondary minerals in basalts from the Leg 83 section of DSDP Hole 504B, Costa Rica Rift. In Anderson, R.N., Honnorez, J., Becker K., et al., *Init. Repts. DSDP, 83*, Washington, (U.S. Govt. Printing Office), 289-296.

Gente, P., 1987. *Etude morphostructurale comparative de dorsales océaniques à taux d'expansion variés*, in Thèse de Doctorat, Université de Bretagne Occidentale, Brest.

Kappel, E.S., and Ryan, W.B.F., 1986. Volcanic episodicity and a non-steady state rift valley along northeast Pacific spreading centers: evidence from Sea MARC I, *J. Geophys. Res., 91*: 925-940.

Lewis, B.R.T., 1979. Periodicities in volcanism and longitudinal magma flow on the East Pacific Rise at 23°N, *Geophys. Res. Lett., 6*, 753-756.

Pezard, P.A., 1990. Electrical properties of MORB, and implications for the structure of the upper oceanic crust at Site 504, *J. Geophys. Res.*, in press.

Pezard, P.A., and Anderson, R.N., 1990. In situ measurements of electrical resistivity, formation anisotropy, and tectonic context, *SPWLA Transactions*, 31st Annual Meeting, Lafayette, Louisiana.

Figure Captions

Figure 1. Location of Site 504 on the south flank of the Costa Rica rift, Panama basin, eastern equatorial Pacific.

Figure 2. Electrical resistivity measurements in Hole 504B, and related shipboard analysis of apparent porosity on the basis of Archie's law [1942]. An estimate of fracture porosity (grey shading) is derived from the comparison of the two laterolog measurements [Pezard and Anderson, 1990]. The different seismic Layers are indicated in the porosity track, and the alteration zones derived from thin-sections analysis in the resistivity track [Alt et al., 1986].

Figure 3. Morphotectonic accretion model of Kappel and Ryan [1986]. A crestal ridge grows from T1 to T2, then the elongated summit-depression (ESD) collapses into the crestal ridge during T3, followed by a growth of a new crestal ridge in the middle of the ESD during T4. The axial structure is allowed to vary in width during the different accretion phases.

Figure 4. Evolution of a vertical volcanic pile (column) equivalent to that penetrated at Site 504, as it is created near the ridge-axis, then grows with time as it travels through the neo-volcanic zone (NVZ). The arrows represent fluid circulation within the crust, and M.C. stands for magma chamber.

Figure 5. Evolution with increasing time of the axial structure, starting with (a) flooding of the ESD and eventual overspilling on the ridge-flanks constituting an off-axis permeability barrier, (b) fracturing on-axis, then (c) renewed volcanism with splitting of the thick axial flow by numerous dike intrusions, and (d) development of a crestal ridge, until (e) that of a new axial ESD.

Figure 6. Hydrological evolution of the crust with respect to successive accretion phases described in Figure 4.

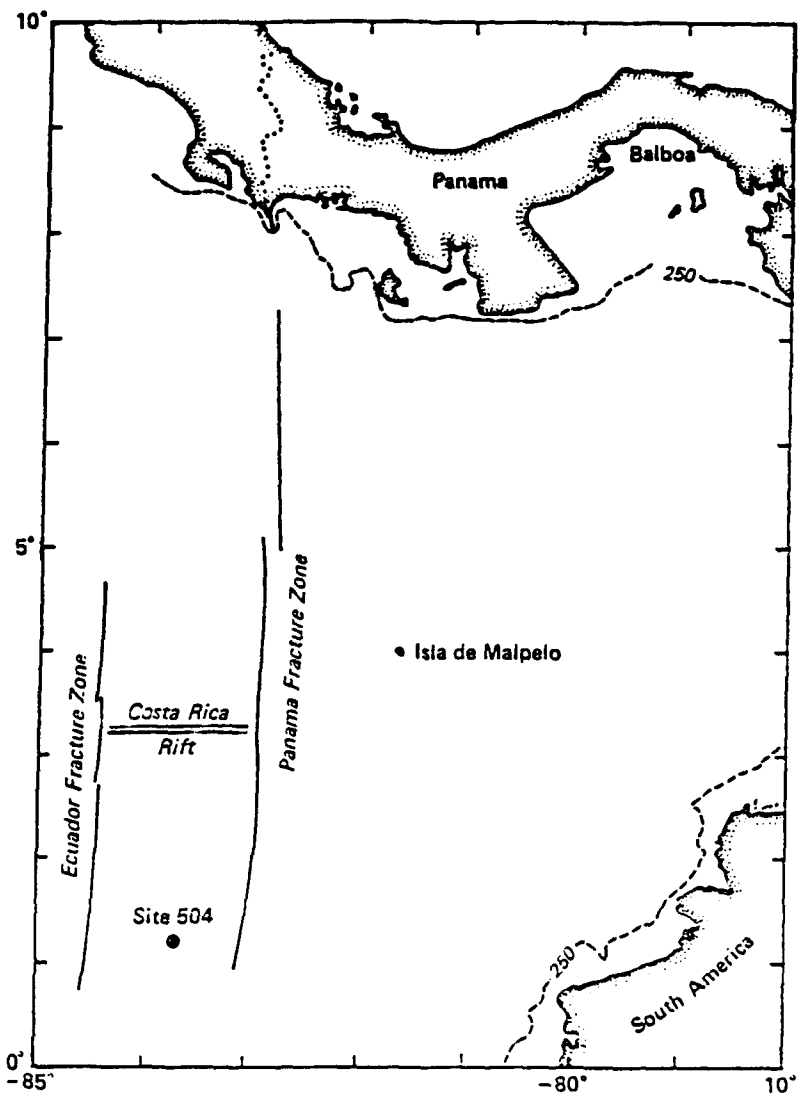
10°
5°
0°
-85°
-80°
10°
Panama
Balboa
250
Isla de Malpelo
Costa Rica
Rift
Ecuador Fracture Zone
Panama Fracture Zone
Site 504
250
South America

Figure 1

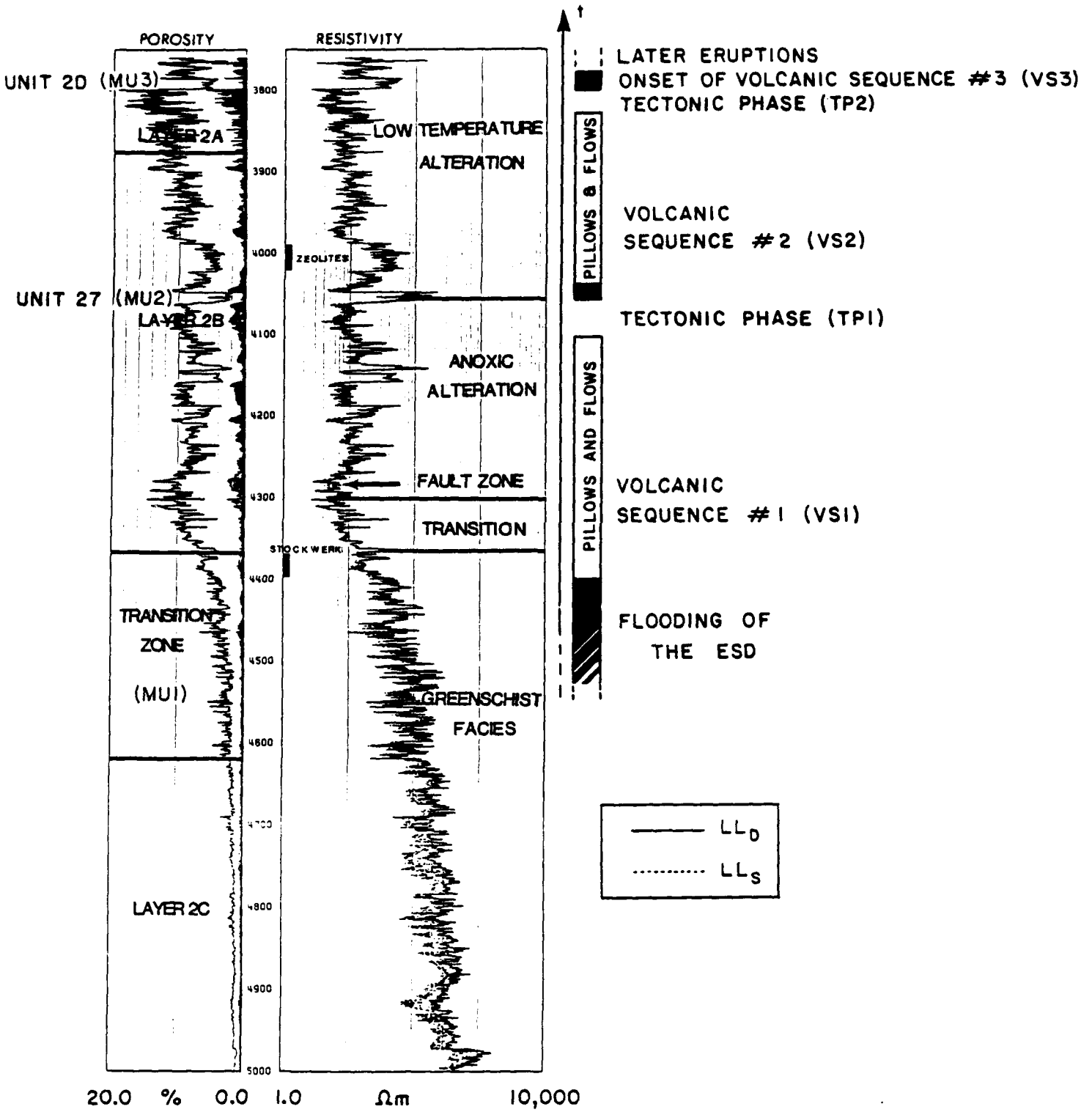
POROSITY
RESISTIVITY
UNIT 20 (MU3)
LAYER 2A
UNIT 27 (MU2)
LAYER 2B
TRANSITION ZONE (MU1)
LAYER 2C
3800
3900
4000
4100
4200
4300
4400
4500
4600
4700
4800
4900
5000
ZEOLITES
STOCKWERK
LOW TEMPERATURE ALTERATION
ANOXIC ALTERATION
FAULT ZONE
TRANSITION
GREENSCHIST FACIES
20.0 % 0.0
1.0 Ωm 10,000
t
LATER ERUPTIONS
ONSET OF VOLCANIC SEQUENCE #3 (VS3)
TECTONIC PHASE (TP2)
PILLOWS & FLOWS
VOLCANIC SEQUENCE #2 (VS2)
TECTONIC PHASE (TP1)
PILLOWS AND FLOWS
VOLCANIC SEQUENCE #1 (VS1)
FLOODING OF THE ESD
LL_D
LL_S

Figure 2

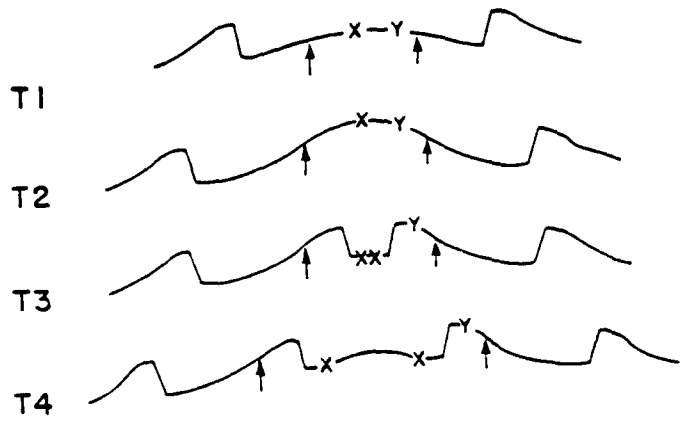

Figure 3

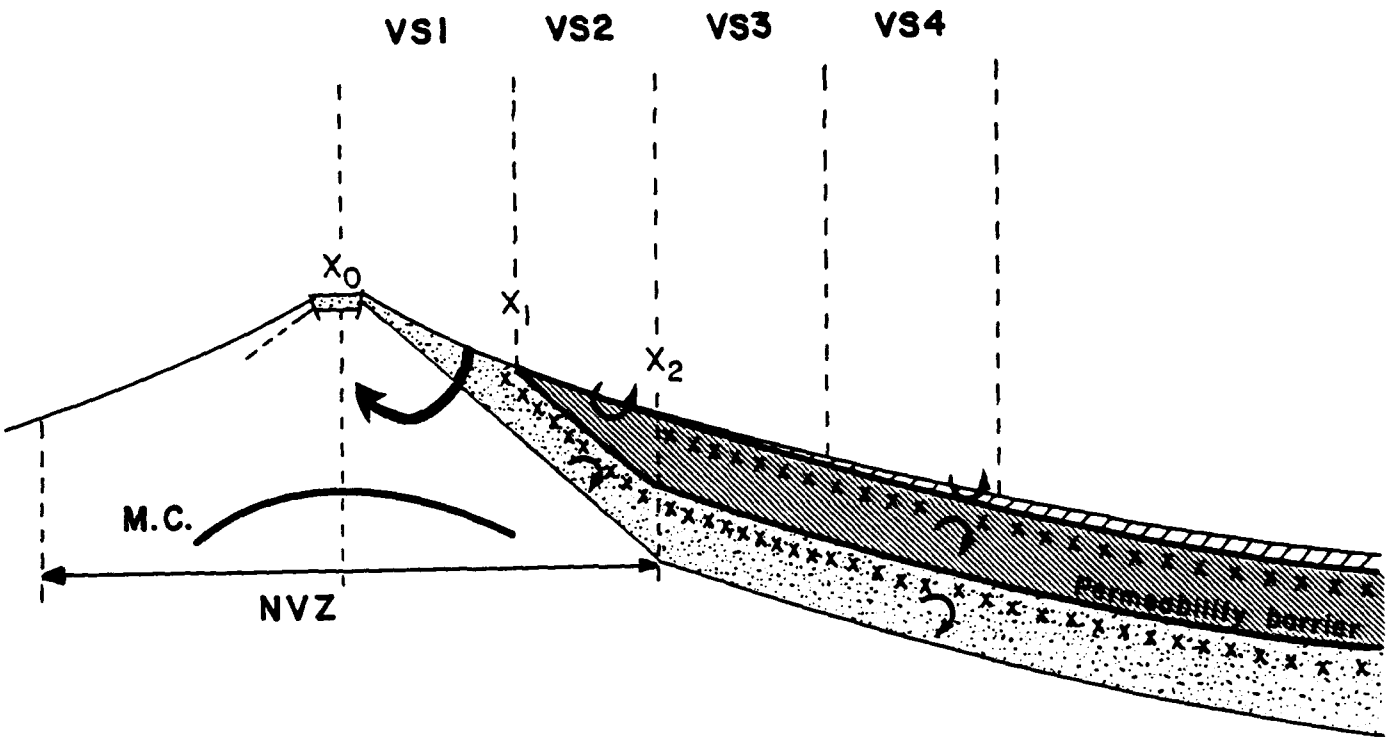

Figure 4

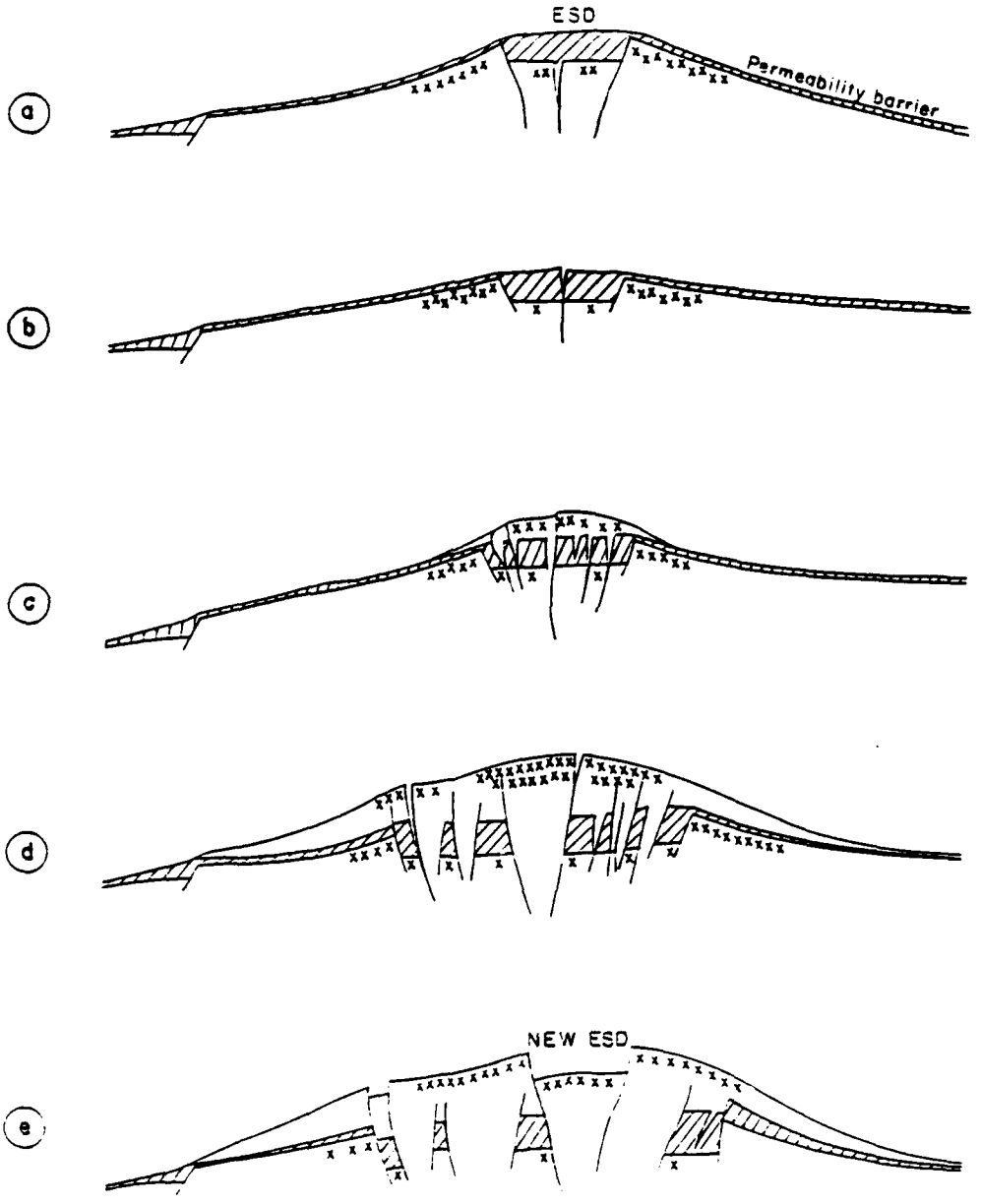

Figure 5

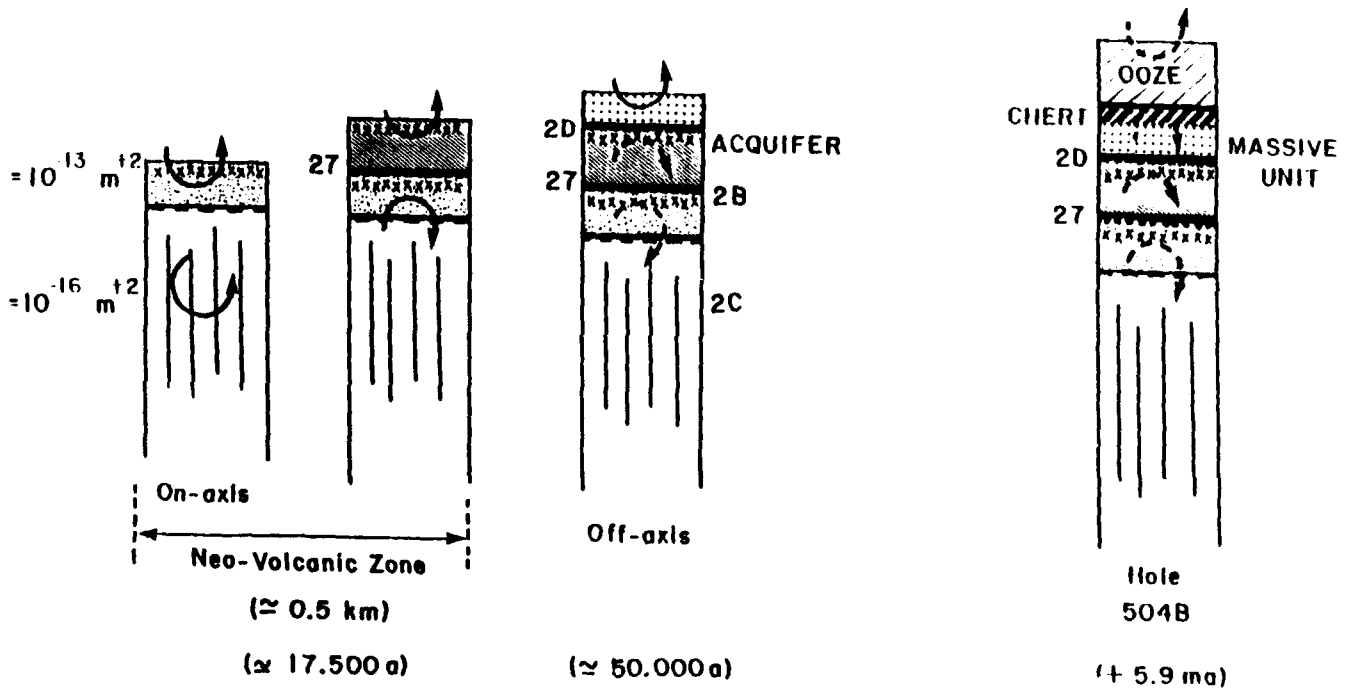
$=10^{-13}$ m^{+2}
$=10^{-16}$ m^{+2}
27
On-axis
Neo-Volcanic Zone
(≃ 0.5 km)
(≃ 17.500 a)
2D
27
ACQUIFER
2B
2C
Off-axis
(≃ 50.000 a)
OOZE
CHERT
2D
27
MASSIVE
UNIT
Hole
504B
(+ 5.9 ma)

Figure 6

Section C2: Techniques

1: The Fine Scale Magnetic Structure of Young Ocean Crust: M.A. Tivey and H.P. Johnson

2: Effects of Rough Bathymetry on the Seismic Resolution of Upper Crustal Structure: I.I. Kim and J.A. Orcutt

3: The Variation of Backscatter with Incidence Angle for Sonar Data over MOR Volcanics: N.C. Mitchell

4. Crustal Studies Using Interface Waves: L.M. Dorman, J.A. Hildebrand, L.D. Bibee

5. Sea Floor Transient Electromagnetic Sounding: R.N. Edwards

6. Key Downhole Measurements for In-Situ Crustal Studies: An Example from Ocean Drilling Program Hole 735B: D. Goldberg

THE FINE SCALE MAGNETIC STRUCTURE OF YOUNG OCEAN CRUST

Maurice A. Tivey, Woods Hole Oceanographic Institution
H. Paul Johnson, University of Washington

What can the fine-scale magnetic structure of young ocean crust tell us about the processes of crustal evolution? To address this question we have investigated the detailed magnetic structure of young ocean crust over the Endeavour ridge segment of the northern Juan de Fuca Ridge using both a high-resolution aeromagnetic survey and near-bottom magnetometer tows. These data show that the observed high frequency magnetic signal is not simply a result of geomagnetic or bathymetric sources but may be responding to processes of crustal evolution such as crustal fissuring and faulting and subsequent enhanced alteration in these disrupted areas.

SHORT WAVELENGTH MAGNETIC ANOMALIES

Short wavelength anomalies are often observed within the normal polarity Brunhes epoch. A particularly well-developed short-wavelength magnetic anomaly, the Central Anomaly Magnetic High (CAMH), occurs directly over the spreading axis of many mid-ocean ridges and is often flanked by other short-wavelength anomalies. The width of the CAMH anomaly does not appear to be a function of spreading rate eliminating the geomagnetic signal as a source of this anomaly. The widespread occurrence of the CAMH anomaly over ridges of varying spreading rate and tectonic environment suggests an interplay between the primary geomagnetic signal and crustal evolution processes such as tectonic and volcanic activity and accompanying alteration processes.

Aeromagnetic Data

An aeromagnetic survey with 1 nautical mile spacing was flown over the Endeavour Ridge at an altitude of 330m by Canadian Defence Research Establishment Pacific in collaboration with the University of Washington in 1987. A 3D view of a portion of this data is presented in Figure 1 and shows the central Brunhes anomaly and a number of short-wavelength anomalies within it including the CAMH anomaly which overlies the axis of spreading and bisects the Brunhes. Typically the CAMH anomaly has the following characteristics:

amplitude of 300 nT
lineated along the axis of spreading
variable in amplitude and wavelength along ridge-strike
flanked by lower amplitude anomalies to the west and east

Deeptow data

Near-bottom magnetic data were collected over the Endeavour Ridge and flanking ridges using the University of Washington Deeptow Magnetometer System in 1984, 1986 and 1988 (see trackline map in Figure 2 for locations). These data were corrected to a level plane 1.8 km below the sea level (300-500m above the seafloor) and then inverted for their crustal magnetization using the Parker and Huestis (1974) Fourier inversion technique. The main results of these deeptow surveys are summarized below:

a) The CAMH anomaly has structure and is not simply a peak as observed at the sea surface but actually has an axial magnetic low (AML) over the rift valley (see profile DTM88-1, Figure 3).

b) The CAMH has very sharp boundaries corresponding to the bathymetric expression of Endeavour ridge, but as indicated by the aeromagnetic data, the CAMH is still well-developed (see profiles DTM88-2 and DTM88-3, Figures 4, 5) where the positive expression of Endeavour Ridge is absent.

c) The structure of the CAMH varies along the strike of the ridge with a well-developed axial magnetic low at the summit area of Endeavour ridge 47°57'N (where hydrothermal activity has been documented) which disappears on profiles further north which show increasing complexity.

d) As observed in the aeromagnetic data flanking anomalies are measured each side of the CAMH. The western anomaly coincides with West Endeavour ridge approximately 7 km off-axis (0.26 Ma) (see profile DTM88-1). Equivalent anomalies are seen to the east of the CAMH at about the same offset (7 km) but with no obvious bathymetric feature (see profiles DTM88-2 and -3, Figures 4, 5).

Tectonic observations

On the Endeavour segment, the axial ridge flanks are relatively unfissured compared with the adjacent fissured crust and axial graben. SeaMARC II data and submersible observations demonstrate the existence of adjacent kilometer-sized blocks of fissured crust and unfissured crust, which can extend along ridge-strike for many tens of kilometers. Magnetic highs are present over zones of unfissured crust and magnetic lows appear over areas of fissured and cracked crust. The correlation of fissure patterns with the observed short-wavelength magnetic anomalies has led to a model for the evolution of shallow crustal structure at a spreading ridge and the source of these magnetic anomalies.

POSSIBLE SOURCES OF SHORT-WAVELENGTH MAGNETIC ANOMALIES

Bathymetry Source

The strong correlation of the CAMH with the positive expression of Endeavour Ridge suggests a bathymetric source, but this correlation fails towards the distal ends of the segment. Forward modeling a strictly bathymetric source for the CAMH cannot reproduce the observed CAMH anomaly. To the northern end of the Endeavour Ridge segment the CAMH anomaly is present even though the bathymetric expression of Endeavour Ridge has disappeared.

Geomagnetic Source

A number of short reversal events within the Brunhes have been identified in terrestrial lavas and sediment cores. The short length of these events combined with the episodicity of mid-ocean volcanic processes makes their correlation to marine magnetic anomalies problematical. Little or no correlation is seen when the deeptow profile magnetizations over Endeavour Ridge are compared with a simple block magnetization model for short reversal events.

Pillow Alteration

Early studies of the CAMH by Klitgord et al., [1975] suggested that the anomaly is caused by a two-stage alteration of pillow basalts in which the outer fine-grained, more magnetic part of the pillow alters first followed by the coarser-grained, less-magnetic interior. However such as process could not explain the presence of the axial magnetic low or flanking anomalies.

A PROPOSED MODEL

Crustal Alteration and Tectonics

We propose that crustal alteration influenced by the tectonic state of the crust is giving rise to the observed fine-scale magnetic signature [Tivey and Johnson, 1987]. This model hypothesizes that large-scale crustal fissuring provides pathways for the continuous penetration of oxygenated seawater deep into the magnetic source layer. Extensively fissured oceanic crust will thus undergo rapid, pervasive, low-temperature oxidation of the magnetic minerals in the extrusive rocks of the entire magnetic anomaly source layer, resulting in a reduction in magnetization. In contrast, unfissured crust (i.e., the flanks of Endeavour Ridge) will have only limited penetration of oxygenated seawater into the magnetic crustal layer. In this case, low-temperature alteration proceeds relatively slowly within the unfissured crustal section, and the crust maintains its initial high magnetization for a longer period of time. The juxtaposition of zones of fissured, altered, low magnetization crust adjacent to zones of unfissured, unaltered, highly magnetic crust provides the necessary magnetic contrast that is the source of the CAMH anomaly. A combination of this crustal alteration process with the tectonic evolution of a medium-rate spreading center, such as proposed by Kappel and Ryan [1986], will produce the pattern of magnetic highs and lows that is observed. The tectonic model similar to that proposed by Kappel and Ryan [1986] outlines the evolution of a medium-rate spreading center through several stages. The fundamental features of this model are:

(1) spreading and crustal extension are relatively continuous, over a scale of tens of thousands of years.
(2) volcanic activity is discontinuous, with periods of high volcanic output followed by quiescent periods.
(3) crustal topographic highs formed during these periods of intense volcanic activity can be subsequently "split" and then each half-ridge transported relatively intact laterally for some distance from the axis of spreading.

The evolution of a typical spreading center can be summarized by four tectonic phases outlined below:

Stage 1: an axially centered ridge has formed during a period of high volcanic activity. The axial ridge crust is relatively unfissured compared with adjacent crust.

Stage 2: as volcanic activity wanes but spreading continues, a down-dropped axial graben forms, splitting the axial ridge in half. This collapse process probably occurs over a relatively short period of time. Fissuring is concentrated at the graben valley walls and there may be some minor volcanic output in the valley proper. The two halves of the split axial ridge raft away as whole units as the crust continues to spread apart with some faulting and fissuring occurring on the axis-facing walls.

Stage 3: If volcanic activity is low for a long enough period of time, a wide and fissure-dominated valley will be present on axis.

Stage 4: Renewal of cycle. When volcanic activity resumes, a new axial ridge begins to form, and the cycle repeats. This tectonic cycle results in two types of crust being produced, unfissured intact blocks compared with fissured and faulted blocks.

The model described above satisfies the observed Endeavour data and can account for the almost universal presence of the CAMH over medium- to fast-spreading ridges in general with a tectonic/alteration process that is common to all mid-ocean spreading centers.

PREDICTIONS OF THE MODEL

The model predicts two fundamentally different types of near-axis crust: crust which is (as yet) unfissured and unaltered, and crust which is fissured, broken, and subjected to pervasive low-temperature alteration by seawater. Several other geophysical parameters should vary systematically for these two types of crust in addition to crustal magnetization.

Seismic Properties

Fractured crust will have increased porosity relative to unfractured crust, resulting in reduced seismic velocities. Seismic velocities of young upper crust could vary on a scale of kilometers depending on the tectonic state of the crust. The filling of fractures by alteration products tends to increase crustal seismic velocities, offsetting the velocity reduction due to fracturing alone. This effect has been noted previously e.g., on the East Pacific Rise by McClain et al. [1985], where shallow seismic velocities decreased as crust aged to 0.1 Ma and then increased again. The strong preference for off-axis fissuring to be aligned along ridge-strike in type B crust should also produce dramatic shallow seismic velocity anisotropy, with shallow seismic velocities being faster along-strike than across-strike.

Gravity

Near-bottom gravity measurements should be higher over intact, unaltered, and presumably denser, uncracked rock but lower over fissured and altered crust with cracks filled with low-density alteration products.

Heat Flow

The presence of crustal zones of varying permeability due to the alternating zones of fissured and unfissured crust will also have a modifying influence upon hydrothermal circulation cell geometry, such as proposed in models by Fehn et al. [1983]. A consequence of the model is that low-level off-axis hydrothermal activity can be predicted to occur along major faults bounding unfractured crust.

SUMMARY

In summary, near-bottom studies of magnetic fields show a fine-scale structure that maybe linked to the tectonic and alteration state of the crust and which vary on a scale of kilometers. This scale is equivalent to the scale of hydrothermal circulation within the crust or at least the cyclic heat flow patterns as seen at the Galapagos Rift. Further synergistic studies are needed on a kilometer scale to understand the evolution of ocean crust and the processes that act upon it.

REFERENCES

Fehn, U., K.E. Green, R.P. Von Herzen, and L.M. Cathles, Numerical models for the hydrothermal field at the Galapagos Spreading Center, *J. Geophys. Res.*, *88*, 1033-1048, 1983.

Kappel, E.S., and W.B. Ryan, Volcanic episodicity and a non-steady state rift valley along Northeast Pacific spreading centers: Evidence from SeaMARC I, *J. Geophys. Res.*, *91*, 13,925- 13,940, 1986.

Klitgord, K.D., Sea-floor spreading: The central anomaly magnetization high, *Earth Planet. Sci. Lett.*, *29*, 201-209, 1976.

McClain, J., J. Orcutt, and M. Burnett, The East Pacific Rise in cross-section: A seismic model, *J. Geophys. Res.*, *90*, 8627-8639, 1985.

Parker, R.L., and S.P. Huestis, The inversion of magnetic anomalies in the presence of topography, *J. Geophys. Res.*, *79*, 1587-1593, 1974.

Tivey, M.A., and Johnson, H.P., The Central Anomaly Magnetic High: Implications for ocean crust construction and evolution, *J. Geophys. Res.*, *92*, 12685, 1987.

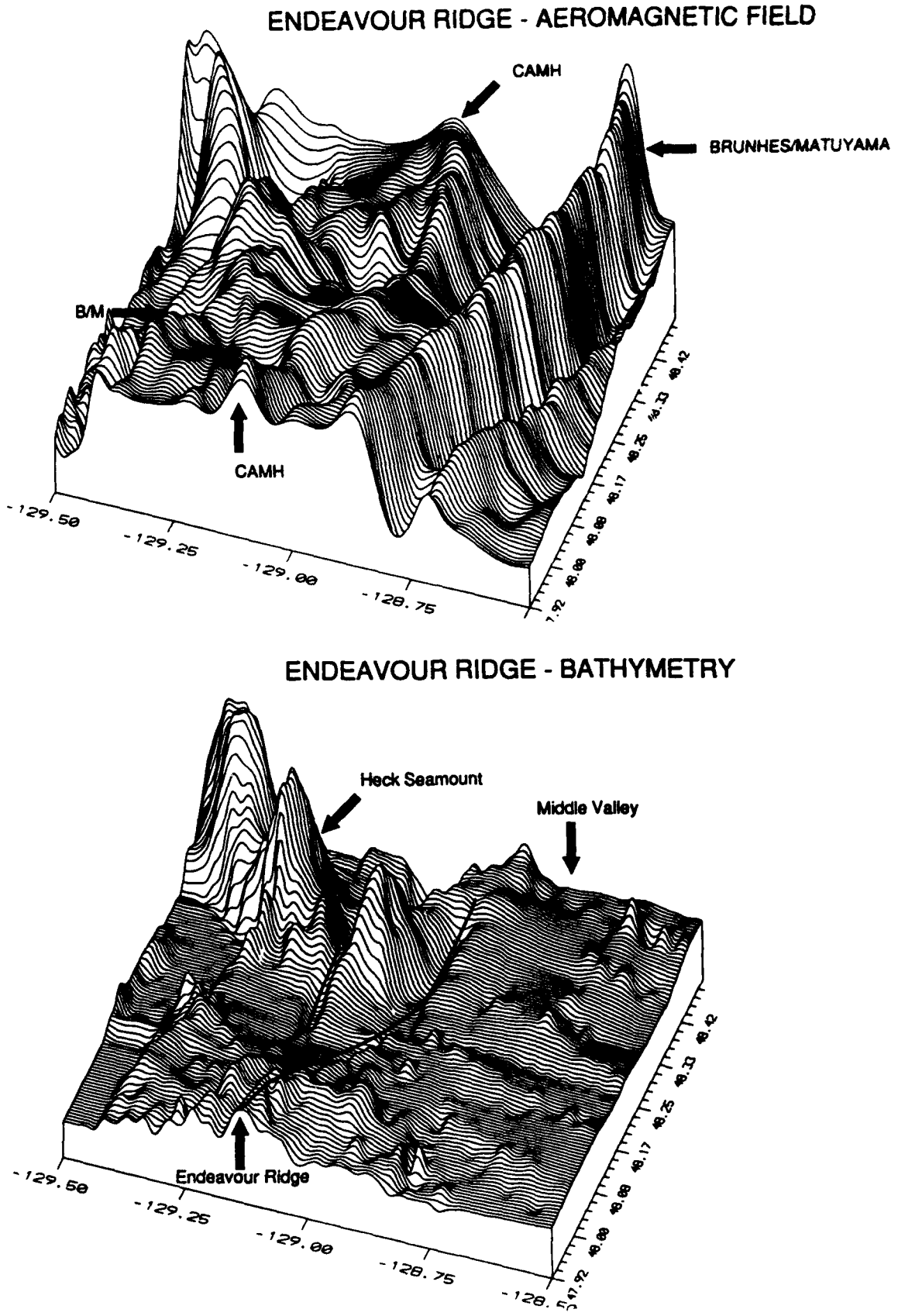

Figure 1 : The top figure shows a three-dimensional view of total magnetic field over the Endeavour ridge on the northern Juan de Fuca Spreading center. Bathymetry is shown in the bottom figure. Note the well-developed central anomaly magnetic high (CAMH) and flanking anomalies within the Brunhes anomaly.

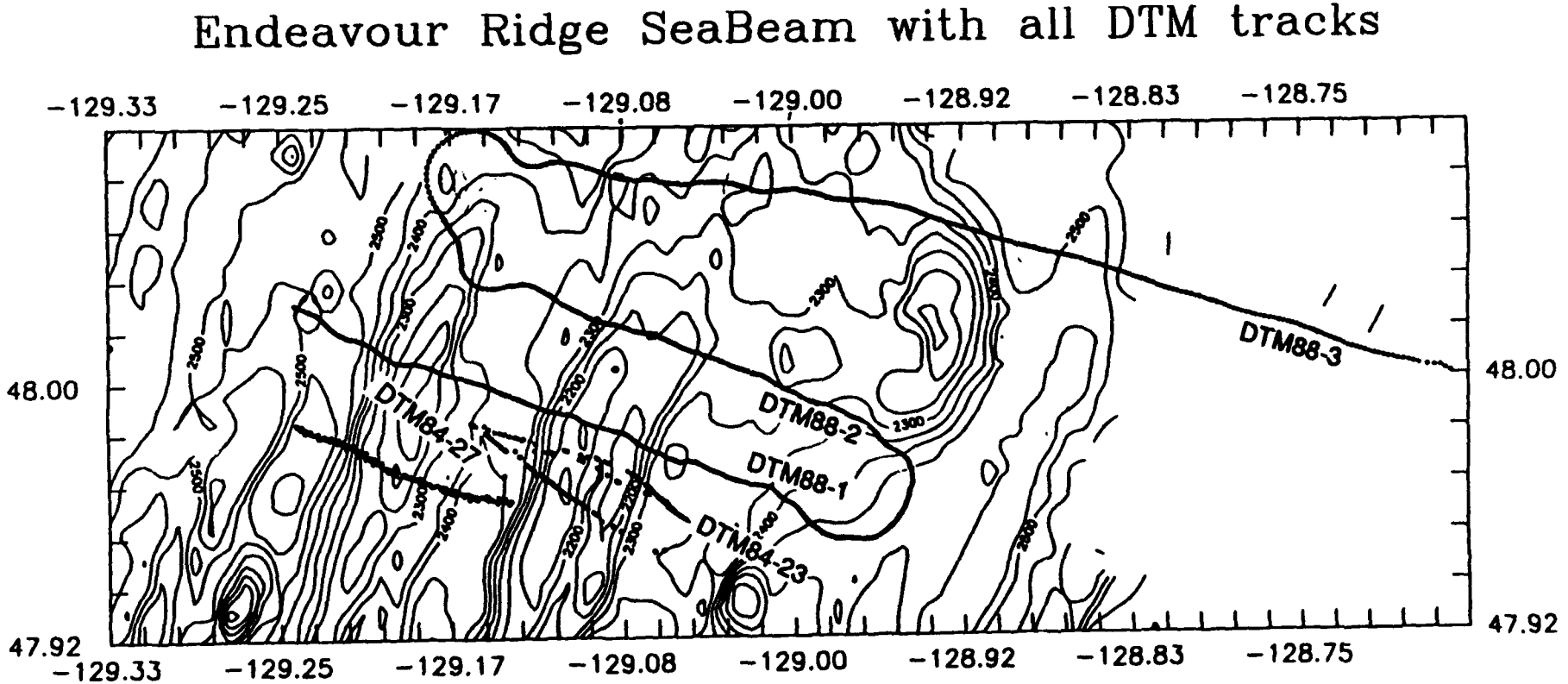

Figure 2 : Trackline map of deeptow magnetic profiles over the Endeavour ridge segment on the northern Juan de Fuca Ridge.

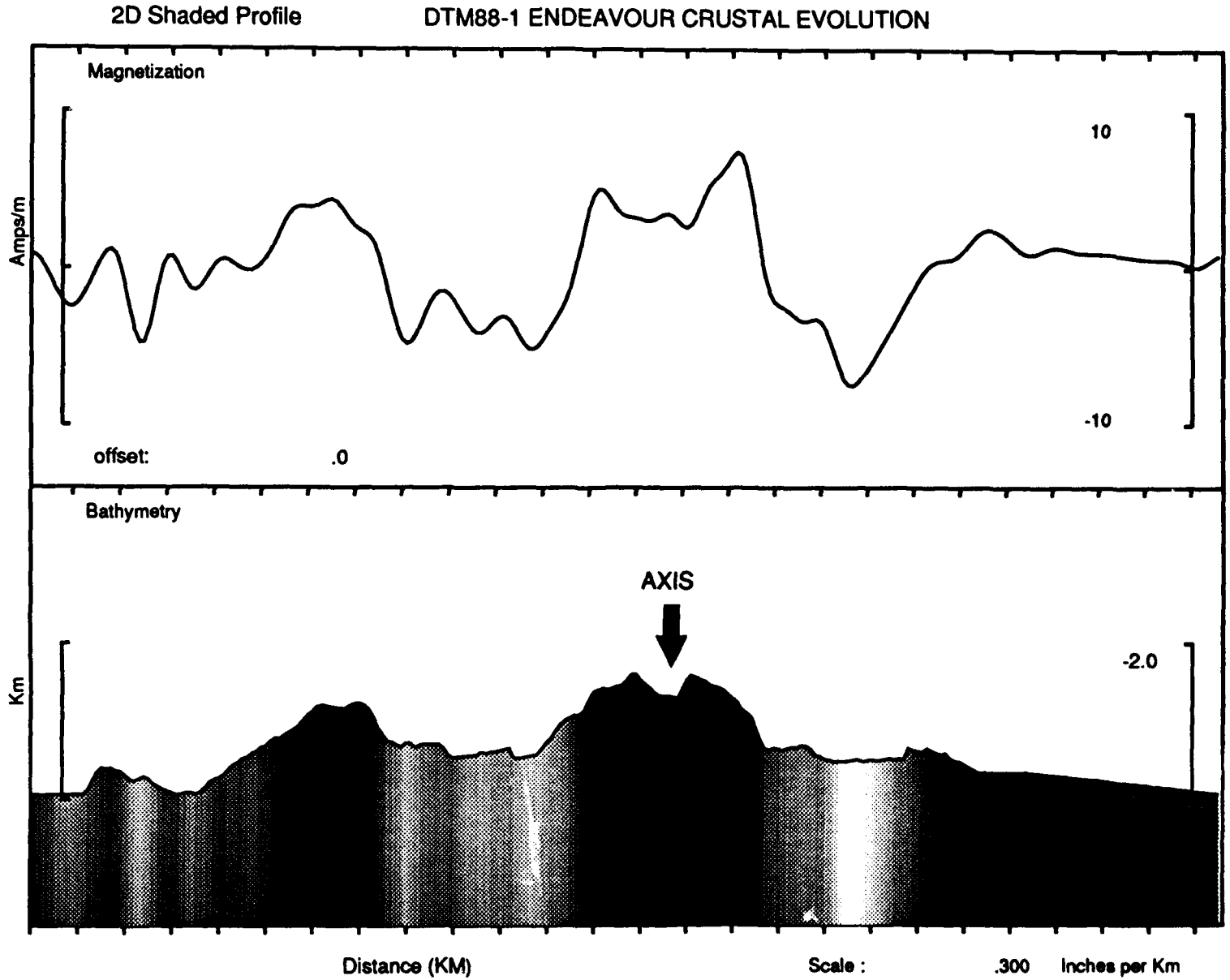

Figure 3 : Magnetization profile DTM88-1 showing magnetization in upper box and bathymetry shaded to the intensity of the magnetization. Dark areas are most magnetic, white areas are least magnetic. Note the high magnetization (CAMH) associated with Endeavour Ridge and flanking West Endeavour Ridge.

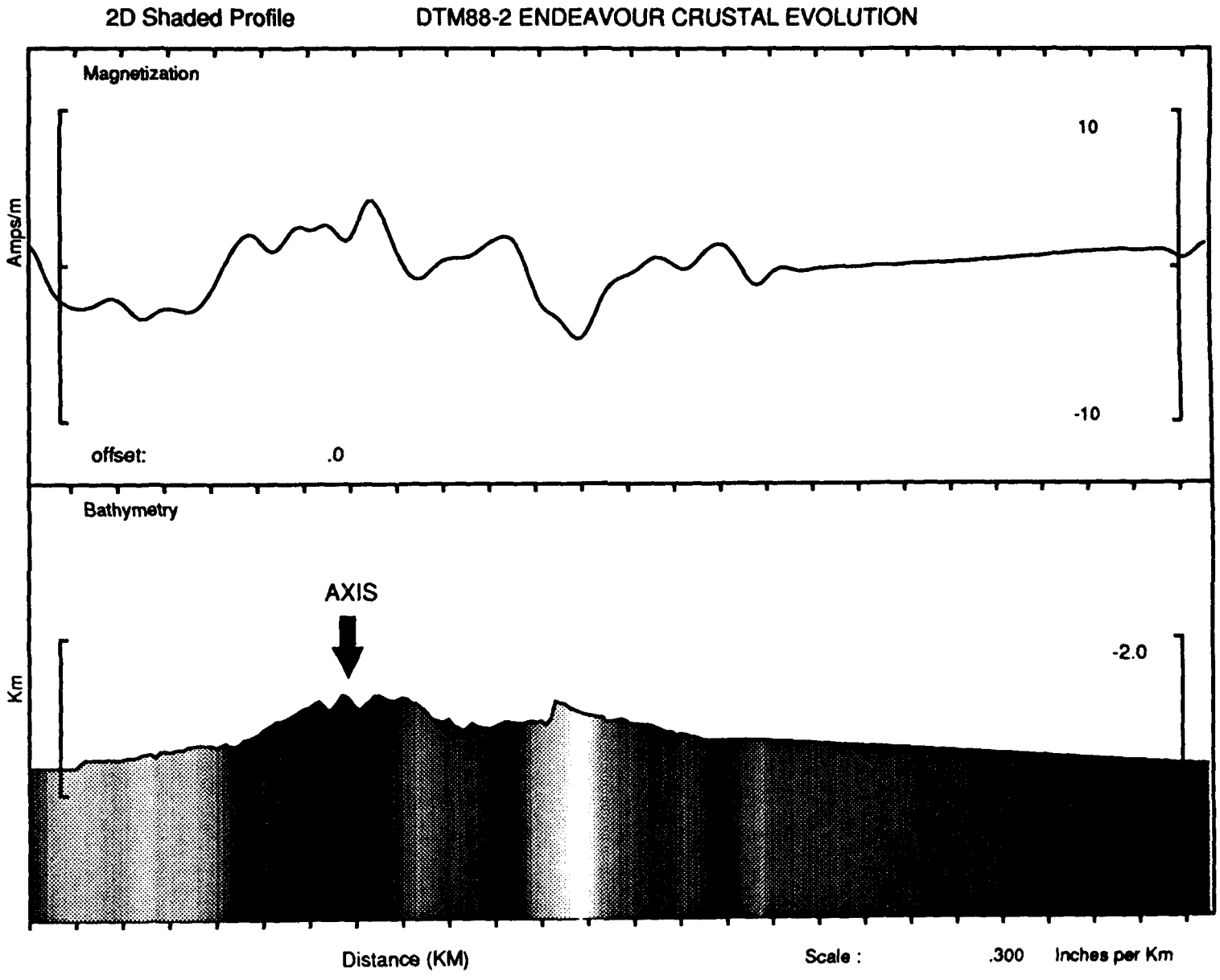

Figure 4: Magnetization profile DTM88-2 showing magnetization in upper box and bathymetry shaded to the intensity of the magnetization. Dark areas are most magnetic, white areas are least magnetic. Note the high magnetization (CAMH) associated with Endeavour Ridge.

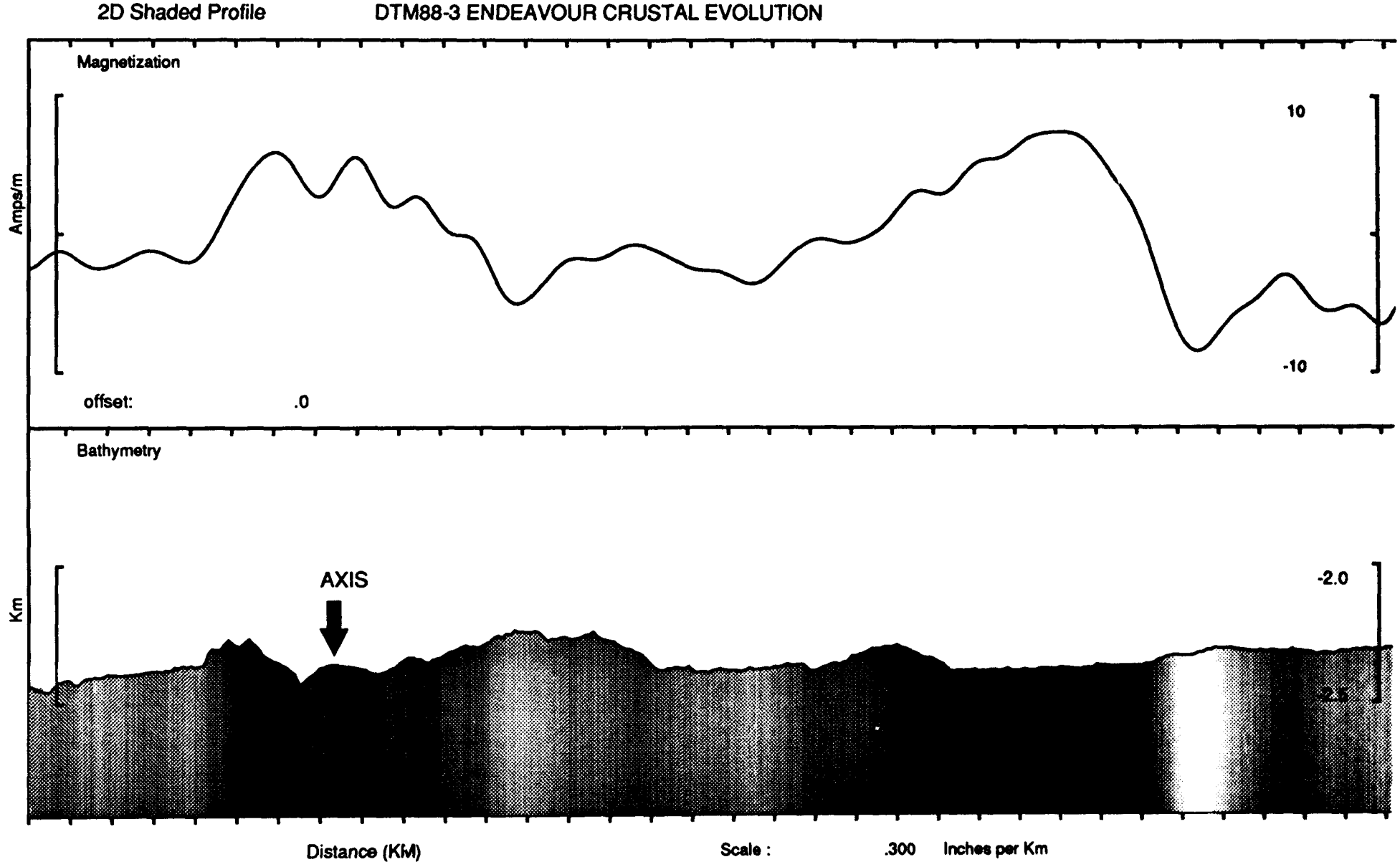

Figure 5: Magnetization profile DTM88-3 showing magnetization in upper box and bathymetry shaded to the intensity of the magnetization. Dark areas are most magnetic, white areas are least magnetic. Note the high magnetization (CAMH) associated with the axial zone.

EFFECTS OF ROUGH BATHYMETRY ON THE SEISMIC RESOLUTION OF UPPER CRUSTAL STRUCTURE

Isaac I. Kim and John A. Orcutt
Scripps Institution of Oceanography

The highest resolution of the fine-scale structure of the oceanic crust is obtained from seismic reflection surveys. Unfortunately, these marine reflection data are often plagued with specular reflections and diffractions from seafloor features such as abrupt fault scarps, abyssal hills, seamounts and troughs. These scattered seafloor events can mimic subsurface reflections and also contribute significantly to the noise in a reflection profile - possibly masking weaker subsurface reflections. An example of such a contaminated seismic reflection profile from the Mid-Atlantic Ridge in the MARK area will be shown. In addition, a variable seafloor can distort the the amplitude strength and arrival time of crustal reflections, resulting in misleading interpretations. We will show an example of this from the East Pacific Rise survey of the small overlapping spreading center at 12°54'N.

Scattering Example from the Mid-Atlantic Ridge

Past statistical methods for dealing with interference from this "seafloor noise" have been based on the assumption that these topographic events can be modelled as simple point source diffractions (Larner, et al., 1983; Neuman, 1984). However, this assumption is not well founded since the the generation of the seafloor at mid-ocean spreading centers leads to strong anisotropy in the tectonic grain. Profiler data collected parallel to these elongated bathymetric features are frequently contaminated with continuous reflections which dip slowly through the observed sections. We have developed a deterministic method of using the actual bathymetry to identify seafloor scatter in reflection data. Maps produced using digital SeaBeam bathymetry data, although not perfect, are of high enough resolution to calculate realistic band-limited synthetic reflection profiles consisting solely of scattering from the larger features of the seafloor. The calculation of this acoustic scattered wavefield involves the numerical evaluation of the Kirchhoff-Helmoltz integral over the surface of seafloor. The physical properties of the seafloor are assumed to be constant in these calculations. Comparisons between these Kirchhoff-Helmholtz synthetics and real data are very helpful in distinguishing between actual subsurface reflections and scattered events originating from the seafloor.

Line 841 is an along-axis multichannel seismic reflection line that runs through the Snake Pit Hydrothermal Field (23°N) on the Mid-Atlantic ridge (Detrick, et al., 1989) (Figure 1a). Many dipping events in the section could be interpreted as intra-crustal reflections. A Kirchhoff-Helmholtz synthetic from a 200 meter grid of SeaBeam bathymetry is shown in Figure 1b. All of the events in the synthetic profile originate from the seafloor. Figure 1b shows that most of these apparent intra-crustal reflections are actually out-of-plane scattering from the seafloor. A few of the major scattered events were picked and located using a back-projection algorithm. Figure 2a shows the picked events and Figure 2b shows their points of origin on the seafloor. It is interesting that the sources of these events seem to be from the smaller holes in the bathymetry. Although most of the large-scale scattering can be reproduced from a 200 meter grid, the background scattering seen in the data is not well reproduced in the synthetic. Most of this background scattering we assume is coming from small-scale faulting not resolvable in a 200 meter grid. Future work includes adding finer scales of roughness to the bathymetry by merging, for example, Goff and Jordan (1989) realizations to the 200 meter SeaBeam grid. We expect that scattering calculations from this rougher grid will reproduce the small-scale scattering.

Transmission example from the East Pacific Rise

A rough seafloor cannot only produce apparent subsurface reflections, it can also distort actual subsurface reflections. This is seen in the top of the magma chamber reflection seen in CDP 24, an along-axis East Pacific Rise seismic reflection line that passes through the 12°54'N overlapping spreading center (OSC) (see Figure 3). This small OSC has an offset of 1.6 km between axial limbs. Both the Lonsdale (1983, 1986) non-transform offset model and the Macdonald et al. (1984, 1986) OSC model propose that the crustal magma chamber should be continuous across this small offset. Refraction data from the MAGMA experiment (Burnett, et al., 1989) show that the 7 km wide crustal low velocity zone is continuous through the OSC area. However, CDP 24 shows a distinctive break in the magma chamber reflector at the OSC (Detrick, et al., 1987), and the reflector from the southern limb appears to be dipping into the overlap basin. A closer look at the track position of CDP 24 with respect to the bathymetry, intersecting cross-axis lines, and some Kirchhoff-Helmholtz transmission modeling reveal that this apparent dipping is likely to be an out-of-plane effect associated with a very narrow magma lens.

CDP 24's track location across the bathymetry is shown in Figure 3. Deep tow bathymetry and magnetic observations indicate that the northern limb is more tectonically active with younger volcanic flows, and the southern limb appears to be dying (Antrim, et al., 1988). Over this northern limb, the top of the magma chamber reflector, at about 4.1 seconds, remains horizontal as it fades away almost exactly where the mapped axial graben dies out (Macdonald and Fox, 1988). No reflector is observed as the ship passes over the portion of the northern limb without a graben. However, a much deeper magma chamber reflector is picked up again once the ship track enters the western portion of the overlap basin. Assuming that the reflector is in the profile plane, the apparent depth of the magma chamber is 2500 meters deeper in the overlap basin than on the rise axis, using an average Layer 2 crustal velocity of 5.0 km/s (Harding, et al., 1989). The magma chamber reflector then rises to a normal depth as the ship track joins up with the southern limb about 8 km south of the limb tip. Cross-axis line control on both the northern limb (CDP 11) and southern limb (CDP 13) show a 700 meter wide magma body centered under the axial high. Cross-axis CDP 18 shows that the magma lens is again centered under the axial high, although the crossing of CDP 24 is about 1 km west of the edge of the magma lens reflector. CDP 24 has already wandered off the narrow magma lens and thus the image of this magma reflector in CDP 24 at this point is an out-of-plane feature. Since the reflector in CDP 24 (see Figure 3) begins to dip as soon as the track leaves the southern limb, all of the apparent dip is likely to be an artifact of the track's distance from the edge of the reflector. To determine how much of the dip could be due to ship track displacement and a change in seafloor morphology as the shiptrack wanders from the rise axis to the overlap basin, transmission Kirchhoff-Helmholtz synthetics were calculated for various magma lens geometries.

The first obvious model is a magma lens that remains centered below the axial graben (Macdonald and Fox, 1988) with no dip. Once the ship track wanders off the reflecting body, the image becomes a diffraction from the edge rather than a specular reflection (Trorey, 1970). The transmission program (Kim and Orcutt, 1989) places a series of point sources on the edge of this arbitrarily placed magma lens. Each shot illuminates a 5 km by 5 km area of the Sea Beam bathymetry where secondary source strengths are calculated. Plane-wave transmission coefficients were determined assuming a seawater velocity of 1.492 km/s and a P-wave uppermost crustal velocity of 3.0 km/s (Harding, et al., 1989). These transmission synthetics are combined with Kirchhoff-Helmholtz scattering synthetics (Kim and Orcutt, 1988) to give the three synthetic profiles shown in Figure 4. The synthetic profile with the magma lens parallel to the axial graben with no dip (Figure 4b) did not produce the same dip as was observed in the data. To reproduce the same dip that

is seen in the data, the magma lens had to dip down 1100 meters to the tip of the axial graben (Figure 4c). However, like any good geophysical inverse problem, the 3-D magma lens location that matches the observed profile dip is nonunique. An increase in apparent profile dip can also arise by placing the magma lens further east of the axial graben. This displacement of the magma body away from the OSC has been observed in cross axis lines near the 9°03' OSC by Mutter et al. (1989) and has been numerically modeled by Sempere and Macdonald (1986). For a magma body with no dip, the edge of the magma lens has to be displaced only 600 meters to the east at the end of the axial graben to reproduce the apparent dip seen in CDP 24 (Figure 3d). This is well within the 7 km wide low velocity zone. A surface of possible magma body geometries exists between these these two extreme geometries that match the observed profile dip equally well. In this case, the shiptrack wander was the dominant cause of the apparent dip. The rough seafloor was responsible for secord-order reflection distortions like the slight hump in the dipping reflector.

Before any conclusions are drawn about upper oceanic crustal structure from marine reflection data, it is important to identify the scattering artifacts from the seafloor which compete with the actual subsurface reflections. Also, it is important to take into account possible distortions of real subsurface reflections due to transmission through a rough seafloor. The type of analysis presented here has only become possible because of the detailed bathymetry provided by high resolution multibeam systems like SeaBeam. As more accurately-navigated SeaBeam surveys become available in areas of seismic reflection surveys, these techniques will improve the resolution of seismic reflection methods for exploring oceanic crustal structure.

Acknowledgements

We would like to thank Bob Detrick, John Mutter and Peter Buhl for providing the MAR reflection data and Jim Dolan for assistance with the gridded Sea Beam bathymetry

References

Antrim, L., J.C. Sempere, and K.C. Macdonald, 1988, Fine scale study of a small overlapping spreading center system at 12°54' N on the East Pacific Rise, *Mar. Geophys. Res.*, 9: 115-130.

Burnett, M.S., D.W. Caress, and J.A. Orcutt, 1989, Tomographic image of the magma chamber at 12°50' N on the East Pacific Rise, *Nature*, 339: 206-208.

Detrick, R.S., P. Buhl, E. Vera, J. Mutter, J. Orcutt, J. Madsen and T. Brocher, 1987, Multi-channel seismic imaging of a crustal magma chamber along the East Pacific Rise, *Nature*, 326: 35-41.

Detrick, R.S., J.C. Mutter and P. Buhl. Multichannel seismic data across the Snake Pit Hydrothermal field (Mid-Atlantic Ridge, 23°N): No evidence for a crustal magma chamber, *EOS Trans. AGU*, 70: p. 1325.

Goff, J.A. and T.H. Jordan, 1990, Pacific and Atlantic models of small-scale seafloor topography, *ONR SRP Technical Report No. 1.*

Harding, A.J., J.A. Orcutt, M.E. Kappus, E.E. Vera, J.C. Mutter, P. Buhl, R.S. Detrick, and T.M. Brocher, 1989, Structure of young oceanic crust at 13°N on the East Pacific Rise from expanding spread profiles, *J. Geophys. Res.*, 94: 12163-12196.

Kim, I.I. and J.A. Orcutt, 1988, Comparison in scattering character between along-axis and cross-axis seismic reflection lines at the East Pacific Rise, *EOS Trans. AGU*, 69: 1440.

Kim, I.I. and J.A. Orcutt, 1989, Effects of disrupted axial morphology on the amplitude strength of the crustal magma chamber reflection at the East Pacific Rise, *EOS Trans. AGU*, 70: 1317.

Larner, K., R. Chambers, M. Yang, W. Lynn, and W. Wai, 1983, Coherent Noise in Marine Seismic Data. *Geophysics*, 48: 854-886.

Mutter, J.C., G.A. Barth, P. Buhl, R.S. Detrick, J. Orcutt and A. Harding, 1988, Magma distribution across ridge-axis discontinuities on the East Pacific Rise from multichannel seismic images, *Nature*, 336: 156-158.

Lonsdale, P., 1983, Overlapping rift zones at the 5.5°S offset of the East Pacific Rise, *J. Geophys. Res.*, 88: 9393-9406.

Lonsdale, P., 1986, Comments on "East Pacific Rise from Siqueiros to Orozco Fracture Zones: Along-strike continuity if axial neovolcanic zone and structure and evolution of overlapping spreading centers" by K. Macdonald, J. Sempere and P.J. Fox, *J. Geophys. Res.*, 91: 10493-10499.

Macdonald, K.C. and P.J. Fox, 1988, The axial summit graben and cross-sectional shape of the East Pacific Rise as indicators of axial magma chambers and recent volcanic eruptions, *Earth Planet. Sci. Lett.*, 88: 119-131.

Macdonald, K.C., J.C. Sempere and P.J. Fox, 1984, East Pacific Rise from Siqueiros to Orozco Fracture Zones: Along-strike continuity if axial neovolcanic zone and structure and evolution of overlapping spreading centers, *J. Geophys. Res.*, 89: 6049-6069.

Macdonald, K.C. and J.C. Sempere, 1986, Reply: The debate concerning overlapping spreading centers and mid-ocean ridge processes, *J. Geophys. Res.*, 91: 10501-10511.

Newman, P., 1984, Seismic Response to Sea-floor Diffractors. *First Break*: 9-19.

Sempere, J.C. and K.C. Macdonald, 1986, Overlapping spreading centers: Implications from crack growth simulation by the displacement discontinuity method, *Tectonics*, 5: 151-163.

Trorey, A.W., 1970, A simple theory for seismic diffractions, *Geophysics*, 35: 762-784.

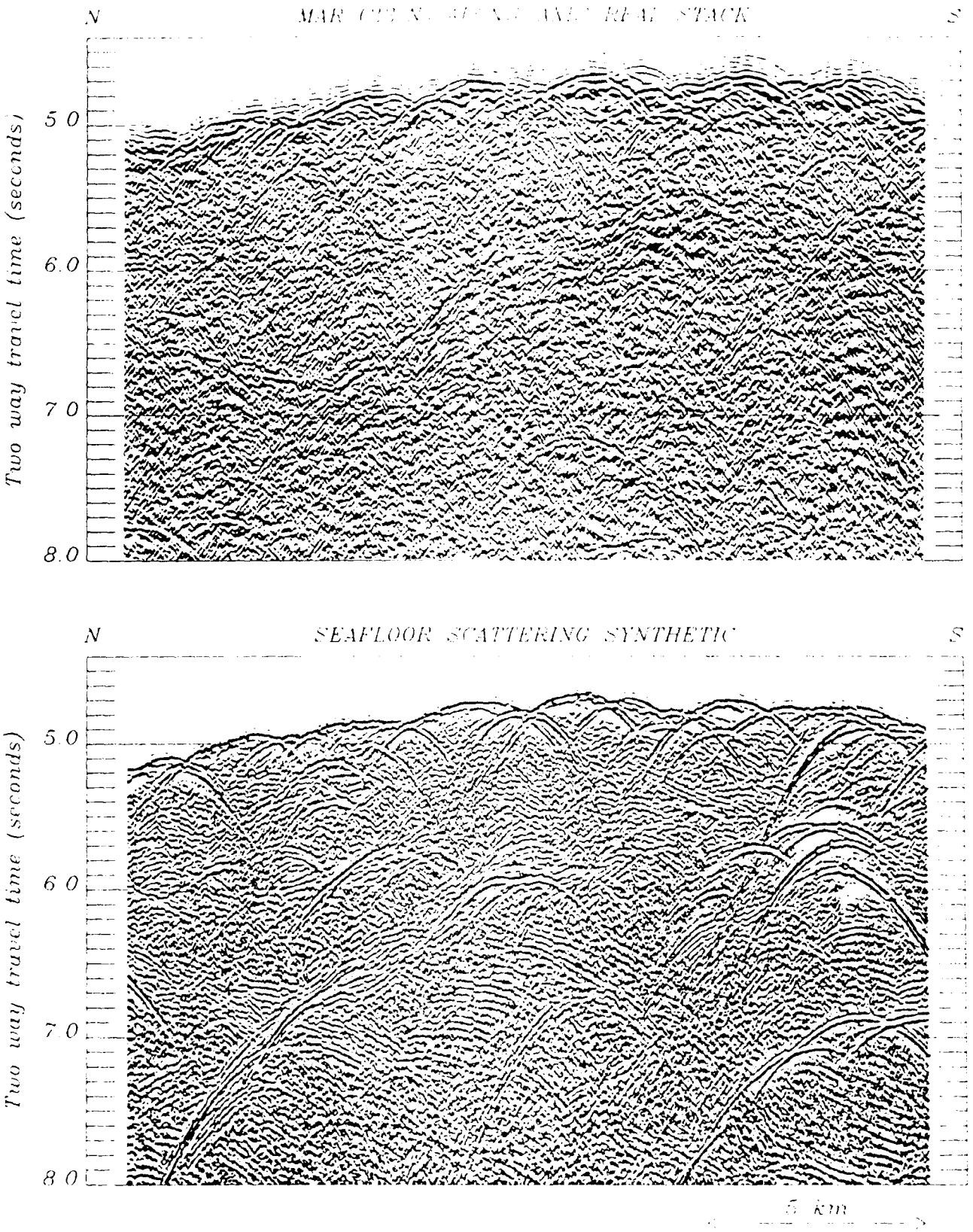

Figure 1a (top). 48-fold CDP seismic reflection data which runs along the MAR rift valley and through the Snake Pit Hydrothermal Field

Figure 1b (bottom). Kirchhoff-Helmholtz zero-offset synthetic profile calculated only using the seafloor. Many of the apparent intra-crustal reflections seen in the real data that are also seen in the synthetic are actually out-of-plane scattering from the rough seafloor.

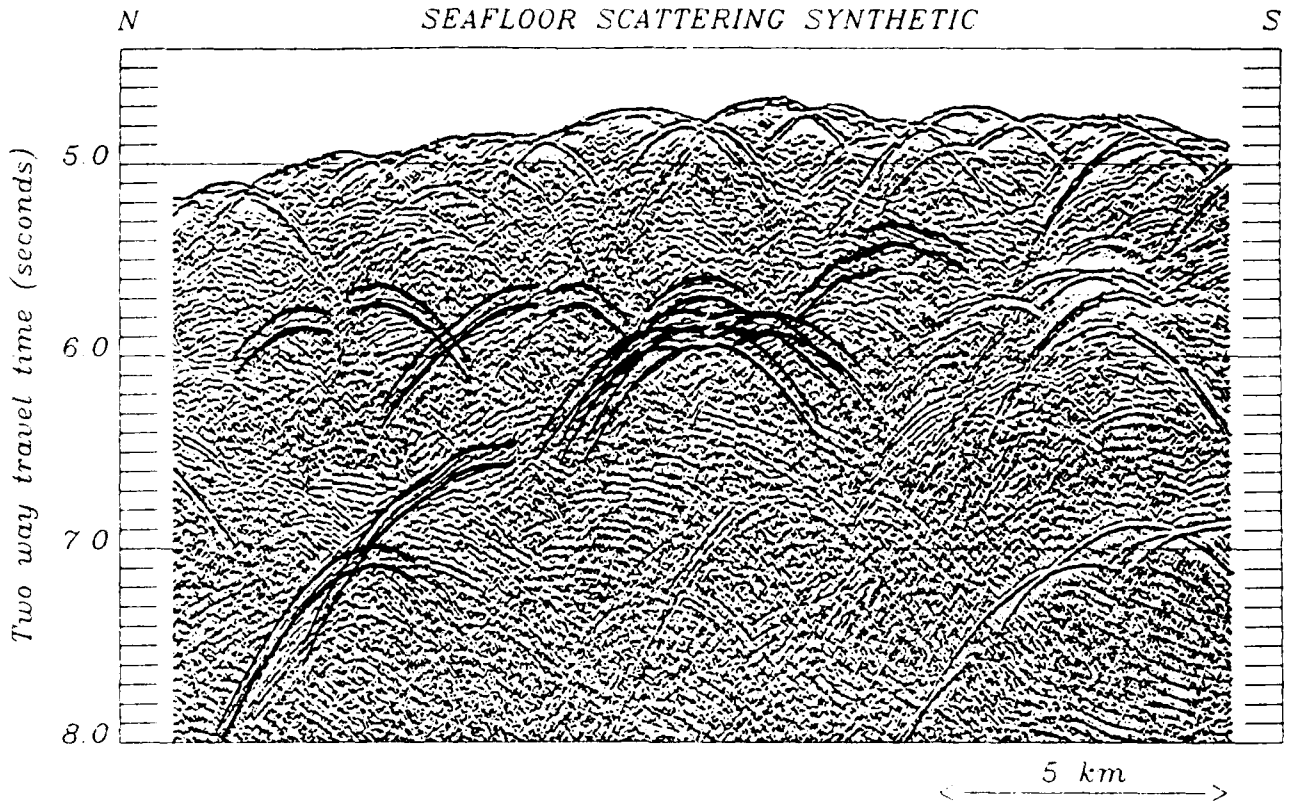

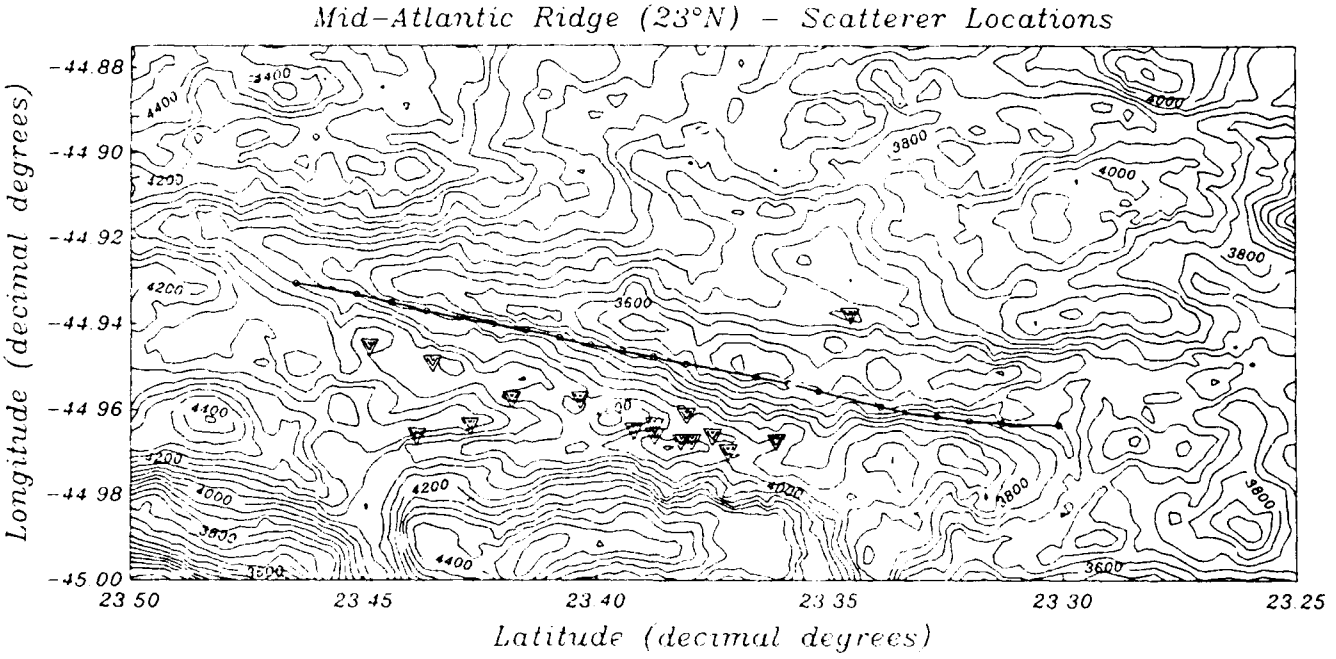

Figure 2a (top). Picks from the synthetic of a few major scattered events that are observed in the real data.

Figure 2b (bottom). Location of the sources on the seafloor of those picked events. Locations derived using a back-projection algorithm. Note that mpst of the scattered events seem to originate from smaller holes in the bathymetry, rather than from larger features.

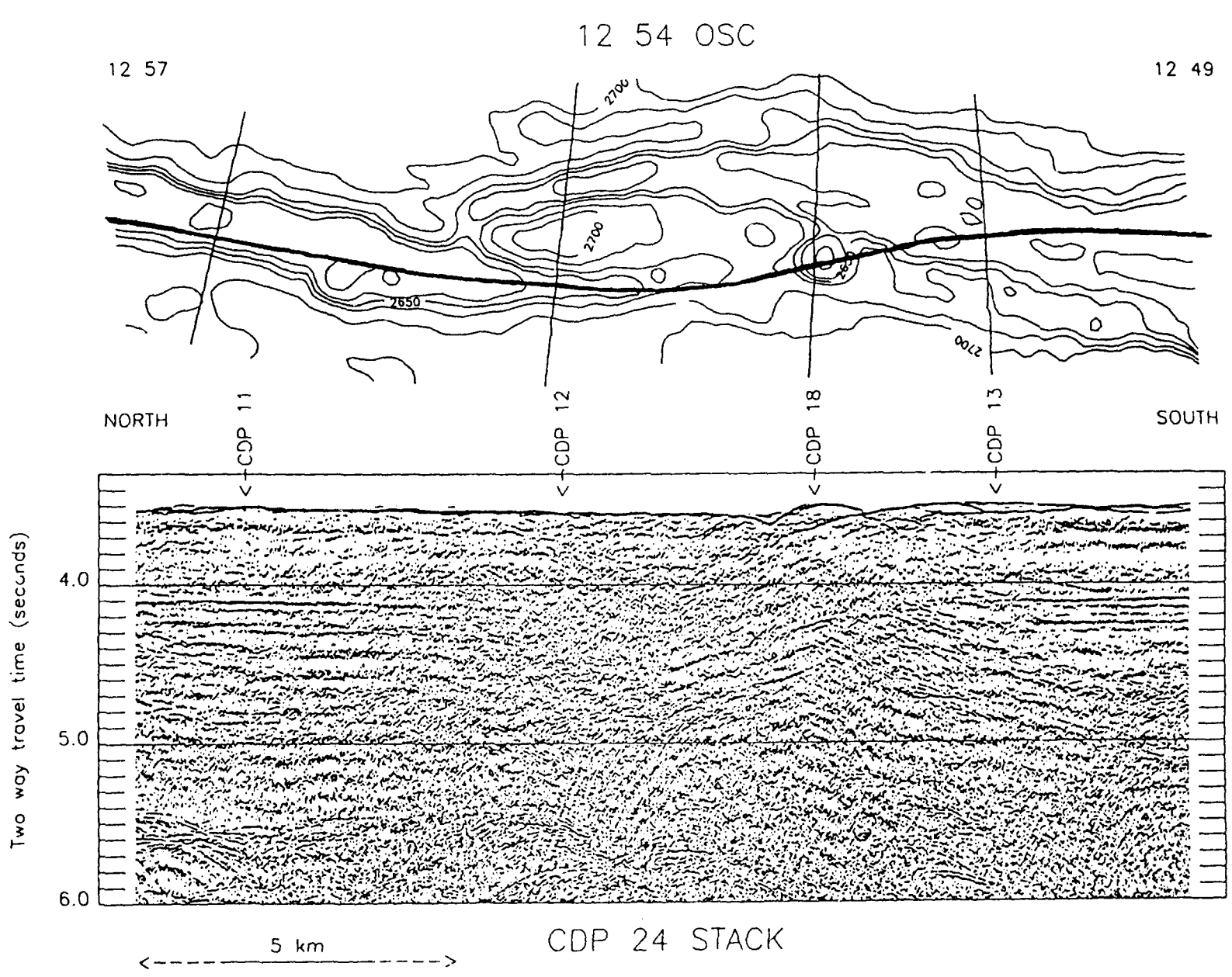

Figure 3: Along-axis CDP 24. On the northern limb, the top of the magma chamber reflector at 4.1 seconds remains horizontal and fades just where the mapped axial graben dies out. On the southern limb, the reflector seems to dip as the line enters the overlap basin. Bathymetric effects are not responsible for the break in the reflector. However, the apparent dip of the reflector is at least partially due to the shiptrack wandering away from the southern limb.

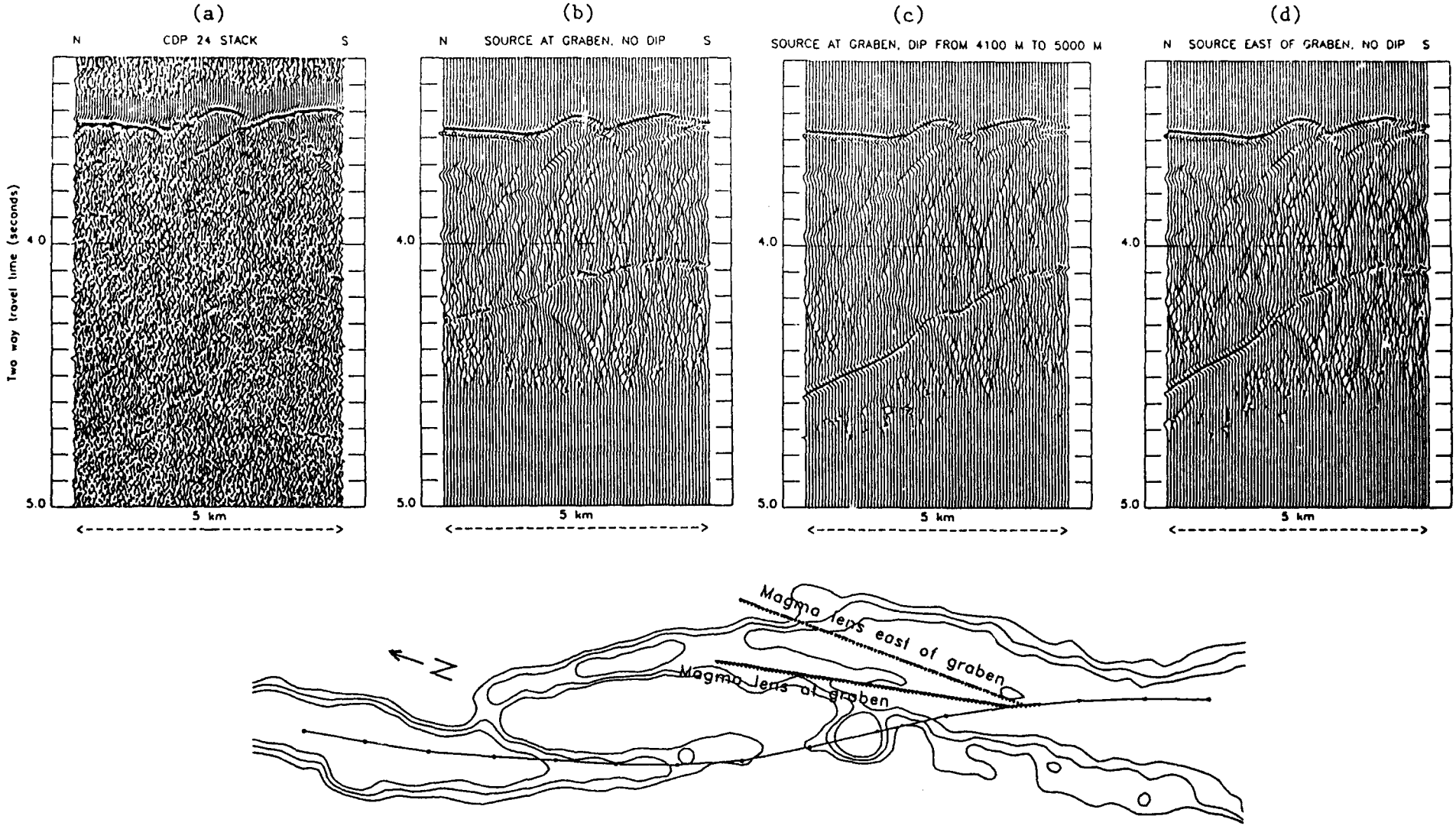

Figure 4: (a) A portion of CDP 24 which shows the apparent dip of the magma lens reflector from the southern limb as it enters the overlap basin. (b) Kirchhoff-Helmholtz transmission synthetics from a magma lens model that is parallel to the southern limb's axial graben with no dip. The apparent dip in the synthetic is not steep enough. (c) Synthetics from a magma lens model that is parallel to the axial graben but dips down 1100 meters. The synthetics apparent dip matches the real data. (d) Here the magma lens is displaced to the east of the graben with no dip. The synthetic apparent dip matches the real data. Many possible magma lens geometries exist between these two end models that will also match the apparent dip in the real data.

THE VARIATION OF BACKSCATTER WITH INCIDENCE ANGLE FOR SONAR DATA OVER MOR VOLCANICS

N.C. Mitchell
Lamont-Doherty Geological Observatory, Palisades, NY 10964

Quantitative sea-floor backscatter strengths have been estimated using an acoustic propagation model [*Mitchell and Somers*, 1989] from 6.5 kHz GLORIA long-range side-scan sonar data collected in the Indian Ocean [*Parson et al.*, 1988]. This model corrects the recorded signal for intensity loss during propagation and allows for the beam patterns and time-varied amplifier gain of the instrument to give the intensity of the backscattered signal at 1m from the sea floor. The intensity of the wavefield incident on the sea floor can also be estimated, using a similar method, from the known power radiated from the transducers. The backscatter strength can then be computed as the logarithm in dB of the surface backscatter coefficient, $P_b/(I_iA)$, where P_b is the power backscattered from the surface per unit solid angle (W/steradian), I_i is the acoustic intensity incident on the surface (Wm^{-2}) and A is the effective insonified surface area (m^2).

To investigate how the sea-floor topography influences the tone variations observed in GLORIA images, the computed backscatter strengths may be correlated with a crude measure of the angle of grazing of the acoustic signal with the sea floor where Sea Beam or other high-resolution bathymetry is available. Figure 1 is a distribution from a limited area of a deep V-shaped median valley [*Mitchell and Somers*, 1989]. This shows a 10-15 dB gradient with grazing angles in the range 10-50°, similar to a Lambert Law for diffuse surface scattering [e.g., *Mackenzie*, 1961; *Urick*, 1983]. Correlating the backscatter strength with the grazing angle is more difficult over larger areas because of problems with co-registering the Sea Beam and side-scan data and because the artifacts of the calculation may have magnitudes similar to the variation being studied. An example of this is shown in Figure 2; a relatively flat distribution for data collected with the sonar scanning 10 km down a relatively flat median valley of a mid-ocean ridge. In this case, the grazing angle is mostly varied by the decreasing depression of the rays with range, rather than by the sea floor's relief measured with Sea Beam. Contributing to the errors in the calculation are the estimate of the beam pattern of the sonar, possible reflections off the sea-surface, and a correction for refraction that may be poor for the shallowly-projected rays. Although difficult to quantify, the sea surface reflections would contribute to the recorded signal increasingly with range because the sea surface becomes acoustically smoother towards grazing incidence [e.g., *Ulaby et al.*, 1982] and tending to raise the strength for the low angles. This would flatten gradients such as in Figure 1.

The 10 dB variation in Figure 1 is smaller than that due to acoustic shadowing by the topography and to different bottom types and roughnesses [*Urick*, 1983]. Sedimentation has been found to increase the acoustic contrast between volcanic abyssal hills and the ponded muds between them to as much as 25-30 dB [*Mitchell*, 1989]. Preliminary results, therefore, suggest that the tone variations observed in GLORIA images are mostly due to different rock or sediment types (i.e., the physical properties and roughness of the sea floor) and to acoustic shadowing; the effect of the sea floor's slope is secondary and often indirect (e.g., talus and breccia form along steep fault scarps).

The almost Lambertian relation in Figure 1 implies that, at 6.5 kHz, volcanic terraines behave as diffuse scatterers of the incident sound field and are not complicated by the effects of bottom penetration and volume scattering that are typical of sedimented sea-floors [*Jackson et al.*, 1986b; *Patterson*, 1969]. Similar shallow variations in backscatter

averaged with grazing angle have been found by other authors [*Bunchuk and Zhitkovskii*, 1980; *Jackson et al.*, 1986a; *McKinney and Anderson*, 1964; *Wong and Chesterman*, 1968]. Other much steeper backscattering relationships over abyssal hills, such as given by Zhitkovskii [1987, Figure 6], may be artifacts of acoustic shadowing by the sea-floor topography and of sediment distributions that are difficult to recognize and correct when explosive sources are used. A knowledge of the surface scattering may have wider uses. For example, where there is significant bottom penetration, the magnitudes of volume scattering and surface scattering off sub-surface layers may be investigated by extracting the surface scattering component, if the surface can be demonstrated to act as a diffuse scatterer of the incident sound field. Jackson et al. [1986b] used an approach similar to this to study 30 kHz backscatter over sands.

Acknowledgements

The acoustical calculations that initiated this work were patiently guided by M.L. Somers. I am also grateful for the hard work of the officers and crew of the RRS Charles Darwin, L.M. Parson and R. Schlich who have furnished the sonar data, and the Royal Commission for the Exhibition of 1851 for providing generous financial support.

Figure 1. The distribution of backscatter strengths falling within a small region of a valley of the South West Indian Ridge near the Indian Ocean Triple Junction [*Mitchell*, 1989]. For comparison, the continuous line shows the relationship to be expected from a Lambert law of diffuse scattering ($20\log10(\sin\theta_g)$). (22 000 samples.)

Figure 2. The distribution of backscatter strengths falling within the South East Indian Ridge median valley (with the sonar scanning parallel with the lineated topography), but for an extent of range greater than in Figure 1. The data within 3 km of the nadir were excluded because of errors in the correction for the system's beam directivity pattern. (31 000 samples.)

References

Bunchuk, A.V., and Y.Y. Zhitkovskii, Sound scattering by the ocean bottom in shallow-water regions (review), *Soviet Physics - Acoustics, 26,* 363-370, 1980.

Jackson, D.R., A.M. Baird, J.J. Crisp, and P.A.G. Thomson, High-frequency bottom backscatter measurements in shallow water, *J. Acoust. Soc. Am., 80,* 1188-1199, 1986a.

Jackson, D.R., D.P. Winebrenner, and A. Ishimaru, Application of the composite roughness model to high-frequency bottom backscattering, *J. Acoust. Soc. Am., 79,* 1410-1422, 1986b.

Mackenzie, K.V., Bottom reverberation for 530- and 1030-cps sound in deep water, *J. Acoust. Soc. Am., 33,* 1498-1504, 1961.

McKinney, C.M., and C.D. Anderson, Measurements of backscattering of sound from the ocean bottom, *J. Acoust. Soc. Am., 36,* 158-163, 1964.

Mitchell, *Investigation of the Structure and Evolution of the Indian Ocean Triple Junction Using GLORIA and Other Geophysical Techniques*, D.Phil. Thesis, Oxford, 1989.

Mitchell, N.C., and M.L. Somers, Quantitative backscatter measurements with a long range side-scan sonar, *IEEE J. of Oceanic Engineering, 14*, 368-374, 1989.

Parson, L.M., and ship's party, RRS Charles Darwin cruise 23/87, 13 May - 11 June 1987. Geophysical investigation of the Indian Ocean Triple Junction, *Cruise report 201*, Wormley, Surrey: Institute of Oceanographic Sciences, 1988.

Patterson, R.B., Relationships between acoustic backscatter and geological characteristics of the deep ocean floor, *J. Acoust. Soc. Am., 46*, 756-761, 1969.

Ulaby, F.T., R.K. Moore, and A.K. Fung, *Microwave remote sensing: active and passive. Volume II: radar remote sensing and surface scattering and emission theory.*, 605 pp., Addison-Wiley Publishing Company, Reading, Massachusetts, 1982.

Urick, R.J., *Principles of underwater sound (3rd Edn)*, McGraw-Hill, New York, 1983.

Wong, H.-K., and W.D. Chesterman, Bottom backscattering near grazing incidence in shallow water, *J. Acoust. Soc. Am., 44*, 1713-1718, 1968.

Zhitkovskii, Y.Y., The sea bottom backscattering of sound (the history and modern state), pp. 15-23 in *Progress in underwater acoustics. Proc. of 12th Int. Congress on Acoustics, 1986.*, edited by H.M. Merklinger, 1987.

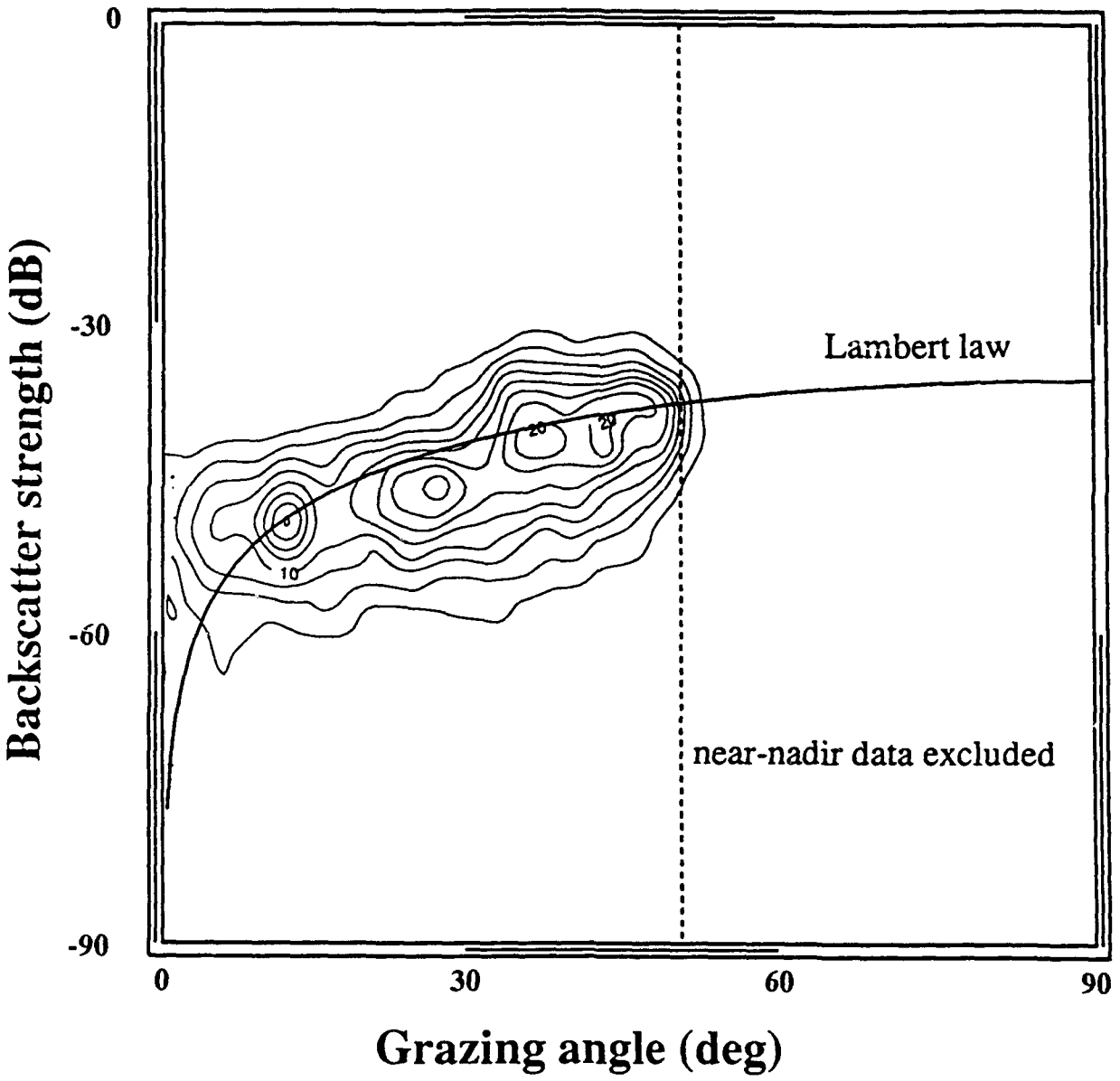
0
-30
-60
-90
Backscatter strength (dB)
0
30
60
90
Grazing angle (deg)
Lambert law
near-nadir data excluded
10
20
20

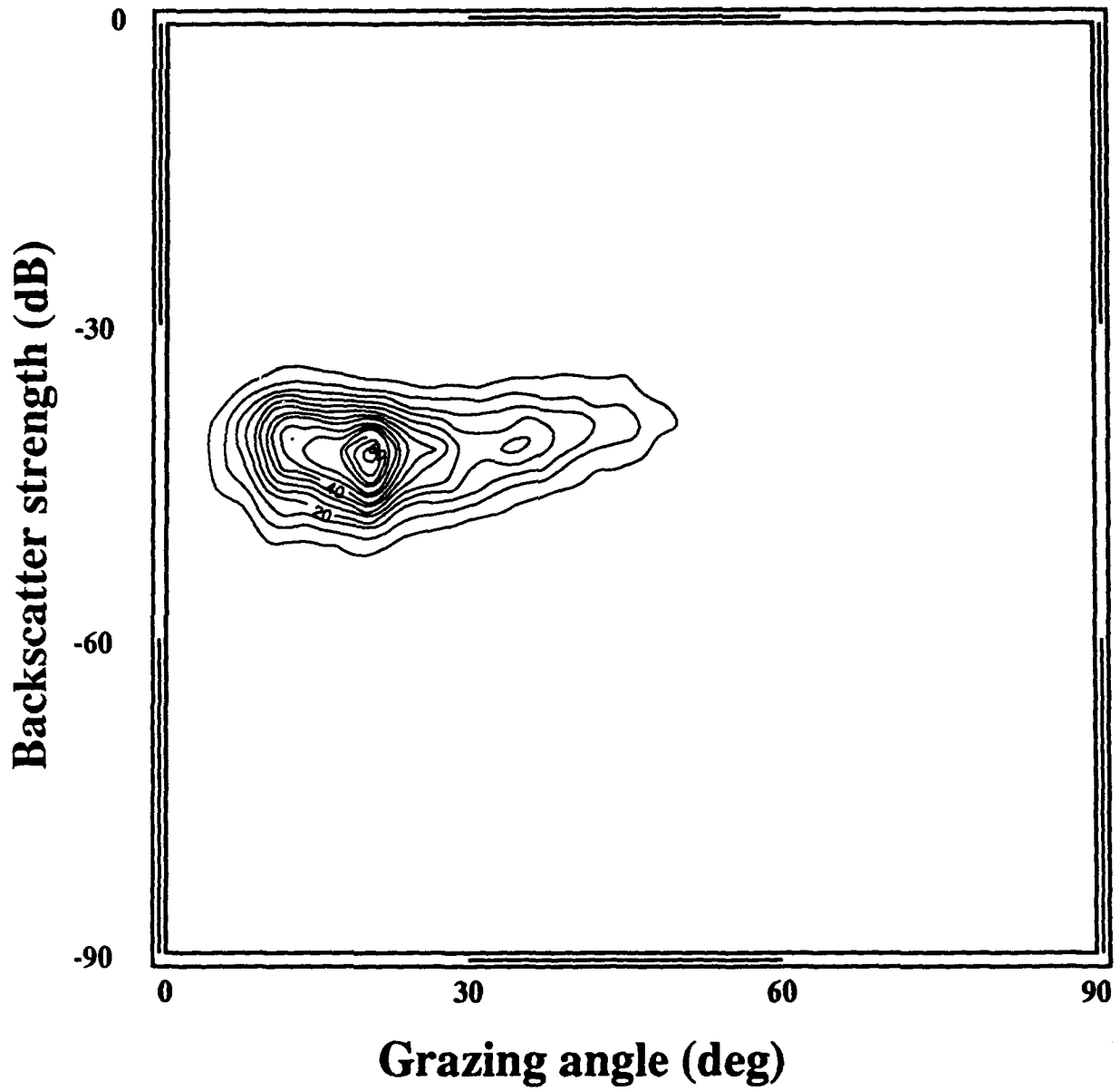
0
-30
-60
-90
Backscatter strength (dB)
0
30
60
90
Grazing angle (deg)
40
20

CRUSTAL STUDIES USING INTERFACE WAVES

LeRoy M. Dorman, Scripps Institution of Oceanography, John A. Hildebrand, Scripps Institution of Oceanography, L. Dale Bibee, NOARL

Recent improvements in the reliability and recording capacity of Ocean Bottom Seismometers (OBS) has allowed their use in more challenging and productive experiments. Concurrently, we have developed the ability to fire sizeable charges (100 lbs.) at ambient pressure on the seafloor, enabling us to conduct experiments with both source and receiver on the seafloor. This permits efficient generation of shear waves and, with precisely navigated sources, provides excellent control of the location where seismic energy enters the bottom, providing a "zero radius" Fresnel zone. We have used these methods in a tomographic study (Hildebrand, Dorman et al., 1989) and to study interface waves in seafloor sediments (Schreiner and Dorman, 1990). The next logical step is to address the problems of the upper crust, specifically the determination of the shear modulii, using these new methods.

Recent seismic studies of the upper crust show compressional velocities much lower than those found in the samples returned by dredging and drilling. This difference has been attributed to alteration and to the presence of pervasive porosity. Some of this porosity is inherent in the formation of pillow lavas and, no doubt, more is introduced by the faulting accompanying isostatic adjustment of the very young crust. Lithostatic pressure closes cracks by rock deformation and hydrothermal circulation fills cracks with deposited mineralization, thus the effects of porosity will be greatest on young, shallow crust.

Characterization of the seismic effects of porosity is complicated, as the effects on the elastic tensor depend critically on the geometry (aspect ratio and orientation) of the water-filled voids (see Fryer et al. (1990) for example, for amplification). The introduction of asymmetry destroys much of the simplicity we have come to enjoy through use of the scalar wave equation for an isotropic medium. In dealing with an anisotropic medium, we are immediately faced with the challenge of determining many more elastic modulii than in the isotropic case.

The first consequence we find is that simply measuring the velocity of one compressional arrival simply doesn't provide enough information to fix the requisite number of elastic parameters. The solution to this problem requires measurement of additional propagation properties including shear arrivals, amplitudes, wave polarizations, and surface or interface waves. Shear waves are the most important parameter affecting the acoustic reflectance of the shallow crust since the existence of a shear critical angle depends upon whether the shear velocity is greater than 1500 m/sec. Using both shots and receivers on the seafloor allows generation and detection of shear waves. Thus far, few reliable measurements of seafloor shear crustal velocity are available; existing measurements are due to P-to-S wave conversions under anomalous conditions. Seafloor shots and receivers give the most direct and reliable means for generating and detecting shear waves within the shallow seafloor.

Seafloor shots also generate interface waves, which are trapped at the boundary between the seafloor and the water column. Earthquake seismology teaches us that interface waves are much simpler to exploit than the body-wave polarizations with their problems of overlapping waveforms and site-dependent effects. We have experience with interface waves generated by seafloor explosions, although primarily from regions with

sedimentary cover. This very low surficial shear velocity of sediment forms a pronounced waveguide which, in turn, yields severe dispersion and wave trains of long duration. Although attenuation in the upper sediments is high, the attenuation of individual modes is not always high, since modes whose phase velocity is near that of water will have their modal amplitude raised by the influence of the high-Q water.

Figure 1 shows frequency-time/slowness analyses of two seismograms, one from a sedimentary pond just off the Patton Escarpment (DSDP site 469) and one from a site near the distal end of the Monterey Fan. The dispersion curves are significantly different; the Patton Escarpment site gives a smoothly dispersed wavetrain, modeled by a smooth shear velocity gradient with depth. In contrast the Monterey Fan site gives a large change in group-slowness over a small frequency range, suggesting a simple two-velocity model with depth.

There have been no experiments designed to measure interface wave dispersion on unsedimented crust. We have calculated interface wave synthetic seismograms for a crust typical of the East Pacific Rise (see Figure 2). The wave trains are not nearly as greatly dispersed as for sedimented crust, yet these waves are very sensitive to the shallow elastic modulii of the oceanic crust.

To address the need for better understanding of shallow elastic properties, we propose a seafloor OBS and seafloor shot array with circular geometry (see Figure 3). This provides a data-set for two experiments; 1) it determines shallow elastic properties controlling compressional and shear propagation, providing a homogeneous but anistropic model and 2) it allows a tomographic inversion with lateral inhomogeneity but isotropic structure. These analyses can be conducted both with body-waves and with interface waves which are slower and offer the greatest spatial resolution.

In summary, studies using explosive sources and seafloor receivers offer the opportunity to measure the greatest number of elastic properties of the upper oceanic crust, as well as anisotropy and inhomogeneity.

References

Hildebrand, J.A., L.M. Dorman, P.T.C. Hammer, A.E. Schreiner and B.D. Cornuelle, Seismic Tomography of Jasper Seamount, *Geophys. Res. Lett., v. 16*, 1355-1358, 1989.

Schreiner, A.E. and L.M. Dorman, Coherence and correlation lengths of sea floor noise, influence of sea floor structure, *J. Acoust. Soc. Am.*, in press, 1990.

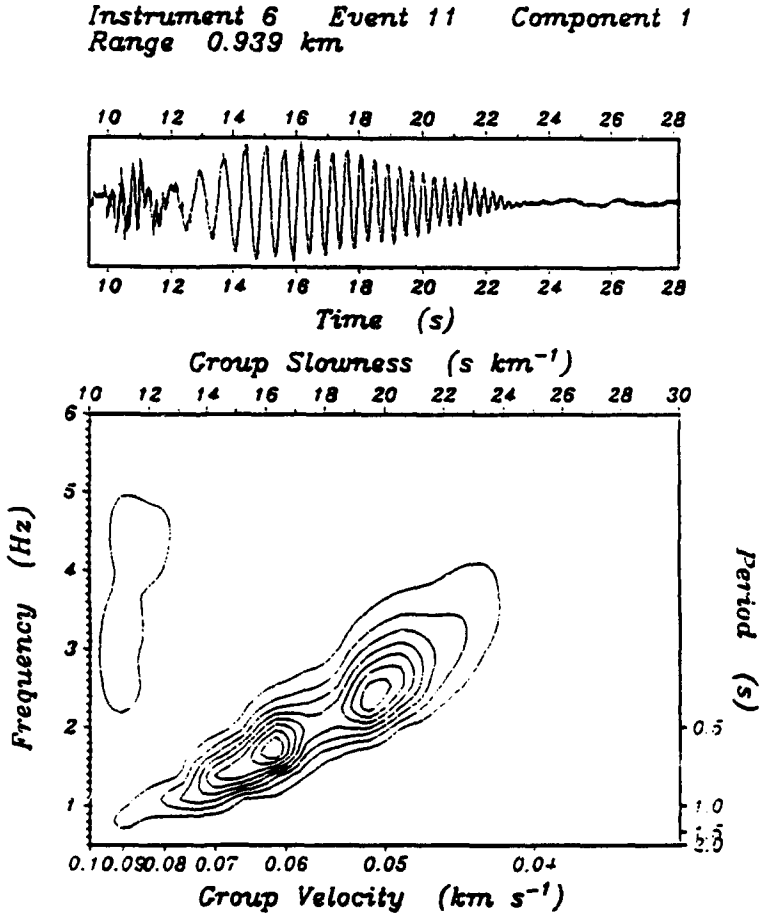

A frequency/period vs. time/slowness decomposition (sonogram) of a Stoneley wave from DSDP site 469, in 3800 m water depth at the base of the Patton Escarpment off San Diego. The source was a small explosion on the seafloor and the record is a vertical component seismogram. We have analyzed this record and determined the seafloor shear velocity structure.

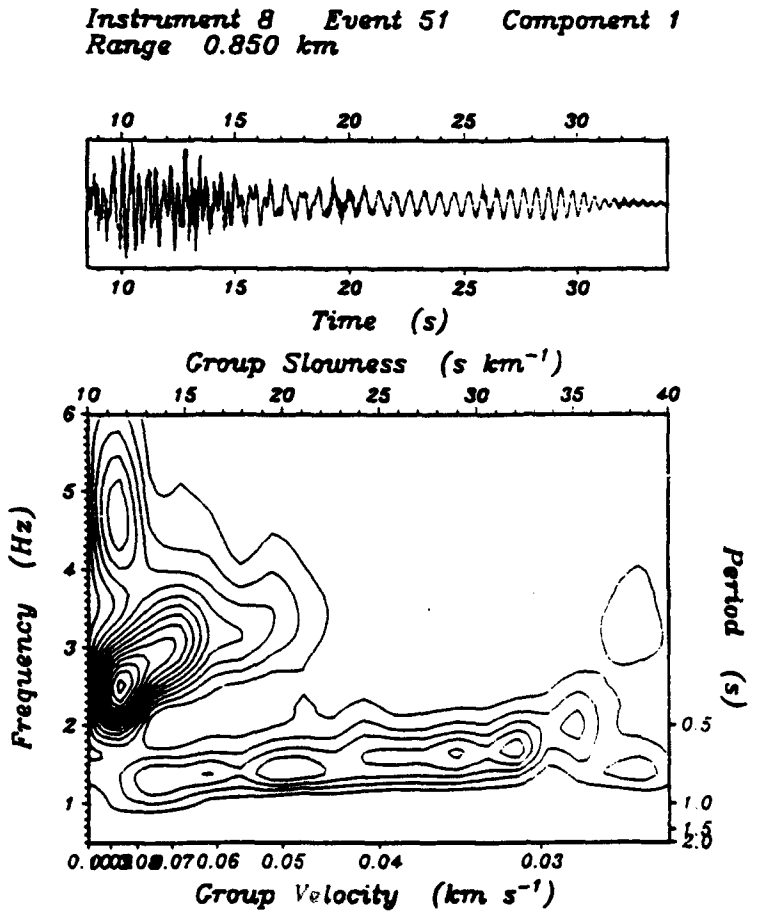

A sonogram of a Stoneley wave observed near the proposed SWAPP site (35 N, 127 W). It exhibits lower velocities at the higher frequencies, indicating lower surficial velocities.

Figure 1

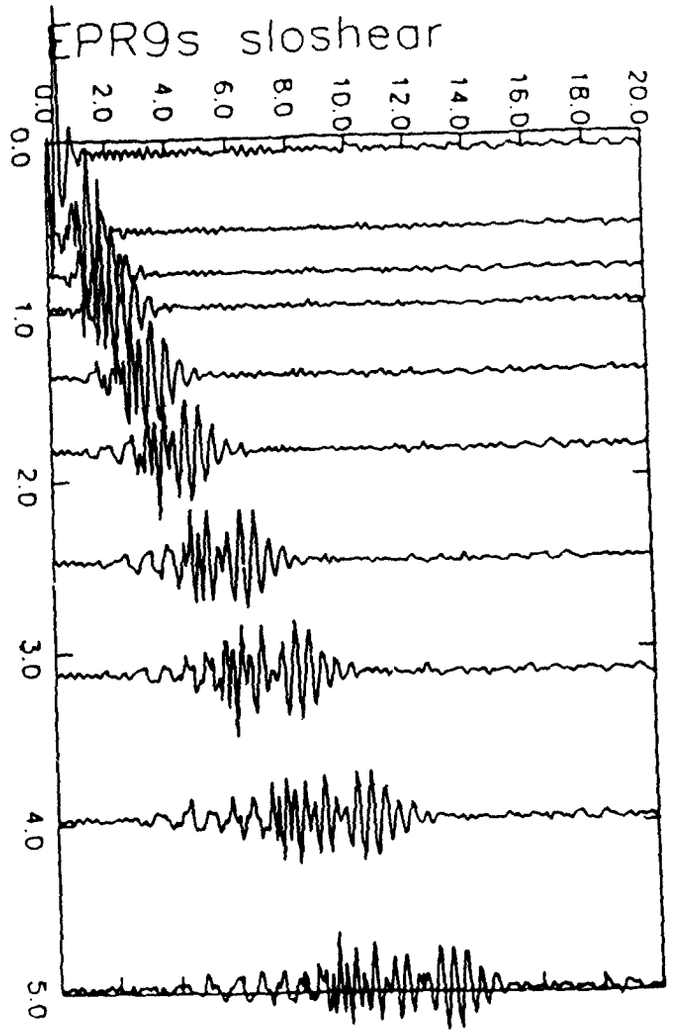

A record section of the 0-5 km distance range computed by the reflectivity method of Kennett (1983). In this case the range of integration includes the Stoneley wave poles so the full medium response in the slowness range 0.0001-2.0 s/km results. These contain all possible reflections and conversions for the frequency band 0.1 - 5.0 Hz. The appearance of the Stoneley wave train differs slightly from the mode seismogram because the frequency response was restricted to 5 Hz due to limits of computer speed and the author's patience. The source is at one meter above the seafloor.

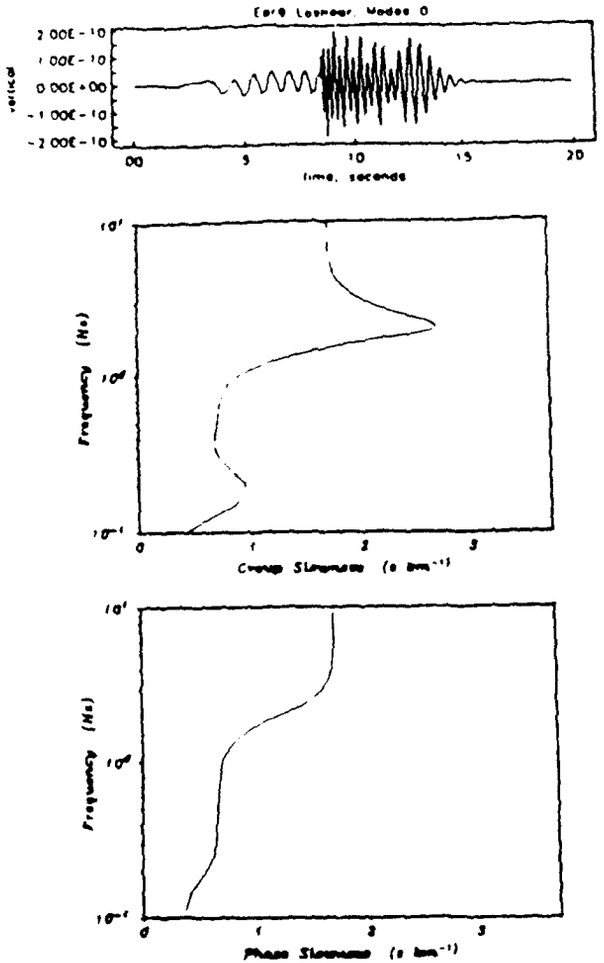

A fundamental mode synthetic seismogram of a Stoneley wave from an explosion at 5 km range on the seafloor. The calculation used a source at one meter below the seafloor. One meter is the bubble size for 50 lbs. of high explosive. The trace shown *is vertical motion observed at the seafloor.* The dispersion curves and synthetic seismogram were calculated using the theory described by Woodhouse (1980) and implemented by Gomberg and Masters (1988). Displaying the dispersion curve using group slowness as a coordinate (instead of group velocity) allows the plotting coordinate to correspond to travel time, in this case scaled for 5 km range. Appropriate integral representation of a synthetic seismogram (*viz.* Aki and Richards Eq. 7.18, 1980) shows that spectral amplitude is inversely proportional to the frequency derivative of group slowness, and explains the prominence of the Airy phase associated with the group slowness maximum. It may seem unlikely that frequencies this low can be observed from sources with bubble frequencies above 100 Hz but we show seafloor examples in Appendix 1.

Figure 2

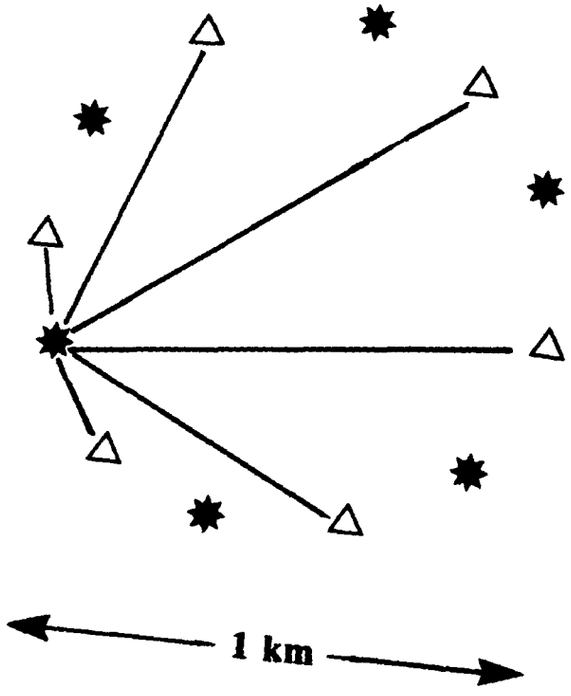

Figure 3. Geometry of an interface wave tomography experiment. The dense concentration of ray paths within the circle provides a stable geometry for the inversion.

SEA FLOOR TRANSIENT ELECTROMAGNETIC SOUNDING

R. Nigel Edwards
Department of Physics, University of Toronto
Toronto, Ontario M5S 1A7

Innovative transient electromagnetic techniques are being developed by research groups at the University of Toronto, the Pacific Geoscience Centre and the Scripps Institution of Oceanography to map the electrical conductivity of the sea floor to a depth of the order of 100 metres. The implementation of each technique requires the construction of apparatus, including sensitive magnetic and electric field sensors and associated computer hardware, and the development of computer algorithms to interpret data collected over complex structures.

Any electromagnetic technique used for mapping sea floor conductivity, has to compensate for the adverse effects of the sea. The conductivity of (generally) resistive rock has to be measured accurately in the presence of conductive sea water. The DC-resistivity method was the first used for marine electromagnetic exploration. A quasi-dc current is injected into the earth through a current dipole and electric potential difference measurements are made across a second pair of electrodes, the potential dipole. While this method can accurately measure the electrical conductivity of very conductive parts of the seafloor (e.g., sulphide deposits), accurate measurements of the seafloor conductivity σ_1 are inhibited if the seafloor has a conductivity of order, or less, than that of seawater σ_0. The poor resolution of the seafloor conductivity occurs because the electric potential is determined principally by the more conductive seawater.

Edwards and Chave (1986) showed that problems associated with the low inherent sensitivity of the resistivity method could be overcome by measuring the EM *transient* response with the same electric dipole-dipole array and determining the crustal conductivity directly from the shape of the response. The rate of diffusion of an EM transient through a medium is inversely proportional to the conductivity of the medium, so that for the usual case of a resistive sea bed, the field diffusing through the sea floor will arrive first. At later times, the signal diffusing through the sea water will arrive, and ultimately the measured field should approach the DC limit.

The analytic solutions for the step-on transient response of two half-spaces in contact, representing the sea floor and the sea water respectively, were derived by Edwards and Chave (1986). Figure 1 illustrates the step-on responses of the electric dipole-dipole system to this model for a range of conductivity ratios of the ocean to seafloor σ_0/σ_1. Clearly, there are two distinct parts to the response. The position in time of the initial rise in the response is a direct measure of sea floor conductivity while the second rise corresponds to the arrival of the signal through the seawater and occurs at the same time for all models. From theory, the delay time τ it takes for the signal to diffuse from the receiver to the transmitter through the seafloor is given by

$$t = \frac{\mu\sigma_1\rho^2}{10}$$

where ρ is the transmitter/receiver separation. For ρ=500 m and σ_1=0.01 S/m the delay time is 0.3 ms. The delay time for the signal travelling through the seawater is 100 ms and thus the ocean signal arrives orders of magnitude later than the earth signal. For most other typical ocean to seafloor conductivity ratios and receiver/transmitter separations, the initial

rise is clearly separated from the seawater signal allowing exceptional resolution of sea floorconductivity.

Apart from the transient electric dipole-dipole system are there other towed EM systems suitable for seafloor exploration? Cheesman, Edwards and Chave (1987) derived the transient response for a crustal layer beneath the sea to several common configurations of both electric and magnetic dipole sources and detectors. Several systems used in land exploration were found to be unsuitable for seafloor work. The response of these systems is determined principally by the conductive seawater, and except for situations of extremely conductive seafloors, the response is not sensitive to the underlying conductivity structure. One additional system was however found to be sensitive to the seafloor conductivity and suitable for a towed seafloor transient sounding: the horizontal coaxial magnetic dipole-dipole system.

Figure 2 shows the step-on response of this system to the double half-space model for a range of conductivity ratios. Again there are two distinct parts to the response with the time of the initial rise being indicative of the underlying conductivity. First order electrical maps of the sea floor could be obtained by simply contouring this delay time. A measurement of the diffusion time between a receiver and a source is a robust estimator of the apparent or average resistivity between the two sites even in a heterogeneous conductivity structure. With additional processing it is possible to obtain layered earth and two-dimensional representations of the underlying conductivity from a transient recording, through inversion of the entire response.

Short baseline ($\rho < 100$m) prototypes of both the electric dipole-dipole and co-axial magnetic dipole-dipole systems have been constructed. The streamers employ a single, multiple conductor, armored cable of sufficient mechanical strength to be towed behind a ship. The transmitter and receiver dipoles are connected both electrically and mechanically to the cable and the whole assembly is towed on or very close to the seafloor. The switched current used to energize the coil (magnetic dipole transmitter) or long wire (electric dipole transmitter) is generated from batteries. The signals received by the electrodes are returned to the ship for stacking and processing. Receiver sensors consist of either an induction coil (magnetic system) or an array of Ag-AgCl electrodes (electric system). Each receiver is encased in a seafloor pressure vessel and includes both pre-amplification and delay circuitry. The latter delays the returning signals by about 1 ms to avoid electrical interference with the outgoing transient.

A ship-towed magnetic system developed jointly by the University of Toronto and the Pacific Geoscience Centre (Cheesman, Edwards and Law, in press) has been operated in the straits between Vancouver Island and the mainland, successfully mapping the seafloor sediment conductivity. The sea floor consists of bedrock overlain by varying thicknesses of mud, ranging from zero to tens of meters, so that the response of the system to varying thicknesses of sediment could be ascertained. A total of 38 measurements were made at 19 sites along three lines. All of the measurements are consistent with a model in which a varying thickness of 0.8 Ωm mud overlies rock with a resistivity of about 10 Ωm. The interpretation was supported by independent seismic information. These are the first measurements taken systematically at sea in deep water with any towed transient electromagnetic system. Another magnetic system, developed at Scripps (Spahr Webb, pvt. comm.) as a package which can be towed by DEEP-TOW, has just completed an electrical survey over the top of a seamount in the Pacific Ocean 500 miles west of San Diego.

The quality of data obtained, the speed of its acquisition and the ease of its interpretation are extremely encouraging, and suggest that it may be possible in the near

future to produce in real time a continuous map of the apparent resistivity of the sea floor using towed TEM systems. Where should such systems be used? Electromagnetic methods map the variation of electrical conductivity, a property of material related to porosity, pore water salinity, pore or fracture geometry, temperature, degree of partial melt and composition. These parameters are highly variable in the vicinity of an active spreading centre. Further, electromagnetic and seismic data, already available at some locations such as the East Pacific Rise, are complementary. In many cases, a combined analysis of the electrical and the seismic properties of earth materials, measured in situ, has proven to be a vital link in the development of a geological model.

A simple model for the formation of submarine volcanic rocks includes a magmatic heat source within a few kilometres of the seafloor to drive the circulation of seawater through the rocks, sufficient permeability to allow deep penetration of the fluid enabling chemical exchanges with a large volume of rock, and fractures to focus the discharge of large volumes of fluid onto the seafloor. Major unknowns include the time scales of the magmatism; the shapes, dimensions and longevity of individual crustal magma chambers; whether a spreading centre acts as a single magmatic unit or is segmented on a finer scale; and the spatial and temporal variation of porosity and permeability which will be relevant to fluid flow. Collaborative research projects, involving the integrated analysis of geophysical, geological and geochemical data have been established to investigate the fundamental science of the conversion of mantle to oceanic crust and to characterize environments of polymetallic massive sulphide deposits at mid ocean ridges. Actively forming and fossil sea-floor sulphide deposits have been discovered at more than two dozen locations worldwide, including on the Juan de Fuca plate and the East Pacific Rise. Sea floor mineral deposits warrant study even if they never become economic. They contain a wealth of scientific information and can reveal the geologic settings and processes by which ancient massive sulphide deposits that are now on land have been formed and preserved. Massive sulphide ores are a major source of copper, zinc, lead, silver and gold.

A fast interpretation of the seafloor conductivity uses the observed delay times to define an apparent conductivity of the seafloor. Forward modeling techniques, both analytical and numerical, can be used to provide an interpretation of an apparent resistivity map in terms of more detailed geological structure. Whereas the response of simple geometries such as a layered earth to excitation by an active electromagnetic source can be found analytically, the response of more complicated structures requires the application of a numerical technique (Edwards and Cheesman, 1987; Edwards, 1988). Everett and Edwards (1988) have used the CRAY-XMP/24 vectorizing supercomputer at the Ontario Center for Large Scale Computation to model the transient response of complicated two-dimensional structures. A finite element representation of the governing Maxwell electromagnetic equations for several prescribed values of the Laplace variable σ is solved and the results converted into the time domain by an inexpensive Laplace inversion algorithm. Modeling of mid-ocean ridge structures indicates that electromagnetic methods are capable of detecting large conductors located at depths below the seafloor greater than one kilometer. A videotape, available from the authors, shows the complete progression of transient eddy currents into, through and around such a conducting body. The use in the finite element package of an automatic mesh generator and digitizing tablet combined with the fast turnaround time of the CRAY (we have attained speeds of 30 Mflops) affords flexible model selectivity, permitting quick access to the responses of relevant off-shore structures. The fast machine speeds also allows the forward code to become a core routine in an integrated tomographic and/or inversion package. The forward code fills a target-specific design role since it can readily assess response sensitivities to proposed TEM source/receiver configurations.

REFERENCES

A. Chave, S.C. Constable and R.N. Edwards, Sea floor electromagnetic exploration techniques, in Electrical Methods in Geophysics 2, Society of Exploration Geophysicists, Tulsa, OK, Invited paper, in press, 1990.

S.J. Cheesman, R.N. Edwards and A.D. Chave, On the theory of sea floor conductivity mapping using transient EM systems, *Geophysics, 52*, 204-217, 1987.

S.J. Cheesman, R.N. Edwards, and L.K. Law, A short baseline transient electromagnetic method for use on the sea floor, *Geophysical Journal*, in press, 1990.

R.N. Edwards, Controlled source electromagnetic mapping of the crust, in *The Encyclopedia of Solid Earth Geophysics*, David E. James Editor, Van Nostrand Reinhold Co. Inc., Stroudsburg, Invited paper, 126-139.

R.N. Edwards, Two-dimensional modeling of a towed electric dipole-dipole sea floor EM system: The optimum time delay for target resolution, *Geophysics, 53*, 846-853, 1988.

R.N. Edwards and A. Chave, On the theory of a transient electric dipole-dipole method for mapping the conductivity of the sea floor, *Geophysics, 51*, 984-987, 1986.

R.N. Edwards, and S.J. Cheesman, Two dimensional modeling of a towed transient magnetic dipole-dipole seafloor EM system, *Geophysics, 61*, 110-121, 1987.

M.E. Everett and R.N. Edwards, Controlled source electromagnetic responses of fast spreading mid-ocean ridge models, submitted to *Journal of Geophysical Research.*

M.E. Everett and R.N. Edwards, Electromagnetic expression of axial magma chambers, *Geophysical Research Letters, 16*, 1003-1007, 1989.

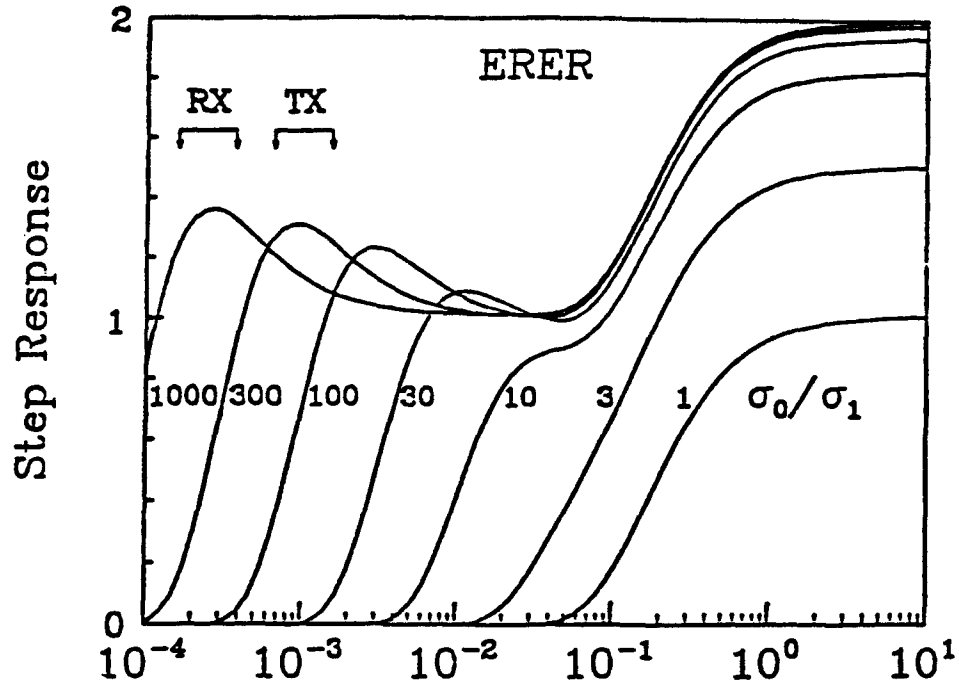

Figure 1 The step–on response of an electric dipole–dipole system to a double half–space model for a range of conductivity ratios of the ocean to seafloor σ_0/σ_1. The time axis has been normalized to the characteristic diffusion time of the signal through the seawater; for a transmitter/receiver separation of 500 m the time axis can be taken as true time. The magnitude of the response has been scaled by the magnitude of the DC response in a whole–space $E_r^{DC} = M_E/2\pi\sigma_0\rho^3$ where M_E is the dipole moment of the electric dipole source and ρ is the transmitter/receiver separation.

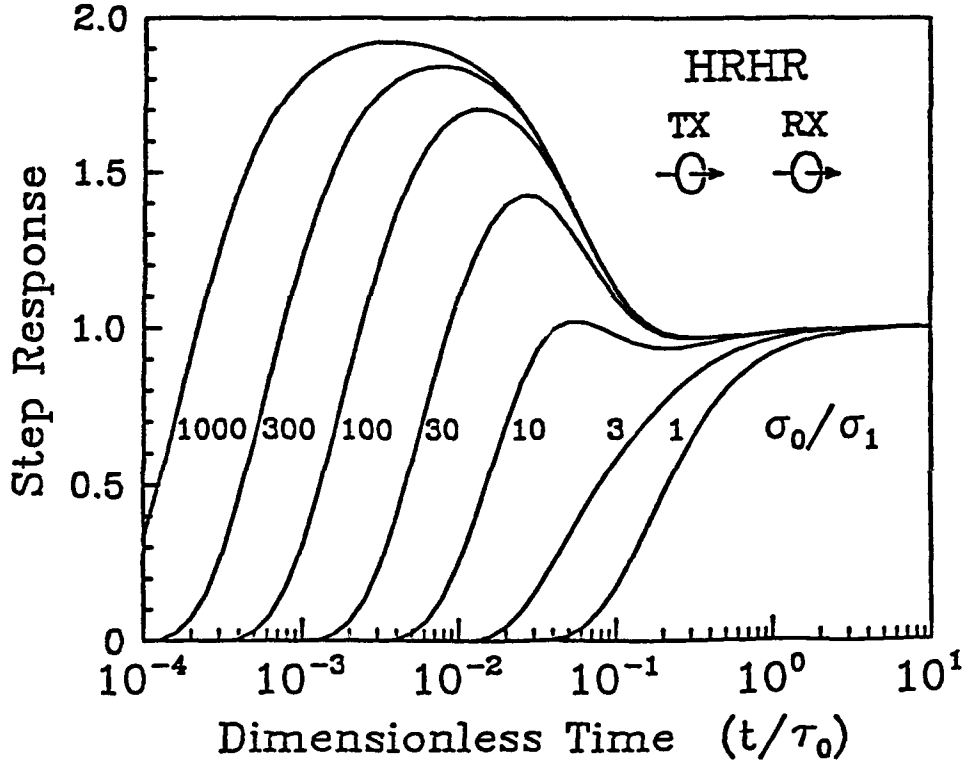

Figure 2 The step–on response of the magnetic dipole–dipole system to the double half–space model for a range of conductivity ratios. The time axis is scaled as in Figure 2. The magnitude of the response has been scaled by the magnitude of the DC response $B_r^{DC} = M_B\mu/2\pi\rho^3$ where M_B is the dipole moment of the magnetic dipole source.

KEY DOWNHOLE MEASUREMENTS FOR IN-SITU CRUSTAL STUDIES: AN EXAMPLE FROM OCEAN DRILLING PROGRAM HOLE 735B

D. Goldberg
Lamont-Doherty Borehole Research Group, Palisades, NY 10964.

INTRODUCTION

To gain insight into the tectonic, chemical, and hydraulic behavior of crust, certain key measurements of its *in situ* properties are essential. This short note describes a suite of downhole measurements, including electrical, acoustic and nuclear logs and hydraulic packer tests, which were used to interpret the properties of the crust near the Atlantis II fracture zone in the southwest Indian Ocean. Hole 735B drilled by the Ocean Drilling Program afforded the unique opportunity to investigate 500m into layer 3 rocks with the first nearly continuous recovery of core in fresh and altered oceanic gabbro and these downhole measurements (Robinson, Von Herzen, *et al.*, 1989). The methods and time required to measure such *in situ* properties, as acquired in Hole 735B and discussed below, should be considered early in any plan investigating crustal behavior through drilling.

IN-SITU PROPERTIES

Alteration and porosity

Since most rocks contain hydrogen in the form of bound water associated with clays and other alteration minerals, the neutron log is crucial to measure the hydrogen in the formation (porosity) and determine the degree of alteration in basaltic and gabbroic rocks in the form of hydrous clay mineralization (e.g., celadonite, palagonite, amphiboles, talc, zeolites, and Fe-hydroxides). This can be accomplished using core measurements of the hydrous mineral concentration or other log measurements such as the natural gamma log or the hydrogen yield log from the GST (Geochemical Spectroscopy Tool) to predict the concentration of hydroxyls bound in alteration minerals (Broglia and Ellis, 1990). In Hole 735B, the alteration volume derived from the GST hydrogen yield log, H weight fraction measurements on dry core samples, the raw and corrected neutron porosity logs, and the core-derived porosities show a good correspondence between log values and core-derived values; differences may be attributed to fracture porosity unsampled in the core (see Fig. 1).

Fracturing and regional stress

The acoustic borehole televiewer can be used to identify fractures intersecting the borehole and stress-induced spalling along the borehole walls (Zemanek et al., 1970). The cumulative aperture of identified fractures in Hole 735B decreases with depth, and the fracture density more or less mirrors the cumulative aperture log (Fig. 1). Similar results have been observed for sub-horizontal fractures closing gradually with increasing overburden pressure (Seeberger and Zoback, 1982; Haimson and Doe, 1983). In this hole, however, many fractures are high-angle, as expected from the steep tectonic uplift at this site, and some remain open at depth. As no wellbore spalling was observed in the televiewer data to indicate the minimum horizontal stress direction, it seems most likely that the high-angle fracturing resulted from normal faulting during uplift of this ridge, rather than a direct result of horizontal plate motion.

Temperature

In dense crystalline rocks, fluid flow is likely to occur through fractures, which shifts the temperature profile and yields an anomalously low or negative temperature gradient. High-precision temperature logs (within 0.01°C) were run before and after the completion of the other logging experiments in Hole 735B (Robinson, Von Herzen, et al., 1989). In Figure 1, negative gradient anomalies occur over intervals containing fractures, although not all of the observed fractures correspond to negative gradient anomalies. Consequently, the observed negative gradient anomalies in this hole are interpreted as due to the presence of fractures which are transmissive and contribute cool fluid back into the borehole that was displaced by warm bottom water during drilling (Von Herzen and Scott, in Robinson, Von Herzen, et al., 1989). During hydraulic packer tests, it is likely that the same transmissive fractures influencing the temperature profile are hydraulically active.

Permeability

Standard measurement techniques to estimate the in-situ permeability with about 30% accuracy can be performed either by monitoring the decays of nearly instantaneous pressure pulses applied to the isolated zone ("slug tests", Bredehoeft and Papalopulos, 1980) or by monitoring the gradual pressure increases as seawater was pumped at a constant rate into the isolated zone ("injection tests", Matthews and Russell, 1967). In Hole 735B, an inflatable single-element drill string packer was used to measure the average hydraulic transmissivity of four different intervals isolated between the bottom of the hole and the depths at which the packer was inflated (Becker, in Robinson, Von Herzen, et al., 1989). The calculated permeabilities between these packer inflation depths show a decreases of over 2 orders of magnitude in the deepest 200m of Hole 735B (Fig 1).

Elastic properties

Full-waveform sonic log data can be analyzed to yield compressional, shear, and guided wave velocities and amplitudes. Borehole wave amplitudes, and in particular guided-wave amplitudes, have been related to hydraulic transmissivity in previous studies of fractured rocks (e.g., Paillet, 1980; Hardin et al., 1987; Barton and Moos, 1988). Observations suggest that velocity and semblance also decrease as a result of hydraulic mechanisms (e.g., Moos and Zoback, 1983; Kimball and Marzetta, 1984; Goldberg and Gant, 1988). In Figure 1, sonic velocities computed by semblance show considerable variation in Hole 735B, and nearly all low Vp anomalies correspond with elevated porosities and low semblance (shaded below the mean). Because acoustic logs can achieve greater depth resolution than hydraulic or temperature measurements, decreases in velocity and semblance can be useful for detailed correlation of fracture transmissivity to the measured permeability.

DISCUSSION

Indicators of fracturing from downhole experiments (e.g., acoustic, porosity, temperature, and televiewer logs) may be used to distinguish fractures that are transmissive from those that are not. For example, the weak correlation of in-situ permeability with porosity and its strong correlation with temperature gradient and televiewer logs gives evidence that fracturing controls the measured permeability in Hole 735B. The transmissive fractures near 40 and 264 mbsf in Hole 735B likely contribute most of the cool fluid flow back into the borehole and generate negative temperature gradients. In a similar manner, these fractures may generate measurable decreases in acoustic amplitudes due to scattering and inelastic dissipation from formation and borehole fluid movements. As a result, low Vp and semblance anomalies and high-porosity fractures, notably at 40, 100-150, 200 and 264 mbsf, are spatially coincident with negative temperature gradient anomalies. These

coincident anomalies may be the best indicators as to which fractures intersecting the borehole are transmissive, because they reflect the result of fluid movement through fractures by independent physical measurements. In combination, the downhole measurements available in this hole provide an essential in-situ data set for interpretation of the physical, chemical, and hydraulic properties of the ocean crust.

REFERENCES

Barton, C.A., and Moos, D., 1988. Analysis of macroscopic fractures in the Cajon Pass scientific drillhole: over the interval 1829-2115 meters. *Geophys. Res. Lett., 15*:1013-1016.

Bredehoeft, J.D., and Papadopulos, I.S.,1980. A method for determining the hydraulic properties of tight formations. *Water Resources Res., 16*:233-238.

Broglia, C., and Ellis, D., 1990. The effect of alteration, formation absorption, and standoff on the response of the thermal neutron porosity log in gabbros and basalts: examples from DSDP-ODP Sites. *J. Geophys. Res.*, in press.

Goldberg, D., and Gant, W.T., 1988. Shear-wave processing of sonic log waveforms in a limestone reservoir. *Geophysics, 53*:668-676.

Hardin, E.L., Cheng, C.H., Paillet, F.L., and Mendelson, J.D., 1987. Fracture characterization by means of attenuation and generation of tube waves in fractured crystalline rock at Mirror Lake, New Hampshire. *J. Geophys. Res., 92*:7989-8006.

Haimson, B.C., and Doe, T.W., 1983. State of stress, permeability and fractures in Precambrian granite of northern Illinois. *J. Geophys. Res., 88*:7355-7371.

Kimball, C.V., and Marzetta, T.L. 1984. Semblance processing of borehole acoustic array data. *Geophysics, 39*:587-606.

Matthews, C.S., and Russell, D.G., 1967. Pressure build-up and flow tests in wells. *Amer. Inst. Min. Met. Pet. Eng., SPE monograph, 1.*

Moos, D., and Zoback, M.D., 1983. In-situ studies of velocity in fractured crystalline rocks. *J. Geophys. Res., 88*:2345-2358.

Paillet, F.L., 1980. Acoustic propagation in the vicinity of fractures which intersect a fluid-filled borehole. SPWLA 21st Annual Logging Symposium Trans., paper D.

Robinson, P.T., Von Herzen, R.P., et al., 1989. Site 735. In Robinson, P. T., Von Herzen, R. P., *Proc. ODP, Init. Repts., Leg 118*: College Station, TX (Ocean Drilling Program), 89-816.

Seeberger, D.A., and Zoback, M.D., 1982. The distribution of natural fractures and joints at depth in crystalline rock. *J. Geophys. Res., 87*:5517-5534.

Zemanek, J., Glenn, E.E., Norton, L.J., and Caldwell, R.L., 1970. Formation evaluation by inspection with the borehole televiewer. *Geophysics, 35*:254-269.

FIGURE CAPTION

Figure 1. Geophysical logs in Hole 735B: Vp and Vs, (track 1), mean semblance (track 2), corrected neutron porosity and alteration (tracks 3 and 4), temperature gradient (track 5), 2-m cumulative fracture aperture (track 6), and bulk permeability (track 7). Locally the alteration can be as high as 60%, and alteration and porosity decrease downhole. Differences between log and core porosities are attributed to the presence of open fractures. Uncertainty in permeability estimates is represented by the line width, and mean semblance (shaded below the mean) decreases systematically at 140 mbsf due to a malfunction of the pre-set receiver gains. As indicated by low-velocity and low semblance, high porosity, and negative temperature gradient perturbations, large fractures identified at 40 and 264 mbsf contribute most to the measured permeability.

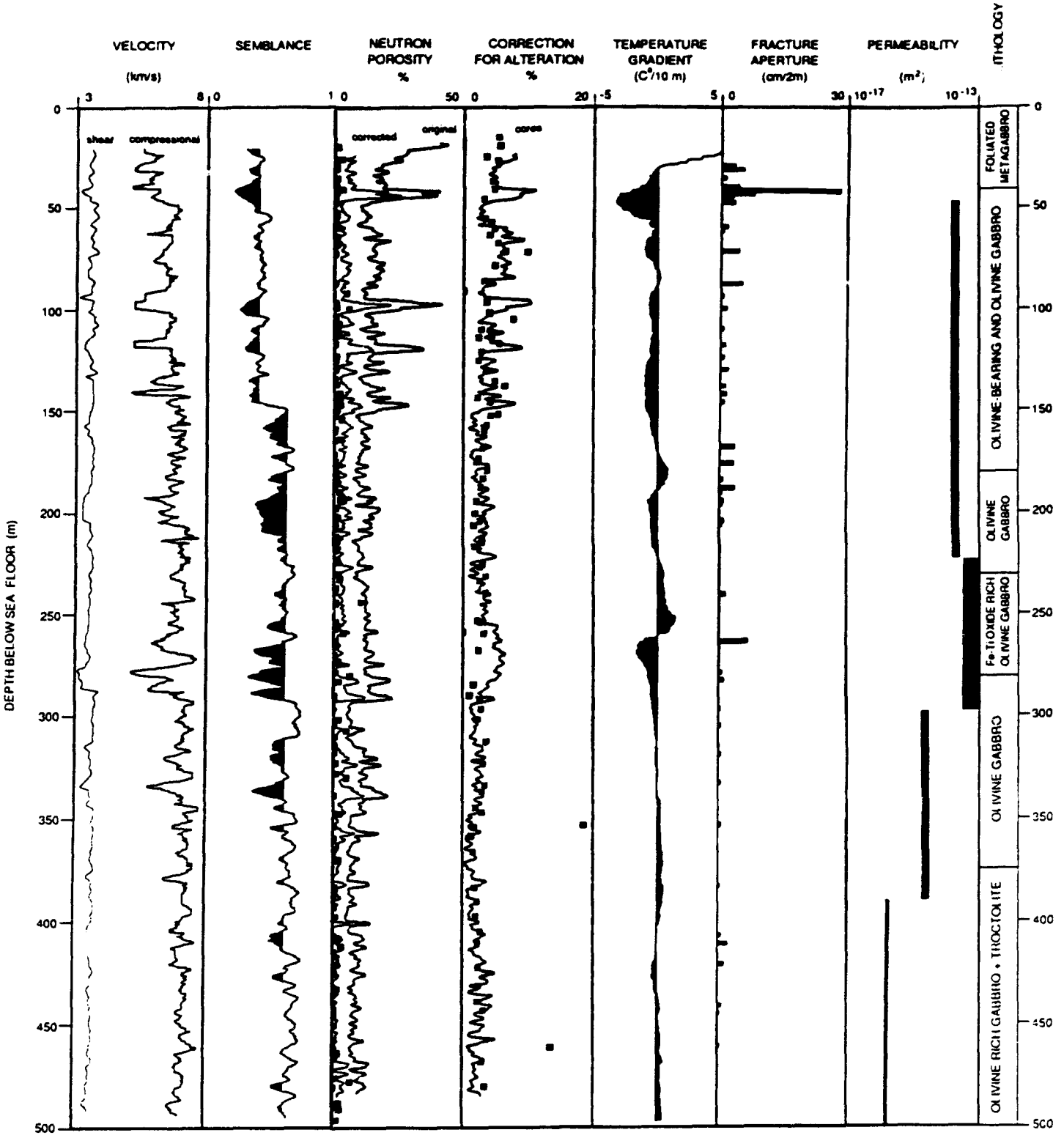
VELOCITY
(km/s)
3
8
shear
compressional
SEMBLANCE
0
1
NEUTRON POROSITY
%
0
50
corrected
original
CORRECTION FOR ALTERATION
%
0
20
cores
TEMPERATURE GRADIENT
(C°/10 m)
-5
5
FRACTURE APERTURE
(cm/2m)
0
30
PERMEABILITY
(m²)
10⁻¹⁷
10⁻¹³
LITHOLOGY
DEPTH BELOW SEA FLOOR (m)
0
50
100
150
200
250
300
350
400
450
500
FOLIATED METAGABBRO
OLIVINE-BEARING AND OLIVINE GABBRO
OLIVINE GABBRO
Fe-Ti OXIDE RICH OLIVINE GABBRO
OLIVINE GABBRO
OLIVINE RICH GABBRO + TROCTOLITE

Section C3: Seismics

1: Tomographic Evidence for Upper Crustal Heterogeneity of the East Pacific Rise Near 9°30'N: D.R. Toomey, G.M. Purdy, S.C. Solomon

2: Seismic Studies of Upper Oceanic Crust on the Juan de Fuca Ridge: K.M.M. Rohr

3: Interpreting Oceanic Crustal Seismic Profiles: D.A. Lindwall

4. Near Surface Velocity Structure through Wide Aperture Profiling: M. Kappus, A. Harding

5. Multichannel Seismic Reflection Observations of the Uppermost Crust near the East Pacific Rise: G.A. Barth

6. Compressional and Shear Wave Velocities in the Upper Crust: O. Diachok, S. Wales, R. Dicus, F. Feirtag, D. Shirley, J. Siegel

TOMOGRAPHIC EVIDENCE FOR UPPER CRUSTAL HETEROGENEITY OF THE EAST PACIFIC RISE NEAR 9°30'N

Douglas R. Toomey*, G.M. Purdy†, Sean C. Solomon*

*Department of Earth, Atmospheric, and Planetary Sciences, Massachusetts Institute of Technology, Cambridge

†Department of Geology and Geophysics, Woods Hole Oceanographic Institution, Massachusetts

---

A seismic experiment, conducted during January 1988 as a cooperative project by the Woods Hole Oceanographic Institution (WHOI) and the Massachusetts Institute of Technology (MIT), was centered on the East Pacific Rise (EPR) at 9°30'N. Fifteen ocean bottom instruments, eight analog and five digital WHOI ocean bottom hydrophones and two digital MIT ocean bottom seismometers, recorded energy from 480 explosive shots and several airgun profiles, yielding more than 8000 seismic records. The majority of the shots lie within a 18x16 km^2 area centered on the rise axis and the nominal shot spacing is 1 km, except that within 3 km of the axis the shot separation was decreased to approximately 0.5 km. A crustal volume underlying this area was tomographically imaged using a subset of the first arriving P wave energy from 375 shots.

Three-dimensional images of upper crustal seismic structure beneath the East Pacific Rise show pronounced axial heterogeneity on the scale of a few kilometers. At shallow depths seismic layer 2 undergoes considerable evolution in physical properties and the responsible processes are heterogeneous along axis. A map view cross section through the three-dimensional seismic velocity image is shown in Figure 1. This figure illustrates velocity heterogeneity averaged over the uppermost 500m of basement or equivalently seismic layers 2a and a large part of 2b at this site. The prominent anomaly is a narrow zone of axis-parallel high velocities. The observed ribbon of axial high velocities persists throughout the array aperture (~16 km) and the anomaly varies in width and intensity along axis. While previous one- and two-dimensional seismic studies have discovered high velocities at shallow depths beneath the rise crest near 9°N [*Rosendahl et al.*, 1976; *Herron*, 1982], 12°50'N [*McClain et al.*, 1985; *Burnett et al.*, 1989], and at this site (9°30'N) [*Vera et al.*, in prep.], the results shown here are the first to demonstrate the axial continuity and heterogeneity of this near-seafloor anomaly. In conjunction with other seismic data, our results strongly suggest that a laterally heterogeneous high velocity anomaly is a ubiquitous feature of the shallow crust at the EPR axis.

Within 2 to 4 km of the summit the shallow axial high-velocity anomaly is flanked by an abrupt decrease in velocities of 0.6 to 1.2 km/s (Figure 1). In some areas this decrease occurs in less than a kilometer. Further off axis the average shallow structure appears to increase gradually by about 0.2-0.4 km/s, relative to the average structure between 2 and 4 km of the rise summit. Our results are thus broadly consistent with an age dependent evolution of shallow velocities (<500m depth) that is characterized by a precipitous decrease within 15-65 k.y., followed by a more gradual increase. This characterization is symptomatic of the entire experimental area. A similar age-dependent evolution of shallow velocities at young crustal ages was previously suggested in this region [*Vera et al.*, in prep.], to the south near 9°N [*Rosendahl et al.*, 1976; *Herron*, 1982], and on the EPR near 12°50'N [*McClain et al.*, 1985; *Burnett et al.*, 1989; *Caress et al.*, in prep.]. Not surprisingly, heterogeneity is superimposed on this average age dependence, with relative contrasts exceeding 0.4 km/s along isochrons; this degree of off-axis heterogeneity within

the uppermost crust is consistent with previous refraction experiments [e.g., *Purdy*, 1982; *Bratt and Purdy*, 1984]. The evolution of upper crustal velocities is not only time dependent, but is also the result of processes that vary along axis.

A commonly held view of the upper crustal velocity structure is that it evolves in response to progressive changes in the nature and magnitude of crustal porosity within the extrusive basaltic layer [*Houtz and Ewing*, 1976; *McClain et al*, 1985; *Purdy*, 1987; *Burnett et al.*, 1989; *Caress et al.*, in prep.]. Consequently, at zero-age crust it is inferred that velocity highs indicate low bulk porosity within recently erupted basaltic pillow and sheet flows [*McClain et al.*, 1985; *Burnett et al.*, 1989; *Caress et al.*, in prep., *Vera et al.*, in prep.]. Shortly after eruption this basaltic layer is supposedly fractured by tectonic forces, such as fissuring and faulting, that presumably increase bulk porosity and decrease bulk seismic velocity. The tectonic fracturing is suggested to initiate a few kilometers away from the neovolcanic zone as evidenced by on-bottom mapping of the onset of surficial faulting [*Macdonald*, 1982].

The interpretation of the evolution in upper crustal velocities solely in terms of variations in the nature and magnitude of porosity assumes that the on- and off-axis stratigraphy is identical. Several models of shallow crustal magmatism [e.g., *Cann*, 1974], however, suggest that directly beneath the neovolcanic zone the sheeted dike complex rises close to the seafloor. Such a configuration seems plausible given the need to transport magma vertically through existing flows. Thus an alternative explanation of the axially continuous high velocity anomaly is a relatively shallow sheeted dike complex at the locus of eruption. The rapid decrease in upper crustal velocities away from the axis, consequently, may be the result of a rapid increase in the thickness of extrusive basalts as a function of age.

An initial analysis of the seismic tomography data shows significant three-dimensional heterogeneity within the shallow (<500m) volcanic crust. The heterogeneity is characterized by both age-dependent and age-independent variability. The processes responsible for the observed seismic heterogeneity are not well understood. However, future analysis of the seismic tomography data will constrain hypotheses by defining in more detail the three-dimensional upper crustal velocity structure.

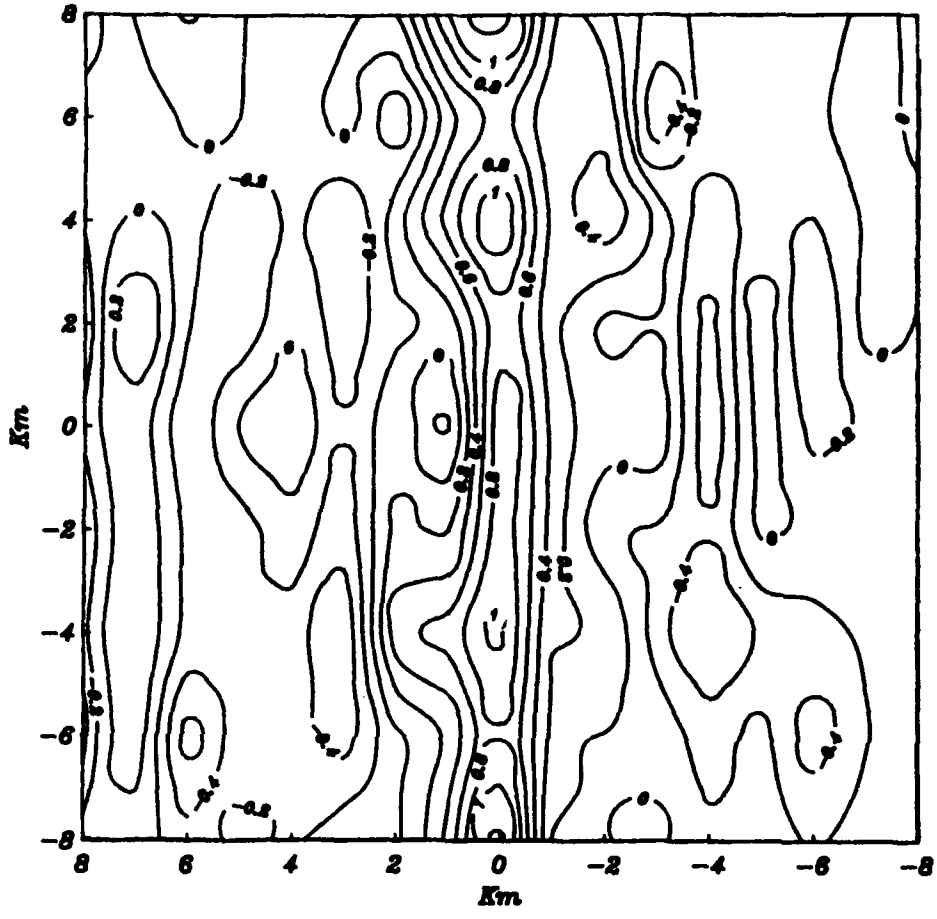

Plan-view cross-section at the seafloor through a three-dimensional P wave velocity structure resulting from tomographic inversion. The velocity model is represented by perturbations (km-s^{-1}) relative to an average one-dimensional model over the area. Between nodal locations velocity is linearly interpolated, in agreement with the model representation used in the inversion algorithm. The plan view origin coincides with the center of the shooting grid (9°31.72'N, 104°14.66'W), and the regional trend of the East Pacific Rise (N8°W) is aligned with the y axis; north is upwards. For reference, a multi-channel reflection line (#561) reported by Detrick et al. [1987] at 9°30'N crossed the rise axis approximately 3 km south of the center of the model.

References:

Bratt, S.R. & Purdy, G.M. *J. geophys. Res.* **89**, 6111-6125 (1984).

Burnett, M.S., Caress, D.W. & Orcutt, J.A. *Nature* **339**, 206-208 (1989).

Cann, J.R. *Geophys. J.R. Astr. Soc.* **39**, 169-187 (1974).

Caress, D.W., Burnett, M.S. & Orcutt, J.A. *J. geophys. Res.* (in prep.).

Detrick, R.S., Buhl, S., Vera, E., Mutter, J., Orcutt, J., Madsen, J. & Brocher, T. *Nature* **326**, 35-41 (1987).

Herron, T.J. *Geophys. Res. Lett.* **9**, 17-20 (1982).

Houtz, R. & Ewing, J. *J. geophys. Res.* **81**, 2490-2498 (1976).

Macdonald, K. C. *Annu. Rev. Earth Planet. Sci.* **10**, 155-190 (1982).

McClain, J.S., Orcutt, J. A. & Burnett, M. *J. geophys. Res.* **90**, 8627-8639 (1985).

Purdy, G.M. *J. geophys. Res.* **92**, 9351-9362 (1987).

Purdy, G.M. *J. geophys. Res.* **87**, 8403-8416 (1982).

Rosendahl, B.R., Raitt, R.W., Dorman, L.M., Bibee, L.D., Hussong, D.M. & Sutton, G.H. *J. geophys. Res.* **81**, 5244-5304 (1976).

Vera, E.E., Mutter, J.C., Buhl, P., Orcutt, J.A., Harding, A.J., Kappus, M.E., Detrick, R.S. & Brocher, T.M. *J. geophys. Res.* (in the press).

SEISMIC STUDIES OF UPPER OCEANIC CRUST ON THE JUAN DE FUCA RIDGE

Kristin Rohr
Geological Survey of Canada

My current research on upper oceanic crustal structure has demonstrated that reflections exist in upper crust of the JDF ridge; OBS refraction work aims to quantify the velocity structure associated with these events. These data sets allow a measurements of velocity increase with age in crust with different thermal histories. These projects are in collaboration with Earl Davis and Roy Hyndman of GSC and Mike Purdy of WHOI.

An increase in seismic velocity of the upper crust with age has been known since 1976 (Houtz and Ewing) and has been confirmed and enlarged upon by a variety of seismic experiments since then. Nevertheless the rate of increase is poorly constrained and causes of the increase are poorly understood. Hydrothermal circulation must be a major factor affecting the increase in velocity; different hydrothermal regimes, e.g., open to oceanic circulation or sealed by sediments, should produce different rates of increase.

The JDF ridge is a natural laboratory to study rates of seismic velocity increase since its eastern flank is blanketed with sediments and the western flank is more lightly sedimented and peppered with seamounts. Hydrothermal circulation on the western flank has probably remained open to sea water out to 3 Ma whereas circulation on the eastern flank is sealed by sediments in crust older than 1 Ma. We expect the flanks have different rates of seismic velocity increase. In June, 1989 Mike Purdy and I performed 9 refraction experiments on either side of the ridge on crust 0-3 Ma old; interpretations are in progress.

Reprocessing a multi-channel reflection line across the Juan de Fuca ridge discovered an upper crustal reflector on both sides of the ridge in crust 0-0.4 ma old (Rohr et al., 1988). The reflector is laterally discontinuous on the scale of a kilometer and heterogeneous in stacking velocities. Interval velocities and thicknesses are typically 3000-3500 m/s and 400-1000m respectively, which are similar to definitions of layer 2A by Houtz and Ewing (1976). In October, 1989 this reflection line was extended out to crust 4 Ma old on the JDF plate; preliminary stacks of subsets of the data show strong upper crustal reflectors. For crust 1-3 Ma old interval thicknesses to the reflector are the same as near the ridge, 400-1000m, but interval velocities increase to 4500-5500 m/s. Interval velocities are crude averages of velocity gradients, but I believe the 1000-2000 m/s increase in velocities measured on older sedimented crust is significant. These velocity measurements will be compared to OBS refraction results for a more complete interpretation of velocity structure.

References

Houtz, R. and J. Ewing, Upper crustal structure as a function of plate age, *J. Geophys. Res., v. 31*, p. 2490-2498, 1976.

Rohr, K.M.M., B.Milkereit and C.J.Yorath, Asymmetric structure across the Juan de Fuca ridge, *Geology, v. 16*, p. 533-537, 1988.

INTERPRETING OCEANIC CRUSTAL SEISMIC PROFILES

Dennis A. Lindwall, NOARL, Stennis Space Center, MS 39529

To interpret a velocity profile of a seismic line obtained over 80 Ma old Pacific crust, I used the measured velocities of samples from three ophiolites (*Salisbury and Christensen*, 1978; *Nichols et al.*, 1980; *Christensen and Smewing*, 1981) and the borehole measured velocities from DSDP site 504B (*Newmark et al.*, 1985a, b; *Salisbury et al.*, 1985). Since this approach relies on the physical properties of the various rock types and ignores the stratigraphic thicknesses of the ophiolites from field measurements, I derived the average stratigraphic thicknesses directly from the velocity-depth solutions.

The BOI ophiolite study of *Salisbury and Christensen* [1978] is used more often than others for making lithological interpretations of seismic profiles (e.g., *Spudich and Orcutt*, 1980a, b; *Au and Clowes*, 1984; *Bratt and Purdy*, 1984) but it has considerably higher velocities for the pillow and dike basalts than the other two ophiolites and the 504B measurements.

Using velocities that are too high for pillow and dike basalts will result in an interpretation that has overly thick pillow and dike layers. The velocity profiles of *Bratt and Purdy* [1984] and *Spudich and Orcutt* [1980a] are very similar to the one presented here and the lithological interpretations based on the BOI velocities give a thickness for the pillows and dikes of about 40% of the total crustal thickness. Using the velocities from the Oman (*Christensen and Smewing*, 1981) and Point Sal ophiolites (*Nichols et al.*, 1980) and from DSDP hole 504B (*Salisbury et al.*, 1985) gives a total thickness of from 1 to 1.3 km for the pillow and dike layers for the velocity profile shown here, 1.3 km for the results of *Bratt and Purdy* [1984], and less than 1 km for those of *Spudich and Orcutt* [1980a].

Rather than relying only on the velocities from the BOI ophiolite, *Spudich and Orcutt* [1980a] argued that the pillow and dike basalt layers should have a high porosity, which raises the Poisson's ratio. Since their Poisson's ratios below 1 km are less than 0.26, requiring low porosity, they concluded that their pillow and dike layers are only 1 km thick, which is much thinner than what a comparison with just the BOI velocities would imply. There is some additional information besides the V_S and V_P values that can be used for assigning lithologies. The zone of zero velocity gradient at 0.7 to 0.95 km depth is certainly not a region of transition from one major division to another. The region with a Poisson's ratio of 0.26 (0.8 to 1.9 km depth) must have low porosity and is probably below the pillow and sheet flow layer.

Based on all of the above arguments, the lithological interpretations derived from the Point Sal and Oman ophiolites and the 504B borehole as shown in the figure are preferred over that from the BOI ophiolite. The interpretations using the 504B, Point Sal, and Oman velocities are very similar to each other, the zone of no gradient (0.7 to 0.9 km depth) is within the sheeted dikes and the area of low Poisson's ratio is below a zone of extensive cracking.

References

Au, D. and R.M. Clowes, Shear-wave velocity structure of the oceanic lithosphere from ocean bottom seismometer studies, *Geophys. J.R. Astr. Soc.*, *77*, 105-123, 1984.

Bratt, S.R. and G.M. Purdy, Structure and variability of oceanic crust on the flanks of the East Pacific Rise between 11 and 13 N, *J. Geophys. Res.*, *89*, 6111-6125, 1984.

Christensen, N.I. and J.D. Smewing, Geology and seismic structure of the northern section of the Oman ophiolite, *J. Geophys. Res.*, *86*, 2545-2555, 1981.

Newmark, R.L., R.N. Anderson, D. Moos, and M.D. Zoback, Structure, porosity and stress regime of the upper oceanic crust: Sonic and ultrasonic logging of DSDP hole 504B, *Tectonophys.*, *118*, 1-42, 1985a.

Newmark, R.L., R.N. Anderson, D. Moos, and M.D. Zoback, Sonic and Ultrasonic logging of hole 504B and its implication for the structure, porosity, and stress regime of the upper 1 km of the oceanic crust, *Initial Reports, DSDP*, *83*, 479-510, U.S. Govt. Printing Office, Washington, D.C., 1985b.

Nichols, J., N. Warren, B.P. Luyendyk, and P. Spudich, Seismic velocity structure of the ophiolite at Point Sal, southern California, determined from laboratory measurements, *Geophys. J.R. Astr. Soc.*, *63*, 165-185, 1980.

Salisbury, M.H. and N.I. Christensen, The seismic velocity structure of a traverse through the Bay of Islands ophiolite complex, Newfoundland, an exposure of oceanic crust and upper mantle, *J. Geophys. Res.*, *83*, 805-817, 1978.

Salisbury, M.H., N.I. Christensen, K. Becker, and D. Moos, The velocity structure of layer 2 at deep sea drilling project site 504 from logging and laboratory experiments, *Initial Reports, DSDP*, *83*, 529-539, Washington, D.C., 1985.

Spudich, P. and J. Orcutt, Petrology and porosity of an oceanic crustal site: Results from wave form modeling of seismic refraction data, *J. Geophys. Res.*, *85*, 1409-1433, 1980a.

Spudich, P. and J. Orcutt, A new look at the seismic velocity structure of the oceanic crust, *Rev. Geophys., Space Phys.*, *18*, 627-645, 1980b.

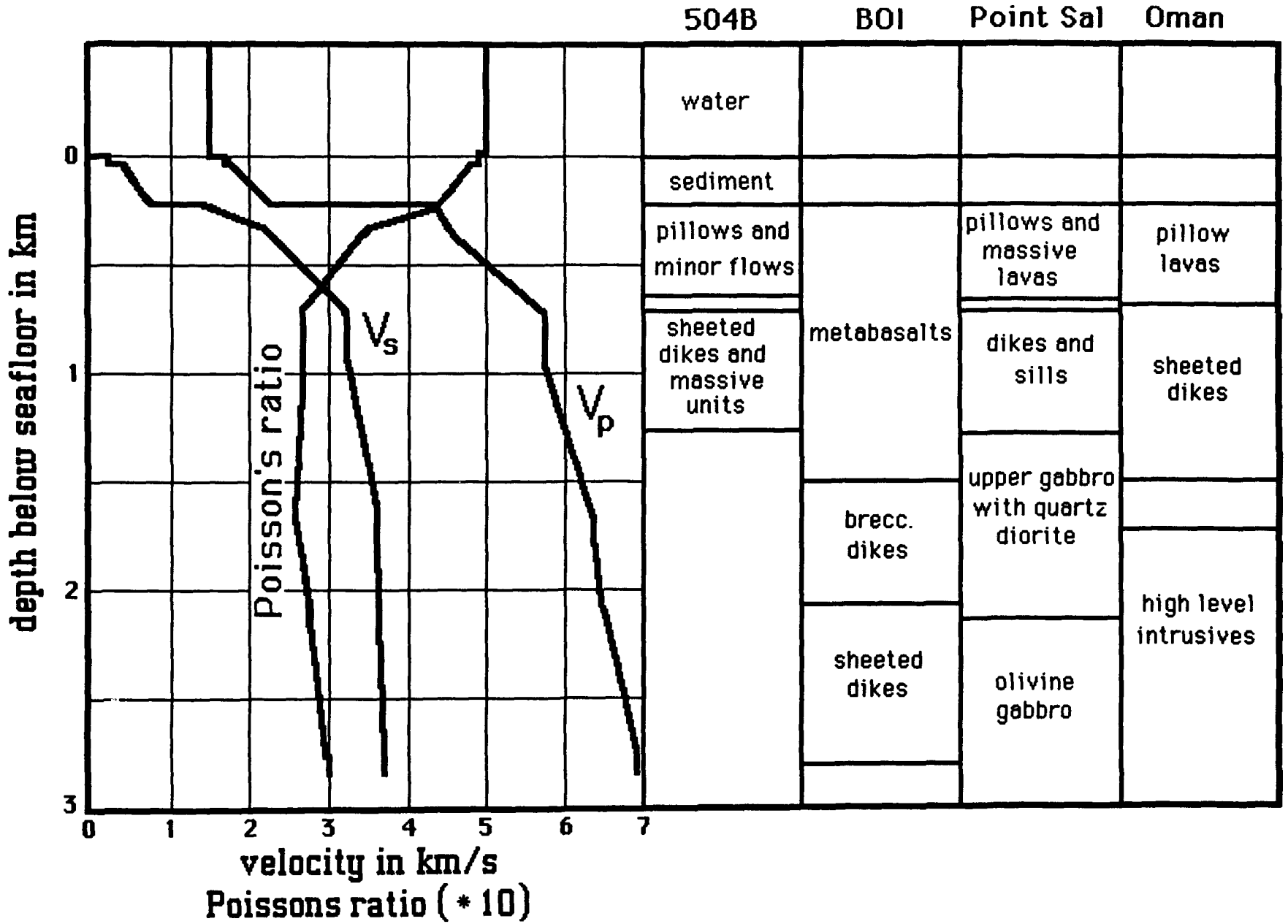
504B
BOI
Point Sal
Oman
water
sediment
pillows and minor flows
sheeted dikes and massive units
metabasalts
brecc. dikes
sheeted dikes
pillows and massive lavas
dikes and sills
upper gabbro with quartz diorite
olivine gabbro
pillow lavas
sheeted dikes
high level intrusives
depth below seafloor in km
0
1
2
3
Poisson's ratio
V_s
V_p
0 1 2 3 4 5 6 7
velocity in km/s
Poissons ratio (*10)

NEAR SURFACE VELOCITY STRUCTURE THROUGH WIDE APERTURE PROFILING

Mary Kappus and Alistair Harding,
Scripps Institution of Oceanography

One of the most interesting questions in marine geophysics concerns the evolution of the upper kilometer of oceanic crust. There has been evidence since 1976 (Houtz and Ewing) that the seismic velocity of the upper crust increases with age, especially within the first 30 million years (Figure 1). Conventional seismic experiments have limited resolution in the upper crust, but experiments using near bottom shots and receivers (i.e., Purdy, 1987) have provided further evidence that over time the upper crustal velocity increases from approximately 2 km/s at the ridge crest to over 4 km/s. Focusing on more recent results from the East Pacific Rise (EPR), both tomographic analysis of Ocean Bottom Seismometer data at 12°50' N (Toomey et al., 1989) and Expanding Spread Profiles (ESP's) at 9°30' N (Vera et al., in press) have been interpreted as showing upper crustal velocities which initially decrease with increasing age. However, ESP's at 13° N (Harding et al., 1989) do not reveal this systematic variation. A hypothesis for age-dependent variation is that velocities initially decrease off-axis as the crust faults and cracks; then as hydrothermal circulation fills in the cracks the velocities increase. The lack of this systematic pattern at the 13° N site does not necessarily invalidate this interpretation, but may indicate that the processes of cracking and infilling trade off in a complicated way. Variations in velocity structure along axis have been related (Macdonald et al., 1984) to segmentation of magma supply and distribution. The degree of homogeneity along strike of the upper crust has direct relevance to continuity of the underlying processes.

The current tomographic data does provide two-dimensional structure, but the vertical resolution is limited to about 1 km. The ESP data are high quality with a vertical resolution on the order of 50m in the upper crust, but the experimental geometry images only one location on the seafloor, and therefore provides no measure of the degree or scale of along-axis variability. Bridging the gap between these two techniques is the Wide Aperture Profile (WAP), initially described by Stoffa and Buhl (1979). The WAP synthesizes a large aperture array by using two ships, one of which tows a multichannel streamer. Figure 2 shows that the two ships maintain a constant separation of twice the streamer length and alternately act as the source ship. At steaming speeds of 5 kts and a 1 minute shot interval, the WAP method provides full-fold midpoint reflection spacing of approximately 300m, and rapidly yields continuous coverage of long sections of seafloor. A single experimental leg generates a sufficiently large number of independent profiles that questions about the variability of the crustal velocity structure can be addressed in a statistically meaningful way. The effectively double-length streamer when used in conjunction with a properly-tuned source array can provide better resolution in the upper crust than either conventional multichannel or OBS experiments. The drawbacks of the WAP experiment are related to the local bathymetry and the accuracy with which it is known. Rough topography invalidates the implicit plane-layer assumption of common-depth-point (CDP) gathers, and increases the likelihood of side-swipe arrivals. Given the precision to which we desire to know the shallow structure, the usefulness of WAP shooting is restricted to intermediate to fast spreading ridges, such as the East Pacific Rise, where the bathymetric relief is relatively small and the data are sufficiently free from out-of-plane energy.

In 1985 a consortium of three institutions collected data at both 9° and 13° N on the EPR in conventional, ESP and WAP geometries (Detrick et al., 1987). The ESP's have

given excellent results (Harding et. al, 1989, and Vera et al., in press) for crust from 0 to 180 ka., as shown in the consolidated velocity-depth profiles for 13° N in Figure 3. In the WAP experiments, the data had offsets from approximately 0.3 - 5.0 km (twice the aperture of the 2.35 km streamer), with a trace spacing of 50m and a midpoint spacing for CDP gathers of 50m. The WAP data consistently recorded a continuous P wave refraction arrival from its separation from the water wave, through a triplication caused by a 100-200m thick layer 2A, and out to the maximum offset of the data, which corresponded to a turning depth of approximately 700m. Figure 4 is an example of the data from 50 ka. crust. By assuming local lateral homogeneity, each synthesized CDP gather can be inverted to create a velocity profile of the upper crust with a spacing comparable to the CDP spacing.

First stages of the processing addressed the degree to which layer 2A and 2B velocity variations are resolvable. The WAP data were processed as a series of ESP's with limited offset or as CDP gathers with expanded offset, which assumes a locally horizontally layered crust. This was a reasonable assumption for the rise axis and for the flatter portions of the horst and graben structures that characterize the off-axis topography. For the sections of the off-axis data where topographic variations on the scale of 100 meters invalidated the assumption, this approach did not always yield results which could be reliably analyzed. We developed a standardized processing sequence in order to efficiently handle the large quantity of data. Individual shots were predictively deconvolved and in some cases the source wavelets were waveshaped so as to better match the different sources of the two ships. The data were then resorted into conventional CDP gathers. Along the ridgecrest line a 300 meter bin size gave a complete 96 trace gather from 0.28 to 5 km with adequate signal to noise ratio. The rougher off-axis topography and lower signal to noise ratio of the data necessitated vertical stacking of 6 adjacent gathers forming a 1500m bin spacing. On the assumption that the underlying structure closely mirrors the seafloor topography, we made small static shift corrections to the off-axis gathers to line up the water bottom reflection. Tau-p stacking and travel time inversion of the data have provided initial estimates of the layer 2A and 2B velocities as well as the thickness of layer 2A. Along axis the velocities vary by less than 5%, with layer 2A at 2.45 km/s and 2B at 5.35 km/s. Variations off-axis are greater, but by 180 ka. the layer 2A velocities approach 3 km/s and layer 2B 5.7 km/s (Figure 5).

The amplitude-offset behavior of the data contain more information about the fine-scale structure than can be modelled from the travel-times alone. This is particularly true of the behavior of the triplication associated with the transition between layer 2A and 2B. Exploiting this information requires an automated method of generating velocity models that closely match the recorded waveforms. One means of achieving this is to use a Monto Carlo method of model generation combined with waveform inversion (Cary & Chapman, 1988) to rapidly test and select from a suite of starting models. These refined models will better constrain the limits on velocity variations estimated from the initial processing. Any method based on CDP gathers avoids tackling the problems associated with bathymetry, a problem that is compounded by the shallowness of subbasement target structure compared to the water depth. While CDP gathers can be reasonably successful for along-axis lines, the variability in depth on cross-axis lines almost certainly requires a different approach that directly constructs a 2-D velocity model directly from the shot gathers using, for example, a refraction tomography approach.

The results of the WAP-geometry experiment are proving useful in extending results from more spatially-limited investigations and show potential for characterizing variations both along-axis and with respect to age. Future experiments could collect higher quality data if targeted explicitly at investigating the upper crustal structure. Airgun arrays could be designed specifically for the upper structure with a broader frequency spectrum and a

reduced bubble pulse. The sources on the two ships should be matched with better control over towing depths and separation to ensure a consistent, known signal. A longer streamer such as that available on the R/V Bernier, would extend the length of the layer 2B refraction recorded and would also provide better amplitude-offset constraints on seafloor reflection coefficients. An experiment designed to specifically study the crustal aging process would obviously increase the maximum crustal age surveyed. WAP data does not offer the horizontal or vertical spatial resolution achievable with a combination of near bottom seismic sources and receivers, but is the most promising method of profiling variations in upper crustal structure created at intermediate to fast spreading ridges.

References

Detrick, R.S., P. Buhl, E. Vera, J. Mutter, J. Orcutt, J. Madsen and T. Brocher, Multi-channel seismic imaging of a crustal magma chamber along the East Pacific Rise, *Nature, 326*, 35-41, 1987.

Harding, A.J., J.A. Orcutt, M.E. Kappus, E.E. Vera, J.C. Mutter, P. Buhl, R.S. Detrick and T.M. Brocher, Structure of young oceanic crust at 13° N on the East Pacific Rise from expanding spread profiles, *J. Geophys. Res., 94*, 12163-12196, 1989.

Houtz, R. and Ewing, J., Upper crustal structure as a function of plate age, *J. Geophys. Res., 81*, 2490-2498, 1976.

Macdonald, K.C., J. Sempere and P.J. Fox, East Pacific Rise from Siqueiros to Orozco fracture zones: along strike continuity of axial new volcanic zone and structure and evolution of overlapping spreading centers, *J. Geophys. Res., 89*, 6049-6069, 1984.

Purdy, G.M., The variability in seismic structure of layer 2 near the East Pacific Rise at 12° N, *J. Geophys. Res., 87*, 8403-8416, 1982.

Stoffa, P.L. and P. Buhl, Two-ship multichannel seismic experiments for deep crustal studies: expanded spread and constant offset profiles, *J. Geophys. Res., 84*, 7645-7660, 1979.

Toomey, D.R., G.M. Purdy, and S.C. Solomon, Three-dimensional seismic structure of the East Pacific Rise at 9° 30' N, *EOS, 70*, 1317, 1989.

Vera, E.E., J.C. Mutter, P. Buhl, J.A. Orcutt, A.J. Harding, M.E. Kappus, R.S. Detrick and T. Brocher, The structure of 0- to 0.2 m.y. old oceanic crust at 9° N on the East Pacific Rise from expanded spread profiles, *J. Geophys. Res.*, in press, 1990.

Figures

1. Measured velocities from acoustic basement plotted as a function of crustal age. From Houtz and Ewing (1976).

2. Geometry of Wide Aperture Profile (WAP) experiment. Two ships steam in the same direction maintaining constant separation of approximately twice the hydrophone streamer length. The ships alternate shooting, timed to image adjacent sections of the seafloor. At time 0 the ships are shown in white; the ship C acts as the source and records arrivals at ranges typical of multichannel reflection work. When the ships reach the position indicated by the shaded profiles, the ship W acts as source, and the streamer records the arrivals at wide aperture.

3. Comparison of upper crustal velocity models for the ESP's from 13° N with the Fanfare 2 model of Spudich and Orcutt. From Harding et al. (1989). The shallow low velocity layer is resolved by the ESP's.

4. A typical WAP gather from 50 ka crust at 13° N on the EPR. The P wave refraction emerges from the water wave at approximately 3.75 km, but can be traced back to the triplication at approximately 2.75 km behind the water wave.

5. Compilation of layer 2A and layer 2B velocities from 3 parallel WAP's at 0, 50 and 180 ka. The spread in values increases with age due to the rough topography. There is a slight trend toward increasing velocity with age, although it is not statistically significant in layer 2B. Further refinement in velocity models is needed to put tighter bounds on the velocity variations.

Houtz and Ewing: Upper Crustal Structure

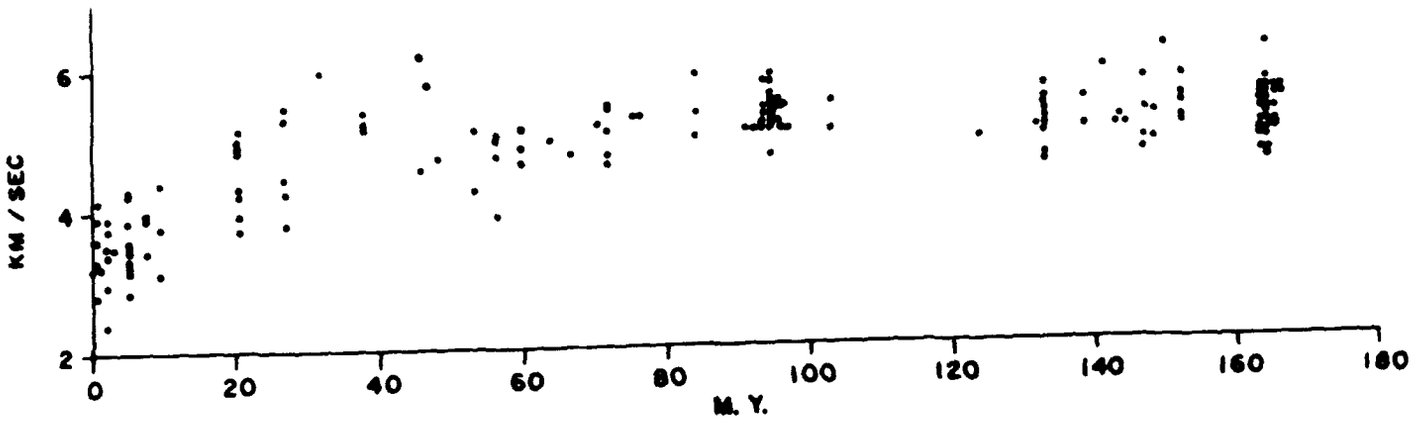

Figure 1

GEOMETRY OF WIDE APERTURE PROFILE EXPERIMENT

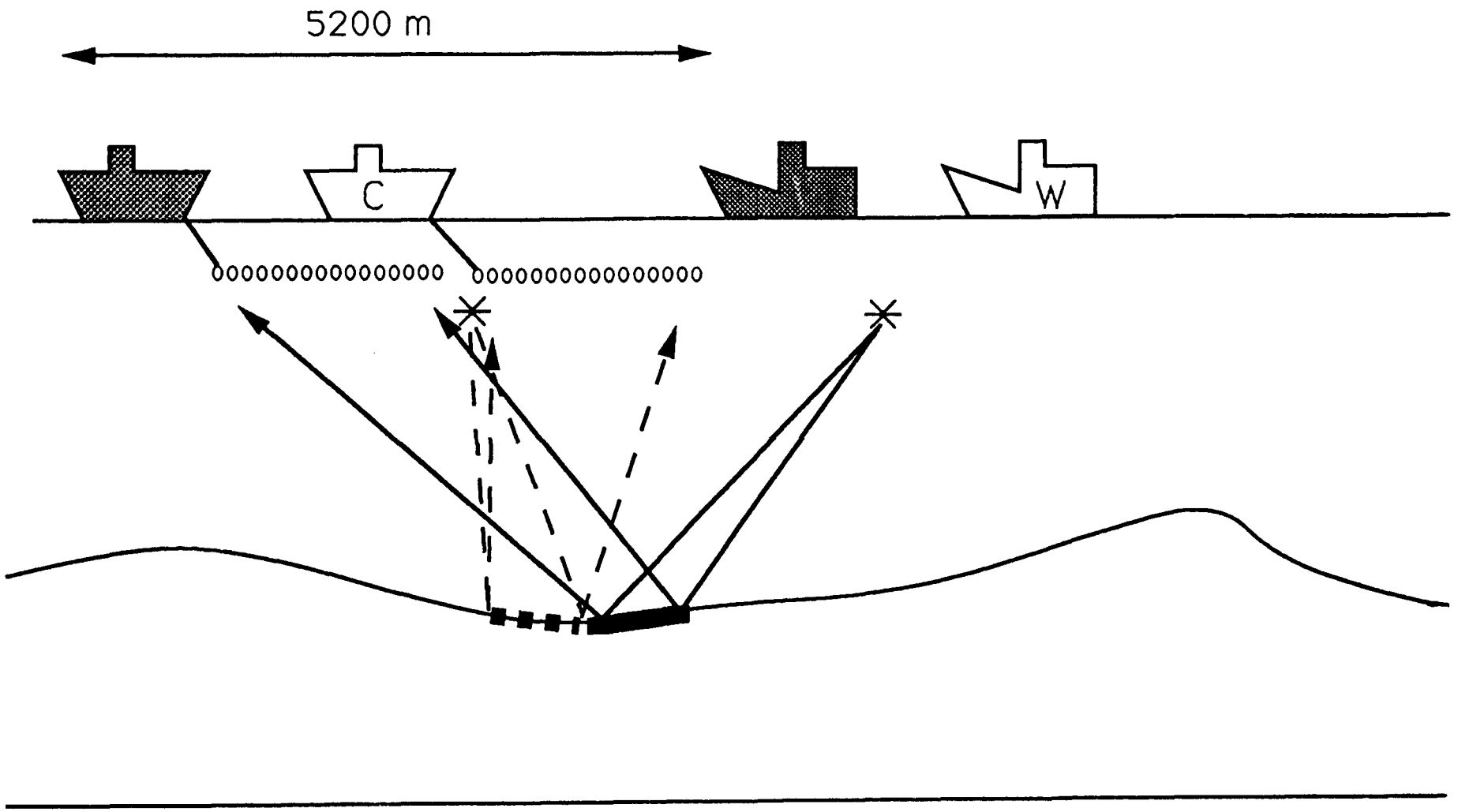

Figure 2

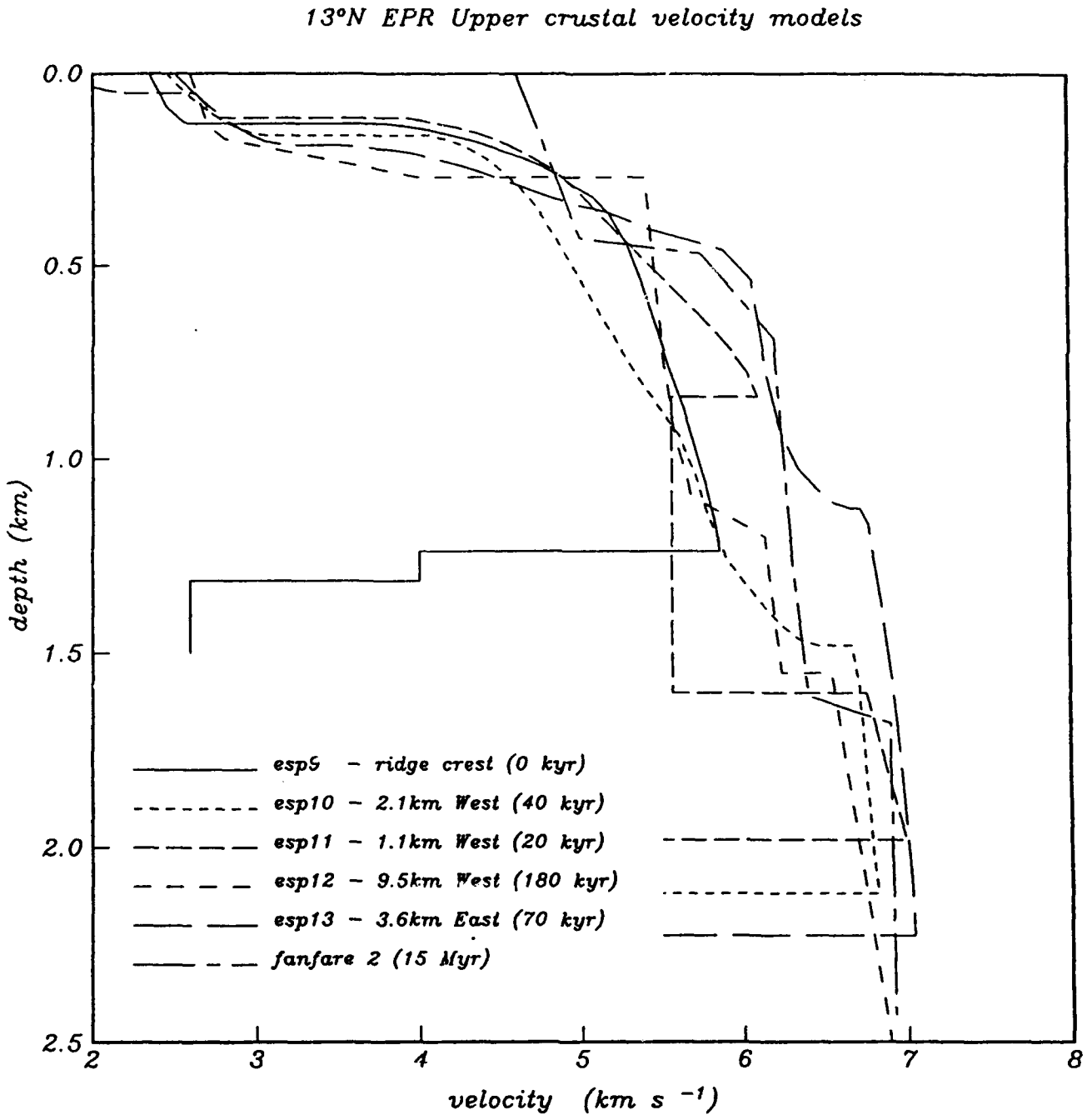
13°N EPR Upper crustal velocity models
0.0
0.5
1.0
1.5
2.0
2.5
depth (km)
2
3
4
5
6
7
8
velocity (km s $^{-1}$)
esp9 - ridge crest (0 kyr)
esp10 - 2.1km West (40 kyr)
esp11 - 1.1km West (20 kyr)
esp12 - 9.5km West (180 kyr)
esp13 - 3.6km East (70 kyr)
fanfare 2 (15 Myr)

Figure 3

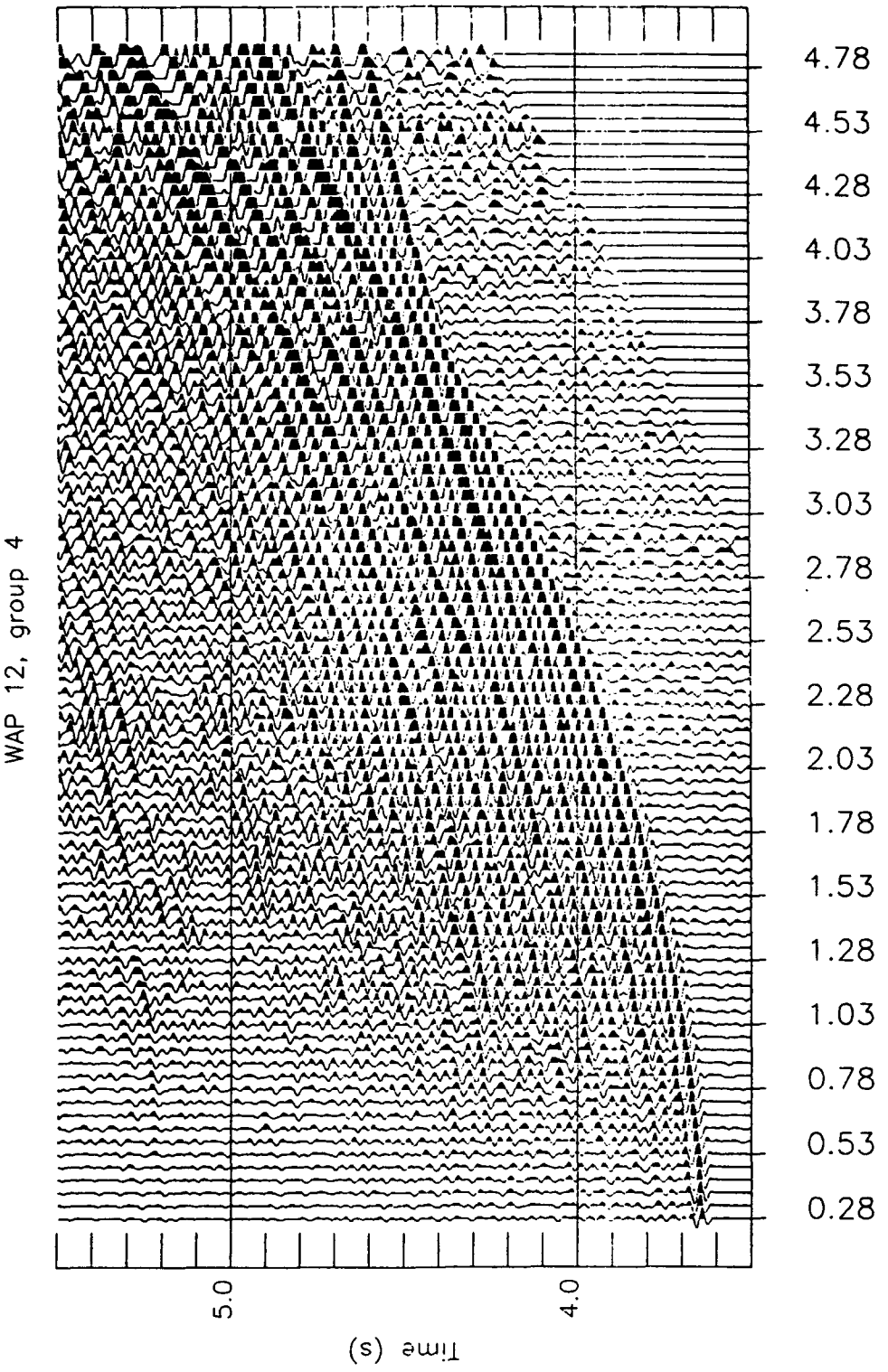
WAP 12, group 4
4.78
4.53
4.28
4.03
3.78
3.53
3.28
3.03
2.78
2.53
2.28
2.03
1.78
1.53
1.28
1.03
0.78
0.53
0.28
Range (km)
5.0
4.0
Time (s)

Figure 4

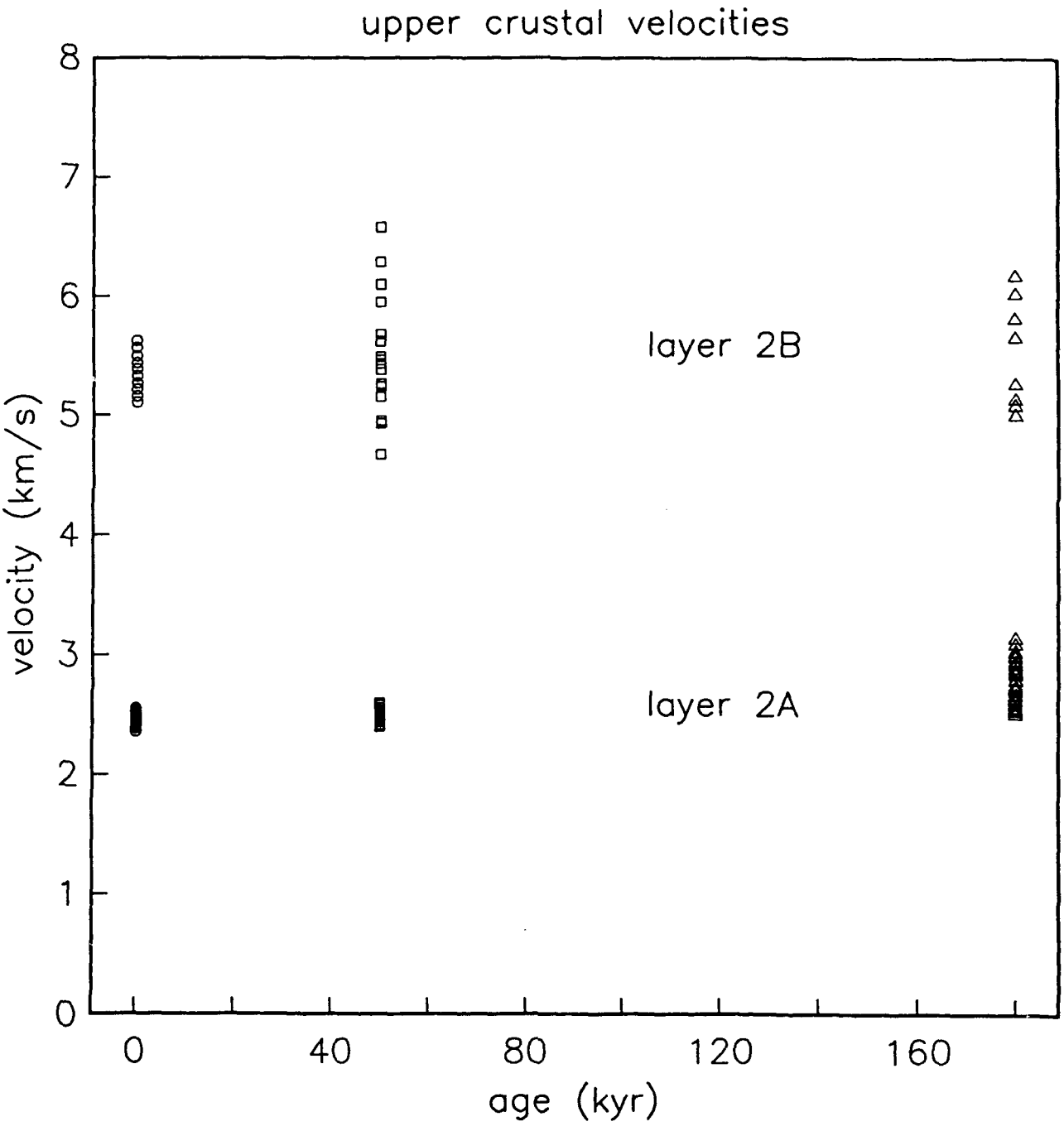
upper crustal velocities
velocity (km/s)
age (kyr)
layer 2B
layer 2A
0
1
2
3
4
5
6
7
8
0
40
80
120
160

Figure 5

MULTICHANNEL SEISMIC REFLECTION OBSERVATIONS OF THE UPPERMOST CRUST NEAR THE EAST PACIFIC RISE

G.A. Barth
Lamont-Doherty Geological Observatory
Palisades, NY 10964

The 1985 East Pacific Rise multichannel seismic experiment collected over one thousand kilometers of single ship multichannel reflection data between 8°50'N and 13°30'N over crust from zero-age to 1.4 Ma. These data have a maximum source-receiver offset of 2.4 km. Two events are identified within these data that pertain to the uppermost several hundred meters of the young oceanic crust.

The first event is a reflection from a horizon located approximately 180 to 240m below the volcanic seafloor. This event is not always clearly present within the single ship CDP gathers. Where observed, it occurs near the first bubble pulse multiple of the seafloor, .15 to .2 seconds (two-way travel time) below the primary seafloor reflection. Where measured, on crust of 1.4 my age, the interval velocity from the seafloor to this event is between 2.35 and 2.45 km/sec. These results are in agreement with recent results derived from the larger-offset portions of the same 1985 experiment, which indicate very low compressional velocities in the upper several hundred meters of seafloor followed by a steep velocity gradient (Harding et al., 1989; Vera, 1989; Kappus et al., 1989). The reflection results indicate that this gradient may sometimes be steep enough to act as a velocity discontinuity, producing reflections even at vertical incidence.

The second event has been labeled 'frozen top' by Detrick et al. (1987). It is the image of a steep velocity gradient (Vera, 1989) located approximately 1.35 to 1.6 km below seafloor. It is a low amplitude event having a lower frequency content than expected based on the attenuation estimates of Vera (1989) and Harding et al. (1989) for the upper crust. This characteristic is consistent with the identification of the horizon as a region of steep velocity gradient rather than a velocity discontinuity. The location of this event in the seismic sections is remarkably regular, occurring between .55 and .6 seconds below seafloor in crust created between 20 ky and 1.4 my ago (Barth et al., 1989). There is no evidence to support coincident changes in velocity and thickness to maintain constant travel time despite variable seismic or geologic structure. In the axial region, the 'frozen top' event is always located at or above the level of the axial magma chamber top (AMC) event. It is hypothesized that the event marks the brecciated to unbrecciated boundary in the upper crust (Vera, 1989), or the maximum depth of water penetration above the active magma body. This may in turn be controlled by the depth of neutral buoyancy of the magma itself, which would be approximately constant over time (Ryan, 1987). Regardless of the process which creates the 'frozen top' horizon, its nearly constant position in the seismic sections indicates noteworthy regularity in the seismic and geologic structure of the upper 1.5 km of crust in this study area.

References:

G.A.Barth, J.C.Mutter, P.Buhl, E.E.Vera, and J.A.Madsen, Spatial and Temporal Variations in Crustal Accretion Processes at the East Pacific Rise, *Eos Trans. AGU., 70*, 1307, 1989

R.S.Detri P.Buhl, E.Vera, J.Mutter, J.Orcutt, J.Madsen, and T.Brocher, Multi-channel Seismic Imaging of a Crustal Magma Chamber Along the East Pacific Rise, *Nature, 326*, 35-41, 1987

A.J.Harding, J.A.Orcutt, M.E.Kappus, E.E.Vera, J.C.Mutter, P.Buhl, R.S.Detrick, and T.M.Brocher, Structure of Young Oceanic Crust at 13°N on the East Pacific Rise from Expanding Spread Profiles, *J. Geophys. Res., 94*, 12163-12196,1989

M.E.Kappus, A.J.Harding and J A.Orcutt, Upper Crustal Velocity Variations at 13°N on the East Pacific Rise, *Eos Trans. AGU., 70*, 1317, 1989

M.P.Ryan, Neutral Buoyancy and the Mechanical Evolution of Magmatic Systems, in Magmatic Processes: Physicochemical Principles (ed B.O.Mysen), *Geochemical Society Special Publication No.1*, 1987

E.E.Vera, *Seismic Structure of 0- to 4.5-my old Oceanic Crust Between 9°N and 13°N on the East Pacific Rise*, PhD Thesis, Columbia University, 1989

COMPRESSIONAL AND SHEAR WAVE VELOCITIES IN THE UPPER CRUST

Orest Diachok, Stephen Wales, Ronald Dicus, Fred Feirtag, David Shirley and John Siegel
Naval Research Laboratory, Code 5120
Washington, DC 20375-5000

ABSTRACT. New reflectivity vs. grazing angle data at a number of thinly sedimented sites in the Pacific Ocean spanning 0.5 to 64 m.y. reveal that compressional and shear wave velocities, V_p and V_s of the uppermost crust increase with geologic age. Measurements between 40 and 64 m.y reveal compressional and shear critical angles of 60±3° and 9°±3° respectively. The corresponding compressional and shear speeds are 3090±300m/s and 1564±15 m/s respectively. The relatively high estimated shear speeds are in sharp contrast to inferred shear speeds in 0.5 m.y. old crust, viz., 800 m/s, whereas the estimated compressional speeds in the older crust only slightly exceed V_p in young crust, which is about 2400 m/s.

1. Introduction

Bottom interacting acoustic fields at small grazing angles in the deep ocean are primarily dominated by sediment-refracted energy when the sediment thickness is greater than about 100 meters, [1-4] and to a large extent by the upper crust when the sediment thickness is below about 100 meters. Consequently, detailed knowledge of upper crustal geoacoustic properties is essential for acoustic field prediction in thinly sedimented regimes. These include seamounts, substantial areas in the vicinity of mid-ocean ridges, and most significantly the majority of the Pacific Ocean.

Unconsolidated sediments on the ocean floor originate primarily from land (terrigenous), volcanoes and deceased oceanic plants and animals (pelagic). Deep trenches surrounding the Pacific Ocean limit terrigenous sediments from flowing into this ocean. As a result the mean sediment thickness in the central North Pacific is low, generally below 100 meters (based on Lamont-Doherty Geophysical Observatory data contoured by B. Hersey)[5]. Exceptions occur in areas in close proximity to land and volcanoes, and in the high biological productivity zone near the equator. As seismic-acoustic properties of the upper crust are age-dependent, it is noteworthy that the sediment thickness overlying crust as old as 150 m.y. in non-equatorial regions of the western Pacific[6] is generally less than 100 meters.

The most significant acoustic parameter affecting the reflection process at the upper crustal boundary at small grazing angles in the absence of a sediment layer is V_s. If V_s is higher than the speed of sound in water, V_w, then total reflectivity occurs at grazing angles less than the critical angle. This type of behavior is illustrated in Figure 1, where $\theta_s = 9°$. If $V_s < V_w$, then there is no shear critical angle, and nearly total mode conversion to shear waves occurs accompanied by large interfacial reflection losses. In a previous paper[7] the results of a low frequency reflectivity vs. grazing angle experiment conducted at a sediment-free site in the vicinity of the East Pacific Rise (Project ROSE) were documented; estimated V_p was shown to be consistent with a limited set of well-sampled seismic refraction measurements at a near-by site[8]. The following conclusion was drawn about the V_s:

> The interfacial V_s in the upper crust at a geologically young, sediment-free Pacific site, was estimated to be 800 m/s, substantially lower than V_w.

This estimate, which is based on single hydrophone data, should be considered a lower bound. Array measurements of the coherent component of the reflection coefficient would probably have resulted in lower reflectivity at small grazing angles and higher inferred V_s.

All of the data analyzed in this paper are limited to the Pacific, where rms roughness is relatively small, to minimize effects of roughness on the reflection coefficient. The conclusions, however are expected to be applicable to other oceans.

The objectives of this paper are to: 1) describe new measurements of the coherent component of the reflection coefficient vs. grazing angle and inferred V_p and V_s in older crust (40-64 m.y.) for comparison with previous measurements in very young crust; and 2) discuss the implication of these results on acoustic field prediction in thinly sedimented regions of the world's oceans.

In Section 2 of this paper the age dependence of interfacial V_p and V_s in thinly sedimented regions of the Pacific will be summarized. In Section 3 results of the reflectivity experiments will be described. Effects of boundary roughness and a thin sediment layer will be considered in Sections 4 and 5, respectively. Reflectivity data will be presented and discussed in terms of critical angles in Section 6. Wave field prediction will be considered in Section 7. Conclusions and recommendations for future research are outlined in Section 8.

2. The Nature of the Upper Crust

The upper crust is formed at mid-ocean ridges and is transported over periods of millions of years to great ranges. Over this period the density and velocities of the solid basalt component of this medium, measured on dredged samples from sediment-free sites at high frequencies and high pressures[9], decrease as a result of chemical alteration. Aging makes this material progressively "softer". Recently formed crust is cracked and porous. As it ages the cracks and pores are thought to be filled primarily by calcite and sediments from above and to limited extent by minerals brought from below by circulating water.

As a result of these effects, the effective low frequency seismic properties of this composite are age-dependent. Estimates of the effective interfacial V_p in thinly sedimented regions of the Pacific Ocean, extrapolated from well sampled seismic refraction data[10-13] and inferences from far field reflectivity vs. angle measurements (to be subsequently discussed in this paper), are shown as a function of geologic age in Figure 2. Since V_p and V_s may be anisotropic, data shown in this figure are restricted to measurements made parallel to the ridge, hypothetically the high speed direction. Excluded from this compilation are measurements made at ridge crests, fracture zones, thickly sedimented sites, near seamounts and those characterized by a low sampling rate. The data shown here suggests that V_p and V_s increase with crustal age, hypothetically due, at least in part, to the filling of cracks and pores.

The variance ΔV_p, of young crust has been estimated by Toomey et. al[10] to be less than or approximately equal to $\pm$ 10%; the corresponding correlation lengths normal and parallel to the axis were estimated to be approximately 2 and 6 km respectively. These lengths are comparable to bathymetric correlation lengths of Pacific abyssal horsts (hills).

3. Reflectivity Measurements

New reflectivity vs. grazing angle measurements were made at 12 sites over the age range 40 to 64 m.y. The sediment thickness, measured with a water gun, was estimated to be less than 40 meters at all sites. To minimize scattering due to roughness all measurements (reported here) were made parallel to the dominant horst-graben structure. Sea-beam maps

were recorded to reveal seamount locations. The rms roughness, determined from the Sea-beam profiler, will be discussed in Section 4. The acoustic signals were detected on a 1100 m long array of hydrophones towed broadside to the propagation path at a depth of 300 m from the Canadian research ship, CFAV Endeavour. Standard Mk 61 2 lb. underwater explosives were dropped from the USNS Desteiger every two degrees (grazing angles) and detonated at a depth of 240 m.

The data was tape recorded over a 5-300 Hz bandwidth and subsequently processed on a single hydrophone and coherently added (beamformed) to provide estimates of the total energy and the coherent component of the reflection coefficient vs. grazing angle. The data were filtered in third octave bands. Only the data centered around 8 Hz will be presented in this paper. After beamforming, reflection coefficients were computed essentially as described in reference 7. Details of the processing are described elsewhere.[14]

Prior to presentation and interpretation of the data, two effects which may confound the identification of critical angles will be discussed, viz. bottom roughness and the thin sediment layer.

4. Effects of Boundary Roughness

Scattering loss from a Gaussian randomly rough surface, a reasonable approximation for the basalt boundary[7], may be simply described and readily implemented with a theory developed by Eckart.[21] According to this theory, scattering loss obeys the relationship:

$$R = e^{-g2}$$

where R = coherent energy reflection coefficient, $g = 2kr \sin \theta$, k = wave number, r = rms roughness, and θ = grazing angle. This model is considered applicable provided $r < \lambda << L$, where λ = wavelength, r = rms roughness and L = correlation length. For the experimental sites reported here, these parameters were derived from the Sea Beam vertical profiling beam. The data was spatially averaged over about 50 km, thereby encompassing many abyssal hills. The resultant $r \approx 50$ m and $L \approx 2000$ m. At 8 Hz, $\lambda = 191$ m. Consequently, the Eckart equation is considered reasonable for this application.

According to this model the scattering loss in the vicinity of the compressional and shear critical angles is about 5 and 1 dB respectively. Consequently scattering effects may be expected to be significant for estimation of θ_p and negligible for estimation of θ_s.

5. Effects of a Thin Elastic Sediment Layer

A thin sediment layer, generally less than 100 m, overlies the upper crustal boundary in the Northeast Pacific. Such sediment layers are known to be spatially variable in thickness (nominally ± 50%) on a scale of about 2 km normal and 6 km parallel to the dominant horst-graben structure. The approximate V_p and V_s values of this medium are 1550 and 150 m/s respectively.

Reflectivity from the flat boundary of a fast (V_s = 2500 m/s) elastic solid covered by a thin horizontally stratified elastic sediment layer has been theoretically investigated by Hawker[18-19] and Vidmar[20-22]. Vidmar demonstrated that a thin elastic layer can diminish the reflection coefficient by a few dB in the angular range $\theta_s < \theta < \theta_p$, and by tens of dB when $\theta < \theta_s$ at frequencies as low as 10 Hz. In contrast, a thin fluid sediment layer produced essentially no effect.

Hawker demonstrated that at sufficiently high frequencies, when $\lambda << H$ where H is the sediment thickness, the angle of the reflection minimum corresponds to mode conversion (according to Snell's law) of compressional to Stoneley waves at the sediment-rock interface. At lower frequencies (where λ is comparable to H) the reflection minimum persists, but shifts to smaller grazing angles than predicted by the Stoneley wave phase speeds.

When V_s is only slightly greater than V_w, e.g., when $V_w < V_s < 1600$ m/s, the interference minimum disappears, and the reflection process becomes transparent to the sediment layer. In older crust[13], where V_s may be as high as 2400 m/s, interference nulls due to the thin sediment layer will undoubtedly affect the reflectivity, and thereby complicate estimation of the shear speed.

6. Estimation and Interpretation of V_p and V_s

At the compressional critical angle θ_p the theoretical plane wave specular reflection coefficient equals unity in the absence of a thin sediment layer or rough boundary scattering. Rough boundary scattering and spherical wave effects diminish and angularly broaden the compressional critical angle peak.

Calculations that incorporate these effects agreed reasonably well with previously reported measurements on a single hydrophone at 0.5 m.y. old sediment-free site. A comparably comprehensive data-theory comparison of the new measurements does not appear to be necessary for identification of critical angles. Measurements made at the 58 m.y. site, shown in Figure 1, clearly reveal compressional and shear critical angles at 59° and 9° respectively.

Inspection of critical angle measurements made at other sites in the 40-64 m.y. age range yields compressional and shear speeds graphically displayed in Figure 2. The relatively large scatter in V_p may be attributed to 1) real spatial variability (Toomey et al. estimated that $\Delta V_p < 10\%$ on a scale of 2 and 6 km along and across strike respectively in the vicinity of the East Pacific Rise), and 2) the mean slope of reflecting surfaces, averaged over a Fresnel Zone. A 1° departure from the horizontal translates into a 2° error in the critical angle measurement. The radial and transverse Fresnel zone dimensions in the vicinity of θ_p are nominally 1 km x 1 km, which are small compared to the correlation lengths of the horst and graben geometry (6 and 2 km in the radial and transverse directions). Consequently significant contributions to ΔV_p may be expected from both effects. The radial and transverse Fresnel zone dimensions in the vicinity of θ_s are nominally about 3 and 18 km respectively, which are relatively large compared to the correlation lengths of V_s and the geometrical structure resulting in spatially averaged (over about 6 "grains") estimates of V_s. Consequently, the contributions of the two effects to the variance in the shear speed are relatively small. The difference in the measured variances in V_p and V_s is also due in part to the low sensitivity of V_s to θ_s at small angles, and the high sensitivity of V_p to θ_p at large angles. Although it is not clear from Figure 2, V_s increases slightly, viz. from 1560 to 1580 m/s over the age range 40-64 m.y. In view of the variance in V_s and the small number of samples, this trend may not be significant.

7. Acoustic Field Prediction

The angular region over which bottom interacting rays (modes) are required for acoustic field prediction is dependent on the amplitude, phase and coherence of reflected signals. Conditions under which the reflectivity and spatial coherence are high, and the phase may be expected to be predictable, occur at angles less than the shear critical angle in the 40-64 m.y. age range. At sufficiently low frequencies the reflectivity, coherence, and phase predictability is hypothetically high due to diminished rough boundary scattering losses and thin layer effects. In young crust ($\lesssim$ 20 m.y.) the lack of a shear critical angle diminishes the

need for incorporating bottom interacting modes in acoustic field prediction. In much older crust interference effects due to the thin sediment layer will probably unpredictaoly scramble the phases of modes that interact with the crust at small grazing angles.

8. Conclusions

Reflectivity vs. grazing angle data at a number of thinly sedimented sites spanning 0.5 to 64 m.y. reveal that compressional and shear speeds of the upper-most crust increase with geologic age, hypothetically a result of crack filling. Measurements between 40 and 64 m.y. reveal compressional and shear critical angles of 60°±3° and 9°±3° respectively. The corresponding compressional and shear speeds are 3090±300 and 1564±15 m/s respectively. The relatively high shear speeds are in sharp contrast to inferred shear speeds in 0.5 m.y. old crust, viz 800 m/s. The existence of shear critical angles in the older crust implies that prediction of acoustic fields in the ocean at very low frequencies in this age range requires incorporation of bottom interacting modes.

9. Recommendations for Future Research

a) Develop methods for probing the physical properties of both the basalt and the thin sediment layer at small grazing angles where multipath arrivals are not separable using modal decomposition and/or matched field processing. Develop analytical search algorithms for rapidly estimating geo-acoustic parameters.

b) Conduct acoustic sensing measurements of the upper crust with horizontal and/or vertical arrays particularly in ocean crust older than 65 m.y. and younger than 20 m.y. Test theoretical predictions that reflectivity from sufficiently old crust characterized by very high shear speeds (~2500 m/s) is affected by sediment-related interference effects. Refine estimates of the shear speed in young crust with towed array measurements.

c) Experimentally determine the magnitude of sound speed anisotropy, and adapt existing and if deemed appropriate, develop new theories of reflectivity from anisotropic solids.

d) Incorporate effects of sub-bottom refracted modes, including boundary scattering upon re-entry into water.

ACKNOWLEDGEMENTS

This work was supported by the Office of the Chief of Naval Research Geology & Geophysics Program, Code 1125GG, and the AEAS Program, Code 124A. The authors appreciate the encouragement from numerous OCNR program managers, particularly Dr. Randy Jacobson, Mr. Ed Estalot and Dr. Leonard Johnson. The measurements reported here would not have been possible without the strong commitment of the management, and the high level of at sea expertise of the technical staff of the Defense Research Establishment Pacific (DREP). The authors are particularly grateful to Dr. Ross Chapman of DREP for his interest, enthusiasm, technical contributions and commitment to this project.

REFERENCES

1. Hill, M.N. (1952) "Seismic Refraction Shooting in an Area of the Eastern Atlantic", Phil Trans. R. Soc. London A244:561.

2. Morris, H.E. (1970) "Bottom Reflection Loss Model with a Velocity Gradient", J. Acoust. Soc. Am. 48:1198.

3. Dicus, R.L. (1976) "Preliminary Investigations of the Ocean Bottom Impulse Response at Low Frequencies", Naval Oceanographic Office, NSTL Station, MS.

4. Hamilton, E.L. (1980) "Geoacoustic Modeling of the Ocean Floor", J. Acoust. Soc. Am. 68:1313.

5. Spofford, D. (1983) "Blug Overview", Science Applications Inc., McLean, VA.

6. Larson, R.L. and Pitman, W.C. (1985) The Bedford Geology of the World, W.H. Freeman and Co., New York, NY.

7. Diachok, O., Dicus, R. and Wales, S. (1986) "Effects of Upper Crustal Geoacoustic Parameters on Low Frequency Sound", in Seismo-Acoustics, T. Akal and J. Berkson, Plenum.

8. Purdy, G.M. (1982) "The Variability in Seismic Structure of Layer 2 Near the East Pacific Rise at 12°N", J. Geophys. Res., 87, 8403.

9. Christensen, N.I. and Salisbury, M.H. (1973) "Velocities, Elastic Moduli and Weathering - Age Relations for Pacific Layer Basalts", Earth and Plan. Science Let. 19:461.

10. Toomey, D.R. et al. (in press) "The Three Dimensional Seismic Velocity Structure of the East Pacific Rise Near Latitude 9°30".

11. Harding, A.J. et al (1989) "Structure of Young Oceanic Crust at 13°N on the East Pacific Rise from Expanding Spread Profiles", J. Geophys. Res., 94, 163.

12. Vera, E.E. and Mutter, J.C. (1988) "Crustal Velocities in the Rose Area of the East Pacific Rise: One Dimensional Travel Time and Expanded Spread Profiles", J. Geophys. Res., 93, 6635.

13. Shearer, P. and Orcutt, J. (1985) "Anisotropy in the Oceanic Lithosphere - Theory and Observations from the Ngendei Seismic Refraction Experiment in the Southwest Pacific", Geophys. Jr. Astr. Soc. 80:493.

14. Dicus, R.L. et. al, in preparation.

15. Eckart, C. (1953) "The Scattering of Sound from the Sea Surface", J. Acoust. Soc. Am. 25:566.

16. Lonsdale, P. unpublished results.

17. Lonsdale, P. (1977) "Regional Shape and Tectonics of the Equatorial East Pacific Rise", Mar. Geophys. Res., 3, 295.

18. Hawker, K. (1978) "Influence of Stoneley Waves on Plan-Wave Reflection Coefficient: Characteristics of Bottom Reflection Loss", J. Acoust. Soc. Am. 64:548.

19. Hawker, K. (1979) "The Existence of Stoneley Waves as a Loss Mechanism in Plane Wave Reflection Problems", J. Acoust. Soc. Am. 65:682.

20. Vidmar, P. (1980) "The Dependence of Bottom Reflection Loss on the Geoacoustic Parameters of Deep Sea (Solid)Sediments", J. Acoust. Soc. Am. 68:1442.

21. Vidmar, P. (1980) "Ray Path Analysis of Sediment Shear Wave Effects on Bottom Reflection Loss", J. Acoust. Soc. Am. 68:639.

22. Vidmar, P. (1980) "The Effect of Sediment Rigidity on Bottom Reflection Loss in a Typical Deep Sea Sediment", J. Acoust. Soc. Am. 68:634.

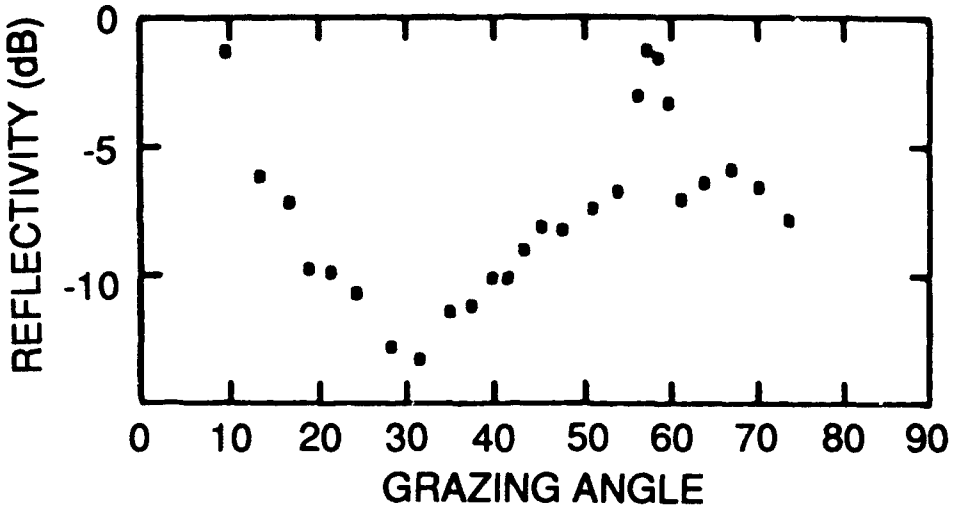

Figure 1. Reflectivity vs grazing angle at 8Hz at 59 m.y. old site

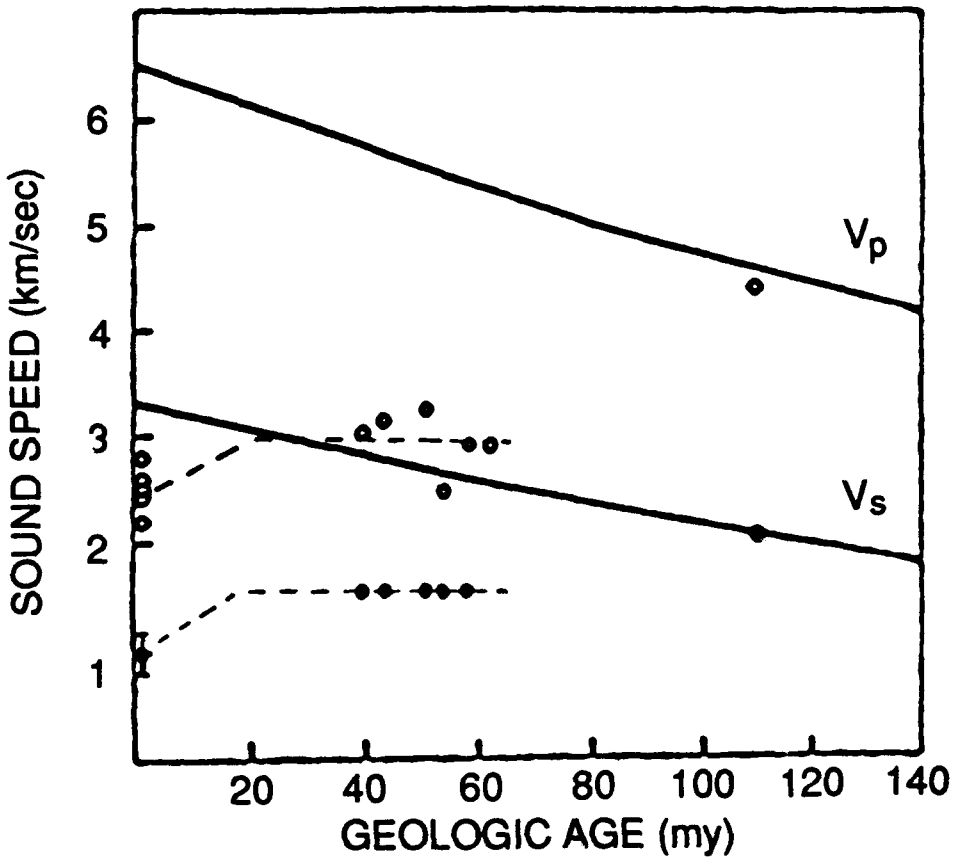

Figure 2. Seismo-acoustic (lower curves and data) and ultrasonic (——) measurements of compressional and shear speeds in sediment-free/thinly sedimented volcanic rock (basalt) vs. geologic age.

Section C4: Physical Properties

1: The Physical Properties of Seafloor Hydrothermal Flow Revealed in Mineralized Veins: Possible Avenues of Research: D.A. Vanko

2: Relationships Between Elastic-Wave Velocities and Morphology Within Oceanic Pillow Basalts: D. Moos, D. Marion

3: Low-Frequency Electrical Properties of MORB: P.A. Pezard

4. Structure of Shallow Basement from Downhole Logs: D. Moos

5. Physical Properties of the Seafloor Exposed at the Hess Deep: J. Hildebrand, L. Dorman

6. Laboratory Physical Properties of a Highly Vesicular Basalt Breccia: K.A. Dadey and the Leg 126 Scientific Party

7. Vertical and Lateral Variations of the Structure of Oceanic Layer 2: R.L. Carlson

8. Evolution of Porosity and Seismic Properties of Shallow Oceanic Crust: R. Wilkens, J. Karsten, G. Fryer

9. Shear Modulus and Porosity Measurements of Deep Ocean Floor: T. Yamamoto, A. Turgut

THE PHYSICAL PROPERTIES OF SEAFLOOR HYDROTHERMAL FLOW REVEALED IN MINERALIZED VEINS: POSSIBLE AVENUES OF RESEARCH

David A. Vanko
Department of Geology, Georgia State University, Atlanta, GA 30303

A major feature of altered oceanic layer 2 is the presence of hydrothermal veins that were formed at high temperature. Recent studies have used petrography and fluid inclusion analysis to document the mineralogy and conditions of origin (temperatures and fluid compositions) of these veins, and their relation to seafloor hydrothermal systems. The dominant vein-filling minerals include quartz, epidote, prehnite, and calcite. Other phases include metal sulfides, actinolite, chlorite, and analcime. A wealth of vein mineralogical data are available from deep-sea drilling (e.g., Bohlke et al., 1981; Alt and Honnorez, 1984; Honnorez et al., 1985; Vanko and Stakes, 1990). More data can be found in studies of dredged or submersible-sampled seafloor rocks. However, detailed studies of vein types, sizes, vein density and vein orientation are lacking. One study that combines vein petrography with a consideration of the hydrodynamics of fluid flow through the original fracture is that of Delaney et al. (1987), which documented fluid flow "in excess of 1 m/s" based on the sizes of rounded pebbles that were apparently carried upward by the flow. Many studies of on-land seafloor rocks do incorporate aspects of vein morphology and mineralogy, e.g., Cathles' (1983) analysis of the Kuroko ore deposits.

One result of investigating the mineralogy and fluid inclusion characteristics of veins is an appreciation of the range of temperatures, pressures, and fluid compositions that one might expect within a "typical" seafloor hydrothermal system. Processes such as the chemical evolution of the seawater fluid (e.g., from a Na-dominant fluid to a Ca-dominant brine; Vanko et al., 1988), possible phase separation of that fluid (e.g., Vanko, 1988), and conductive heat loss within the hydrothermal system (e.g., leading to the precipitation of quartz commingled with massive sulfide; Vanko et al., 1989) have been documented by evaluating fluid inclusion characteristics. The ultimate goal of this line of research is to develop a general model for hydrothermal systems that incorporates each of these processes at their appropriate place and time within the context of the origin, evolution, and extinction of the system.

Certain observations and measurements may be made on veined rock samples that can lead to new constraints for hydrothermal fluid flow models. Mineral textures in veins often show that the minerals grew as the vein became dilated (yielding a cross-fiber texture, for example). This means that the fracture aperture at any particular time could have been substantially less than that obtained by simply measuring the vein width. Veins often occur in small swarms of oriented (subparallel) features, illustrating that fracture permeability may have been significantly anisotropic. Vein density (number of veins per unit length or unit volume) is also a highly variable property. These observables have not been systematically documented, however it is proposed that this type of study could allow one to ask and answer a number of important new questions. The study could be done with samples from the seafloor already in hand, or those archived at the various sample and core repositories.

A more detailed understanding of the life of a seafloor hydrothermal system will lead to a significantly better picture of the spatial variation of different crustal properties. In particular, detailed knowledge of the distribution, density, sizes, and orientations of veins, and how these properties depend on tectonic setting (i.e., spreading rate, position within a spreading segment) will affect the degree to which the seismic and other properties of the upper crust can be understood.

References

Alt, J.C., and J. Honnorez, 1984, Alteration of the upper oceanic crust, DSDP site 417: mineralogy and chemistry. *Contrib. Mineral. Petrol., v. 87*, p. 149-169.

Bohlke, J.K., J. Honnorez, B.-M. Honnorez-Guerstein, K. Muehlenbachs, and N. Petersen, 1981, Heterogeneous alteration of the upper oceanic crust: correlation of rock chemistry, magnetic properties, and O isotope ratios with alteration patterns in basalts from site 396B, DSDP. *J. Geophys. Res., v. 86*, p. 7935-7950.

Cathles, L.M., 1983, An analysis of the hydrothermal system responsible for massive sulfide deposition in the Hokuru Basin of Japan. *Economic Geology, Monograph 5*, p. 439-487.

Delaney, J.R., D.W. Mogk, and M.J. Mottl, 1987, Quartz-cemented breccias from the Mid-Atlantic Ridge: samples of a high-salinity hydrothermal upflow zone. *J. Geophys. Res., v. 92*, p. 9175-9192.

Honnorez, J., J.C. Alt, B.-M. Honnorez-Guerstein, C. Laverne, K. Muehlenbachs, J. Ruiz, and E. Saltzman, 1985, Stockwork-like sulfide mineralization in young oceanic crust: Deep Sea Drilling Project Hole 504B. In Anderson, R.N., J. Honnorez, K. Becker, et al., 1985, *Initial Reports of the Deep Sea Drilling Program, v. 83*, Washington (U. S. Government Printing Office), p. 263-282.

Vanko, D.A., 1988, Temperature, pressure, and composition of hydrothermal fluids, with their bearing on the magnitude of tectonic uplift at mid-ocean ridges, inferred from fluid inclusions in oceanic layer 3 rocks. *J. Geophys. Res., v. 93*, 4595-4611.

Vanko, D.A., R.J. Bodnar, and S.M. Sterner, 1988, Synthetic fluid inclusions. VIII. Vapor-saturated halite solubility in part of the system NaCl-$CaCl_2$-H_2O, with application to fluid inclusions from oceanic hydrothermal systems. *Geochim. Cosmochim. Acta, v. 52*, 2451-2456.

Vanko, D.A., B.J. Milby, and S.W. Heinzquith, 1989, Massive sulfide dredged from a young East Pacific Rise-flank seamount at 14°09'N: petrographic, fluid inclusion, and trace element characteristics. *Trans. Amer. Geophys. Union, v. 70*, p. 494.

Vanko, D.A., and D.S. Stakes, 1990, Fluids in oceanic layer 3: evidence from veined rocks, hole 735B, Southwest Indian Ridge. In Robinson, P., R. Von Herzen, et al., 1990. *Proc. ODP, Sci. Results, 118*: College Station, TX (Ocean Drilling Program), in press.

RELATIONSHIPS BETWEEN ELASTIC-WAVE VELOCITIES AND MORPHOLOGY WITHIN OCEANIC PILLOW BASALTS

D. Moos, D. Marion
Department of Geophysics, Stanford University

Understanding the processes related to creation of the oceanic crust at mid-ocean ridges, and of the changes within the crust as it ages, require precise measurements of in situ porosity and structure. Because of the difficulties of direct measurements of these properties, we have been forced to rely on estimates based on interpretation of seismic velocities. Consequently, the seismic velocities of the oceanic crust have been extensively studied over the last 20 years, first with explosive sources and hydrophones within a few hundred meters of the seawater surface, and later with ocean bottom receivers and finally with both ocean bottom sources and receivers. Unfortunately, the relationship between porosity and velocity is not simple, and porosity cannot be uniquely determined from seismic velocity, especially when only compressional velocity has been measured.

New results [Ewing and Purdy, 1982; Purdy, 1987; Harding et al, 1989; Vera, 1989] suggest that compressional velocities in the top 100-200m of "0-age" crust within the axial valley of the Mid-Atlantic Ridge are as low as 2.5 km/s, and at the East Pacific Rise in crust as old as 4 Ma are as low as 2.35-2.6 km/s with S-wave velocities below 0.8 km/s. These results seem to imply large porosities within very young pillows, accompanied by large changes in pore space distribution in a very short period of time. These new results have since been interpreted using an effective medium approach [Toksöz et al., 1976] based on selective infilling of thin aspect ratio fractures [Fryer and Wilkens, 1988].

A new analysis based on Hertz' contact theory [e.g., Timoshenko and Goodier, 1951] using an approach developed by Digby [1981] to calculate the effective elastic moduli of porous granular materials can explain these data. One advantage of this and of other effective medium models is that they allow simultaneous calculation of V_p and V_s, and therefore both velocities can be used to constrain the results.

The physical model we propose for pillow basalts to explain the in situ velocity variations with depth and age described above is the following. Pillows are initially extruded as discrete bodies and form an aggregate material whose "grains" are the pillows themselves and whose structure is determined by processes occurring within the neovolcanic zone. We will assume that the properties of the basalt within the pillows are adequately described by laboratory measurements, and do not change with age (i.e., progressive alteration does not affect the basalt's intrinsic elastic properties). This is almost certainly incorrect, but the consequence of a small overestimation of the basalt intrinsic properties is much smaller than the primary effects we consider here. The model requires that the seismic wavelength be at least an order of magnitude greater than the size of the pillows. This is reasonable, as a 100 Hz seismic wave travelling at 2.5 km/s has a wavelength of 25m.

The properties of the aggregate are determined simply by the effective length of contact between the pillows. However, this can be difficult to determine, as the morphology of pillows is complicated (see Ballard and Moore [1977]); from these observations the length of the contacts is quite large. However, the outer carapace of the pillows on contact is relatively stiff. Thus although the length of the contact may be large, the surfaces are physically in contact at only a few points, and it is only at these points that stresses are efficiently transmitted. Similar models for the contact area of cracks are common (e.g.,

Gangi [1978]; Walsh and Grosenbaugh [1979]). The first-order model described here similarly does not attempt to account for the presence of radial cracks within the pillows, or of collapse features or empty pillow tubes, both of which are observed in situ.

The initial effective area of contact of the pillows is very small, corresponding to very low velocities. Cementation of the pillows in the first few million years increases the effective contact area by the addition of a very small volume of cementation products, resulting in a rapid velocity increase. Matching Purdy's [1987] data requires a decrease of porosity of 10% over a time period of 7.3 MY. More gradual infilling of pillow voids, modeled using Gassman's [1951] relationship, results in a slow continued velocity increase with age.

Figure 1 compares the results of our model to recent seismic data. The results provide an excellent match between the compressional velocities both at the top of the crust as a function of age and as a function of depth for a given age. For example, at the top of basement compressional velocities of 2.0 to 2.3 km/s and shear velocities of 0.6 to 1.0 km/s are found in material with an initial radius of contact (b/R) between pillows of 0.01 to 0.05. The rapid velocity increase with depth observed by Purdy [1987] below the MAR requires a progressive increase in contact radius with depth independent of the increase due to compaction. Note that with the exception of constraints on shear velocities by Harding et al. [1989], for which our model provides a good match, no shear velocity models have been published to date. However, the model predictions can be compared to future results as they become available. In fact, combined measurements of shear and compressional velocities are required in order to differentiate both between parameter variations in this model, and the various allowable crack aspect ratio distributions used in models such as that of Toksöz et al. [1976].

Although the model we propose matches the seismic data well, it assumes an overly simplistic pillow geometry. Work in progress extends the model to pillows of arbitrary shape, and will provide the opportunity to test the importance of different observed morphologic features such as cracks within pillows on their seismic velocities.

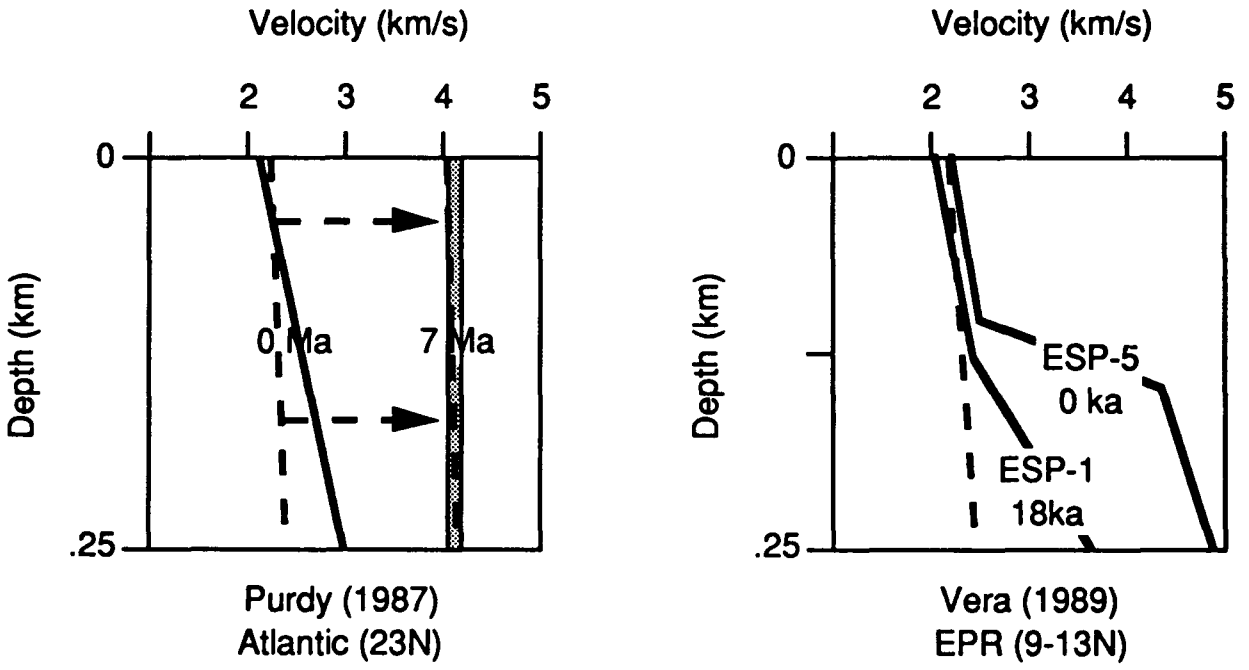

Figure 1: Comparison of velocity-depth profiles (solid lines and shading) to our model predictions (dashed). The arrows illustrate the effect of increased cementation on the velocities. The predictions match both the data from the zero-age EPR and the 7 Ma Atlantic well, but underestimate the zero-age velocity gradient at the MAR. A small increase in cementation with depth would fit the zero-age MAR data.

REFERENCES

Ballard, R.D. and Moore, G.M., 1977. *Photographic Atlas of the Mid-Atlantic Ridge Rift Valley*, Springer-Verlag, New York, 114 pp.

Digby, P.J., 1981. The effective elastic moduli of porous granular materials, *J. App. Mech., 48*, 803-808.

Ewing, J.I. and Purdy, G.M., 1982. Upper crustal velocity structure in the Rose area of the East Pacific Rise, *J. Geophys. Res., 87*, 8397-8402.

Fryer, G.J. and Wilkens, R.H., 1988. Porosity, aspect ratio distributions, and the increase of seismic velocity with age in young oceanic crust, *EOS, Trans. AGU (69)*:1323.

Gangi, A.F., 1978. Variation of whole and fractured porous rock permeability with confining pressure, *Int. J. Rock Mech. Min. Sci., 15*, 249-257.

Harding, A.J., Orcutt, J.A., Kappus, M.E., Vera, E.E., Mutter, J.C., Buhl, P., Detrick, R.S., and Brocher, T.M., 1989. The structure of young oceanic crust at 13°N on the East Pacific Rise from expanding spread profiles, *J. Geophys. Res., 94*, 12,163-12,196.

Timoshenko, S., and Goodier, J.N., 1951. *Theory of elasticity (2nd edn.)*, pp. 372 *ff*, McGraw-Hill, New York.

Purdy, G.M., 1987. New observations of the shallow seismic structure of young oceanic crust, *J. Geophys. Res., 92*, 9351-9362.

Toksöz, M. N., C.H. Cheng, and A. Timur, 1976. Velocities of seismic waves in porous rocks, *Geophys., 41*, 621-645.

Vera, E.E., 1989. *Seismic structure of 0- to 4.5-M.Y.-old oceanic crust between 9° and 13° N on the East Pacific Rise*, PhD. Thesis, Columbia University, New York, NY., 127 pp.

Walsh, J.B., and Grosenbaugh, M.A., 1979. A new model for analyzing the effect of fractures on compressibility, *J. Geophys. Res., 84*, 3532-3536.

LOW-FREQUENCY ELECTRICAL PROPERTIES OF MORB

Philippe A. Pezard
Borehole Research Group of the Lamont-Doherty Geological Observatory.

The extreme sensitivity of electrical properties to a large number of parameters makes electromagnetic methods a powerful technique to study large- and small-scale structures of rock formations. In the oceanic crust, measurements of electrical properties of rocks have covered so far 6 orders of magnitude [Olhoeft, 1981]. In situ, the measurements of electrical resistivity respond to conductivity changes in the rock surrounding the borehole, to the nature of the saturating-fluid and to the influence of crustal stresses. The presence of vesicular pores, cracks and microcracks, either fluid-filled, or plugged with precipitated conductive alteration minerals such as chlorites, zeolites, and smectites creates a path for current flow. In tholeiitic basalts, the electrical conduction is thus a combination of electrolytic mechanisms for the fluid-filled fractures, and of surface-mediated ion transport for conductive alteration minerals. Since an order of magnitude separates the resistivity of alteration minerals (a few Ω.m in situ), to that of seawater (about 0.2 Ω.m at 25°C), the electrical resistivity is sensitive to the progressive sealing of the oceanic crust with basalt alteration products.

A series of laboratory measurements on cores were made to evaluate the contribution of alteration minerals to current conduction in situ. If significant, such contribution would cause estimates of porosity through Archie's law [1942] to be too high. The electrical resistivity (at five different fluid salinites), porosity and cation exchange capacity (CEC) of MORB samples recovered in DSDP Hole 504B were measured at room temperature and atmospheric pressure. A frequency of 50 Hz was chosen to match that used in situ with the Dual Laterolog (DLL). The presence of chlorites, zeolites and particularly smectites as alteration products of MORB is reflected by high values of CEC (Figure 1). Whereas the massive units of Layers 2A and 2B are defined by high and uniform CEC values, the more fractured and altered pillows are characterized by even higher values of CEC and a large variability (Figure 1). The formation factor is related to porosity by an inverse power law similar to Archie's formula, with m of the order of 1.0 and a as large as 10.0 (Figure 2). This result is similar to those of Flovenz et al. [1985], Pape et al. [1985], and Broglia and Moos [1988] derived for terrestrial basalts, granite and MORB respectively. A distinction is here necessary to distinguish the apparent formation factor computed from measurements made at a single salinity value (or conductivity; i.e., that of seawater), and the intrinsic formation factor obtained from several measurements made at high salinities. The intrinsic formation factor might therefore be defined as equating to electrolytic conduction in pore volumes (and associated with the notion of free-water). The intrinsic formation factors FF" and porosity $\emptyset$ are also found to be related by:

$$FF'' = [\ \pi 2 / \emptyset\ ] = (10.0) / \emptyset, \qquad [1]$$

where $\pi 2$ is associated with the tortuosity of pore volumes after Walsh and Brace [1984], Katsube and Hume [1987] and Johnson and Schwartz [1989].

Such a low m value with respect to Archie's formula (where m = 2.0) equates to current conduction in cracks and microcracks present throughout the rock at mineral-scale, and elsewhere observed in thin-sections. These microstructures are due to MORB quenching at the ridge axis, and conserved by precipitation of alteration minerals due to hydrothermal circulation. In the massive flows, the in situ conduction mechanism is found to be mostly electrolytic (Figures 3 and 4). In the pillows, however, the main conduction mechanism appears to be cationitic in relation with surface-conduction and the presence of alteration minerals (Figure 5). On that basis, a model of conduction in parallel is used to

describe the propagation of electrical currents in MORB at low frequency (Figure 3). The total conductivity of the rock Co is thus viewed as the sum of the fluid-contribution Cf (dominant at high salinity), and the surface contribution Cs (dominant at low salinity) with:
$Co = [Cf + Cs] = [[Cw / FF'] + [(B.Qv) /(\mu 2 . FF')]] = [Cw + (B.Qv / \mu 2)] / FF'$, [2]
where Cw is the conductivity of the pore fluid, B is the equivalent conductance of the sodium ions absorbed onto alteration mineral surfaces, Qv is the CEC normalized to unit pore volume, and $\mu 2$ is a dimensionless number accounting for the increased tortuosity of the pore surfaces with respect to that of the pore space.

A continuous electrical-resistivity profile was recorded with a DLL during Leg 111 of the Ocean Drilling Program in DSDP Hole 504B [Pezard, 1990]. Onboard ship, an apparent porosity profile was computed from Archie's formula [1942]. The intrinsic porosity estimate deduced from the previous analysis accounts for surface conduction, and therefore yields lower porosity estimates than those obtained from Archie's formula. In particular, high values of porosity are obtained in Layer 2A only (Figure 5). A permeability profile computed after Hubbert [1956] and Brace [1977] on the basis of laboratory and in situ resistivity measurements reproduces those obtained in situ from packer experiments (Figure 6), and therefore provides a key to the low-permeability high-apparent-porosity paradox obtained in the past when comparing in situ experiments conducted in Hole 504B [Becker, 1985].

References

Alt, J.C., Honnorez, J., Lavene, C., and Emmermann, R., 1986. Hydrothermal alteration of a 1-km section through the upper oceanic crust, DSDP Hole 504B: the mineralogy, chemistry and evolution of seawater-basalt interactions, *J. Geophys. Res., 91*. 309-335.

Archie, G.E., 1942. The electrical resistivity log as an aid in determining some reservoir characteristics, *Journal of Petroleum Technology, 5*, 1-8.

Becker, K., 1985. Large-scale electrical resistivity and bulk porosity of the oceanic crust, DSDP Hole 504B, Costa Rica Rift. In Anderson, R.N., Honnorez, J., Becker, K., et al., *Init. Repts. DSDP, 83*: Washington (U.S. Govt. Printing Office), 419-427.

Becker, K., Sakai, H., et al., 1989. Drilling deep into young oceanic crust, Hole 504B, Costa Rica Rift, *Rev. of Geophysics, 27*, 1, 79-102.

Brace, W.F., 1977. Permeability from resistivity and pore shape, *J. Geophys. Res., 82*: 3343-3349.

Broglia, C., and Moos, D., 1988. In situ structure and properties of 110 ma crust from geophysical logs in DSDP Hole 418A. In Salisbury, M.H., Scott, J. et al., *Proc. ODP, Sci. Results, 102*: College Station, Texas (ODP), 29-47.

Flovenz, O.G., Georgsson, L.S., and Arnason K., 1985. Resistivity structure of the upper crust in Iceland, *J. Geophys. Res., 90*: 10136-10150.

Hubbert, M.K., 1956. Darcy's law and the field equation of the flow of underground fluids, Trans, AIME, 207: 222-239.

Johnson, D.L., and Schwartz, L.M., 1989. Unified theory of geometrical effects in transport properties of porous media, *SPWLA, 30th Ann. Logging Symp.; Paper E*; Denver, Colorado.

Katsube, T.J., and Hume, J.P., 1987. Permeability determination in crystalline rocks by standard geophysical logs, *Geophysics, 52*: 342-352.

Olhoeft, G.R., 1981. Electrical properties of rocks. In Touloukian, Y.S., Judd, W.R., and Roy, R.F., *Physical Properties of Rocks and Minerals*, McGraw-Hill (New York), 257-330.

Pape, H., Riepe, L., and Schopper, J.R., 1985. Petrophysical detection of microfissures in granites, *SPWLA, 26th Ann. Log. Symp.; paper P*; Dallas, Texas.

Pezard, P.A., 1990. Electrical properties of MORB, and implications for the structure of the upper oceanic crust at Site 504, *J. Geophys. Res.*, in press.

Walsh, J.B., and Brace, W.F., 1984. The effect of pressure on porosity and the transport properties of rocks, Ward, S.H., and Fraser, D.C., 1967. Conduction of electricity in rocks, in Musgrave, A.W., Ed., *Mining Geophysics, 2*, 197-223, Soc. Explor. Geophys.

Figure Captions

Figure 1. Laboratory measurements of CEC plotted as a function of depth. The decrease in amount of smectites from the upper part of the basement (Layers 2A and 2B), to the sheeted dikes of Layer 2C (characterized by greenschist facies of alteration), is reflected in a gradual decrease of the CEC within Layer 2C. The fracture-free samples of Layers 2A and 2B have the lowest CEC values in this part of the crust. The three main alteration zones observed in thin-sections [Alt et al.,1986] are indicated as UPAZ (upper alteration zone), LPAZ (lower alteration zone) and GFAZ (greenschist facies alteration zone).

Figure 2. [A] Apparent formation factor (determined at Rw = 0.2 Ωm) plotted versus measured porosity for MORB samples from Hole 504B. The samples from the sheeted-dikes and breccias of Layer 2C (solid triangles) are more resistive at equivalent porosity than those from Layers 2A and 2B. The fracture-free samples of Layers 2A and 2B (small solid circles) have the lowest porosity and the highest apparent formation factor. The dataset can be represented by a regression similar to Archie's law with a=9.1 and m=1.05. [B] Apparent formation factor (determined at Rw = 0.2 Ωm) plotted versus CEC. An inverse correlation is observed in the upper part of the basement (Layers 2A and 2B), but the samples from Layer 2C do not follow this trend. The fracture-free samples of Layer 2A and 2B (small solid circles) are those with the highest apparent formation factor and the lowest CEC values (i.e., alteration). The largest CEC values within Layers 2A and 2B are recorded in the pillow units.

Figure 3. Electrical conductivity Co of sample 527 from Unit 2D (a massive flow), plotted versus saturating-fluid conductivity Cw. The hollow squares represent measurements made at different saturating-fluid salinities, and the black square on the vertical axis is derived from the CEC measurement using the surface conduction model (Equation 2). The horizontal asymptote is related to cationitic conduction on pore surfaces (in the bound-water domain), while the asymptote at high saturating-fluid conductivity (or salinity) corresponds to electrolytic conduction within the pore space (in the free-water domain). The shaded domain on the horizontal axis represents sea-water conductivity in Hole 504B due to downhole temperature variations. A higher temperature, or a larger CEC value, tends to

increase surface conduction Cs. The intrinsic formation FF" factor is determined by the location of the high-salinity asymptote.

Figure 4. Same as Figure 3. The data are plotted per lithologic units for samples from three massive units penetrated in the volcanic section of Hole 504B. [A] Unit 2D, [B] Unit 27 and [C] Unit 34.

Figure 5. Same as Figure 3 for [A] pillow units and [B] samples from the sheeted-dikes complex.

Figure 6. [A] Apparent porosity profile computed from Archie's law (PHIR) during ODP Leg 111. The conduction due to the presence of alteration minerals is not taken into account. [B] Clay-corrected free-water porosity profiles computed from the new model with $\mu 2 = 10.0$ (PHIP3), and $\mu 2 = 1.0$ (PHIP4). The square diamonds represent porosity measurements made on cores. The zonation of the alteration (UPAZ, LPAZ and GFAZ) is indicated as in Figure 1.

Figure 7. Computed permeability profiles obtained with $\mu 2 = 10.0$ (PER32), and $\mu 2 = 1.0$ (PER42), and plotted in millidarcy and m2. The bulk permeabilities measured in situ are represented with elongate vertical rectangles. The vertical extend of the rectangle represents the depth interval over which average permeabilities were measured. The horizontal extend of the rectangles represents the range of estimated errors in the permeability determination [Becker et al.,1989]. The two dashed rectangles indicate new estimates of permeability from in situ packer experiments computed with revised parameters [Becker et al., 1989]. Alteration zonation (UPAZ, LPAZ and GFAZ) as per Figure 1.

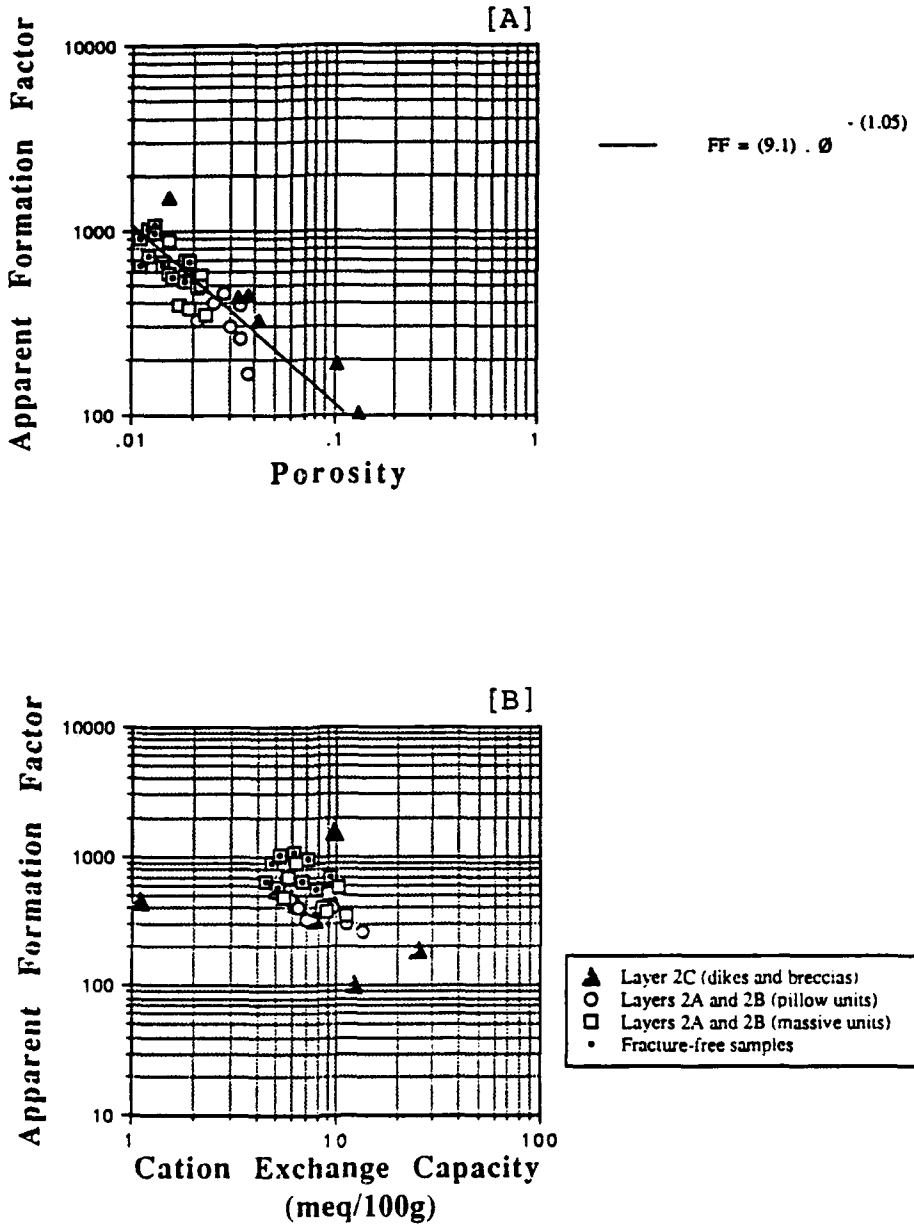
[A]
Apparent Formation Factor
10000
1000
100
.01
.1
1
Porosity
FF = (9.1) . Ø^-(1.05)
[B]
Apparent Formation Factor
10000
1000
100
10
1
10
100
Cation Exchange Capacity
(meq/100g)
Layer 2C (dikes and breccias)
Layers 2A and 2B (pillow units)
Layers 2A and 2B (massive units)
Fracture-free samples

Figure 2

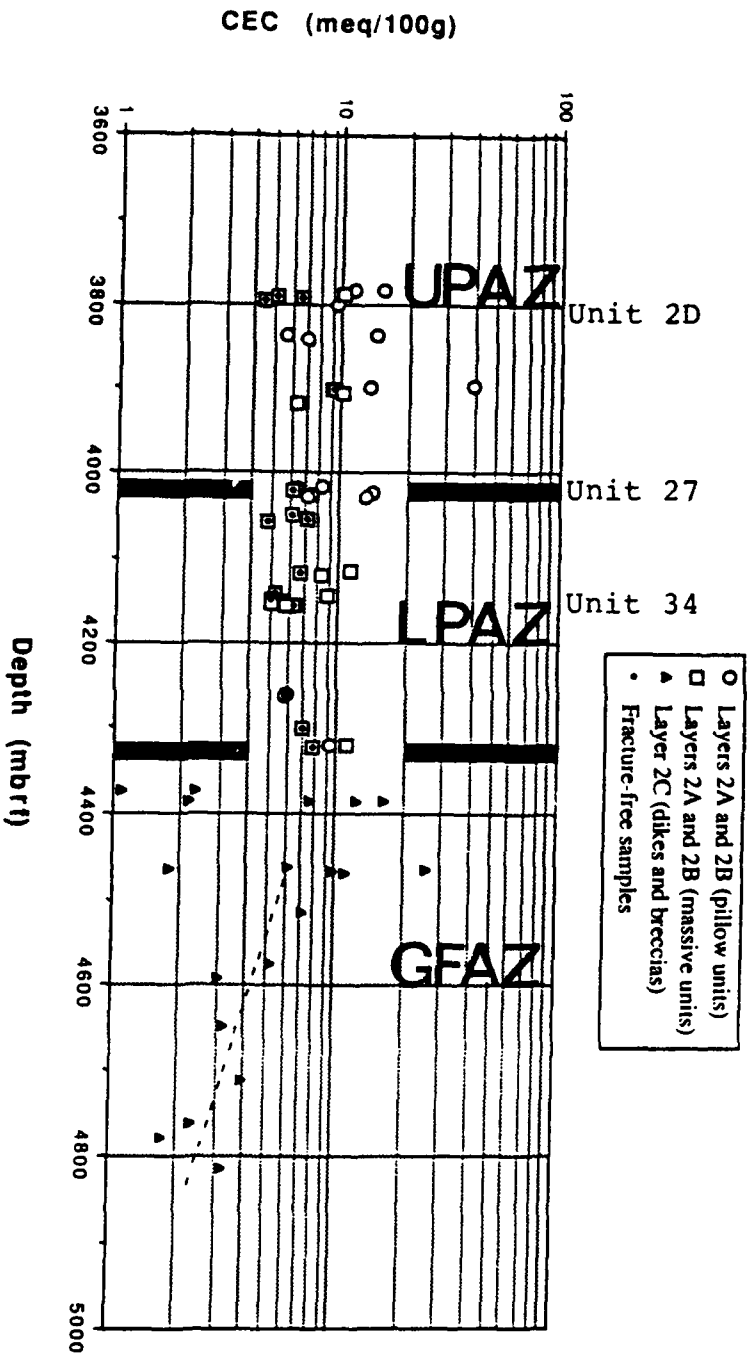
CEC (meq/100g)
1
10
100
3600
3800
4000
4200
4400
4600
4800
5000
Depth (mbrf)
UPAZ
LPAZ
GFAZ
Unit 2D
Unit 27
Unit 34
Layers 2A and 2B (pillow units)
Layers 2A and 2B (massive units)
Layer 2C (dikes and breccias)
Fracture-free samples

Figure 1

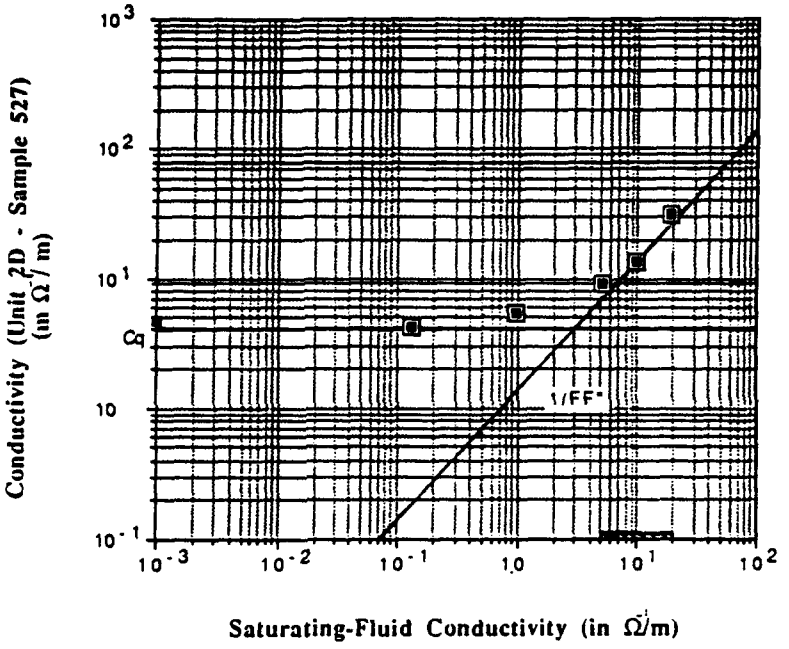
Conductivity (Unit 2D - Sample 527)
(in Ω/m)
10^3
10^2
10^1
Cq
10
10^-1
1/FF*
10^-3
10^-2
10^-1
1.0
10^1
10^2
Saturating-Fluid Conductivity (in Ω/m)

Figure 3

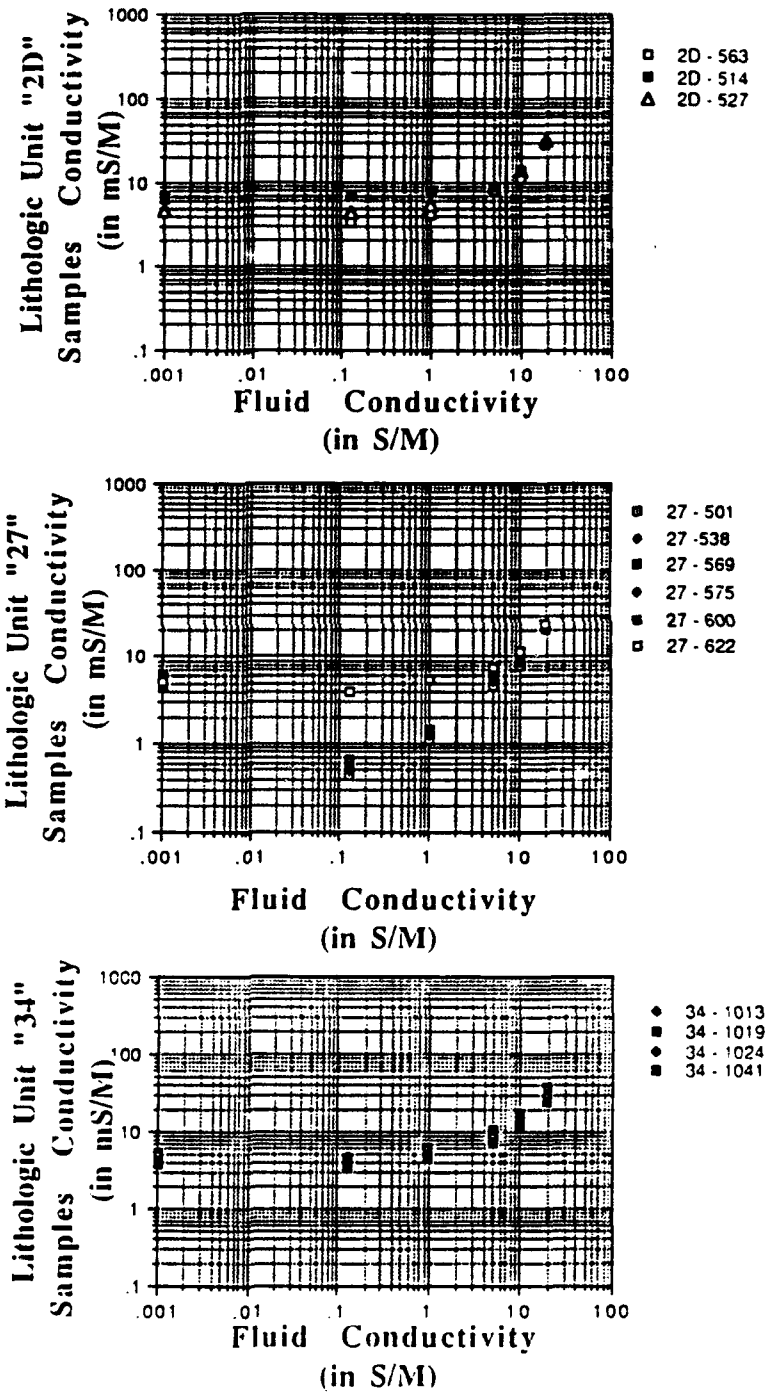
Lithologic Unit "2D"
Samples Conductivity
(in mS/M)
1000
100
10
1
.1
.001
.01
.1
1
10
100
Fluid Conductivity
(in S/M)
2D - 563
2D - 514
2D - 527
Lithologic Unit "27"
Samples Conductivity
(in mS/M)
Fluid Conductivity
(in S/M)
27 - 501
27 -538
27 - 569
27 - 575
27 - 600
27 - 622
Lithologic Unit "34"
Samples Conductivity
(in mS/M)
Fluid Conductivity
(in S/M)
34 - 1013
34 - 1019
34 - 1024
34 - 1041

Figure 4

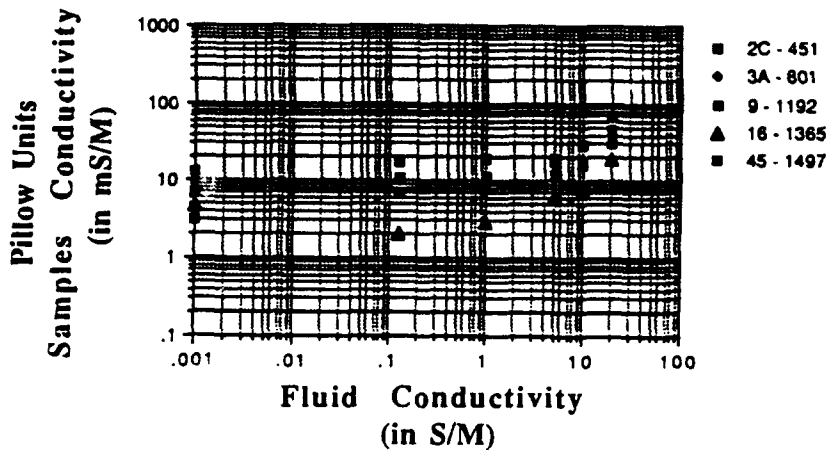
Pillow Units
Samples Conductivity
(in mS/M)
1000
100
10
1
.1
.001
.01
.1
1
10
100
Fluid Conductivity
(in S/M)
2C - 451
3A - 801
9 - 1192
16 - 1365
45 - 1497

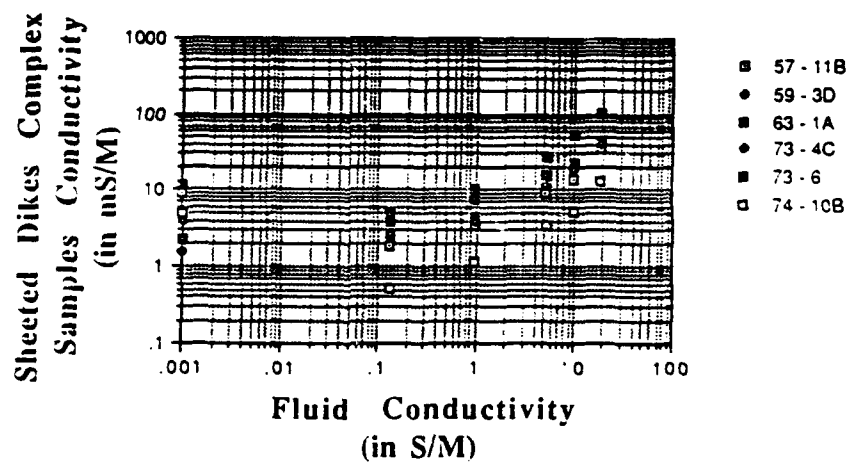
Sheeted Dikes Complex
Samples Conductivity
(in mS/M)
1000
100
10
1
.1
.001
.01
.1
1
10
100
Fluid Conductivity
(in S/M)
57 - 11B
59 - 3D
63 - 1A
73 - 4C
73 - 6
74 - 10B

Figure 5

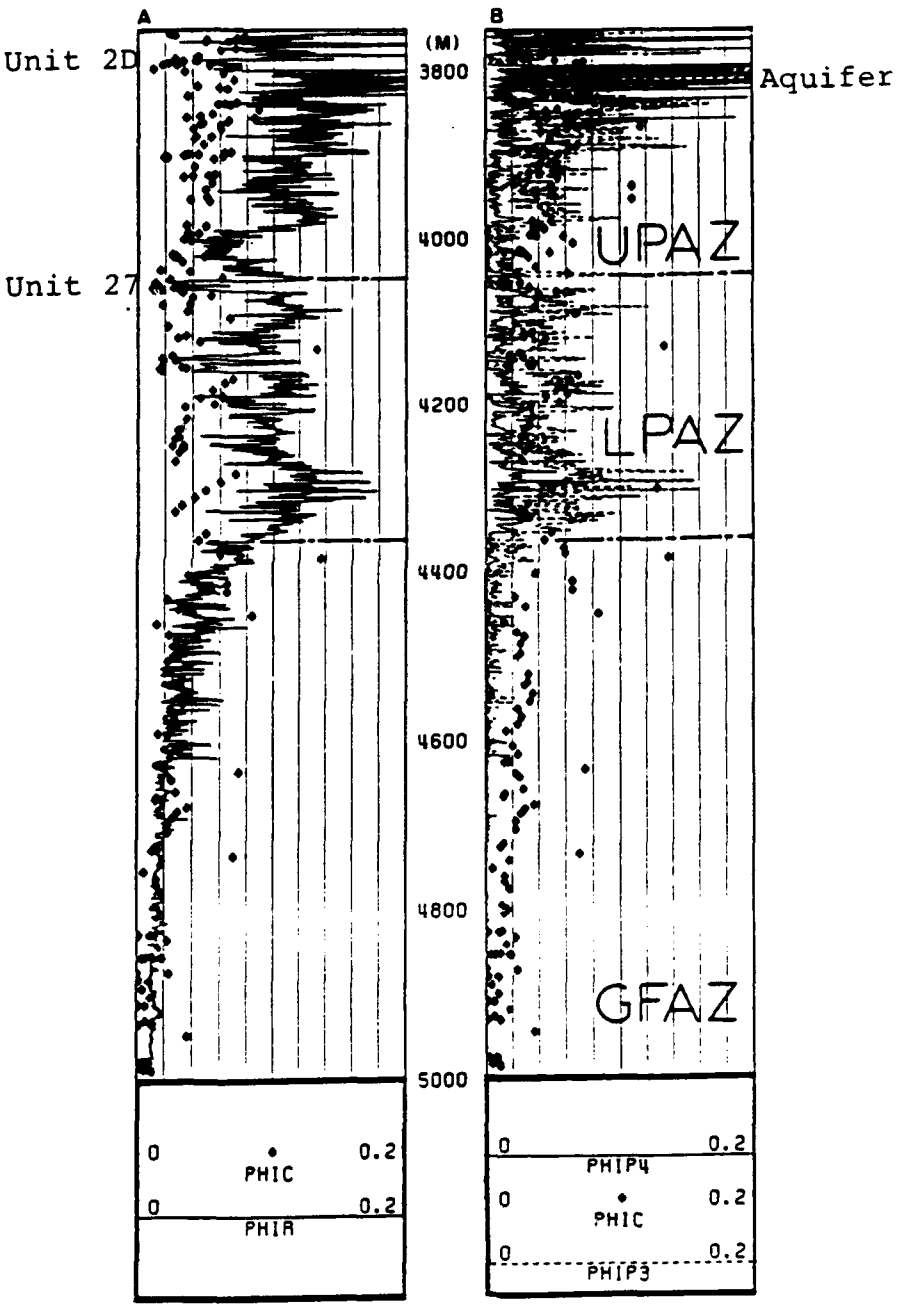
A
B
Unit 2D
Unit 27
(M)
3800
4000
4200
4400
4600
4800
5000
Aquifer
UPAZ
LPAZ
GFAZ
0
0.2
PHIC
0
0.2
PHIR
0
0.2
PHIP4
0
0.2
PHIC
0
0.2
PHIP3

Figure 6

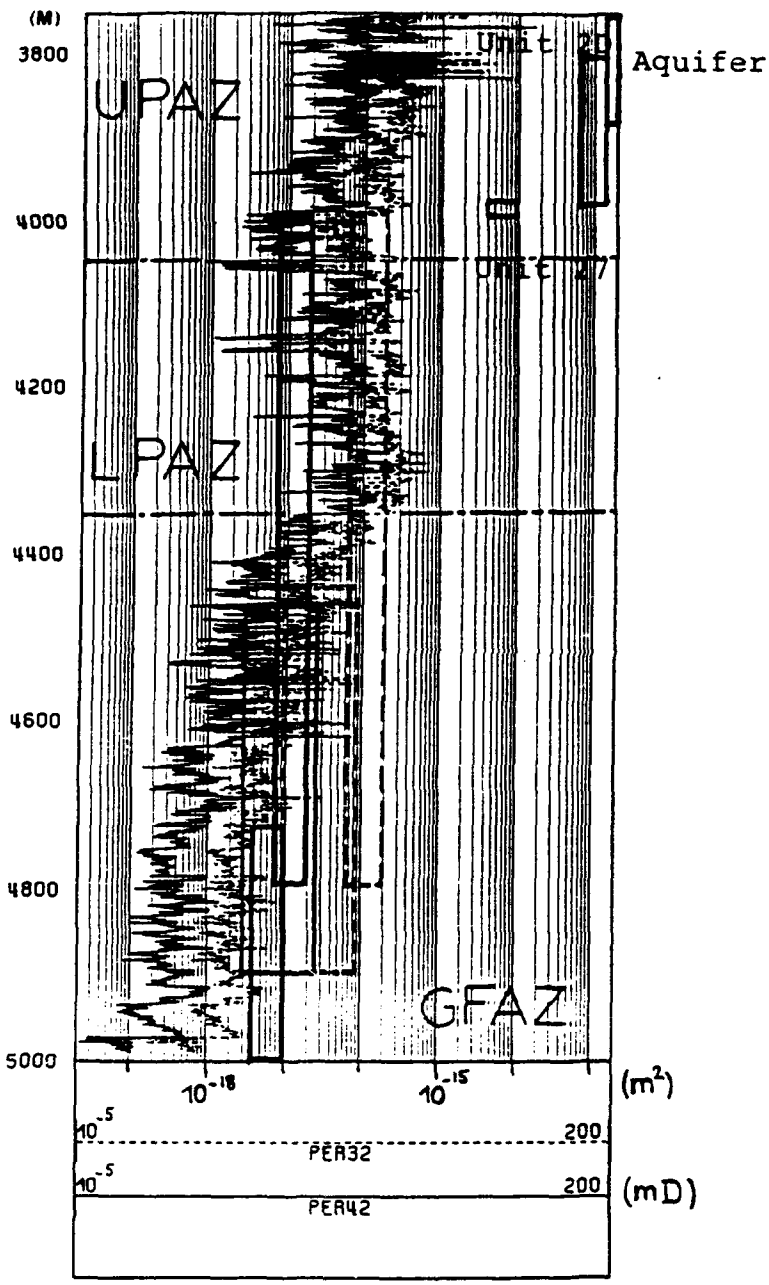
(M)
3800
4000
4200
4400
4600
4800
5000
UPAZ
LPAZ
GFAZ
Unit 20
Unit 27
Aquifer
10^{-18}
10^{-15}
(m^2)
10^{-5}
200
PER32
10^{-5}
200
(mD)
PER42

Figure 7

STRUCTURE OF SHALLOW BASEMENT FROM DOWNHOLE LOGS

D. Moos
Department of Geophysics, Stanford University

One of the goals of the drilling within the oceanic crust has been to determine the lithostratigraphy of Oceanic Layer 2. Unfortunately, core recovery is typically low (often less than 25%) and the recovered samples are not necessarily representative of the in situ material. This is a particular problem in young, shallow crust, where the basalts are structurally weak, as for example in ODP Hole 648B [Shipboard Scientific Party, 1988].

Therefore, downhole logs provide the only continuous determination of physical properties throughout the depth of open hole. Unfortunately, these measurements are generally difficult to "invert" for the first-order information of the thicknesses and characteristics of pillows, massive units, and breccias encountered by the borehole. For example, Figure 1 shows generalized sections determined from density, resistivity, and compressional wave velocity logs for DSDP Holes 395A, 418A, and 504B. Also shown are interpretations of the volume fraction of basalt, alteration products, "fracture" porosity, and "primary" porosity as a function of depth.

Numerous attempts have been made to differentiate between different litho-structural units based on quantitative information from geophysical logs. Moos et al. [1985] determined that in the uppermost 150m of basement at Hole 504B, pillows can be separated from massive units by comparing compressional and shear velocities and their ratio. Later work in DSDP Hole 418A revealed that the peak frequency and the semblance coherence of sonic full waveforms is lower in pillows than in massive units, based on scattering of energy from pillow margins [Moos, 1988]. K. Becker has presented a number of results relating in situ structure to large-scale electrical resistivity (e.g., Becker [1985]). Barton et al. [1989] showed that the stratigraphy of volcanogenic sediments and interlayered flows could be delineated from resistivity, density, and velocity logs. Pezard [in press] compared shallow and deep resistivity measurements to estimate the contribution of horizontal and vertical fractures and of alteration to in situ conductivity in Hole 504B.

Unfortunately, downhole logs to date have been notoriously unsuccessful in determining accurately the density structure of the oceanic crust. Although Broglia and Ellis (in press) have presented a reasonable approach toward removing the effects of alteration products and environmental effects on the porosity log, both this log and the density log, which also has severe problems in the ODP environment, still investigate only a few meters (at best) away from the wellbore. Borehole gravity measurements (BHGM) can resolve density with precisions equivalent to downhole logs, over volumes of many tens of cubic meters around the wellbore, without the calibration and pad standoff problems associated with neutron or density logs (see, for example, LaFehr [1983]). When combined with inversion techniques and surface measurements these logs can resolve both vertical and horizontal variations in density at scales of meters to tens of meters [e.g., Mamonov, 1988]. However, either these measurements must be made via wireline re-entry, or significant modifications must be made to existing probes in order to accommodate the size restrictions of logging through ODP drillpipe.

Elastic properties measurements in pillows are difficult, due to the scattering of high frequencies and the poor propagation of shear sonic waves along large-diameter boreholes. Recent improvements in shear-wave logging technology can overcome these problems, by (1) utilizing lower frequencies (below 1 KHz) and (2) generating dipole or higher-order

modes in the borehole, which propagate more efficiently than axi-symmetric waves (see, for example, Chen [1989]). It is hoped that in the future these new technologies will be adapted for use in ODP drillholes.

The most successful lithostratigraphy has been obtained from interpretation of borehole televiewer (BHTV) images (e.g., Zoback and Anderson [1983]; Newmark et al. [1985]). Unfortunately, before the advent of the ODP, the BHTV had been run in only a few wells, and data quality was generally quite poor. However, the difference between pillows and massive units in BHTV images is striking (see Figure 2), and thus BHTV data can provide perhaps the only unequivocal lithostratigraphic information. In the last few years of the ODP a number of borehole televiewer logs have been run, but complete analyses of these data have yet to be published.

From joint analysis of BHTV lithostratigraphy and other logs (see, for example, Anderson et al. [1984]; Newmark et al. [1985]; Moos et al. [1986]) the systematics of log variations can be compared directly to in situ structure. In the future such comparisons may provide the basis for an understanding of the relationship between crustal structure and seismic, hydro-geologic, and mechanical properties, as shown by Goldberg et al. [in press]. These analyses will be most important as attempts are made to drill and study young, poorly sedimented crust.

References

Anderson, R.N., H. O'Malley, and R.L. Newmark, 1984. Nuclear, multichannel-sonic, ultrasonic analyses for determination of degree of fracturing and alteration in a fast formation: the deep ocean crust, *SPWLA 25th Annual Log. Symp.*, paper Y.

Barton, C., D. Moos and J.-P. Blangy, 1989. Analysis of full waveform acoustic logging data at ODP Site 642 — Outer Voring Plateau, in Eldholm, O., J. Thiede, E. Taylor, et al., *Proc. ODP Sci. Results, 104*: College Station, TX (Ocean Drilling Program), 953-964.

Becker, K., 1985. Large-scale electrical resistivity and porosity of the oceanic crust, DSDP Hole 504B, Costa Rica Rift, In Anderson, R.N., Honnorez, J., Becker, K., et al., *Init. Repts. DSDP, 83*: Washington (US Gov't. Printing Office), 419-427.

Broglia, C., and D. Ellis, in press. The effect of alteration, formation absorption, and standoff on the response of the thermal neutron porosity log in gabbros and basalts: Examples from DSDP - ODP sites, *J. Geophys. Res.*

Chen, S.T., Shear-wave logging with quadruple sources, *Geophys., 54(5)*, 590-597, 1989.

Goldberg, D., C. Broglia and K. Becker, in press. Fracturing, alteration and permeability: in situ properties in Hole 735B, in *Proc. ODP, Sci. Results, 118*: College Station, TX (Ocean Drilling Program).

LaFehr, T.R., 1983. Rock density from borehole gravity surveys, *Geophys. (58)*, 341-356.

Mamonov, A.V., 1988. Two-dimensional inversion of gravity data on external and internal fields, Izvestia, *Earth Physics 24(3)*, 210-215.

Moos, D., D. Goldberg, M.A. Hobart and R.N. Anderson, 1986. Elastic-wave velocities in Layer 2A from full waveform sonic logs at Hole 504B, In Leinen, M., D. Raye, K. Becker, et al., *Init. Repts DSDP, 92*: Washington (U.S. Gov't. Printing Office) 563-570.

Moos, D., 1989. Elastic properties of 110 Ma oceanic crust from sonic full waveforms in DSDP Hole 418A, In Salisbury, M.H., Scott, J.H., et al., *Proc. ODP, Sci. Results, 102*: College Station, TX (Ocean Drilling Program), 49-62.

Newmark, R.L., Anderson, R.N., Moos, D., and Zoback, M.D., 1985. Sonic and ultrasonic logging of Hole 504B and its implications for the structure, porosity and stress regime of the upper 1 km of the oceanic crust, in Anderson, R.N., Honnorez, J., et al., *Init. Repts. DSDP, 83*, Washington (U.S. Gov't. Printing Office), 479-510.

Pezard, P.A., in press, Morphology and alteration of the upper oceanic crust from in situ electrical experiments in DSDP Hole 504B, *J. Geophys. Res.*

Shipboard Scientific Party, 1988. Site 648, In Detrick, R., Honnorez, J., et al., *Proc. ODP, Init. Repts. (Pt. A), 106/109*: College Station, TX (Ocean Drilling Program), 35-134.

Zoback, M.D., and Anderson, R.N., 1983. The implications of fracture distribution, structure, and stratigraphy from borehole televiewer imagery of the oceanic crust on the Costa Rica Rift, *Nature, 295*:375.

Figure Captions:

Figure 1: Average profiles of natural gamma activity (left-hand track), P-wave velocity, resistivity, and density for Holes 504B, 418A, and 395A, plotted as a function of depth below sea level from top of basement to total logged depth in each hole. Also shown on the right are inferred volume percentages of alteration (solid black) basalt (stippled), and "fracture" (dotted) and "primary" (white) porosity inferred from the logs.

Figure 2: Digitized borehole televiewer data recorded during DSDP Leg 68 in Hole 501. Shown are travel-times and amplitudes of reflections from a thick massive unit (logged depth 3757-3765.4 m bsf) between two pillow units. The thickness and characteristics of the pillows and massive units in this well are clearly delineated by the BHTV images. Differences in thickness and size of individual pillows are also apparent.

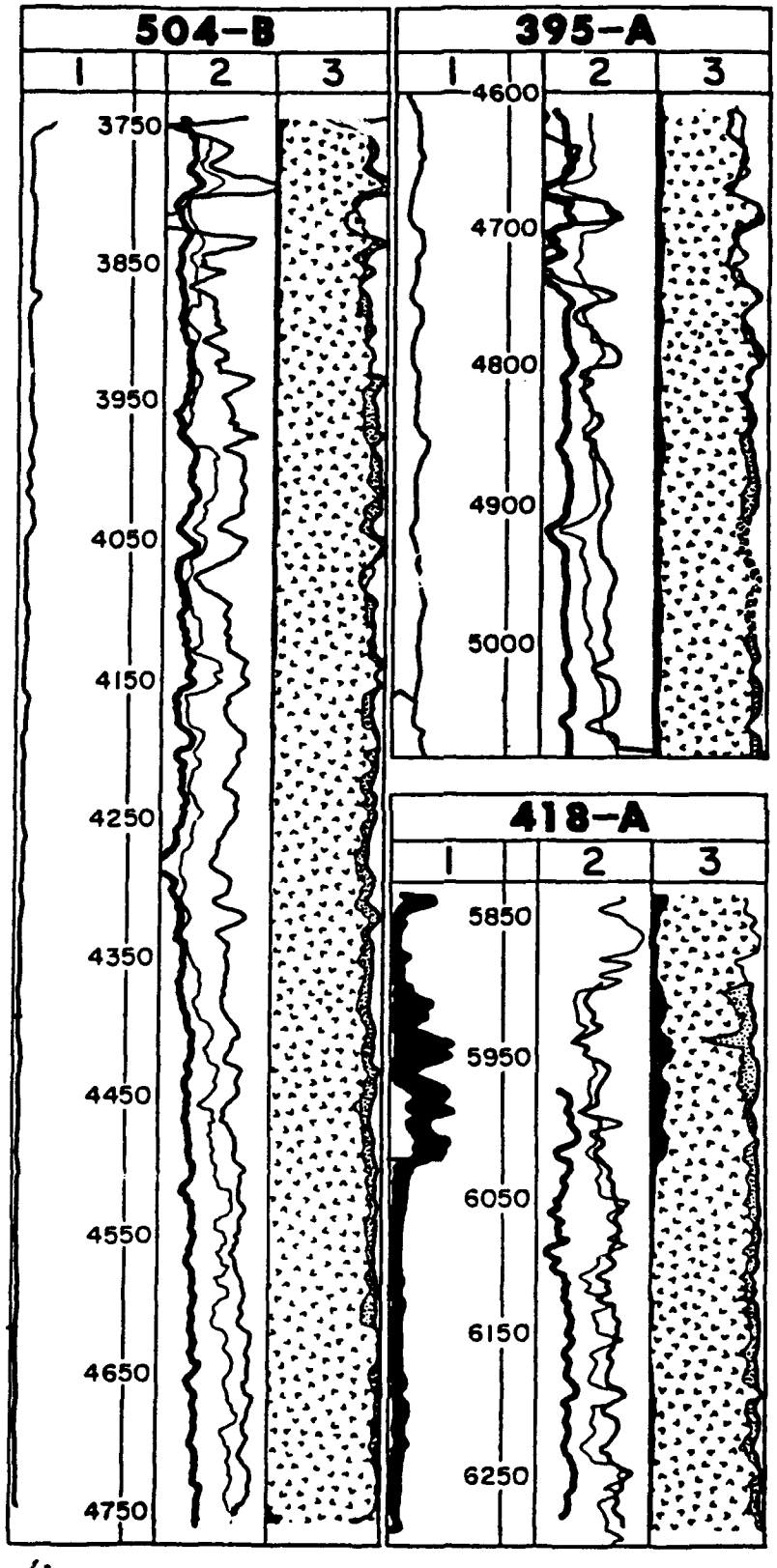

KEY:

ρ ——— DENSITY (2-4.5 gm/cm^3)

Ω ——— RESISTIVITY (2-2000 ohm-m)

V_P ——— VELOCITY (2-7 km/sec)

Figure 1

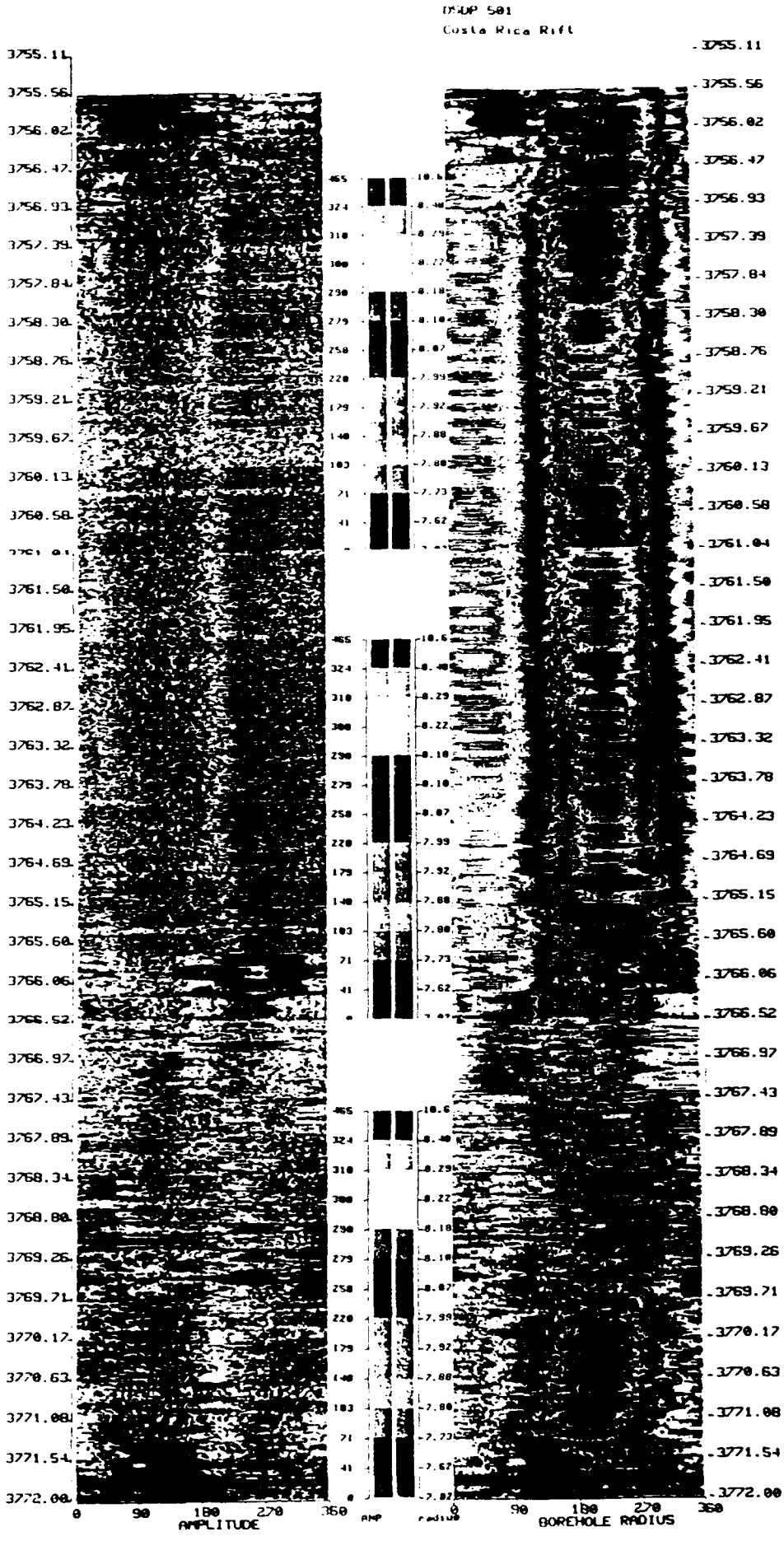
DSDP 501
Costa Rica Rift
3755.11
3755.56
3756.02
3756.47
3756.93
3757.39
3757.84
3758.30
3758.76
3759.21
3759.67
3760.13
3760.58
3761.50
3761.95
3762.41
3762.87
3763.32
3763.78
3764.23
3764.69
3765.15
3765.60
3766.06
3766.52
3766.97
3767.43
3767.89
3768.34
3768.80
3769.26
3769.71
3770.17
3770.63
3771.08
3771.54
3772.00
0
90
180
270
360
AMPLITUDE
AMP
BOREHOLE RADIUS

Figure 2

PHYSICAL PROPERTIES OF THE SEAFLOOR EXPOSED AT THE HESS DEEP

John Hildebrand and LeRoy Dorman
Scripps Institution of Oceanography
University of California at San Diego

We contend that the Hess Deep provides a unique opportunity to study the shallow physical properties of the oceanic crust. The Hess Deep results from rifting at the junction between the Galapagos Rift and the East Pacific Rise. At the Hess Deep, 2000m sections of young volcanic oceanic crust are exposed in nearly vertical rift shoulder walls. The exposed section includes all of layer 2 (pillow basalt, sheeted dikes), and the upper portion of layer 3 (gabbro). The Hess Deep, therefore, presents a unique geological setting with an exposed, fresh section of oceanic crust.

An active seafloor seismic experiment could measure the detailed velocity structure of the upper crust at the Hess Deep. The seismic experiment would consist of placing seafloor receivers (OBSs) on the Hess Deep rift shoulders and placing seafloor shots on the Hess Deep scarp (see Figure 1). This geometry is similar to that used in Vertical Seismic Profiling from boreholes and allows unambiguous determination of velocity structure as a function of depth, even in the presence of velocity inversions. A line of seafloor shots recorded at single OBSs would provide VSP velocity profiles of the shallow crust. Using a number of OBS receivers allows measurement of a three-dimensional tomographic image, revealing variations in shallow structure. Such an experiment program will require seafloor shots and seafloor receivers, since surface shots and receivers would be difficult to analyze in this rough terrain.

Improved shallow resolution is obtained for seismic profiles using precisely navigated seafloor shots and receivers because the entry and exit points of seismic rays are well known, eliminating the need for model dependent topographic corrections. This improves the potential for tomographic inversion of shallow raypaths to provide an image of seafloor velocity structure. We have used this approach successfully to model the vertical seismic structure of a seamount (Hildebrand, Dorman *et al.*, 1989) and similar techniques can be applied to construct vertical sections of the Hess Deep rift shoulders. Another key advantage of seafloor shot and receivers is that they allow the arrivals from waves traveling in the upper few hundred meters of crust to be observed preceding the large amplitude water wave arrivals, in contrast to sea-surface shots where the water wave obscures shallow crustal arrivals. In the geometry of the Hess Deep site, the water arrivals are blocked by the shoulder of the scarp. Forward modeling and our previous experience with shallow seismic experiments suggest that seafloor sources and receivers will provide tight constraints on the shallow crustal structure.

The geometry of the Hess Deep site gives a natural "window" into the shallow crust, providing the same advantages of a borehole seismic experiment, without the cost. Several of the advantages of this geometry are: 1) no direct water wave arrival to obscure arrivals from the shallow crust, 2) velocity measurements derived from analysis of the inflection point in the travel time-range plot, 3) improved coupling of the source to the rocks at depth and 4) direct correlation of seismic velocity and rock samples (collected by P. Lonsdale, May 1990 in Alvin).

Another technique which provides complimentary information on the shallow density structure is seafloor gravity. Gravity profiles conducted on the Hess Deep scarp would provide constraints on shallow density by measuring the local vertical gradient of gravity.

When seafloor gravity measurements are plotted as a function of station depth, the observed vertical gravity gradient results from a combination of the free-water gradient (0.2215 mGal/m) and the seafloor gravitational attraction. By differencing the free-water and observed gravity gradient the water-rock density contrast can be calculated. The value obtained is most sensitive to the shallow crustal density (uppermost 1 km). Seafloor gravity measurements conducted on the Hess Deep rift shoulder would provide incremental layer densities, similar to those measured by borehole gravity. The seafloor gravimeter has been used in steep and rough terrain previously, for example on the side of Axial Volcano (Hildebrand *et al.*, 1990), where patience is required to level the sensor.

References

Hildebrand, J.A., L.M. Dorman, P.T.C. Hammer, A.E. Schreiner, and B.D. Cornuelle, Seismic Tomography of Jasper Seamount, *Geophys. Res. Lett., v. 16*, 1355-1358, 1989.

Hildebrand, J.A., J.M. Stevenson, P.T.C. Hammer, M.A. Zumberge, R.L. Parker, C.G. Fox, and P. Meis, A Seafloor and Sea-Surface Gravity Survey of Axial Volcano, *J. Geophys. Res.*, in press, 1990.

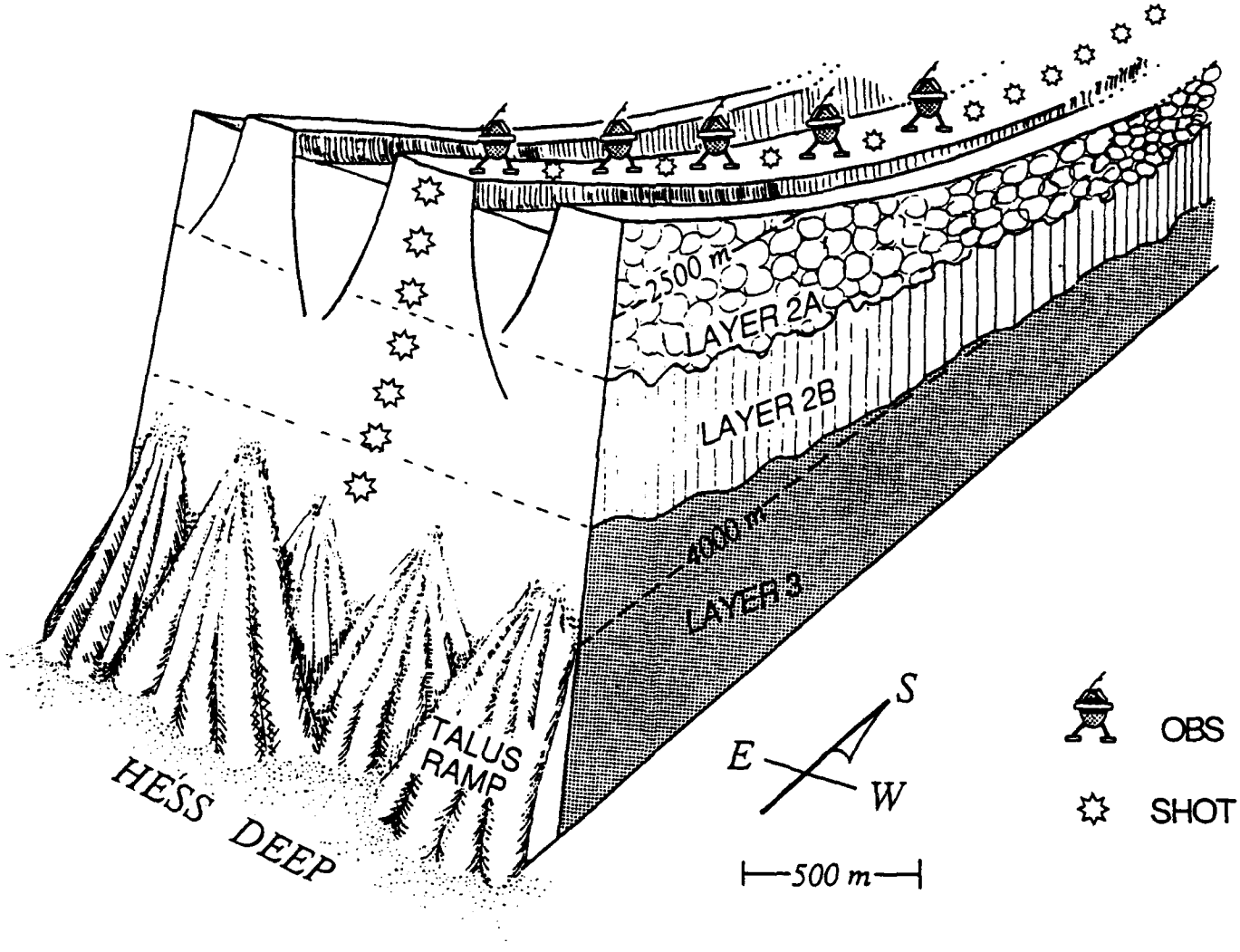

Figure 1. The southern rift shoulder of the Hess Deep is drawn schematically along with locations for seafloor shots and seafloor receivers. The near vertical exposure reveals young oceanic crust including all of layers 2A (pillow basalt), 2B (sheeted dikes), and the top of layer 3 (gabbros). Seafloor shots and gravity stations conducted along the scarp face will yield accurate measurements of shallow crustal velocities and densities.

LABORATORY PHYSICAL PROPERTIES OF A HIGHLY VESICULAR BASALT BRECCIA

K.A. Dadey and the Leg 126 Scientific Party
Graduate School of Oceanography
University of Rhode Island
Narragansett, RI 02882

A recent Ocean Drilling Program cruise (Leg 126) to the Izu-Bonin Arc region (Shipboard Scientific Party, 1989 a, b) recovered approximately 311 meters of igneous basement rocks at Site 791. Of this, 135 meters were composed of scoriaceous basalt breccia consisting of grey clasts in a green-grey matrix. Macroscopic examination indicates that this material is highly vesicular, highly expanded basalt glass (Gill et al., submitted). A prominent seismic reflector observed at approximately four seconds two-way travel time is hypothesized to mark the bottom surface of this unit (Shipboard Scientific Party, in press).

We measured the laboratory physical properties on parallel-sided samples or mini-cores drilled from split cores. Measurements include gravimetric bulk density, water content/porosity and grain density and Hamilton frame sonic velocity. Wherever possible, we tested samples composed of exclusively clast or matrix material. Most samples, however, are mixtures of the two. Because of logistical difficulties, many samples were not removed from the cores for testing until hours or days after splitting. Our unpublished data suggests that igneous rock properties may be significantly altered after only a few hours in the laboratory. As a result, several samples exhibited values which are obviously erroneous. These are not reported here.

The basalt breccia as a whole is characterized by higher porosities and lower bulk densities than the other basement rocks (Figure 1). Porosities average 37%, agreeing reasonably well with the 30-50% vesicularity estimated visually (Gill et al., submitted). Bulk densities average 2.3 g/cm^3. Average porosity and bulk density values of the other igneous units are 18.6% and 2.55 g/cm^3, respectively. Except for three samples between 1050 and 1075 mbsf, all the breccia samples exhibited velocities below 4.0 km/s. In contrast, all but three velocities measured in the other units were above 4.0 km/s. Within the breccia unit, properties display high variability and no strong trends with depth (Figure 1). Bulk density, porosity and velocity values all tend to decrease with depth in the unit. We attribute these trends, as well as the general increase in variability of the properties near the base of the unit to the increase in alteration with depth in the breccia (Gill et al., submitted). Sharp increases in both bulk density and velocity from the breccia to the underlying diabase unit is postulated to be responsible for the strong reflector observed in the seismic stratigraphic section.

A highly vesicular basalt breccia zone in the basement rocks of ODP Site 791 was identified initially by visual inspection. Its distinct nature and characteristic properties were independently confirmed using laboratory physical properties.

References

ODP Leg 126 Shipboard Scientific Party, 1989a. ODP Leg 126 drills the Izu-Bonin arc. Geotimes, 34:36-38.

ODP Leg 126 Shipboard Scientific Party, 1989b. Volcanism and rifting in the Izu-Bonin forearc and backarc. Nature, 342:18-20.

ODP Leg 126 Shipboard Scientific Party, in press. Proc. Init. Repts., 126: College Station TX (Ocean Drilling Program).

Gill, J., Torssander, P. and the Leg 126 Shipboard Scientific Party. Explosive deep water basalt in the Sumisu backarc rift. Submitted to Science

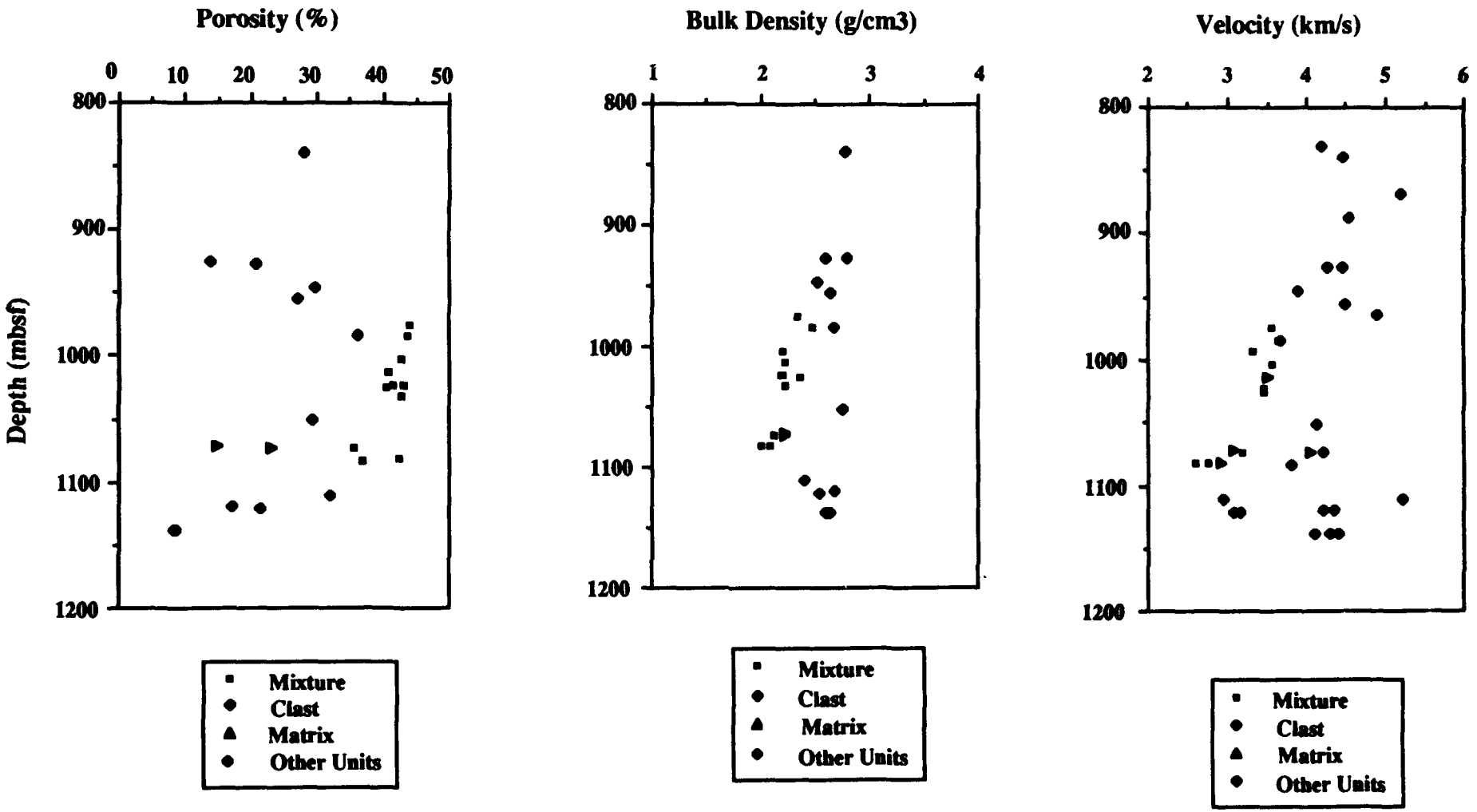
Porosity (%)
0
10
20
30
40
50
800
900
1000
1100
1200
Depth (mbsf)
Mixture
Clast
Matrix
Other Units
Bulk Density (g/cm3)
1
2
3
4
800
900
1000
1100
1200
Mixture
Clast
Matrix
Other Units
Velocity (km/s)
2
3
4
5
6
800
900
1000
1100
1200
Mixture
Clast
Matrix
Other Units

VERTICAL AND LATERAL VARIATIONS OF THE STRUCTURE OF OCEANIC LAYER 2

R.L. Carlson
Department of Geophysics
University of Texas

Seismic and acoustic wave propagation in the uppermost crystalline oceanic basement depend on the density and velocity (both shear and compressional wave) of the medium; studies of ophiolites, seismic surveys and drilling results indicate that layer 2 is both vertically and laterally heterogeneous on a wide range of scales (e.g., Christensen and Salisbury, 1975; Houtz and Ewing, 1976; Spudich and Orcutt, 1980). It is widely recognized that strong vertical gradients are characteristic of layer 2. Houtz and Ewing (1976) have shown that in young oceanic crust, layer 2 may itself be subdivided into layers 2a (3.7 ± 0.4 km $-s^{-1}$), 2b (5.2 ± 0.4 km $-s^{-1}$) and 2c (6.1 ± 0.2 km $-s^{-1}$). Layer 2a gradually disappears because of progressive alteration as the crust ages. Hence, even on large scales, the velocity and density structure of oceanic layer 2 is complex.

Carlson and Herrick (in press) have recently used the measured properties of oceanic rocks, drilling and downhole logging results from Holes 395A and 418H, and seismic structure models to estimate density and porosity variations in the oceanic crust. Carlson and Raskin (1984) found that there is a strong linear relationship between bulk densities and P-wave slowness measured in the laboratory (Figure 1):

$$\rho\ (\text{Mg-M}^{-3}) = (3.81 \pm 0.02) - (6.0 \pm 0.1)\ S_p\ (\text{sec-km}^{-1}) \qquad (1)$$

with an rms error of 0.07 $Mg\text{-}m^{-3}$. Carlson and Herrick found that the relationship between downhole log densities and sonic slownesses from Holes 418A and 395A is statistically undistinguishable from (1), and that in-situ (log) porosity is also a linear function of slowness (Figure 2):

$$\Phi_f = -(0.35 \pm 0.03) + (2.37 \pm 0.15)\ S_p\ (\text{sec-km}^{-1}) \qquad (2)$$

Equations 1 and 2 can be used to estimate densities and porosities from seismic structures models, as shown in Figure 3: as expected, strong density and porosity gradients are seen to be characteristic of layer 2.

Carlson and Herrick (in press) also applied these relationships to the data reported by Houtz and Ewing (1976) to estimate the rates of change in the properties of layer 2a. They found that layer 2a thins at a rate of 20-45 in per m.y. while the velocity increases by about 0.04 km $-s^{-1}$ - $m.y.^{-1}$. The corresponding rates of change of density and porosity are 0.016 ± 0.009 mg m^{-1} $m.y.^{-1}$, and 0.005 ± 0.003 $m.y.^{-1}$, respectively (Figure 4).

These results represent the best available estimates of first-order vertical and lateral variations of the properties of layer 2. A more detailed or refined assessment cannot be made for two reasons: 1) though drilling has shown that progressive alteration does occur (e.g., Salisbury, Scott et al., 1988; Becker, Sakai et al., 1988), there are no significant penetrations of basement less than about 110 or more than 10 million years old, and 2) the seismic data presented by Houtz and Ewing (1976) almost 15 years ago remains the only data set that addresses systematic, lateral (age-dependent) changes in seismic velocity structure.

Recommendation: A crustal aging experiment should be conducted on the 395 - 418 transect in the Western Atlantic. The first phase should consist of a detailed seismic survey along the entire transect with the objective of documenting lateral changes in the seismic structure of layer 2. Based in part on the seismic survey results, at least two new holes should be drilled to a sub-basement depth of >500m in the important age interval 10-50 Ma. There will then be four boreholes on the transect which can be used to interpret the seismic structures along the same transect.

References

Carlson, R.L. and C.N. Herrick, Densities and porosities in the oceanic crust and their variations with depth and age, *J. Geophys. Res.*, in press.

Becker, K., H. Sakai et al., Proc. ODP, *Init. Repts., Pt. A, 111*, Ocean Drilling Program, College Station, TX, 1988.

Carlson, R.L. and G.S. Raskin, Density of the ocean crust, *Nature, 311*, 555-558, 1984.

Christensen, N.I. and M.H. Salisbury, Structure and constitution of the lower oceanic crust, *Res., Geophys, 13*, 57-86, 1975.

Houtz, R. and J. Ewing, Upper crustal structure as a function of plate age, *J. Geophys. Res., 81*, 2490-2498, 1976.

Spudich, P. and J. Orcutt, A new look at the seismic velocity structure of the oceanic crust, *Rev. Geophys., 18*, 627-645, 1980.

Salisbury, M.H., J.H. Scott et al., *Proc. ODP, Sci. Results, 102*, Ocean Drilling Program, College Station, TX, 1988.

Figure Captions

Figure 1 Wet-bulk vs P-wave slowness in laboratory samples from ophiolites and from the upper oceanic crust. Velocities were measured at 40 MPa confining pressure under water-saturated conditions. 'Miscellaneous' includes rock types such as serpentinites and amphibolites which are present but not abundant in the oceanic crust. Solid line is best fit of density on slowness (eq. 2a); dashed lines represent rms error (from Carlson and Raskin, 1984).

Figure 2 Weighted least squares fits of in-situ density and porosity on slowness from Holes 418A and 395A. Error bars indicate 95 percent confidence limits of mean densities and porosities. Solid lines indicate best fits to the data; light lines indicate standard error.

Figure 3 Selected velocity, density and porosity profiles. Densities and porosities estimated from seismic velocity profiles: MA140 (Purdy, 1983), DW121N (Kennett and Orcutt, 1976), DW34 (Kennett and Orcutt, 1976), VMO (Vera and Mutter, 1988). Height of each box represents depth interval, width represents standard deviation.

Figure 4 Variations of layer 2a properties with age of seafloor. Velocity, thickness, and age data from Houtz and Ewing (1976); open circles indicate data from the Atlantic, solid circles indicate data from the Pacific. Error bars indicate standard deviations of the means. Heavy line indicates weighted least-squares fit; light lines indicate standard error of estimate.

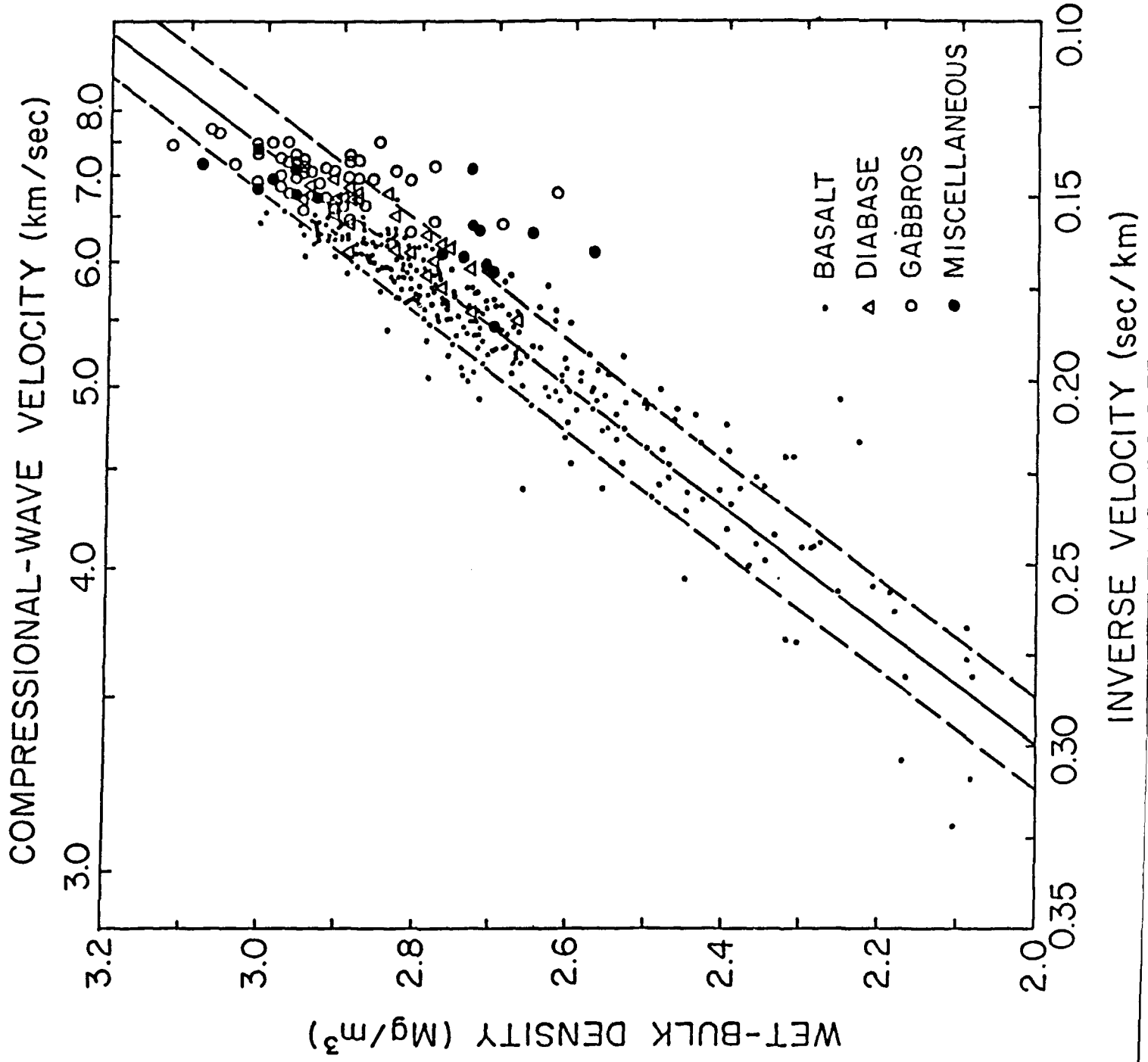

Figure 1 Wet-bulk vs P-wave slowness in laboratory samples from ophiolites and from the upper oceanic crust. Velocities were measured at 40 MPa confining pressure under water-saturated conditions. 'Miscellaneous' includes rock types such as serpentinites and amphibolites which are present but not abundant in the oceanic crust. Solid line is best fit of density on slowness (eq. 2a); dashed lines represent rms error. (From Carlson and Raskin, 1984.)

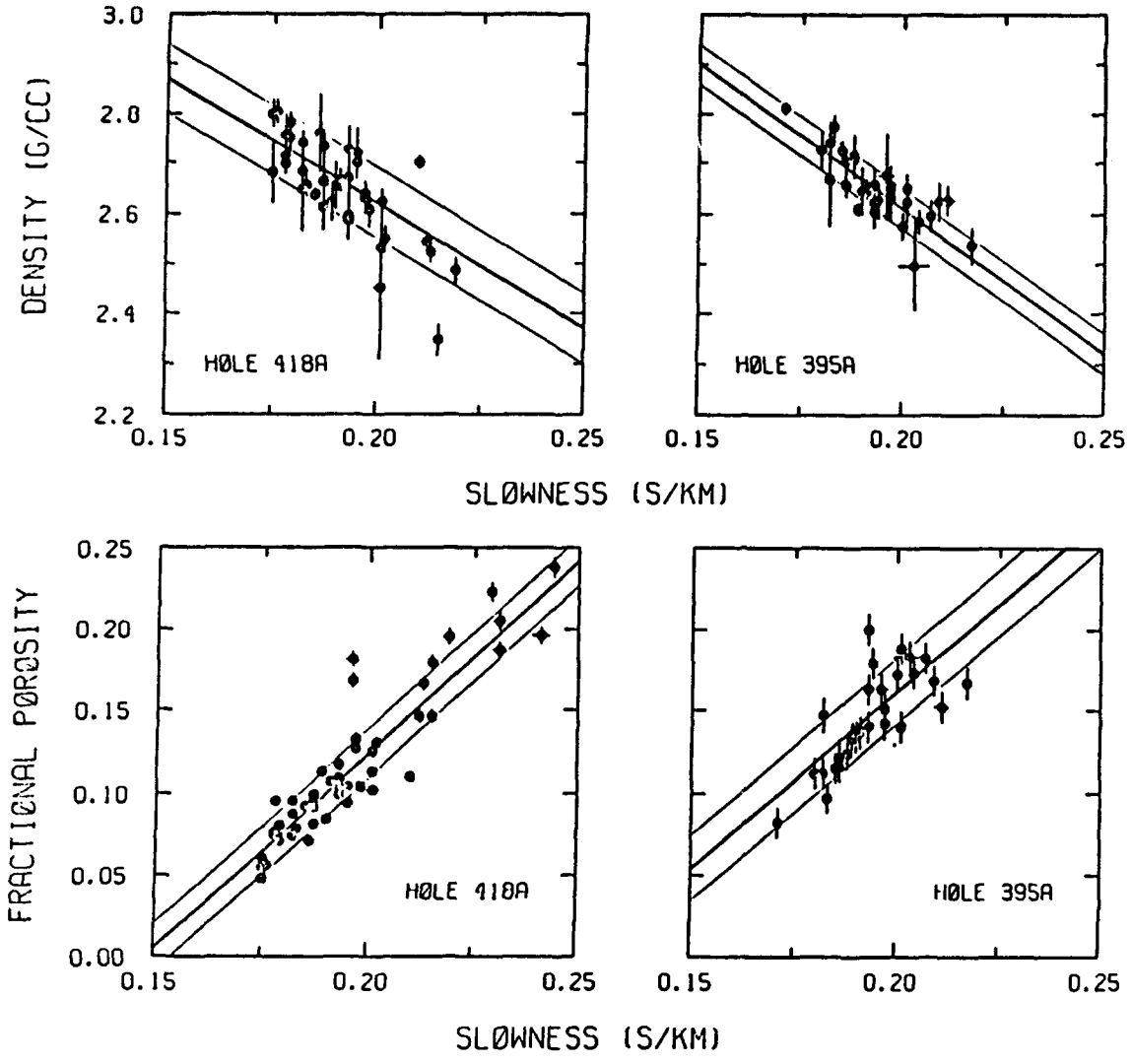

Figure 2. Weighted least squares fits of in situ density and porosity on slowness from Holes 418A and 395A. Error bars indicate 95 percent confidence limits of mean densities and porosities. Solid lines indicate best fits to the data; light lines indicate standard error.

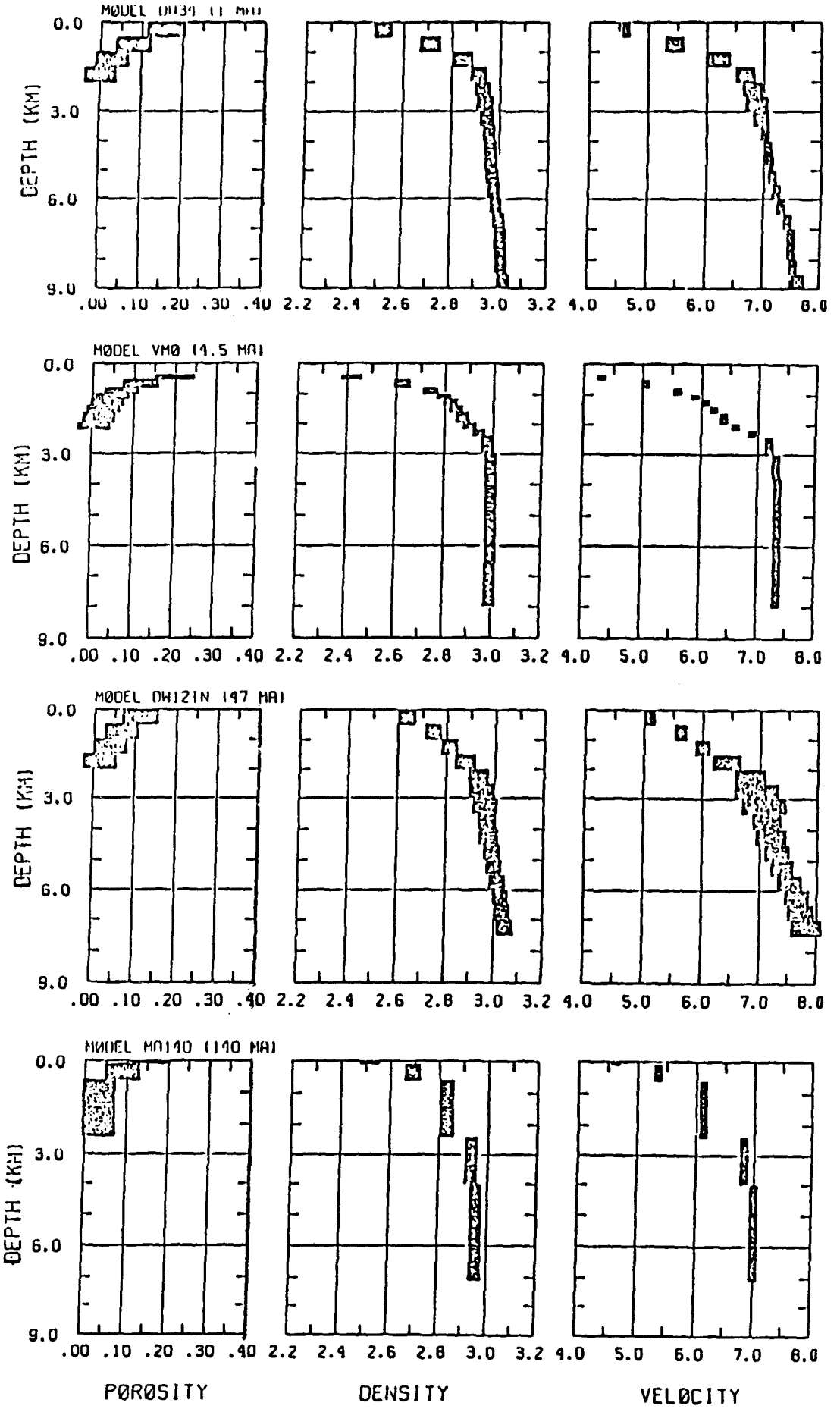

Figure 3. Selected velocity, density and porosity profiles. Densities and porosities estimated from seismic velocity profiles: MA140 (Purdy, 1983), DW121N (Kennett and Orcutt, 1976), DW34 (Kennett and Orcutt, 1976), VMO (Vera and Mutter, 1988). Height of each box represents depth interval, width represents standard deviation.

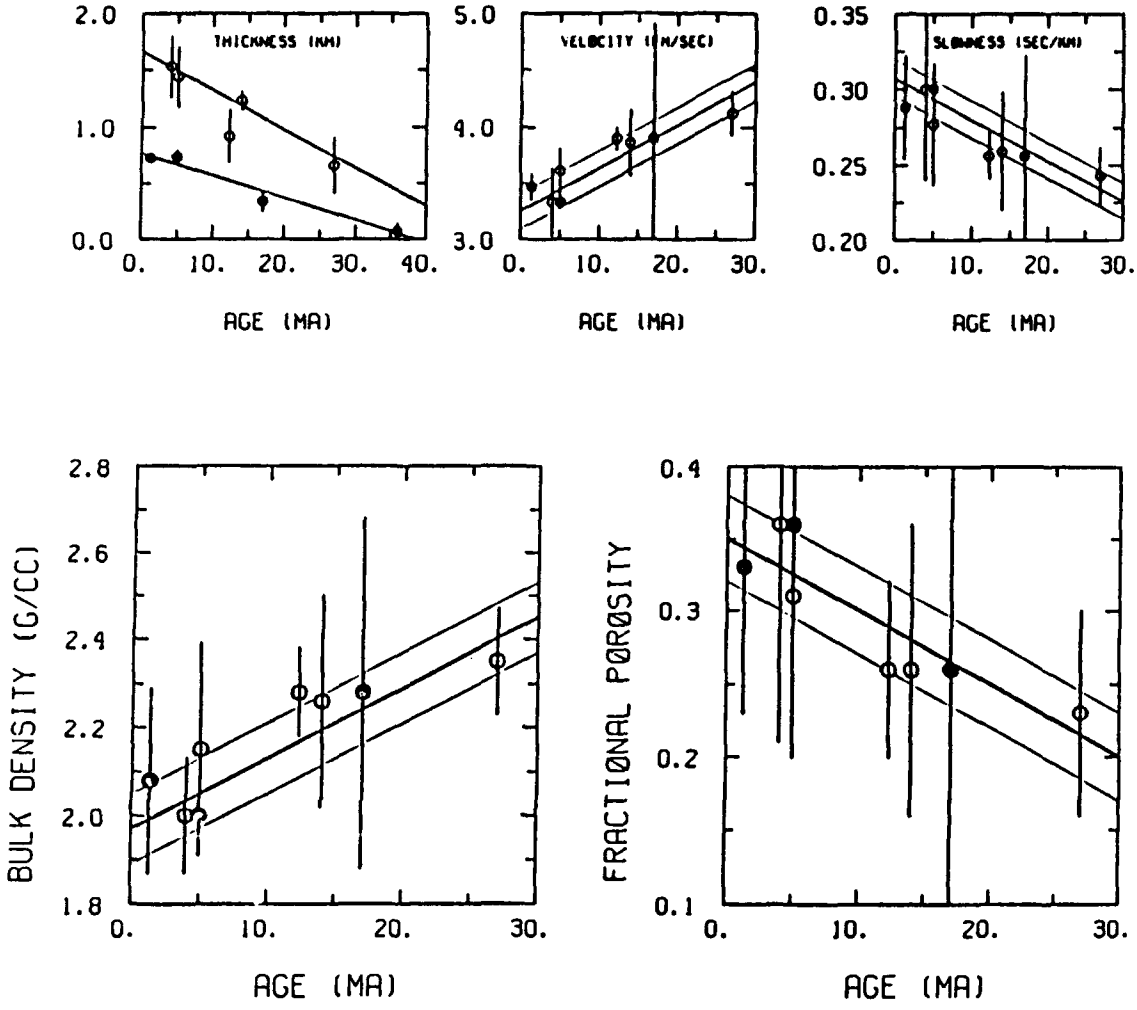

Figure 4. Variations of layer 2a properties with age of sea floor. Velocity, thickness, and age data from Houtz and Ewing (1976); open circles indicate data from the Atlantic, solid circles indicate data from the Pacific. Error bars indicate standard deviations of the means. Heavy line indicates weighted least-squares fit; light lines indicate standard error of estimate.

EVOLUTION OF POROSITY AND SEISMIC PROPERTIES OF SHALLOW OCEANIC CRUST

R. Wilkens, J. Karsten, and G. Fryer
Hawaii Institute of Geophysics

It has long been recognized that the seismic properties of shallow igneous crust are dominated by porosity effects. The goal of our research is to quantify the ways in which bulk porosity, pore geometry, and pore-filling materials control the velocity profile in the light of rock physics theory, laboratory results and field observations. The importance of porosity is due to large differences between seismic properties of basalts and the fluids or alteration assemblages which fill veins and pores. Constraints on the detailed three-dimensional geological structure of shallow oceanic crust can be derived from seafloor and ophiolite observations (e.g., Coleman, 1977; Macdonald, 1982; Adamson, 1985; Anderson et al., 1982; Becker et al., 1989; Nicolas, 1989). The basic structure of the extrusive layer is introduced by volcanic processes occurring at the ridge axis, but there can be significant variability at the scale of several tens of meters in the dimensions of individual flows and flow morphology (pillows versus massive flows). These differences largely depend on tectonic setting (e.g., fast versus slow spreading rate) or stage of the volcanic cycle (e.g., waxing or waning magma supply). Pore space is introduced into this basic structure in several fashions and at a variety of scales, including: microcrack formation during cooling and contraction, vesiculation during eruption, development of large gaps between flow fronts, in collapsed pillows and lava tubes, or in collapse pits of ponded flows. Superimposed on this structure are the effects of tectonic deformation, primarily in the form of fissuring and faulting initiated near the plate boundary zone.

Pore space introduced during the volcanic and tectonic events associated with crustal accretion is later modified by mechanical, weathering, and metamorphic processes. As the crustal pile builds up at the axis, auto-brecciation of flow tops, compaction of collapse features, compression of fractures and late-stage dike intrusion all contribute to a sealing of larger scale void space deeper in the section. As the crust ages, seawater interacts with the basalt, leading to a variety of alteration assemblages which depend on the temperature, pressure and oxygen fugacity of the fluid. Examples of the processes involved in aging are: palagonitization of glassy rinds, cementation of microcracks with anhydrite, carbonates, zeolites and higher temperature assemblages, such as chlorite, quartz and sulfides, and pervasive replacement of the primary igneous phases with clays and zeolites. Results from ophiolites and drill core samples reveal three main zones within the upper kilometer of oceanic crust (e.g., Bednarz and Schminke, 1989; Honnorez et al., 1983; Alt, et al., 1986): an upper region characterized by oxidative cold seawater alteration, a middle region of low temperature seawater interaction and zeolite facies metamorphism, and a deeper region of hot seawater interaction and greenschist facies metamorphism. At sites where high temperature hydrothermal fluids have exited, the crust may be extensively veined at shallow levels with quartz/sulfide assemblages, even at the scale of major fractures.

Alteration effects have intricate feed-back loops with the porosity of the rock matrix. Precipitation along fractures clogs fluid transport pathways, making convective cooling less efficient. This may allow temperature gradients to increase locally, causing some phases to dissolve and others to precipitate. Expansion associated with the volume change of clay formation, however, may cause the formation of new cracks. The wide-spread occurrence of cross-cutting veins in basalts recovered from the seafloor attests to the complex metamorphic history of the oceanic crust (e.g., Alt et al., 1986). Since interconnected void space acts as a conduit for fluid movement, thin cracks tend to close earlier than dispersed

voids. In-filling of open fractures will tend to increase seismic velocities by reducing porosity and changing the aspect ratio of pore spaces which remain open. However, pervasive replacement of the minerals of the basalt with lower density clays and zeolites will generally reduce the matrix seismic velocities. Clearly it is necessary to consider all of these complex effects when trying to relate seismic data to geological structure.

A comparison of well-log compressional wave velocity profiles from DSDP/ODP Holes 504B and 418A (Figure 1) illustrates differences in upper crustal seismic structure. The data have been smoothed with a 10m running average to emphasize larger scale features. Hole 504B, approximately 5 my old, has a relatively high velocity cap, underlain by an interval of low but steadily increasing compressional wave velocity. Hole 418A, on the order of 100 my old, does not exhibit the same low velocities near the top of basement as are seen at Site 504. Other differences in the crust at the two sites can be seen in a plot of the compressional wave velocity versus porosity of samples taken from core at the two holes (Figure 2). While the logging velocities at Hole 418A are generally faster (for a given depth) than those at Hole 504B, the velocities of the samples from Hole 418A are slower (for a given porosity) than those of Hole 504B. Either dataset can be explained by differences in porosity and/or pore geometry, cement, and framework (solid rock) properties. Each velocity profile that is collected in the oceans will probably be the result of a unique set of these factors.

In order to investigate the sensitivity of a velocity profile to the various influences discussed above, we have constructed models of the upper 500m of the oceanic crust based on the rock physics theory of Kuster and Toksöz, 1974, and Cheng and Toksöz, 1979. The Kuster-Cheng-Toksöz theory calculates moduli and velocities of rocks, given framework and pore fluid properties and the distribution of porosity into a spectrum of randomly oriented pores of differing aspect ratio (aspect ratio being defined as the ratio of the lengths of the minor and major axes of an ellipse.) Compressional wave velocity and porosity versus depth for two of the models (generic "FAST" and "SLOW" profiles) are displayed in Figure 3. Each model consists of 100 layers, with each layer having a distinct porosity distributed amongst eight aspect ratios. Compressional wave travel times have been averaged over 10m. Aspect ratio distributions for the models at two depths are shown in Figure 4. These models assume that the framework is fresh basalt (no alteration) and that the pore fluid is seawater. Intervals of lower porosity that increase in abundance with depth are meant to represent massive units (dikes, sills).

The SLOW and FAST models illustrate the manner in which crustal velocities may differ substantially with only a small difference in porosity. The shaded portion of the porosity profile represents the disparity in porosity between the two models. Nowhere in the column does the porosity differ by more than 1%. This small change in porosity, produced by sealing (removing) the lowest aspect ratio cracks from the SLOW model (Figure 4) is sufficient to increase the compressional wave velocity near the top of the basement by 0.7 km/sec and at greater depths by nearly 0.5 km/sec. It should also be noted that while the difference between the two profiles is due to the presence or absence of low aspect ratio pores, the difference in velocity between the 50m and 250m levels in the model are due mainly to contrasts in the volumes of higher aspect ratio pores.

We have superimposed our SLOW model on the well log velocity profile of Hole 504B and our FAST model on the Hole 418A data (Figure 5). Since our SLOW model was conceptual, constrained only by a velocity of 3.0 km/sec at the top of basement, a velocity over 5.5 km/sec at 500m sub-basement, and our own observations and prejudices, it is encouraging to see how well our model matches data. The SLOW model assumes a surface pillow layer 100m thick which has undergone only a minor amount of pore filling and fracture

sealing. The borehole at Site 504 encountered a massive unit at 35m sub-basement, and may have drilled (but not recovered) another massive basalt at a shallower depth.

Hole 418A also discovered massive basalts at shallow levels in the crust which may be partially responsible for the lack of fit of the FAST model to the well log profile. We note, however, that both pillows and massive units have high velocities at Site 418, suggesting that fracture sealing and pore infilling has progressed further at Site 418 than at Site 504. This conclusion may also be supported by the difference in character of the two velocity profiles. Both the FAST model and the Hole 418A data are smoother than their counterparts, suggesting that the processes that tend to generally increase crustal velocity also work towards reducing velocity contrasts between differing structural layers in the crust.

The total volume, distribution, and aspect ratio of void space all must be considered when assessing the effect of porosity on seismic structure. The nature and geometry of pore space within the upper oceanic crust reflects the integrated volcanic, tectonic, and metamorphic history of the plate as it ages and moves away from the site of crustal accretion. Thus, older and deeper oceanic crust has different porosity and seismic structures than younger and shallower crust. The goal of our research is to develop realistic histories for the geologic structure of shallow (<500 m) oceanic crust emphasizing the evolution of porosity and alteration of the basalt framework, and assess the sensitivity of seismic structure to variations in these histories. This program is a multi-disciplinary, multi-scale effort, which consists of four major phases: analysis of the distribution and evolution of pore space within hand samples, for which seismic properties have been determined, extension of porosity-velocity theories to handle high porosity situations typical of young oceanic crust, construction of numerical models for the elastic properties of specific geologic settings which are based on seafloor and ophiolite observations, and investigation and comparison of these models with synthetic seismograms. Results of the study will lead to both a better understanding of existing data and help to formulate the nature of future investigations.

REFERENCES

Adamson, A.C., Basement lithostratigraphy, DSDP Hole 504B, *Init. Repts. DSDP, 83*, Washington (U.S. Govt. Printing Office), 121-127, 1985.

Alt, J.C., J. Honnorez, C. Laverne, and R. Emmerman, Hydrothermal alteration of a 1 km section through the upper oceanic crust, Deep Sea Drilling Project Hole 504B: mineralogy, chemistry, and evolution of seawater-basalt interactions, *J. Geophys. Res., 91*, 10309-10355, 1986.

Anderson, R.N., et al., DSDP Hole 504B, the first reference section over 1 km through layer 2 of the ocean crust, *Nature, 300*, 589-594, 1982.

Becker, K. et al., Drilling deep into young oceanic crust, Hole 504B, Costa Rica Rift, *Rev. of Geophysics, 27*, 79-102, 1989.

Bednarz, U. and H.U. Schminke, Mass transfer during sub-seafloor alteration of the upper Troodos crust (Cyprus), *Contrib. Mineral. Petrol., 102*, 93-101, 1989.

Cheng, C.H., and M.N. Toksöz, Inversion of seismic velocities for the pore aspect ratio spectrum of a rock, *J. Geophys. Res., 84*, 7533-7543, 1979.

Christensen, N.I., S.C. Blair, R.H. Wilkens, and M.H. Salisbury, Compressional wave velocities to 6 kilobars, densities and porosities of basalts from HOLES 417A, 417D, and 418A, DSDP Legs 51-53, *Init. Repts. DSDP, 51-53*, Washington (U.S. Govt. Printing Office), 1467-1472, 1979.

Coleman, R.G., Ophiolites. Ancient oceanic lithosphere?, Springer-Verlag, Berlin, 1977.

Honnorez, et al., Stockwork-like sulfide mineralization in young oceanic crust: Deep Sea Drilling Project Hole 504B, *Init. Repts. DSDP, 83*, Washington (U.S. Govt. Printing Office), 263-282, 1985.

Kuster, G.T., and M.N. Toksöz, Velocity and attenuation of seismic waves in two phase media: Part 1. Theoretical formulations, *Geophysics, 39*, 587-606, 1974.

Macdonald, K.C., Mid-ocean ridges: Fine scale tectonic, volcanic, and hydrothermal processes within the plate boundary zone, *Ann. Rev. Earth Planet. Sci., 10*, 155-190, 1982.

Nicolas, A., Structural Studies of Ophiolites and Dynamics of Ocean Lithosphere, Kluwer Academic Publishers, Amsterdam, 1989.

Salisbury, M.H., N. I. Christensen, K. Becker, and D. Moos, The velocity structure of layer 2 at Deep Sea Drilling Project Site 504B from logging and laboratory experiments, *Init. Repts. DSDP, 83*, Washington (U.S. Govt. Printing Office), 529-539, 1985.

Wilkens, R.H., N.I. Christensen, and L. Slater, High pressure studies of Leg 69 and 70 basalts, *Init. Repts. DSDP, 69-70*, Washington (U.S. Govt. Printing Office), 683-686, 1983.

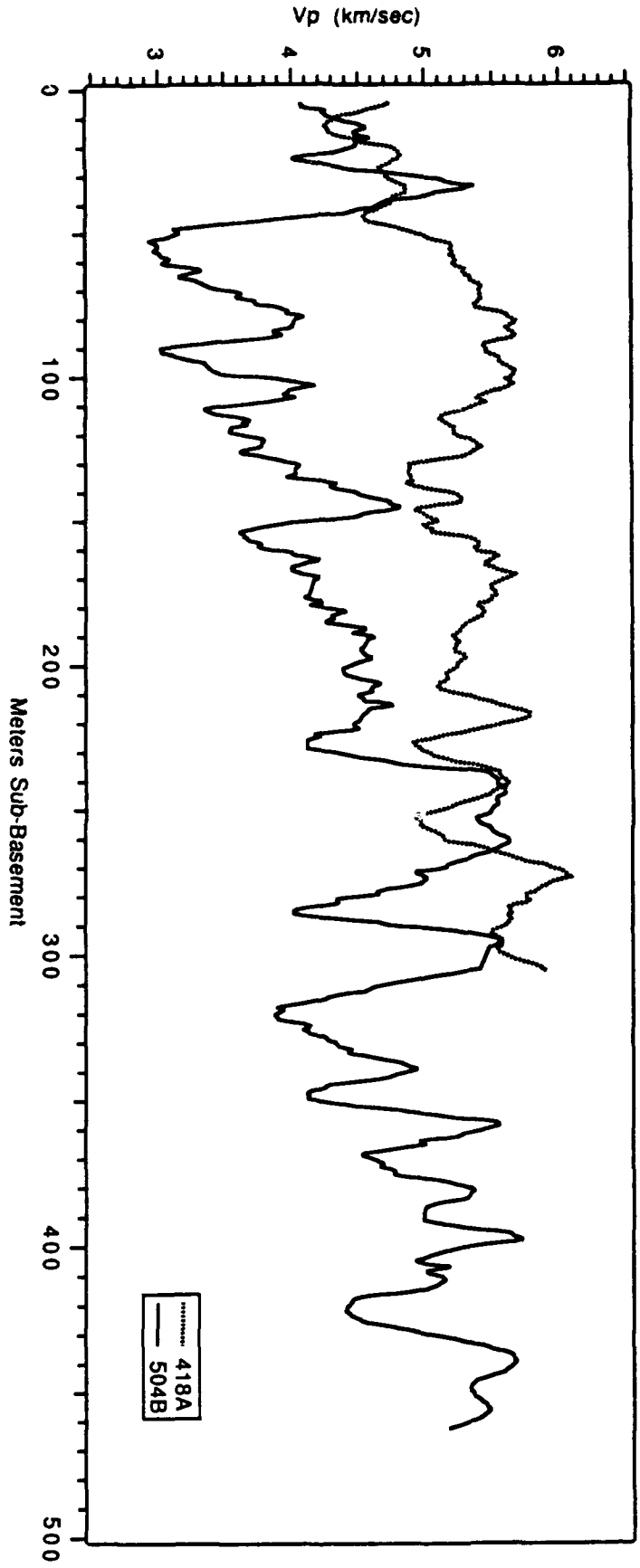

Figure 1. Compressional wave velocity logs from DSDP-ODP Holes 418A and 504B. Only the upper 500 m of basement is shown for Hole 504B. Data have been smoothed with a 10 m running average of travel time.

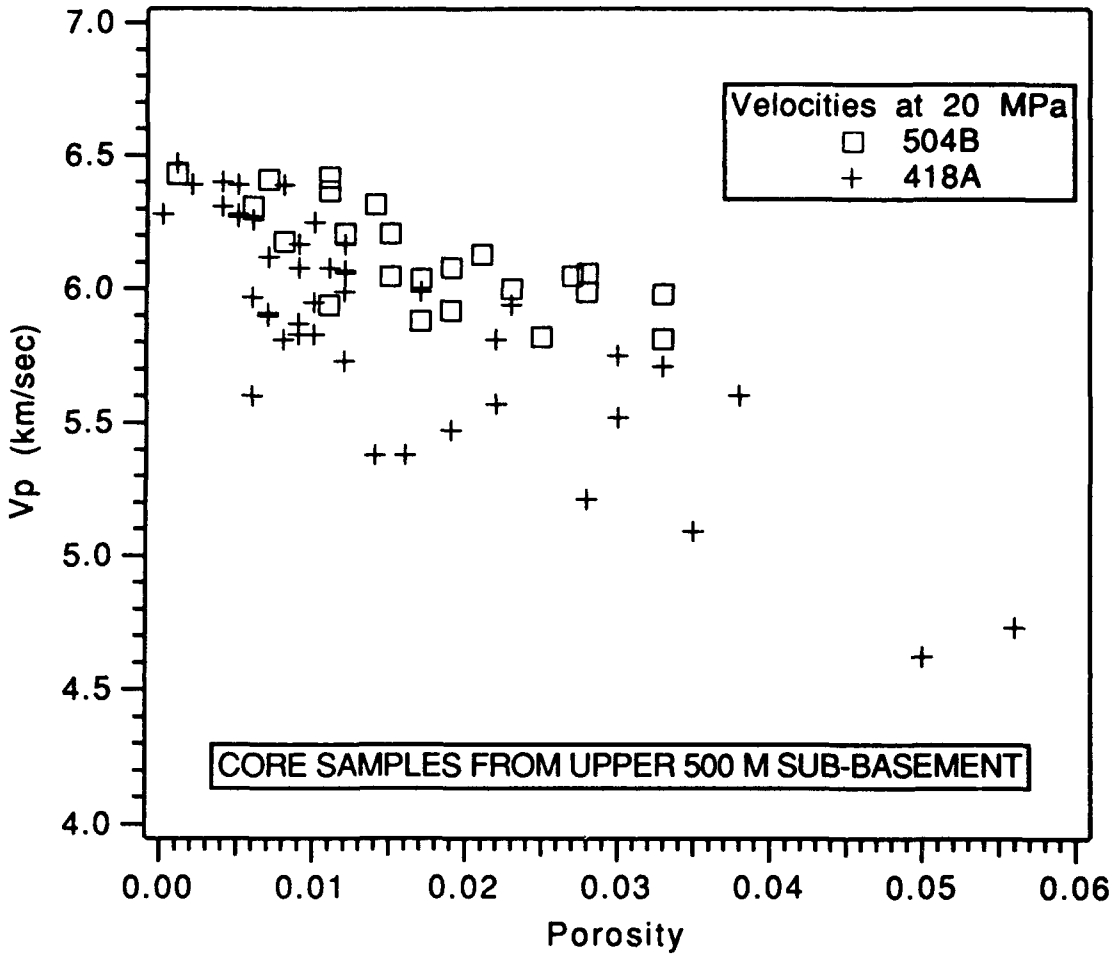

Figure 2. Compressional wave velocities of core samples versus porosity. Measurements were made at 20 MPa confining pressure. Data from Christensen et al., 1979, Wilkens et al., 1983, and Salisbury et al., 1985.

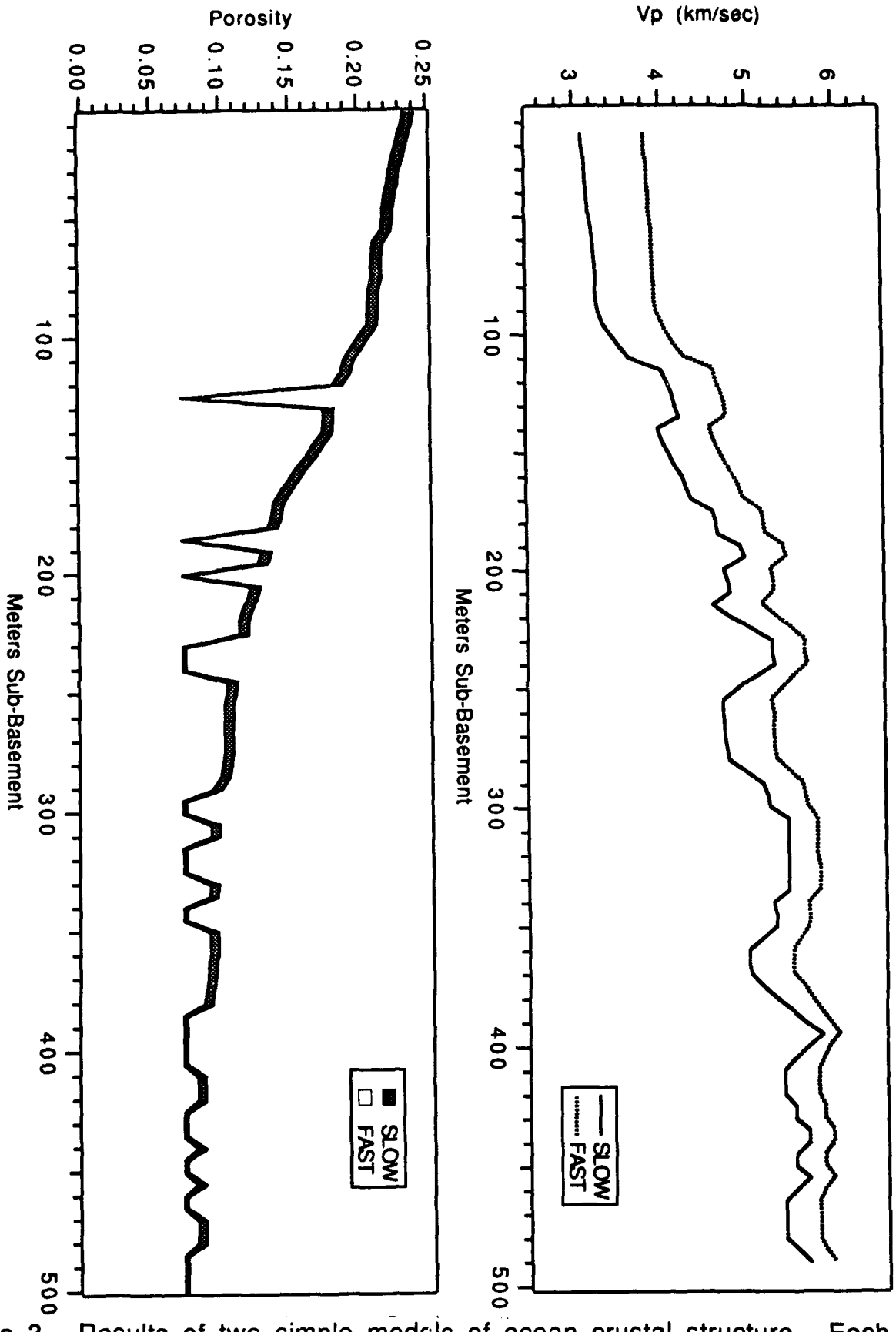

Figure 3. Results of two simple models of ocean crustal structure. Each model contains 100 layers. Each layer comprises porosity distributed amongst 8 different aspect ratios. Velocities were calculated using the theory of Kuster and Toksoz, 1974, and Cheng and Toksoz, 1979. Data were smoothed with a 10 m running average of travel time.

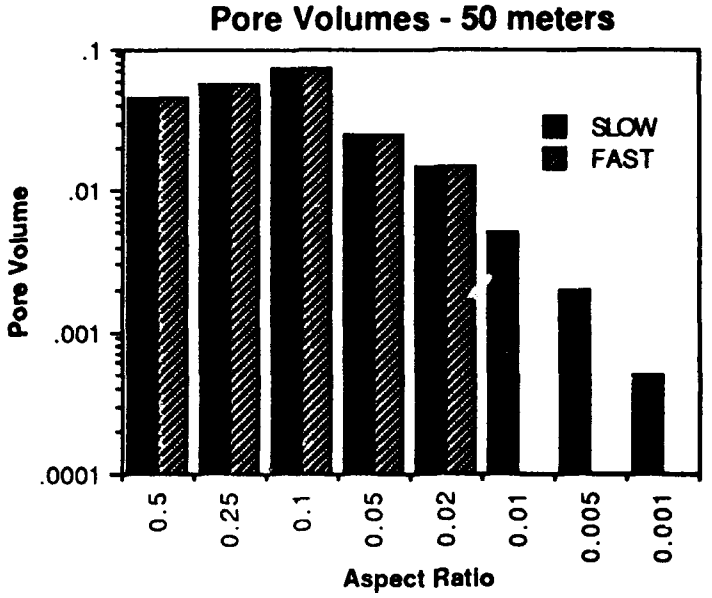

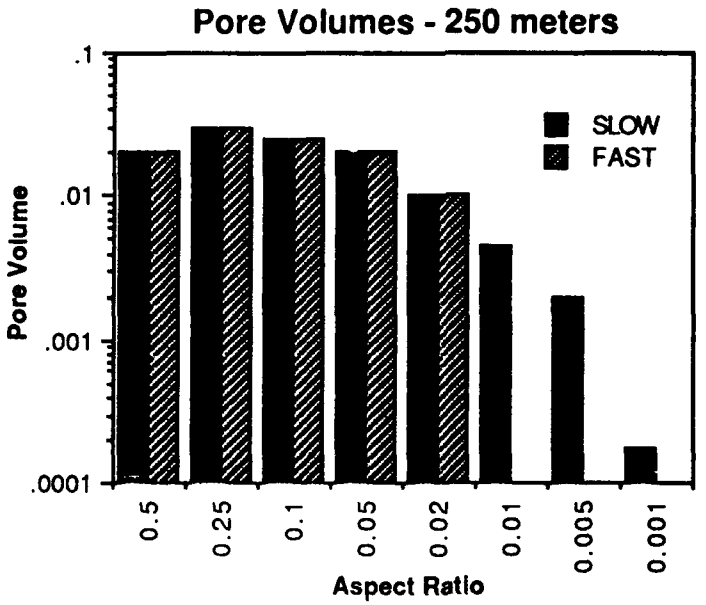

Figure 4. Pore abundance spectrum of two layers from the SLOW and FAST models. The difference in velocity between 50 and 250 m is primarily due to a reduction in volume of pores with aspect ratios greater than 0.01, while the difference between the two models at either depth is a result of the presence of low aspect ratio pores in the SLOW model.

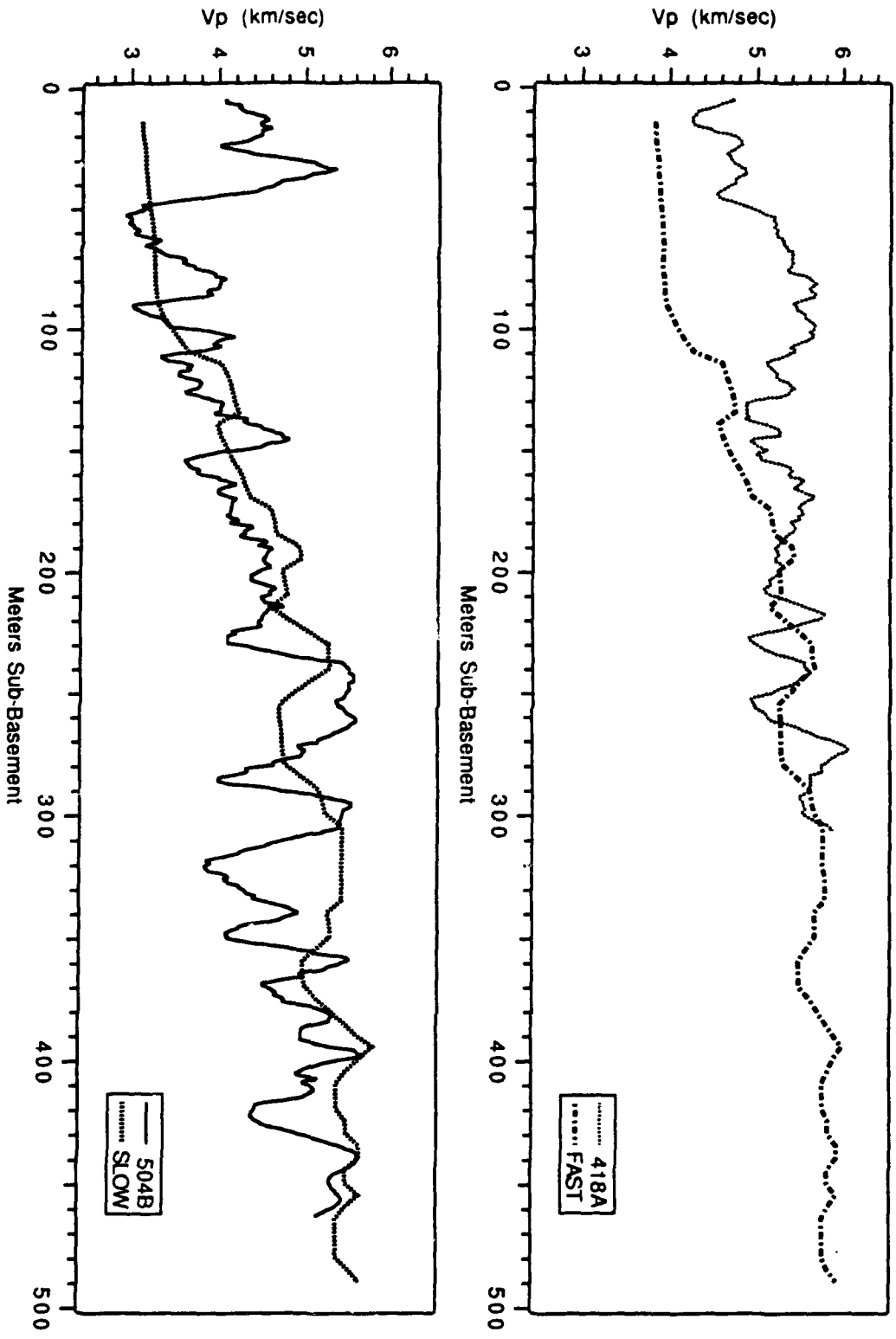

Figure 5. Comparison of logging data with FAST and SLOW models.

SHEAR MODULUS AND POROSITY MEASUREMENTS OF DEEP OCEAN FLOOR

Tokuo Yamamoto and Altan Turgut
Rosenstiel School of Marine and Atmospheric Sciences
University of Miami
Miami, FL 33149

Abstract

An entirely new method for the remote sensing of seabed geophysical properties has recently been developed at the Geo-Acoustics Laboratory. This method, names the Bottom Shear Modulus Profiler (BSMP), uses gravity water wave-induced motion of seabed measured by a buried OBS to extract the shear modulus vs. depth profile of sediment. The mathematical uniqueness and consistency of the BSMP method were demonstrated by Yamamoto and Torii, [1]. Experimental verifications of the BSMP method by comparisons with borehole data at various locations were given by Trevorrow et al., [2] Badiey et al., [3] and Turgut et al., [4]. Existing BSMP system is capable of measuring the seabed shear modulus profile with a maximum resolution of a few meters.

The BSMP method is applicable to the seabeds of deep oceans as well as shallow seas, because the oceans are covered with continuous spectra of gravity water waves ranging from 0.001 to 1 Hz. The BSMP method is potentially capable of measuring the seabed shear modulus profile with a maximum penetration of 20 km into the seabed with depth resolutions of 200m. The lateral resolution of BSMP is about one wavelength or about 6 km in deep ocean.

Introduction:

For the past five years, the Geoacoustics Laboratory at the University of Miami has been undertaking intensive research on remote sensing of sea floor in shallow water. This research utilizes Ocean Bottom Seismometers (OBSs) buried in the seafloor, and includes both theoretical and experimental studies of forward and inverse problems. A theory has been developed for remote sensing of shear modulus structure of seabed using the energy that propagates as natural gravity water waves [1]. In addition to inversion for shear modulus structure of sea floor, the BSMP method is capable of determining the seabed porosity [5]. The physical properties which control acoustic propagation in shallow sediments - shear modulus, porosity, and permeability - are also important in controlling several key processes in deep oceanic sediments and crust, particularly hydrogeological processes, the alteration of the crust, and diagenesis of the sediments. In this paper, we present some experimental results from shallow water measurements and give some numerical examples for deep water applications.

Experimental results from shallow water measurements:

Application of the BSMP method to a real data set collected from New Jersey Shelf can be found in Trevorrow et al. [2]. A comparison of shear modulus profiles obtained from BSMP method and AMCOR coring project [6] data for AMCOR 6010 site (150 km off the coast of New Jersey in 70m of water depth) is given in Figure 1. It can be seen from Figure 1 that there is good agreement between inverted and reference profiles. In Figure 2, porosity profiles converted from the BSMP inverted shear modulus profiles are compared with the borehole porosity logs at AMCOR 6010 site [5]. Resolution and penetration of

porosity predicted by BSMP method are identical to those of the shear modulus predictions. Resolution is determined by the shortest wavelength and penetration determined by longest wavelength in the measured gravity wave spectrum. Existing geophysical methods for measurements of the seabed porosity utilize the effect of seabed electric conductivity on the applied electromagnetic fields, with a limited depth resolution and penetration (e.g., MOSES method). The BSMP method for prediction of porosity seems to have better depth resolution and penetration than these electromagnetic methods.

Applicability of BSMP method to deep water site:

The BSMP method is also applicable to the deep oceans because of the existence of continuous spectra of gravity, wave energy in the oceans ranging from 0.001 to 1 Hz. The deep water BSMP system utilizes the energy between 0.005 and 0.03 Hz which corresponds to infragravity waves. Pressure fluctuations due to infragravity waves have been measured on the seafloor off southern California by Webb and Cox [7].

Because the phase velocity of gravity waves ($\sqrt{gh}$) is of the order of 200 m/s in deep water, which is much slower compared to seismic waves, the response of the seafloor to gravity waves will be essentially equivalent to that of static loading. By correlating the pressure and the vertical acceleration as a function of wavelengths, some properties (shear modulus, porosity, and shear and compressional wave velocities) can be deduced as a function of depth into the earth.

Figure 3 shows the calculated vertical and horizontal admittances (ratio of seabed displacement to wave height) caused by surface gravity wave pressure fluctuations on the sea floor (water depth = 2800m). Two different shear modulus profiles (Case.1 and Case.2) are used to test our BSMP inversion method. In Figure 3b, inverted shear modulus profiles are compared with the input shear modulus profiles. The penetration is 15 km with resolution of 200m at the top 1000m, and 500 to 1000m at the deeper layers. Note the slow velocity layers at 5 km and 8 km also were able to be depicted using the admittance data have 1% uncertainty. Porosity, shear wave velocity, and compressional wave velocity profiles can also be inverted using empirical relations (see Yamamoto et al. [5] and Turgut et al. [8]). Figure 4 shows inverted porosity, shear wave and compressional wave velocities from the shear modulus profiles in Figure 3b.

Conclusion:

Determination of shear modulus structure of upper ocean crust is possible with the BSMP method. In addition, this information can be used to invert porosity, shear wave velocity, and compressional wave velocity of the sea floor.

References:

1. T. Yamamoto, and T. Torii, Seabed Shear Modulus Profile Inversion Using Surface Gravity (Water) Wave-induced Bottom Motion, Geophys. *J.R. Astr. Soc., 85*, 413-431, 1986.

2. M. Trevorrow, T. Yamamoto, M. Badiey, A. Turgut, and C. Conner, Experimental Verification of Seabed Shear Modulus Profile Inversions Using Surface Gravity (Water) wave-Induced Seabed Motion, *Geophys. J. Int., 93(3)*, 419-436, 1988.

3. M. Badiey, T. Yamamoto, A. Turgut, R. Bennett, and C. Conner, Laboratory and in situ Measurements of Selected Geoacoustic Properties of Carbonate Sediments, *J. Acoust. Soc. Am., 84*, 689-696, 1988.

4. A. Turgut, T. Yamamoto, M. Badiey, M. Trevorrow, and C. Conner, Bottom Shear Modulus Profiler, A Remote Sensing Instrument, Current Practices and New Technology in Ocean Engineering, 13, 87-96, 1988.

5. T. Yamamoto, M. Trevorrow, M. Badiey, A. Turgut, Seabed Porosity and Shear Modulus Inversion Using Surface Gravity (Water) Wave Induced Seabed Motion, *Geophys. J. Int., 98(1)*, 173-182, 1989.

6. J.C. Hathaway, J.S. Schlee, C.W. Poag, P.C. Valentine, E.A.G. Weed, M.H. Bothner, F.A. Kohout, F.T. Manheim, R. Schoen, R.E. Miller, and D.M. Schultz, Preliminary Summary of the 1976 Atlantic margin coring project, U.S. Geol. Survey, Open File Report No. 76-944, 1976.

7. S.C. Webb, and C.S. Cox, Observations and Modeling of Seafloor Microseisms, *J. Geophys. Res., 91*, 7343-7358, 1986.

8. A. Turgut, T. Yamamoto, C. Abbott, D. Goodman, M. Trevorrow, and M. Badiey, A Real-time Seismic Array for Seafloor Classification and Directional Spectra Observations, ASME's 4th ETCE Conference, 1966 New Orleans.

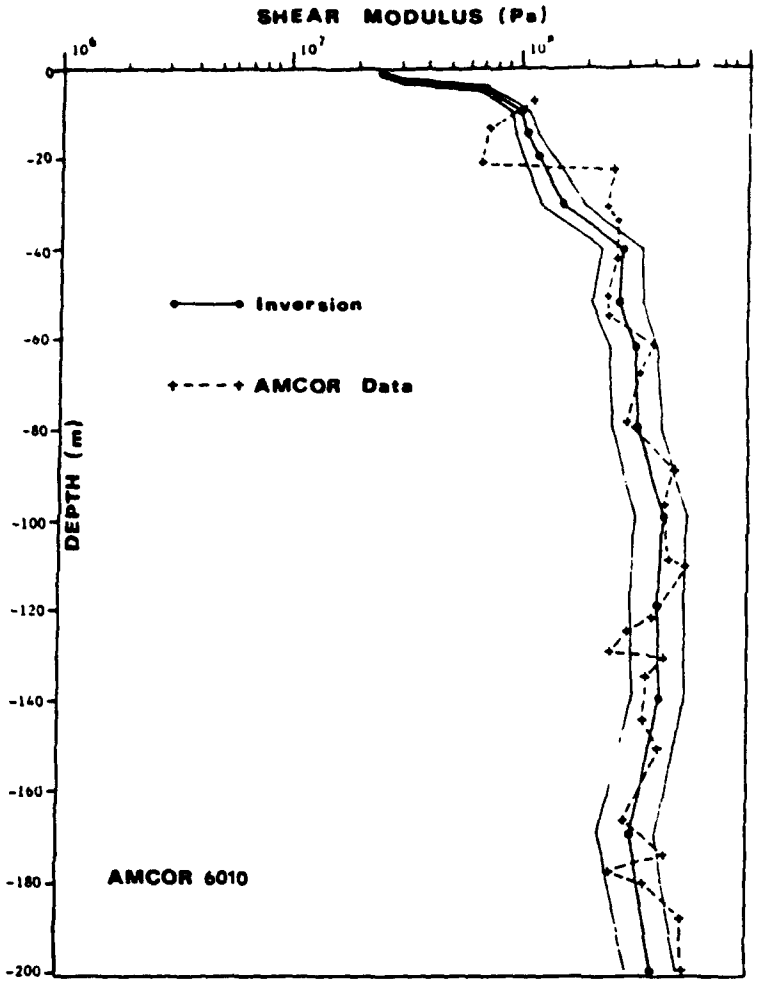

Figure 1. Comparison between inverted shear modulus profile and borehole data at AMCOR 6010 site.

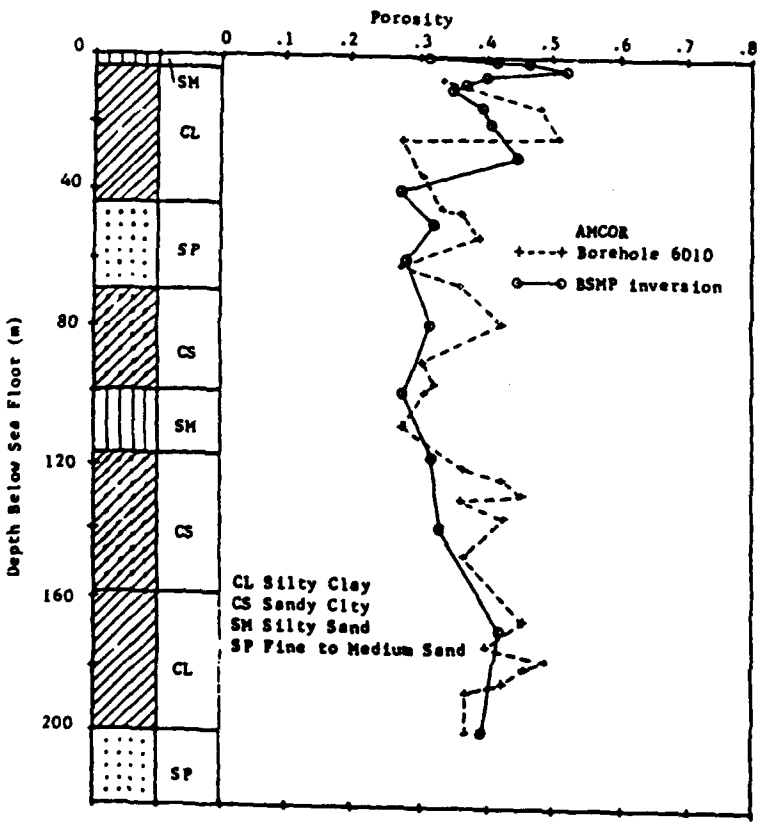

Figure 2. Stratigraphic column, porosity profile measured from cores and density log of AMCOR 6010 borehole [6]. Porosity profile converted from BSMP shear modulus profile are also plotted for comparison

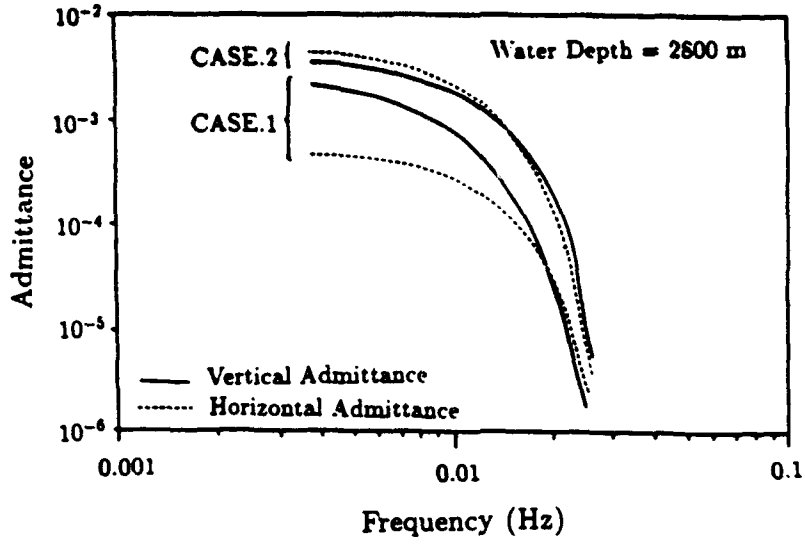

(a)

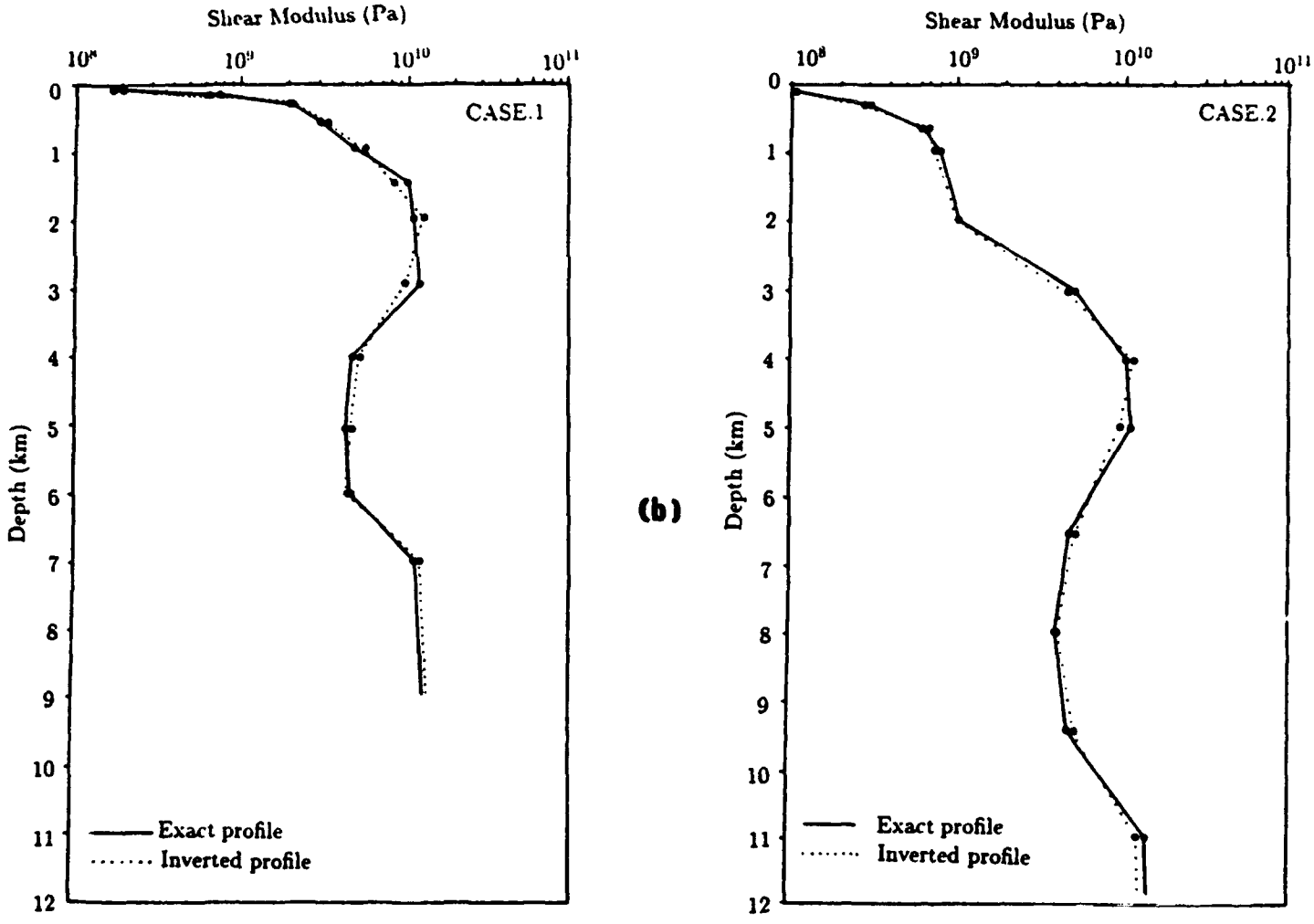

(b)

Figure 3. a) Admittance at the seafloor caused by surface gravity waves. b) inverted shear modulus profiles using the admittance values in (a) with 1% uncertainty.

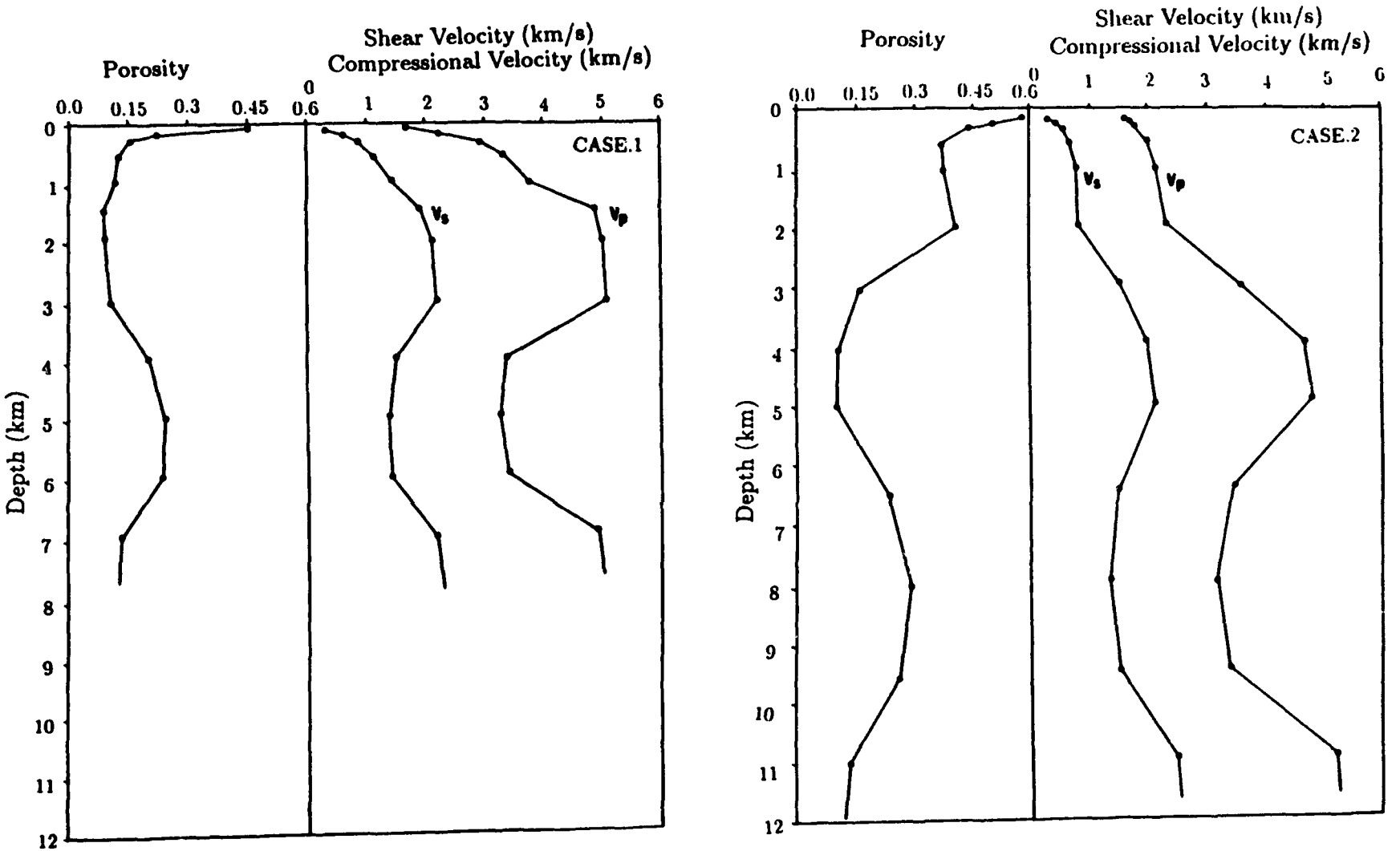

Figure 4. Inverted porosity and compressional and shear wave velocities from shear modulus profiles in Figure 3b.

APPENDIX 1

THE PHYSICAL PROPERTIES OF VOLCANIC SEAFLOOR

Workshop Agenda

Woods Hole Oceanographic Institution, Clark Building, Quissett Laboratories, April 24-26, 1990

Tuesday, April 24th

0730: Coffee and pastries, Registration, Clark Building, 5th floor

0800: Introduction and description of the Workshop Plan: Mike Purdy and Gerard Fryer

KEYNOTE PRESENTATIONS: Clark Building 5th Floor, Chairman, D. Bibee

1) *ACOUSTICS*

0900: Effects of the Upper Crust on the Prediction of the Acoustic Wave Field (30 mins., 15 mins. discussion): O. Diachok.

2) *PROCESSES*

0945: Rock-Seawater Interaction (30 mins., 15 mins. discussion): G. Thompson

1030: Coffee Break

1045 The Physical Properties of Volcanic Seafloor: Volcanic Processes (30 mins., 15 mins. discussion): R. Batiza

1130: Tectonic Regulation of the Physical Properties of Ocean Crust (30 mins., 15 mins. discussion): P. Johnson

1215: Lunch

KEYNOTE PRESENTATIONS (cont'd.): Clark Building 5th Floor, Chairman, R. Jacobson

3) *GEOPHYSICAL MEASUREMENTS*

1315: Seismic Structure of the Uppermost 0.5-1 km of Zero Age Crust (20 mins., 10 mins. discussion): J. Diebold and E. Vera

1345: The Evolution in Seismic Structure of the Uppermost 0.5-1 km of Oceanic Crust (20 mins., 10 mins. discussion): G.M. Purdy

1415: Detailed Resolution of the Structure and Physical Properties of the Upper Oceanic Crust Using Downhole Measurements (20 mins., 10 mins. discussion): K. Becker

4) *PHYSICAL PROPERTIES*

1445: Physical Properties of Oceanic Volcanic Rocks (20 mins., 10 mins. discussion): N. Christensen

1515: Coffee Break

1545: Fractures, Cracks and Large Scale Porosity (20 mins., 10 mins. discussion): G. Fryer

1615: Closing Remarks and Formation of the Process Groups: G.M. Purdy and G. Fryer

1700: Poster Session (Recent Results) and Refreshments

1800: Dinner

1930: Process Group Meetings (preliminary one hour discussion)

Volcanics — Chairman, R.S. Detrick — Clark Building 5th Floor

Tectonics — Chairman, B.T.R. Lewis — Clark 201

Alteration — Chairman, J.R. Cann — Clark 237

Acoustics — Chairman, O. Diachok — Clark 4

Wednesday, April 25th

0730: Coffee and pastries, Clark Building 5th Floor

0800: Process Groups Meetings (to review and define scientific objectives)

Volcanics — Chairman, R.S. Detrick — Clark 5th Floor

Tectonics — Chairman, B.T.R. Lewis — Carriage House

Alteration — Chairman, J.R. Cann — Fenno House

Acoustics — Chairman, O. Diachok — Clark 237

1045: Coffee Break, Clark Building 5th Floor

PLENARY SESSION 1: REVIEW OF THE SCIENTIFIC GOALS
Clark Building 5th Floor — Chairman, G. Frisk

1100: Volcanics — R.S. Detrick

1115: Tectonics — B.T.R. Lewis

1130: Alteration — J.R. Cann

1145: Acoustics — O. Diachok

1200: Formation of Technique Groups and Definition of Their Charge

1215: *Lunch*

1315: **TECHNIQUE GROUP MEETINGS** (to begin formulation of the science plan)

Seismo-Acoustics: Discussion Leaders: R. Stephen, L. Dorman and O. Diachok - Clark Building 5th Floor

Downhole and Other Geophysical Measurements: Discussion Leaders: D. Goldberg, D. Moos and P. Johnson - Carriage House

Laboratory Measurements and Bottom Sampling: Discussion Leaders: J. Karson, R. Carlson and R. Wilkens - Fenno House

1530: Coffee Break: Clark 5th Floor

1600: **TECHNIQUE GROUP MEETINGS** (continued)

1800: Poster Session (New Techniques) and Refreshments — Clark 5th Floor

1900: Dinner: Clark Building, 5th Floor

Thursday, April 26th

0730: Coffee and pastries, Clark Building, 5th Floor

0800: **TECHNIQUE GROUP MEETINGS** (continued)

1000: Coffee Break: Clark Building 5th Floor

1015: **DEFINITION OF TASKS FOR PROCESS GROUPS:** Clark Building 5th Floor, G.M. Purdy and Gerard Fryer

1030: **PROCESS GROUP MEETINGS** (to review plans from the Technique groups)

Volcanics: Chairman, R.S. Detrick, Clark 5th Floor
1030: Seismo-Acoustics Group Report: R. Stephen
1100: Downhole and Geophysics Group Report: D. Moos
1130: Laboratory and Sampling Group Report: R. Wilkens

Tectonics: Chairman, B. Lewis, Carriage House
1030: Seismo-Acoustics Group Report: L. Dorman
1100: Downhole and Geophysics Group Report: D. Goldberg
1130: Laboratory and Sampling Group Report: J. Karson

Alteration: Chairman, J.R. Cann, Fenno House
1030: Seismo-Acoustics Group Report: O. Diachok
1100: Downhole and Geophysics Group Report: P. Johnson
1130: Laboratory and Sampling Group Report: R. Carlson

1200: Buffet Lunch, Clark Building 5th Floor

1230: PROCESS GROUPS RECONVENE (to review Science Plans presented by Technique groups, prioritize objectives and write rationale for the proposed activities)

PLENARY SESSION 2: REVIEW OF THE SCIENCE PLAN — Co-Chairmen G.M. Purdy and G. Fryer, Clark Building 5th Floor

1500: Volcanics — R.S. Detrick (10 mins., 10 mins. discussion)

1520: Tectonics — B.T.R. Lewis (10 mins., 10 mins. discussion)

1540: Alteration — J.R. Cann (10 mins., 10 mins. discussion)

1600: Review of Acoustic Objectives: O. Diachok

1620: Closing Remarks: G.M. Purdy and G. Fryer

1630: End of Workshop

APPENDIX 2

— ATTENDEES —

Dr. Ginger Barth
Lamont-Doherty Geological Observatory
Palisades, NY 10964

Dr. Rodey Batiza
Chairman, JOIDES Lithosphere Panel
Hawaii Institute of Geophysics
2525 Correa Road
Honolulu, HI 96822

Dr. Keir Becker
RSMAS
University of Miami
10 Rickenbacker Causeway
Miami, FL 33149

Dr. Dale Bibee
Seafloor Geoscience Division
Marine Geophysics Branch, Code 362
NORDA
NSTL Station, MS 39529-5004

Dr. Bill Bryan
Department of Geology and Geophysics
Woods Hole Oceanographic Institution
Woods Hole, MA 02543

Dr. Richard L. Carlson
Department of Geophysics
Texas A&M University
College Station, TX 77843

Professor J.R. Cann
Department of Earth Sciences
University of Leeds
Leeds LS2 9JT, England

Dr. Robert Cessaro
Teledyne Geotech, Alexandria Labs
314 Montgomery Street
Alexandria, VA 22314

Dr. Nikolas I. Christensen
Department of Geosciences
Purdue University
West Lafayette, IN 47907

Dr. Kathleen Dadey
The University of Rhode Island, GSO
Narragansett Bay Campus
Narragansett, RI 02882-1197

Dr. John R. Delaney
RIDGE Office
University of Washington
School of Oceanography
Seattle, WA 98195

Dr. Robert S. Detrick
University of Rhode Island
Graduate School of Oceanography
Kingston, RI 02882

Dr. Orest Diachok
Naval Research Laboratory
Attention Code 5120
4555 Overlook Avenue, SW
Washington, DC 20375-5000

Dr. Henry J.B. Dick
Department of Geology and Geophysics
Woods Hole Oceanographic Institution
Woods Hole, MA 02543

Dr. John Diebold
Lamont-Doherty Geological Observatory
Palisades, NY 10964

Dr. LeRoy Dorman
Scripps Institution of Oceanography
Geological Research Division, A-015
University of California, San Diego
La Jolla, CA 92093

Professor R. Nigel Edwards
Department of Physics
University of Toronto
Toronto, Ontario M5S 1A7, Canada

Dr. Neil L. Frazer
Hawaii Institute of Geophysics
2525 Correa Road
Honolulu, HI 96822

Dr. George Frisk
Department of Applied Ocean
Physics and Engineering
Woods Hole Oceanographic Institution
Woods Hole, MA 02543

Dr. Gerard J. Fryer
University of Hawaii at Manoa
SOEST
Department of Geology and Geophysics
2525 Correa Road
Honolulu, Hawaii 96822

Dr. Louis Geli
ARGOS, CNES
2 Place Maurice Quentin
75001 Paris, France

Dr. Kathy Gillis
Department of Geology and Geophysics
Woods Hole Oceanographic Institution
Woods Hole, MA 02543

Dr. David Goldberg
Lamont-Doherty Geological Observatory
Palisades, NY 10964

Dr. Alistair Harding
Scripps Institution of Oceanography
University of California, San Diego
IGPP - A-025
La Jolla, CA 92093

Dr. Stan Hart
Department of Geology and Geophysics
Woods Hole Oceanographic Institution
Woods Hole, MA 02543

Dr. John A. Hildebrand
Scripps Institution of Oceanography
University of California, San Diego
A-005
La Jolla, CA 92093

Dr. W. Steven Holbrook
Department of Geology and Geophysics
Woods Hole Oceanographic Institution
Woods Hole, MA 02543

Dr. R.S. Jacobson
Office of Naval Research
Code 1125GG
800 North Quincy Street
Arlington, VA 22217-5000

Dr. H. Paul Johnson
Department of Oceanography, WB-10
University of Washington
Seattle, WA 98195

Dr. Mary E. Kappus
Scripps Institution of Oceanography
IGPP, A-025
University of California, San Diego
La Jolla, CA 92093

Dr. Jeffrey A. Karson
Department of Geology
211 Old Chemistry Building
Duke University
Durham, NC 27706

Dr. Jill L. Karsten
Hawaii Institute of Geophysics
2525 Correa Road
Honolulu, HI 96822

Dr. Kim Klitgord
USGS
Woods Hole, MA 02543

Dr. Joseph H. Kravitz
Office of Naval Research
Code 1125GG
800 North Quincy Street
Arlington, VA 22217-5000

Dr. Brian T.R. Lewis
School of Oceanography, WB-10
University of Washington
Seattle, WA 98195

Dr. Jian Lin
Department of Geology and Geophysics
Woods Hole Oceanographic Institution
Woods Hole, MA 02543

Dr. Dennis Lindwall
Seafloor Geoscience Division
Marine Geophysics Branch, Code 362
NORDA
NSTL Station, MS 39529-5004

Dr. Susan Lohmann
Department of Chemistry
Woods Hole Oceanographic Institution
Woods Hole, MA 02543

Dr. Neil C. Mitchell
Lamont-Doherty Geological Observatory
Palisades, NY 10964

Dr. Daniel Moos
Department of Geophysics
Stanford University
Stanford, CA 94305

Dr. John A. Orcutt
Scripps Institution of Oceanography
Geophysics/Planetary Phys., A-025
La Jolla, CA 92093

Dr. Philippe H. Pezard
Lamont-Doherty Geological Observatory
Palisades, NY 10964

Dr. G.M. Purdy
Department of Geology and Geophysics
Woods Hole Oceanographic Institution
Woods Hole, MA 02543

Dr. Kristin Rohr
Pacific Geoscience Centre
9680 West Saanich Road
Sidney, BC V8L 4B2
Canada

Dr. Peter Shaw
Department of Geology and Geophysics
Woods Hole Oceanographic Institution
Woods Hole, MA 02543

Dr. Sean C. Solomon
Department of Earth, Atmospheric
and Planetary Sciences, 54-522
Massachusetts Institute of Technology
Cambridge, MA 02139

Dr. Ralph Stephen
Department of Geology and Geophysics
Woods Hole Oceanographic Institution
Woods Hole, MA 02543

Dr. Stephen Swift
Department of Geology and Geophysics
Woods Hole Oceanographic Institution
Woods Hole, MA 02543

Dr. Maurice Tivey
Department of Geology and Geophysics
Woods Hole Oceanographic Institution
Woods Hole, MA 02543

Dr. Geoffrey Thompson
Department of Chemistry
Woods Hole Oceanographic Institution
Woods Hole, MA 02543

Dr. Douglas Toomey
Department of Geological Sciences
Cascade Hall, University of Oregon
Eugene, OR 97403

Dr. Altan Turgut
RSMAS
University of Miami
4600 Rickenbacker Causeway
Miami, FL 33149

Dr. David A. Vanko
Georgia State University
Department of Geology
Atlanta, GA 30303

Dr. Emilio E. Vera
Lamont-Doherty Geological Observatory
Geoscience, Building 103
Palisades, NY 10964

Dr. Richard P. Von Herzen
Department of Geology and Geophysics
Woods Hole Oceanographic Institution
Woods Hole, MA 02543

Dr. Stephen Wales
Naval Research Laboratory
Attention Code 5122
4555 Overlook Avenue, SW
Washington, DC 20375-5000

William S. Wilcock
Department of Geology and Geophysics
Woods Hole Oceanographic Institution
Woods Hole, MA 02543

Dr. Roy H. Wilkens
Hawaii Institute of Geophysics
2525 Correa Road
Honolulu, HI 96822

Dr. John Wolf
Naval Research Laboratory
Attention Code 5120
4555 Overlook Avenue, SW
Washington, DC 20375-5000

END